Oxidative Medicine and Cellular Longevity

Interplay between Oxidative Stress and Metabolism in Signalling and Disease

Guest Editors: Andrés Trostchansky, Adriana Maria Cassina, Celia Quijano, Hariom Yadav, and Eric E. Kelley

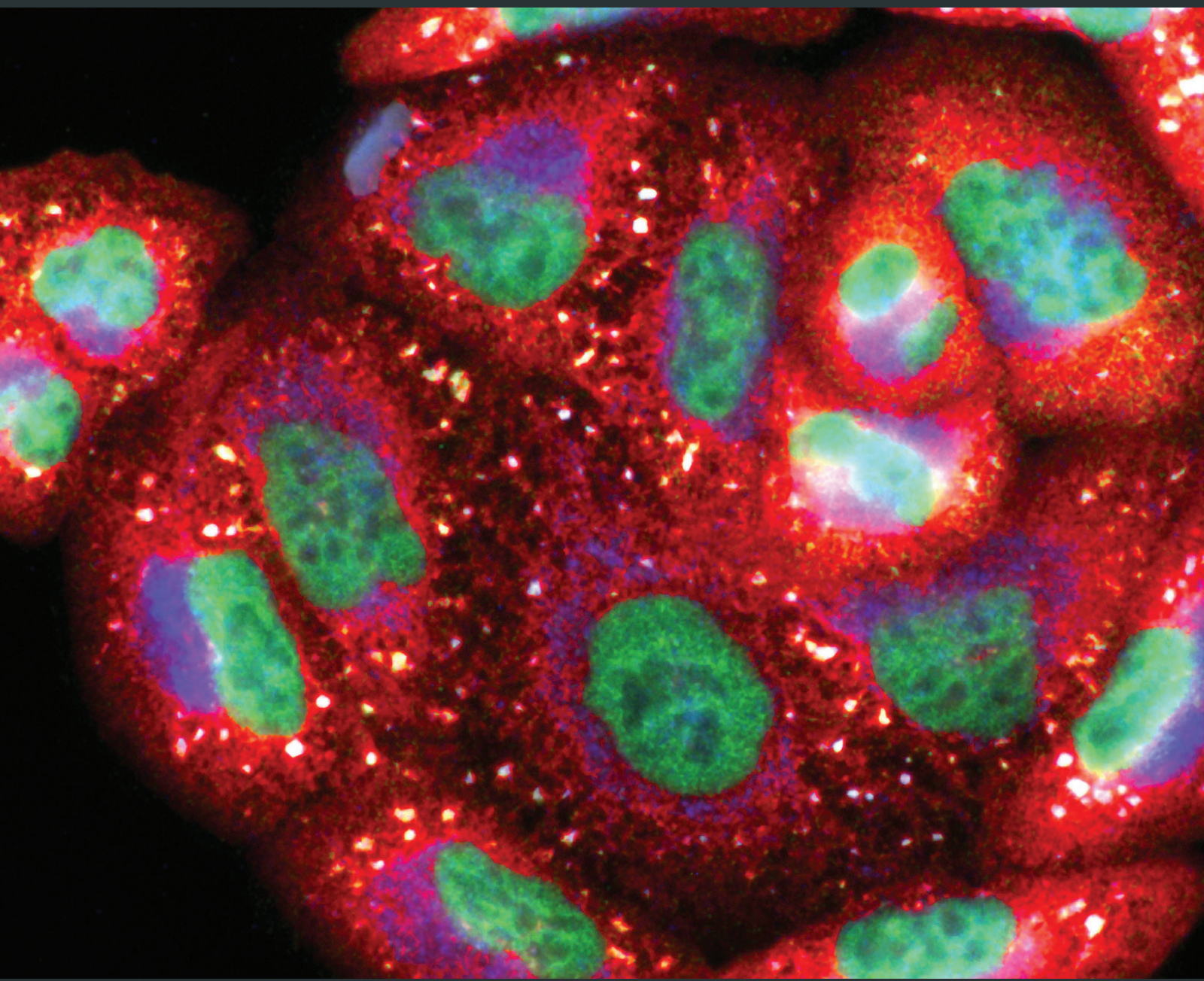

Interplay between Oxidative Stress and Metabolism in Signalling and Disease

Oxidative Medicine and Cellular Longevity

Interplay between Oxidative Stress and Metabolism in Signalling and Disease

Guest Editors: Andrés Trostchansky, Adriana Maria Cassina, Celia Quijano, Hariom Yadav, and Eric E. Kelley

Editorial Board

Contents

Interplay between Oxidative Stress and Metabolism in Signalling and Disease
Andrés Trostchansky, Celia Quijano, Hariom Yadav, Eric E. Kelley, and Adriana Maria Cassina
Volume 2016, Article ID 3274296, 2 pages

Potential Modulation of Sirtuins by Oxidative Stress
Leonardo Santos, Carlos Escande, and Ana Denicola
Volume 2016, Article ID 9831825, 12 pages

Maladaptive Modulations of NLRP3 Inflammasome and Cardioprotective Pathways Are Involved in Diet-Induced Exacerbation of Myocardial Ischemia/Reperfusion Injury in Mice
Raffaella Mastrocola, Massimo Collino, Claudia Penna, Debora Nigro, Fausto Chiazza, Veronica Fracasso, Francesca Tullio, Giuseppe Alloatti, Pasquale Pagliaro, and Manuela Aragno
Volume 2016, Article ID 3480637, 12 pages

Dietary Restriction and Nutrient Balance in Aging
Júlia Santos, Fernanda Leitão-Correia, Maria João Sousa, and Cecília Leão
Volume 2016, Article ID 4010357, 10 pages

Toll-Like Receptor 4 Reduces Oxidative Injury via Glutathione Activity in Sheep
Shoulong Deng, Kun Yu, Qian Wu, Yan Li, Xiaosheng Zhang, Baolu Zhang, Guoshi Liu, Yixun Liu, and Zhengxing Lian
Volume 2016, Article ID 9151290, 9 pages

Correlation between Mitochondrial Reactive Oxygen and Severity of Atherosclerosis
Gabriel G. Dorighello, Bruno A. Paim, Samara F. Kiihl, Mônica S. Ferreira, Rodrigo R. Catharino, Anibal E. Vercesi, and Helena C. F. Oliveira
Volume 2016, Article ID 7843685, 10 pages

Increased Susceptibility of *Gracilinanus microtarsus* Liver Mitochondria to Ca^{2+}-Induced Permeability Transition Is Associated with a More Oxidized State of NAD(P)
Juliana A. Ronchi, Barbara Henning, Felipe G. Ravagnani, Tiago R. Figueira, Roger F. Castilho, Sergio F. dos Reis, and Anibal E. Vercesi
Volume 2015, Article ID 940627, 10 pages

Mitochondrial Retrograde Signaling: Triggers, Pathways, and Outcomes
Fernanda Marques da Cunha, Nicole Quesada Torelli, and Alicia J. Kowaltowski
Volume 2015, Article ID 482582, 10 pages

Toll-Like Receptor 4 Promotes NO Synthesis by Upregulating GCHI Expression under Oxidative Stress Conditions in Sheep Monocytes/Macrophages
Shoulong Deng, Kun Yu, Baolu Zhang, Yuchang Yao, Zhixian Wang, Jinlong Zhang, Xiaosheng Zhang, Guoshi Liu, Ning Li, Yixun Liu, and Zhengxing Lian
Volume 2015, Article ID 359315, 11 pages

Insulin Therapy of Nondiabetic Septic Patients Is Predicted by *para*-Tyrosine/Phenylalanine Ratio and by Hydroxyl Radical-Derived Products of Phenylalanine
Szilárd Kun, Gergő A. Molnár, Eszter Sélley, Lívia Szélig, Lajos Bogár, Csaba Csontos, Attila Miseta, and István Wittmann
Volume 2015, Article ID 839748, 7 pages

Hindawi Publishing Corporation
Oxidative Medicine and Cellular Longevity
Volume 2016, Article ID 3274296, 2 pages
http://dx.doi.org/10.1155/2016/3274296

Editorial

Interplay between Oxidative Stress and Metabolism in Signalling and Disease

Andrés Trostchansky,[1] Celia Quijano,[1] Hariom Yadav,[2] Eric E. Kelley,[3] and Adriana Maria Cassina[1]

[1]*Departamento de Bioquímica and Center for Free Radical and Biomedical Research, Facultad de Medicina, Universidad de la República, 11800 Montevideo, Uruguay*
[2]*NIDDK, NIH, Diabetes, Endocrinology and Obesity Branch, Bethesda, MD 20892, USA*
[3]*Department of Anesthesiology and Vascular Medicine Institute, School of Medicine, University of Pittsburgh, Pittsburgh, PA 15261, USA*

Correspondence should be addressed to Andrés Trostchansky; trocha@fmed.edu.uy

Received 11 October 2015; Accepted 11 October 2015

It is well recognized that energy metabolism is linked to the production of reactive species and critical enzymatic processes allied to metabolic pathways can be affected by redox reactions. Both protein and lipid oxidation are involved in the aging process as well as the onset and progression of many age-related diseases. As such, the capacity to identify specific targets and detect subsequent oxidative modifications is crucial for the understanding of the molecular basis of age-related diseases (i.e., diabetes, metabolic syndrome, or atherosclerosis) and for revealing novel treatment strategies.

Formation of mitochondrial reactive oxygen and nitrogen species (ROS and RNS, resp.) has been extensively studied in the literature. Moreover, mitochondrial dysfunction is observed in many pathological conditions in addition to an increase in ROS and RNS production. Thus, the initiation and progression of diseases whose pathogenesis involves mitochondrial dysfunction may be modulated by decreasing mitochondrial oxidant formation. However, mitochondria are not the only source of reactive species in cells; for example, catabolism of biomolecules can be a source of oxidant formation with critical intracellular outcomes. For example during β-oxidation of fatty acids, the electron transfer flavoprotein (ETF) produces superoxide ($O_2^{\bullet -}$) and hydrogen peroxide (H_2O_2) upon reduction with its substrate, medium chain acyl-CoA dehydrogenase (MCAD). Superoxide and H_2O_2 can be formed in several metabolic pathways where electron transfer reactions are involved and can subsequently lead to the formation of highly oxidizing species such as peroxynitrite and lipid-derived electrophiles. As such, capacity to detoxify reactive species with a battery of antioxidant enzymes is critical in preventing the reactions of oxidants with cellular components.

In this special issue, we present several examples of the interplay between oxidative stress and metabolism.

The manuscript by M. da Cunha and colleagues discusses mitochondria-to-nucleus retrograde signaling in various organisms as well as the differences in effector pathways, molecules, and outcomes. Almost 99% of mitochondrial proteins are encoded in the nucleus; however, mitochondrial DNA does encode some key proteins. The correct communication between mitochondria and the nucleus is seminal in coordinating mitochondrial protein synthesis during biogenesis whereas potential mitochondrial malfunction can influence in this communication. Mitochondrial role in apoptosis, addressed by J. A. Ronchi et al., describes Ca^{2+}-dependent opening of mitochondrial membrane permeability transition pore (PTP) and ROS generation. In their manuscript, the authors propose that PTP opening is a relevant process of mitochondrial Ca^{2+} signaling when a redox imbalance is present. The NADPH/$NADP^+$ ratio was also analyzed in terms of mitochondrial ROS formation in hypercholesterolemic mice after supplementation with citrate or by

inhibition of the NADPH consuming anabolic cholesterol synthesis pathway. Overall, the authors showed a positive correlation of the atherosclerotic lesion with mitochondrial ROS formation in liver.

The NAD-dependent protein deacetylases sirtuins (SIRT) regulate metabolic enzymes maintaining cellular homeostasis. L. Santos et al. present a thorough revision on how sirtuins are regulated at the expression level and/or by proteasomal degradation depending on the degree of oxidative stress. Finally, the authors discuss how SIRT3 may be regulated by oxidant species generated in the mitochondrial matrix.

Santos J. and colleagues addressed nutrient signaling pathways related to caloric restriction (in particular, how aging and caloric restriction interact by overlapping the activation of insulin-derived pathways). Meanwhile, R. Mastrocola et al. analyzed metabolic disorders and its relation with high fat diet. In their original article S. Kun et al. explore how hydroxyl radical- or metabolic-derived Phe or Tyr derivatives alter the gluconeogenic pathway in nondiabetic septic patients and propose that these species may serve as indicators for insulin-based therapies in these patients.

The aim of this special issue was to increase our knowledge of the role of metabolism and oxidative stress in cell signaling and disease, particularly about the molecular mechanisms participating in these processes as well as their role in human diseases and cell physiology.

Acknowledgment

We would like to thank all the reviewers that contributed during the peer-review process.

Andrés Trostchansky
Celia Quijano
Hariom Yadav
Eric E. Kelley
Adriana Maria Cassina

Hindawi Publishing Corporation
Oxidative Medicine and Cellular Longevity
Volume 2016, Article ID 9831825, 12 pages
http://dx.doi.org/10.1155/2016/9831825

Review Article

Potential Modulation of Sirtuins by Oxidative Stress

Leonardo Santos,[1] Carlos Escande,[2] and Ana Denicola[1]

[1]*Laboratorio de Fisicoquímica Biológica, Instituto de Química Biológica, Facultad de Ciencias, Universidad de la República, Iguá 4225, 11400 Montevideo, Uruguay*
[2]*Laboratorio de Patologías del Metabolismo y Envejecimiento, Institut Pasteur de Montevideo, Mataojo 2020, 11400 Montevideo, Uruguay*

Correspondence should be addressed to Ana Denicola; denicola@fcien.edu.uy

Received 30 July 2015; Accepted 20 September 2015

Academic Editor: Eric E. Kelley

Sirtuins are a conserved family of NAD-dependent protein deacylases. Initially proposed as histone deacetylases, it is now known that they act on a variety of proteins including transcription factors and metabolic enzymes, having a key role in the regulation of cellular homeostasis. Seven isoforms are identified in mammals (SIRT1–7), all of them sharing a conserved catalytic core and showing differential subcellular localization and activities. Oxidative stress can affect the activity of sirtuins at different levels: expression, posttranslational modifications, protein-protein interactions, and NAD levels. Mild oxidative stress induces the expression of sirtuins as a compensatory mechanism, while harsh or prolonged oxidant conditions result in dysfunctional modified sirtuins more prone to degradation by the proteasome. Oxidative posttranslational modifications have been identified *in vitro* and *in vivo*, in particular cysteine oxidation and tyrosine nitration. In addition, oxidative stress can alter the interaction with other proteins, like SIRT1 with its protein inhibitor DBC1 resulting in a net increase of deacetylase activity. In the same way, manipulation of cellular NAD levels by pharmacological inhibition of other NAD-consuming enzymes results in activation of SIRT1 and protection against obesity-related pathologies. Nevertheless, further research is needed to establish the molecular mechanisms of redox regulation of sirtuins to further design adequate pharmacological interventions.

1. Introduction

Sirtuins are a conserved family of enzymes, originally defined as histone deacetylases (class III HDAC) [1]. They deacetylate not only histones but also other proteins. In addition, they catalyze the hydrolysis of lysines modified with longer acyl chains (deacylase activity) [2]. Unlike classes I, II, and IV HDAC that utilize zinc for catalysis, sirtuins use a complex mechanism depending on cofactor NAD that already discloses a fine-regulated activity.

Since the discovery of yeast Sir2 (Silent Information Regulator 2) 30 years ago [3], the founding member of the family, an intensive research went on to elucidate the biological functions of sirtuins, especially after the early found connection of sirtuins with lifespan [1, 4]. The number of publications grew exponentially in the search of potential activators or inhibitors of sirtuins that fight against metabolic disorders, cancer, and even aging [5].

In *S. cerevisiae*, besides Sir2, four more sirtuins were described, Hst1–4. In *C. elegans*, four homologs of yeast Sir2 were named Sir2.1–2.4, whereas seven paralogs were described in mammals, SIRT1–7. Phylogenetic analysis groups the mammalian SIRT1, SIRT2, and SIRT3 as subclass I which shows close homology to yeast Sir2, SIRT4, and SIRT5 as subclasses II and III, respectively, and SIRT6-SIRT7 in subclass IV [6].

The seven mammalian SIRT differ in sequence (although they all share a conserved catalytic core), in subcellular location, enzyme activity, and substrate specificity. The list depicted in Table 1 is by no means comprehensive since new *in vivo* substrates and specificities are discovered every day. The most studied human isoform is SIRT1, a nuclear protein reported to regulate critical physiological processes and associated with chronic inflammatory diseases and metabolic dysfunctions like diabetes, obesity, aging, and even cancer [7].

Table 1: General characteristics of mammalian sirtuins.

Human isoforms	Localization	Length	Conserved catalytic core position	Catalytic activity	Substrate	Function	References
SIRT1	Nucleus cytoplasm	747 aa	 254 489	Deacetylase	p53, H3K9, H1K26, H4K16, PGC1α, SREBP-1c, PPARγ NF-κB, AKT, FOXO, HIF-1α, TFAM, AceCS1, APE1, and PARP-1	Lipogenesis ↓ Gluconeogenesis ↑↓ Lipolysis ↑ Inflammation ↓	[31, 42, 45, 94, 123–135]
SIRT2	Cytoplasm	352 aa	 40 294	Deacetylase demyristoylase	PEPCK, α-tubulin, H4K16, and FOXO3a	Gluconeogenesis ↑ Control of mitotic exit	[37, 136–139]
SIRT3	Mitochondria	399 aa	 238 373	Deacetylase	LCAD, HMGCS2, SOD2, IDH2, PDC, and AceCS2	Lipid accumulation ↓ Fatty acid oxidation ↑ Ketone body production ↑ Oxidative stress ↓	[48, 132, 140–143]
SIRT4	Mitochondria	314 aa	 47 308	ADP-ribosyltransferase Lipoamidase	GDH, PDC	Insulin secretion ↓	[17, 144]
SIRT5	Mitochondria	310 aa	 51 301	Desuccinylase Demalonylase Deglutarylase	CPS1	Urea cycle ↑	[18, 145, 146]
SIRT6	Nucleus endoplasmic reticulum	355 aa	 45 257	Depalmitoylase ADP-ribosyltransferase Deacetylase Demyristoylase	H3K9, H3K56, TNFα, and PARP-1	Glucose uptake ↓ Inflammation ↑ DNA reparation ↑	[16, 19, 147–150]
SIRT7	Nucleolus	400 aa	 254 489	ADP-ribosyltransferase Deacetylase	PAF53, H3K18	RNA polymerase I transcription ↑	[151, 152]

SREBP-1c: sterol regulatory element binding protein c, PGC1α: peroxisome proliferator-activated receptor gamma coactivator 1 alpha, FOXO1: Forkhead box protein O1, PPARα: peroxisome proliferator-activated receptor alpha, NF-κB: nuclear factor kappa-light-chain-enhancer of activated B cells, AKT: protein kinase B, UCP-2: uncoupling protein 2, HIF-1α: hypoxia-inducible factor 1 alpha, PPARγ: peroxisome proliferator-activated receptor gamma, TFAM: transcription factor A, mitochondrial, APE1: apurinic/apyrimidinic endonuclease 1, PARP-1: poly(ADP-ribose) polymerase 1, PEPCK: phosphoenolpyruvate carboxykinase, LCAD: long-chain acyl-CoA dehydrogenase, HMGCS2: 3-hydroxy-3-methylglutaryl-CoA synthase 2, SOD2: superoxide dismutase, IDH2: isocitrate dehydrogenase 2, PDC: pyruvate dehydrogenase complex, GDH: glutamate dehydrogenase, CPS1: carbamoyl-phosphate synthase 1, TNFα: tumor necrotic factor alpha, PAF53: RNA polymerase associated factor, and AceCS: acetyl-CoA synthetase.

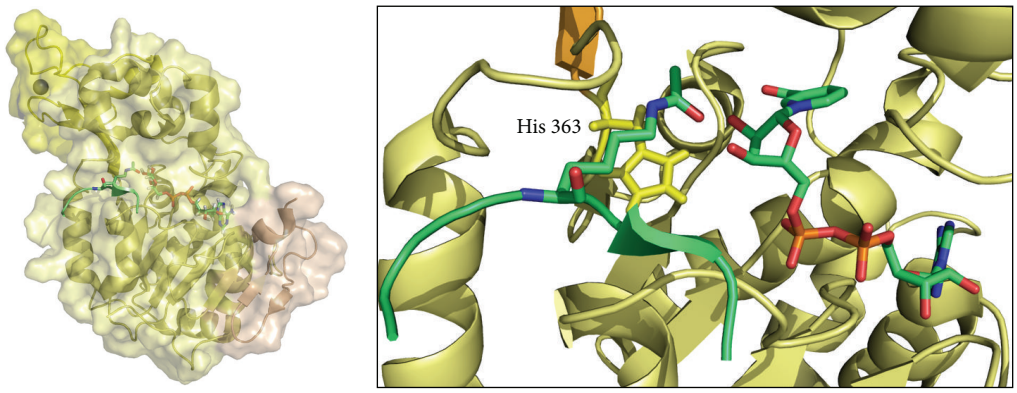

(a) (b)

Figure 1: Structure of sirtuins. (a) Crystal structure of a partial sequence of hSIRT1 (PDB 4KXQ) with bound substrates, acetylated peptide, and NAD. The catalytic core is depicted in yellow with the Zn^{2+} binding domain. (b) Zoom of catalytic site with the catalytic histidine colored in yellow.

This review focuses on the effect of oxidative stress on structure and activity of sirtuins and the biological consequences of their redox regulation. Understanding the role and mechanism of action of sirtuins in the context of a pathophysiological inflammatory condition will help to identify novel interventions to manage important chronic diseases.

2. Sirtuins Structure

Crystal structures of sirtuins from archaea to eukaryotes show a central catalytic core comprised of 245 residues. The core is made up of a large domain containing a Rossmann fold typical of NAD-dependent proteins and a small domain containing a Zn^{2+} ribbon motif, separated by a cleft where the peptide substrate binds (Figure 1). The NAD molecule adopts an extended conformation binding to a grove between the two domains with the adenine base facing the large domain and the nicotinamide group close to the small domain (Figure 1). SIRT1 is the biggest isoform with extended N- and C-terminals very flexible, unstructured, which offers more sites of activity modulation (posttranslational modifications, interaction with proteins and ligands).

The Zn^{2+} binding site is composed of three antiparallel beta strands containing two Cys-X-X-Cys conserved motifs separated by 15–20 residues that coordinate a single zinc ion that has an important structural role. It has long been known that mutation of these cysteine residues by alanine causes loss of activity [8]. Although the zinc tetrathiolate is fairly exposed, only high concentrations of zinc chelator were able to disrupt it with the corresponding loss of activity [9]. Another report on *P. falciparum* Sir2 obtained the inactive apoenzyme by treatment with potent zinc chelator and restored activity upon reconstitution with exogenous zinc chloride [10].

The zinc ion is located in the small domain, far away from the NAD binding pocket, excluding the possibility of participation in the catalysis, in contrast with other HDAC types where zinc is part of the catalytic mechanism [11].

3. Enzymatic Activities of Sirtuins

Sirtuins are defined as protein deacylases. They catalyze the reaction depicted in Figure 2 using NAD as a cofactor, yielding the deacylated protein, nicotinamide (that displays inhibition by product), and acylated ADPR as final products.

Kinetic studies and isotope exchange indicate that sirtuins first bind the acetylated substrate, followed by NAD binding to form a ternary enzyme complex where the carbonyl oxygen of the acetyl group attacks ribose C1′ to form O-alkylamidate intermediate. Crystal structures of binary complexes were solved between Sir2-like enzyme and NAD [9], or ADP-ribose [12], or acetylated p53 [13]. Moreover, the crystal structure of a ternary complex was reported between yeast Hst2, an acetylated histone peptide, and a nonhydrolyzable NAD analog [14]. Crystal data confirm the peptide substrate binds in a narrow channel that positions the acylated lysine residue near the nicotinamide ring of NAD (Figure 1). Upon peptide binding, a conformational change on the NAD site must occur to facilitate the nucleophilic attack on ribose C1′ to cleave the nicotinamide-ribosyl bond, first step in the catalytic pathway. A conserved histidine residue (H363 in hSIRT1) has been identified as critical for the catalysis, first acting as a general base hydrogen bonded to 3″ OH-ribose and, then, as a general acid protonating the lysine residue in the last step of the catalysis.

Besides protein deacetylation, it was early recognized that sirtuins can also catalyze ADP ribosylation of a protein acceptor (or the enzyme itself) via a similar mechanism (Figure 2) [14–17].

More recently, it has been found that some sirtuin isoforms previously considered poor deacetylases are actually good deacylases; that is, they catalyze the hydrolysis of lysine amides derivatized with a longer-chain carboxylic acid, for example, succinate or malonate. Indeed, SIRT5 functions as desuccinylase or demalonylase [18], whereas SIRT6 functions as demyristoylase [2, 19]. Moreover, SIRT6 deacetylase activity has been recently shown to be regulated by free-fatty

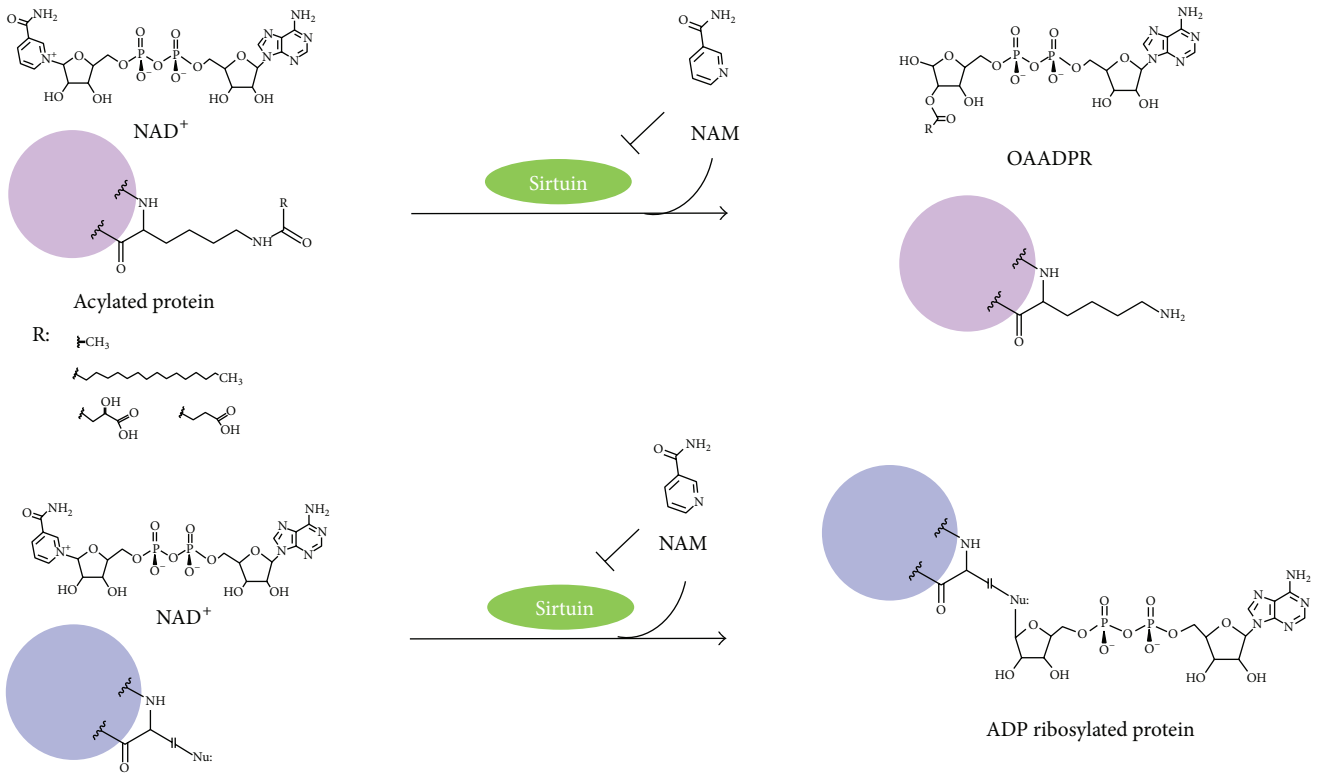

Figure 2: Scheme of reactions catalyzed by sirtuins. Deacetylation is the most common reaction catalyzed by sirtuins, but some sirtuins catalyze deacylation of other posttranslational lysine modifications and mono ADP ribosylation. NAM = nicotinamide, OAADPR = *O*-acetyl-ADP-ribose.

acids *in vitro*, opening the possibility that fatty acids might be acting as endogenous regulators of sirtuin activity *in vivo* [2].

Acetylation is an important posttranslational modification even outside chromatin. The acetylome shows that many proteins are acetylated as a mechanism of regulation of cellular function, and it is even possible that is as common in cellular life as phosphorylation [20, 21]. Comparative studies on *Drosophila* and humans have demonstrated that acetylated lysines are highly conserved [22, 23]. An acetylome peptide microarray has been described that reveals new deacetylation substrate candidates for all sirtuin isoforms [24].

4. Sirtuins and Oxidative Stress

As mentioned above, increasing evidence supports the role of sirtuins in the regulation of cellular homeostasis, in particular metabolism and inflammation [25, 26]. During conditions of metabolic stress, like obesity and metabolic syndrome, an oxidative stress environment is created, mainly due to a state of chronic inflammation. Based on the key role of sirtuins in the regulation of metabolic responses [27, 28], it is pertinent to ask how changes in the redox status of the cells affect the activity of sirtuins and what are the biological consequences of these alterations.

Oxidative stress, considered as an overwhelmed generation of reactive species (ROS/RNS) or a general disruption of redox cellular homeostasis [29, 30], can affect the activity of sirtuins at different levels:

(1) Inducing or repressing the expression of SIRT gene.

(2) Posttranslational oxidative modifications of SIRT.

(3) Altering SIRT-protein interactions.

(4) Changing NAD levels.

4.1. Changes in Sirtuin Expression during Oxidative Stress. It has been observed that *mild oxidative stress conditions induce the expression of SIRT1*, changing its activity and thus affecting SIRT1 targets that are involved in the response to changes in the redox state of the cell [31–33]. The first major SIRT1 substrate identified was p53, a transcription factor involved in activating antioxidant genes like SOD2 (superoxide dismutase 2, MnSOD) and GPx1 (glutathione peroxidase) [34]. Another redox transcription factor deacetylated by SIRT1 (as well as SIRT2 and SIRT3) is FOXO3a which induces an antioxidant response via SOD2 and catalase expression [35–40]. PGC1α, a known substrate of SIRT1, is reported to regulate expression of mitochondrial antioxidants like SOD2 [41–43]. SIRT1 can deacetylate p65 NFκB subunit diminishing its activity and, thus, the production of proinflammatory cytokines [44–46]. In addition, upon increased production of ROS at the mitochondria, induction of SIRT3 was observed [47]. It was reported that SIRT3 deacetylates and thus activates SOD2 reducing oxidative

stress in the mitochondria [48]. In adult mouse hearts, SIRT1 was significantly upregulated (4-fold) in response to oxidative stress (paraquat injection) and, similarly, 3-fold increase in SIRT1 levels was observed in old versus young monkey hearts [49]. In the same way, modest overexpression of SIRT1 retarded age-dependent changes in the heart of transgenic mice [49]. Low levels of H_2O_2 promoted deacetylation of the tumor suppressor protein PLM in HeLa cells via SIRT1 and SIRT5 [50].

On the contrary, *exposure to high levels of H_2O_2 or harsh oxidative stress resulted in* increased proteasomal degradation of SIRT1, desumoylation, and *enzyme inactivation* that leads to apoptosis [51]. Human monocytes exposed to high dose of H_2O_2 (250 μM, 24 h) resulted in a significant decrease in SIRT1 activity (measured as levels of acetylated p53) and lower SIRT1 gene and protein expression [52]. Human lung epithelial cells exposed to oxidants (H_2O_2, aldehyde-acrolein, and cigarette smoke extract) presented decreased levels of SIRT1 concomitant with decreased SIRT1 activity [53]. A recent work on human endothelial cells showed no effect of low doses of H_2O_2 but a drastic drop to 50% SIRT1 activity after exposure to 100 μM H_2O_2 for 30 min, along with a decrease in free thiol content of SIRT1 [54].

An interesting view suggested by Tong et al. [55] is that active sirtuins provide an adequate level of *O*-acetyl-ADP-ribose (OAADPR) (product of the reaction catalyzed by sirtuins with deacetylase activity, Figure 2) that readily converts to ADP-ribose and both may function as cellular signals. Increased ADPR/OAADPR levels protect cells from oxidative stress via two mechanisms: (1) inhibition of Complex I of the mitochondrial electron transport chain with concomitant lower production of ROS and (2) inhibition of glyceraldehyde-3-phosphate dehydrogenase, central enzyme in glycolysis, diverting glucose to the pentose phosphate pathway with the concomitant increase in NADPH, main reductant for detoxifying ROS enzymes.

4.2. Posttranslational Modifications (PTM) of Sirtuins. Phosphorylation was the first PTM found in SIRT1. SIRT1 is the most studied mammalian isoform although a crystal structure of the whole protein is not available and we rely on a simulation model [56]. Apart from the central catalytic structured core, SIRT1 has long C- and N-terminal domains which are flexible and disordered, not present in the other SIRT structures, and considered potential sites of enzyme regulation. Early mass spectrometry (MS) analysis detected several serine/threonine phosphorylation sites at the N- and C-terminal domains of SIRT1 [57]. Several kinases are known to phosphorylate SIRT1, and many of them are regulated by oxidative stress. CdkI (also known as Cdc2), a kinase involved in cell cycle progression and regulated by oxidative stress [58], phosphorylates SIRT1 in its C-terminus domain (T530 and S540) [57]. Mutations of these two sites on SIRT1 affect cell cycle progression [58]. SIRT1 is also phosphorylated by Casein Kinase II (CKII) in serines S154, S649, S651, and S683 [59]. CKII activity is tightly regulated by oxidative stress [60], and, indeed, ionizing radiation activates CKII, leading to SIRT1 phosphorylation and activation [59]. Phosphorylation of SIRT1 in different residues by AMPK has also been shown to regulate its activity mainly by affecting binding to its protein inhibitor DBC1 [61, 62]. AMPK is a key sensor and regulator of redox state of the cell and its biological activity is regulated by oxidative stress [63], although no direct link between oxidative stress and SIRT1 involving AMPK has been shown until now. Finally, phosphorylation of SIRT1 at different C-term residues has been shown to change its enzymatic activity. SIRT1 phosphorylation (T530) triggers a conformational change that increases its deacetylase activity [64–66]. Also, PKA-dependent phosphorylation of SIRT1 (S434) stimulates its activity [67]. Sumoylation at the C-terminal domain of SIRT1 (K734) has been detected and shown to increase activity as well [51]. Phosphorylation sites at the C-terminal of SIRT2 (S368, S372) were also reported to regulate enzyme function [68, 69]. In the case of SIRT6, phosphorylation at T294 and S303 were identified in a proteomic analysis, with no report on functional consequences [70, 71]. Another report shows that phosphorylation of SIRT6 at S338 by AKT leads to its degradation in breast cancer cells [72]. Moreover, mutation of that phosphorylation site made breast cancer cells more sensitive to chemotherapeutic agents [72].

Oxidative modifications of sirtuins are less well studied. Treatment of recombinant hSIRT1 with nitrosoglutathione (GSNO) was first reported [73] to modify C67 (located in the noncatalytic C-terminal domain) by S-glutathionylation, with no effect on basal deacetylase activity but loss of stimulation by resveratrol *in vitro* (although it has to be mentioned that the activity was measured using the fluorimetric assay that it is known to yield an artefactual activation of SIRT by resveratrol [74]). In this work [73], differential alkylation revealed 5 out of the 19 cysteines on human SIRT1 as reactive towards GSNO. Three of those five modified cysteines are solvent exposed residues (C67, C268, and C623) as indicated in the computer generated model of human SIRT1 structure [56]. However, in that same year 2010, it was published that treatment of SIRT1 with GSNO resulted in nitrosylation (not glutathionylation) of the enzyme with loss of deacetylase activity [75]. The residues modified (C387 and C390 from the mouse ortholog that coordinates the zinc ion) were different from those proposed previously [75]. These authors reported that treatment of intact HEK293 cells with GSNO resulted in nitrosylation of SIRT1 (SIRT1-SNO) via transnitrosylation from GAPDH-SNO translocated to the nucleus [75]. Nitrosylation of nuclear SIRT1 inhibited deacetylation of PGC1α in HEK293 cells. Mutational analysis on transfected cells with mouse SIRT1 plasmids identified C387 and C390 from the zinc tetrathiolate motif as the sites of S-nitrosylation. Surprisingly, C363 and C366 that also participate in zinc coordination were not susceptible to transnitrosylation. More recently, C371 and C374 from hSIRT1 (corresponding to C363 and C366 in mSIRT1) have been identified as the cysteines reduced by APE/Ref-1 to stimulate endothelial SIRT1 activity (although the other two cysteines involved in zinc ion coordination were not tested) [54].

When HepG2 cells transiently transfected with mouse SIRT1 WT were treated with increasing concentrations of CysNO or H_2O_2, decrease in p53 deacetylase activity was observed [76]. However, when cells were transfected with

mSIRT1 mutants C61S, C318S, and/or C613S, the deacetylase activity was initially higher than with WT overexpression and less susceptible to oxidants [76]. The authors suggested reversible oxidative modification of SIRT1 forming GSH-adducts with these cysteine residues that are reverted by glutaredoxin 1. In this case, the reported cysteine residues oxidatively modified are not part of the Zn-binding motif.

Treatment of human epithelial cells with alkylating agent NEM diminished SIRT1 protein levels and free cysteine residues on immunoprecipitated SIRT1, although the specific residues modified were not identified [53].

Increased protein carbonylation of SIRT3 was found in liver mitochondrial extracts of ethanol-consuming mice [77]. The authors identified *in vitro* covalent modification of rSIRT3 by the electrophilic compound 4-hydroxynonenal at C280 (critical zinc-binding cysteine residue), resulting in inhibition of rSIRT3 activity [77].

More recently, mapping protein S-sulfenylation in cells treated with exogenous H_2O_2 as well as endogenous H_2O_2 (EGF treatment in A431 cells), SIRT6 was found among the most highly and consistently S-sulfenylated proteins [78]. Cysteine C18, a highly conserved residue close to the amino terminus, was identified as Cys-SOH that could form a covalent complex with HIF1α via disulfide bond, suggesting SIRT6-mediated redox control of HIF1α transcriptional activity [78].

Even though sirtuins do not have critical cysteine residues that participate in the mechanism of catalysis, modification of cysteine residues affects their activity, because it alters either the enzyme structure or the interaction with other proteins. The four cysteines in the zinc tetrathiolate motif, highly conserved, are essential for having a properly folded enzyme; thus, mutation of these cysteines to serine, not surprisingly, diminished deacetylase activity [54].

Another PTM (tyrosine nitration) on SIRT6 was recently reported [79]. Treatment of recombinant SIRT6 with the peroxynitrite donor SIN-1 revealed nitration of the enzyme and diminished activity. The authors identified tyrosine Y257 as one of the amino acid residues modified and mutation Y257F causes loss of deacetylase activity and susceptibility to nitration by SIN-1. Nitrated SIRT6 was also found in retina in a model of endotoxin-induced retinal inflammation [79].

4.3. Regulation of Sirtuins by Protein-Protein Interaction during Oxidative Stress. Oxidative stress regulates the activity of different sirtuins by altering their binding to regulatory proteins. From all sirtuins, the most extensively studied in terms of regulation by protein-protein interaction is SIRT1. The main protein regulators of SIRT1 described so far are DBC1 (deleted in breast cancer 1) [80] and AROS (active regulator of SIRT1) [81], and both have been involved in SIRT1-mediated response to oxidative stress [81, 82]. In the case of AROS, it was shown that its knock-down decreases SIRT1-mediated response to oxidative stress in cells, although it is not clear whether the protein plays an active role in such response or it is binding to SIRT1 the critical event. Oxidative stress also alters the interaction of SIRT1 with its protein inhibitor DBC1. Oxidative stress promotes phosphorylation of DBC1 (Thr454) by an ATM/ATR-dependent mechanism, increasing its affinity for SIRT1 and leading to sirtuin inhibition [82]. Interestingly, in mice, both obesity and aging [83, 84] promote SIRT1 binding to DBC1 [80], leading to a decrease in SIRT1 activity. Finally, it was shown recently that during oxidative stress SIRT1 can be inactivated by cytoplasmic sequestration and localization into caveolae by direct binding to caveolin-1 [85].

Thus, many different mechanisms might be operating to regulate SIRT1 activity during oxidative stress.

4.4. Alterations of Intracellular NAD Levels and Sirtuin Regulation during Oxidative Stress. NAD availability is key in the regulation of all sirtuins [86]. In fact, it has been shown that NAD levels decline during aging, obesity, and other metabolic diseases [87], affecting the activities of sirtuins in different tissues. Importantly, interventions that prevent NAD decline in tissues protect against metabolic and age-related diseases [87–91]. Genetic deletion [90] and also pharmacological inhibition of the protein CD38 [92], the main NAD glycohydrolase in mammalian tissues [92], activate SIRT1 [93] and protect against obesity and metabolic syndrome [90]. Similar results were found by inhibition of other major NAD-consuming enzymes in tissues like PARP-1 [91]. In fact, SIRT1 and PARP-1 activities can influence each other, since it has also been reported that SIRT1 can deacetylate PARP-1, decreasing its activity [94]. Furthermore, pharmacological treatment with NAD precursors, like nicotinamide mononucleotide (NMN) or nicotinamide riboside (NR), prevents NAD decline and protects against many aspects of metabolic syndrome, including glucose intolerance [87, 88]. Altogether, these results open the possibility of using NAD therapy for the treatment of metabolic and age-related diseases.

It is well established that aging and also metabolic disorders like obesity lead to an increased oxidative stress in tissues. In addition, it has been shown that NAD decline inversely correlates with oxidative stress during aging [95] and that oxidative stress negatively impacts on mitochondria, leading to NAD depletion in the matrix [96]. Interestingly, caloric restriction, an intervention shown to increase healthspan and to prevent metabolic syndrome, decreases oxidative stress leading to increased NAD levels and improving mitochondrial function by SIRT3-mediated increase in SOD2 activity [48].

5. Sirtuins as Pharmacological Targets for Metabolic and Age-Related Diseases

There has been considerable debate about pharmacological sirtuin activation and its effect on metabolism, cancer, and aging. The original observation that the polyphenol resveratrol and other small molecules (STACs, for sirtuin activating compounds) extend lifespan in *S. cerevisiae* through activation of Sir2 and that resveratrol could also activate human SIRT1 [97] puts sirtuins on the spot as ideal pharmacological targets for the treatment of aging and age-related diseases. Early on, an intense debate started about the role of resveratrol and other STACs as direct SIRT1 activators,

since such activation appeared to rely on a specific activity assay and could not be reproduced by other means *in vitro* [98]. Since then, many molecular mechanisms have been proposed for SIRT1 activation by resveratrol *in vivo*, including direct SIRT1 activation [97, 99], activation of the AMPK-SIRT1 axis with NAD levels linking AMPK activation to SIRT1 activation [100], activation of the AMPK-SIRT1 axis through SIRT1 phosphorylation and dissociation from DBC1 [61], and SIRT1 activation through increase in cAMP levels by phosphodiesterase inhibition [101].

The development of novel, structurally different STACs by Sirtris Pharmaceuticals showed that SIRT1 activation by these new molecules (SRT1720, SRT1460, and SRT2183) prevents metabolic diseases in mice [99], and in the case of SRT1720, it was later shown that it also increases healthspan and lifespan in mice [102, 103]. Interestingly, the debate rose again about the specificity of these STACs for SIRT1 [104]. Recent research, however, has provided new evidence showing that these STACs, and even more potent new generations (STAC-5, STAC-9, and STAC-10), are indeed SIRT1 activators [105, 106].

Although the mechanism of action of resveratrol and other STACs may still need to be further investigated, it is clear that they provide beneficial effects against age-related disease *in vivo*. Resveratrol protects against high-fat diet induced obesity, type II diabetes, cardiovascular diseases, and cancer [99, 101, 107–114]. Similar results have been found with newly developed STACS [107, 107, 115, 116]. Interestingly, both resveratrol and the newly developed STACs decrease oxidative stress *in vitro* and *in vivo*, either by promoting antioxidant defenses or by improving mitochondrial function [103, 117–122].

The effect of STACS on human subjects has also been debated. Most of the evidence relies on studies conducted on volunteers who received resveratrol at different doses and for different periods of time. The evidence, reviewed in [153], shows that resveratrol might have some beneficial effects in humans, although its bioavailability is poor. Recently, phase I and II clinical trials were published with a new STAC (SRT2104), showing that it is well tolerated by the elderly, who showed decrease in cholesterol, LDL, and triglycerides levels, opening the possibility that STACs might become an available treatment for age-related diseases in humans [154, 155].

Finally, it is worth mentioning that SIRT6 might also be a pharmacological target for the treatment of age-related diseases, including inflammation, genomic stability, and cancer. The fact that SIRT6 is activated by fatty acids [2] might provide new avenues into the treatment of age-related diseases [156, 157].

6. Conclusions and Perspectives

Sirtuins are NAD-dependent deacylases that catalyze not only deacetylation of histones but also deacylation of other proteins including transcription factors and metabolic enzymes thereby regulating cell cycle, differentiation, metabolism, stress resistance, senescence, and aging. Fine regulation of expression and activity of sirtuins is critical to maintain cellular homeostasis. Although it is clear that sirtuins are modulated by oxidative stress, the molecular mechanisms are not well understood. Active sirtuins protect cells from ROS-induced damage via their product OAADPR/ADPR that inhibits mitochondrial ROS production and increases NADPH levels from pentose phosphate pathway. Mild oxidative stress induces sirtuin expression as a compensatory mechanism, while harsh or prolonged oxidant conditions result in dysfunctional modified sirtuins more prone to degradation by the proteasome. The increase in the NAD/NADH ratio under oxidative stress conditions can result in higher availability of the NAD cofactor, thus an apparent increase in sirtuin activity. Oxidative PTM of sirtuins have been identified, both *in vitro* and *in vivo*, to inhibit deacylase activity, although they can also affect the interaction with modulators, like SIRT1 with its endogenous inhibitor DBC1, resulting in a net increase of SIRT1 activity. Further research is needed to establish the mechanisms of redox regulation of sirtuins. Particularly interesting is to investigate redox modulation of SIRT3 in the mitochondrial matrix where most of cellular oxidants are formed. The fact that sirtuins can be activated, either by modulating NAD bioavailability in tissues or by pharmacological activation by small molecules, gives a therapeutic opportunity for the treatment of metabolic and age-related diseases.

Conflict of Interests

The authors declare that there is no conflict of interests regarding the publication of this paper.

Acknowledgments

Comisión Sectorial de Investigación Científica CSIC, UdelaR; Agencia Nacional de Investigación e Innovación ANII, Uruguay; Programa de Desarrollo de las Ciencias Básicas PEDECIBA; and INNOVA II are acknowledged.

References

[1] S.-I. Imai, C. M. Armstrong, M. Kaeberlein, and L. Guarente, "Transcriptional silencing and longevity protein Sir2 is an NAD-dependent histone deacetylase," *Nature*, vol. 403, no. 6771, pp. 795–800, 2000.

[2] J. L. Feldman, J. Baeza, and J. M. Denu, "Activation of the protein deacetylase SIRT6 by long-chain fatty acids and widespread deacylation by Mammalian Sirtuins," *The Journal of Biological Chemistry*, vol. 288, no. 43, pp. 31350–31356, 2013.

[3] D. Shore, M. Squire, and K. A. Nasmyth, "Characterization of two genes required for the position-effect control of yeast mating-type genes," *The EMBO Journal*, vol. 3, no. 12, pp. 2817–2823, 1984.

[4] M. Gotta, S. Strahl-Bolsinger, H. Renauld et al., "Localization of Sir2p: the nucleolus as a compartment for silent information regulators," *The EMBO Journal*, vol. 16, no. 11, pp. 3243–3255, 1997.

[5] B. P. Hubbard and D. A. Sinclair, "Small molecule SIRT1 activators for the treatment of aging and age-related diseases," *Trends in Pharmacological Sciences*, vol. 35, no. 3, pp. 146–154, 2014.

[6] R. A. Frye, "Phylogenetic classification of prokaryotic and eukaryotic Sir2-like proteins," *Biochemical and Biophysical Research Communications*, vol. 273, no. 2, pp. 793–798, 2000.

[7] T. Finkel, C.-X. Deng, and R. Mostoslavsky, "Recent progress in the biology and physiology of sirtuins," *Nature*, vol. 460, no. 7255, pp. 587–591, 2009.

[8] J. M. Sherman, E. M. Stone, L. L. Freeman-Cook, C. B. Brachmann, J. D. Boeke, and L. Pillus, "The conserved core of a human SIR2 homologue functions in yeast silencing," *Molecular Biology of the Cell*, vol. 10, no. 9, pp. 3045–3059, 1999.

[9] J. Min, J. Landry, R. Sternglanz, and R.-M. Xu, "Crystal structure of a SIR2 homolog-NAD complex," *Cell*, vol. 105, no. 2, pp. 269–279, 2001.

[10] S. P. Chakrabarty and H. Balaram, "Reversible binding of zinc in *Plasmodium falciparum* Sir2: structure and activity of the apoenzyme," *Biochimica et Biophysica Acta*, vol. 1804, no. 9, pp. 1743–1750, 2010.

[11] M. S. Finnin, J. R. Donigian, and N. P. Pavletich, "Structure of the histone deacetylase SIRT2," *Nature Structural Biology*, vol. 8, no. 7, pp. 621–625, 2001.

[12] J.-H. Chang, H.-C. Kim, K.-Y. Hwang et al., "Structural basis for the NAD-dependent deacetylase mechanism of Sir2," *The Journal of Biological Chemistry*, vol. 277, no. 37, pp. 34489–34498, 2002.

[13] J. L. Avalos, I. Celic, S. Muhammad, M. S. Cosgrove, J. D. Boeke, and C. Wolberger, "Structure of a Sir2 enzyme bound to an acetylated p53 peptide," *Molecular Cell*, vol. 10, no. 3, pp. 523–535, 2002.

[14] K. Zhao, R. Harshaw, X. Chai, and R. Marmorstein, "Structural basis for nicotinamide cleavage and ADP-ribose transfer by NAD^+-dependent Sir2 histone/protein deacetylases," *Proceedings of the National Academy of Sciences of the United States of America*, vol. 101, no. 23, pp. 8563–8568, 2004.

[15] R. A. Frye, "Characterization of five human cDNAs with homology to the yeast SIR2 gene: Sir2-like proteins (Sirtuins) metabolize NAD and may have protein ADP-ribosyltransferase activity," *Biochemical and Biophysical Research Communications*, vol. 260, no. 1, pp. 273–279, 1999.

[16] G. Liszt, E. Ford, M. Kurtev, and L. Guarente, "Mouse Sir2 homolog SIRT6 is a nuclear ADP-ribosyltransferase," *The Journal of Biological Chemistry*, vol. 280, no. 22, pp. 21313–21320, 2005.

[17] M. C. Haigis, R. Mostoslavsky, K. M. Haigis et al., "SIRT4 inhibits glutamate dehydrogenase and opposes the effects of calorie restriction in pancreatic β cells," *Cell*, vol. 126, no. 5, pp. 941–954, 2006.

[18] J. Du, Y. Zhou, X. Su et al., "Sirt5 is a NAD-dependent protein lysine demalonylase and desuccinylase," *Science*, vol. 334, no. 6057, pp. 806–809, 2011.

[19] H. Jiang, S. Khan, Y. Wang et al., "SIRT6 regulates TNF-α secretion through hydrolysis of long-chain fatty acyl lysine," *Nature*, vol. 496, no. 7443, pp. 110–113, 2013.

[20] C. Choudhary, C. Kumar, F. Gnad et al., "Lysine acetylation targets protein complexes and co-regulates major cellular functions," *Science*, vol. 325, no. 5942, pp. 834–840, 2009.

[21] K. T. Smith and J. L. Workman, "Introducing the acetylome," *Nature Biotechnology*, vol. 27, no. 10, pp. 917–919, 2009.

[22] B. T. Weinert, S. A. Wagner, H. Horn et al., "Proteome-wide mapping of the *Drosophila* acetylome demonstrates a high degree of conservation of lysine acetylation," *Science Signaling*, vol. 4, no. 183, article ra48, 2011.

[23] S. Zhao, W. Xu, W. Jiang et al., "Regulation of cellular metabolism by protein lysine acetylation," *Science*, vol. 327, no. 5968, pp. 1000–1004, 2010.

[24] D. Rauh, F. Fischer, M. Gertz et al., "An acetylome peptide microarray reveals specificities and deacetylation substrates for all human sirtuin isoforms," *Nature Communications*, vol. 4, article 2327, 2013.

[25] M. C. Haigis and D. A. Sinclair, "Mammalian sirtuins: biological insights and disease relevance," *Annual Review of Pathology: Mechanisms of Disease*, vol. 5, pp. 253–295, 2010.

[26] C. Sebastián, F. K. Satterstrom, M. C. Haigis, and R. Mostoslavsky, "From sirtuin biology to human diseases: an update," *Journal of Biological Chemistry*, vol. 287, no. 51, pp. 42444–42452, 2012.

[27] R. H. Houtkooper, E. Pirinen, and J. Auwerx, "Sirtuins as regulators of metabolism and healthspan," *Nature Reviews Molecular Cell Biology*, vol. 13, no. 4, pp. 225–238, 2012.

[28] E. Verdin, "The Many Faces of Sirtuins: coupling of NAD metabolism, sirtuins and lifespan," *Nature Medicine*, vol. 20, no. 1, pp. 25–27, 2014.

[29] D. P. Jones, "Redefining oxidative stress," *Antioxidants and Redox Signaling*, vol. 8, no. 9-10, pp. 1865–1879, 2006.

[30] H. Sies, "Oxidative stress: oxidants and antioxidants," *Experimental Physiology*, vol. 82, no. 2, pp. 291–295, 1997.

[31] S. Nemoto, M. M. Fergusson, and T. Finkel, "Nutrient availability regulates SIRT1 through a forkhead-dependent pathway," *Science*, vol. 306, no. 5704, pp. 2105–2108, 2004.

[32] T. Prozorovski, U. Schulze-Topphoff, R. Glumm et al., "Sirt1 contributes critically to the redox-dependent fate of neural progenitors," *Nature Cell Biology*, vol. 10, no. 4, pp. 385–394, 2008.

[33] C.-H. Peng, Y.-L. Chang, C.-L. Kao et al., "SirT1—a sensor for monitoring self-renewal and aging process in retinal stem cells," *Sensors*, vol. 10, no. 6, pp. 6172–6194, 2010.

[34] A. A. Sablina, A. V. Budanov, G. V. Ilyinskaya, L. S. Agapova, J. E. Kravchenko, and P. M. Chumakov, "The antioxidant function of the p53 tumor suppressor," *Nature Medicine*, vol. 11, no. 12, pp. 1306–1313, 2005.

[35] A. Brunet, L. B. Sweeney, J. F. Sturgill et al., "Stress-dependent regulation of FOXO transcription factors by the SIRT1 deacetylase," *Science*, vol. 303, no. 5666, pp. 2011–2015, 2004.

[36] K. Hasegawa, S. Wakino, K. Yoshioka et al., "Sirt1 protects against oxidative stress-induced renal tubular cell apoptosis by the bidirectional regulation of catalase expression," *Biochemical and Biophysical Research Communications*, vol. 372, no. 1, pp. 51–56, 2008.

[37] F. Wang, M. Nguyen, F. X.-F. Qin, and Q. Tong, "SIRT2 deacetylates FOXO3a in response to oxidative stress and caloric restriction," *Aging Cell*, vol. 6, no. 4, pp. 505–514, 2007.

[38] M. C. Motta, N. Divecha, M. Lemieux et al., "Mammalian SIRT1 represses forkhead transcription factors," *Cell*, vol. 116, no. 4, pp. 551–563, 2004.

[39] P. S. Pardo, J. S. Mohamed, M. A. Lopez, and A. M. Boriek, "Induction of Sirt1 by mechanical stretch of skeletal muscle through the early response factor EGR1 triggers an antioxidative response," *The Journal of Biological Chemistry*, vol. 286, no. 4, pp. 2559–2566, 2011.

[40] A. H. H. Tseng, S.-S. Shieh, and D. L. Wang, "SIRT3 deacetylates FOXO3 to protect mitochondria against oxidative damage," *Free Radical Biology and Medicine*, vol. 63, pp. 222–234, 2013.

[41] Z. Lu, X. Xu, X. Hu et al., "PGC-1alpha regulates expression of myocardial mitochondrial antioxidants and myocardial oxidative stress after chronic systolic overload," *Antioxidants and Redox Signaling*, vol. 13, no. 7, pp. 1011–1022, 2010.

[42] J. T. Rodgers, C. Lerin, W. Haas, S. P. Gygi, B. M. Spiegelman, and P. Puigserver, "Nutrient control of glucose homeostasis through a complex of PGC-1α and SIRT1," *Nature*, vol. 434, no. 7029, pp. 113–118, 2005.

[43] J. St-Pierre, S. Drori, M. Uldry et al., "Suppression of reactive oxygen species and neurodegeneration by the PGC-1 transcriptional coactivators," *Cell*, vol. 127, no. 2, pp. 397–408, 2006.

[44] S. Rajendrasozhan, S.-R. Yang, V. L. Kinnula, and I. Rahman, "SIRT1, an antiinflammatory and antiaging protein, is decreased in lungs of patients with chronic obstructive pulmonary disease," *American Journal of Respiratory and Critical Care Medicine*, vol. 177, no. 8, pp. 861–870, 2008.

[45] H. Vaziri, S. K. Dessain, E. N. Eaton et al., "$hSIR2^{SIRT1}$ functions as an NAD-dependent p53 deacetylase," *Cell*, vol. 107, no. 2, pp. 149–159, 2001.

[46] J.-H. Lee, M.-Y. Song, E.-K. Song et al., "Overexpression of SIRT1 protects pancreatic β-cells against cytokine toxicity by suppressing the nuclear factor-κB signaling pathway," *Diabetes*, vol. 58, no. 2, pp. 344–351, 2009.

[47] Y. Chen, J. Zhang, Y. Lin et al., "Tumour suppressor SIRT3 deacetylates and activates manganese superoxide dismutase to scavenge ROS," *EMBO Reports*, vol. 12, no. 6, pp. 534–541, 2011.

[48] X. Qiu, K. Brown, M. D. Hirschey, E. Verdin, and D. Chen, "Calorie restriction reduces oxidative stress by SIRT3-mediated SOD2 activation," *Cell Metabolism*, vol. 12, no. 6, pp. 662–667, 2010.

[49] R. R. Alcendor, S. Gao, P. Zhai et al., "Sirt1 regulates aging and resistance to oxidative stress in the heart," *Circulation Research*, vol. 100, no. 10, pp. 1512–1521, 2007.

[50] D. Guan, J. H. Lim, L. Peng et al., "Deacetylation of the tumor suppressor protein PML regulates hydrogen peroxide-induced cell death," *Cell Death and Disease*, vol. 5, no. 7, Article ID e1340, 2014.

[51] Y. Yang, W. Fu, J. Chen et al., "SIRT1 sumoylation regulates its deacetylase activity and cellular response to genotoxic stress," *Nature Cell Biology*, vol. 9, no. 11, pp. 1253–1262, 2007.

[52] S. V. de Kreutzenberg, G. Ceolotto, I. Papparella et al., "Down-regulation of the longevity-associated protein sirtuin 1 in insulin resistance and metabolic syndrome: potential biochemical mechanisms," *Diabetes*, vol. 59, no. 4, pp. 1006–1015, 2010.

[53] S. Caito, S. Rajendrasozhan, S. Cook et al., "SIRT1 is a redox-sensitive deacetylase that is post-translationally modified by oxidants and carbonyl stress," *The FASEB Journal*, vol. 24, no. 9, pp. 3145–3159, 2010.

[54] S.-B. Jung, C.-S. Kim, Y.-R. Kim et al., "Redox factor-1 activates endothelial SIRTUIN1 through reduction of conserved cysteine sulfhydryls in its deacetylase domain," *PLoS ONE*, vol. 8, no. 6, Article ID e65415, 2013.

[55] L. Tong, S. Lee, and J. M. Denu, "Hydrolase regulates NAD^+ metabolites and modulates cellular redox," *Journal of Biological Chemistry*, vol. 284, no. 17, pp. 11256–11266, 2009.

[56] I. Autiero, S. Costantini, and G. Colonna, "Human sirt-1: molecular modeling and structure-function relationships of an unordered protein," *PLoS ONE*, vol. 4, no. 10, Article ID e7350, 2009.

[57] T. Sasaki, B. Maier, K. D. Koclega et al., "Phosphorylation regulates SIRT1 function," *PLoS ONE*, vol. 3, no. 12, Article ID e4020, 2008.

[58] A. T. Alexandrou and J. J. Li, "Cell cycle regulators guide mitochondrial activity in radiation-induced adaptive response," *Antioxidants & Redox Signaling*, vol. 20, no. 9, pp. 1463–1480, 2014.

[59] H. Kang, J.-W. Jung, M. K. Kim, and J. H. Chung, "CK2 is the regulator of SIRT1 substrate-binding affinity, deacetylase activity and cellular response to DNA-damage," *PLoS ONE*, vol. 4, no. 8, Article ID e6611, 2009.

[60] K. M. Kim, J. D. Song, H. T. Chung, and Y. C. Park, "Protein kinase CK2 mediates peroxynitrite-induced heme oxygenase-1 expression in articular chondrocytes," *International Journal of Molecular Medicine*, vol. 29, no. 6, pp. 1039–1044, 2012.

[61] V. Nin, C. Escande, C. C. Chini et al., "Role of deleted in breast cancer 1 (DBC1) protein in SIRT1 deacetylase activation induced by protein kinase A and AMP-activated protein kinase," *Journal of Biological Chemistry*, vol. 287, no. 28, pp. 23489–23501, 2012.

[62] A. W. Lau, P. Liu, H. Inuzuka, and D. Gao, "SIRT1 phosphorylation by AMP-activated protein kinase regulates p53 acetylation," *American Journal of Cancer Research*, vol. 4, no. 3, pp. 245–255, 2014.

[63] S.-B. Wu, Y.-T. Wu, T.-P. Wu, and Y.-H. Wei, "Role of AMPK-mediated adaptive responses in human cells with mitochondrial dysfunction to oxidative stress," *Biochimica et Biophysica Acta (BBA)—General Subjects*, vol. 1840, no. 4, pp. 1331–1344, 2014.

[64] X. Guo, J. G. Williams, T. T. Schug, and X. Li, "DYRK1A and DYRK3 promote cell survival through phosphorylation and activation of SIRT1," *The Journal of Biological Chemistry*, vol. 285, no. 17, pp. 13223–13232, 2010.

[65] H. Kang, J.-Y. Suh, Y.-S. Jung, J.-W. Jung, M. K. Kim, and J. H. Chung, "Peptide switch is essential for Sirt1 deacetylase activity," *Molecular Cell*, vol. 44, no. 2, pp. 203–213, 2011.

[66] N. Nasrin, V. K. Kaushik, E. Fortier et al., "JNK1 phosphorylates SIRT1 and promotes its enzymatic activity," *PLoS ONE*, vol. 4, no. 12, Article ID e8414, 2009.

[67] Z. Gerhart-Hines, J. E. Dominy, S. M. Blättler et al., "The cAMP/PKA pathway rapidly activates SIRT1 to promote fatty acid oxidation independently of changes in NAD^+," *Molecular Cell*, vol. 44, no. 6, pp. 851–863, 2011.

[68] F. Nahhas, S. C. Dryden, J. Abrams, and M. A. Tainsky, "Mutations in SIRT2 deacetylase which regulate enzymatic activity but not its interaction with HDAC6 and tubulin," *Molecular and Cellular Biochemistry*, vol. 303, no. 1-2, pp. 221–230, 2007.

[69] B. J. North and E. Verdin, "Mitotic regulation of SIRT2 by cyclin-dependent kinase 1-dependent phosphorylation," *The Journal of Biological Chemistry*, vol. 282, no. 27, pp. 19546–19555, 2007.

[70] Y. Bian, C. Song, K. Cheng et al., "An enzyme assisted RP-RPLC approach for in-depth analysis of human liver phosphoproteome," *Journal of Proteomics*, vol. 96, pp. 253–262, 2014.

[71] N. Dephoure, C. Zhou, J. Villén et al., "A quantitative atlas of mitotic phosphorylation," *Proceedings of the National Academy of Sciences of the United States of America*, vol. 105, no. 31, pp. 10762–10767, 2008.

[72] U. Thirumurthi, J. Shen, W. Xia et al., "MDM2-mediated degradation of SIRT6 phosphorylated by AKT1 promotes tumorigenesis and trastuzumab resistance in breast cancer," *Science Signaling*, vol. 7, no. 336, p. ra71, 2014.

[73] R. S. Zee, C. B. Yoo, D. R. Pimentel et al., "Redox regulation of sirtuin-1 by S-glutathiolation," *Antioxidants and Redox Signaling*, vol. 13, no. 7, pp. 1023–1032, 2010.

[74] M. T. Borra, B. C. Smith, and J. M. Denu, "Mechanism of human SIRT1 activation by resveratrol," *The Journal of Biological Chemistry*, vol. 280, no. 17, pp. 17187–17195, 2005.

[75] M. D. Kornberg, N. Sen, M. R. Hara et al., "GAPDH mediates nitrosylation of nuclear proteins," *Nature Cell Biology*, vol. 12, no. 11, pp. 1094–1100, 2010.

[76] D. Shao, J. L. Fry, J. Han et al., "A redox-resistant Sirtuin-1 mutant protects against hepatic metabolic and oxidant stress," *The Journal of Biological Chemistry*, vol. 289, no. 11, pp. 7293–7306, 2014.

[77] K. S. Fritz, J. J. Galligan, R. L. Smathers et al., "4-hydroxynonenal inhibits SIRT3 via thiol-specific modification," *Chemical Research in Toxicology*, vol. 24, no. 5, pp. 651–662, 2011.

[78] J. Yang, V. Gupta, K. S. Carroll, and D. C. Liebler, "Site-specific mapping and quantification of protein S-sulphenylation in cells," *Nature Communications*, vol. 5, article 4776, 2014.

[79] S. Hu, H. Liu, Y. Ha et al., "Posttranslational modification of Sirt6 activity by peroxynitrite," *Free Radical Biology and Medicine*, vol. 79, pp. 176–185, 2015.

[80] J.-E. Kim, J. Chen, and Z. Lou, "DBC1 is a negative regulator of SIRT1," *Nature*, vol. 451, no. 7178, pp. 583–586, 2008.

[81] E.-J. Kim, J.-H. Kho, M.-R. Kang, and S.-J. Um, "Active regulator of SIRT1 cooperates with SIRT1 and facilitates suppression of p53 activity," *Molecular Cell*, vol. 28, no. 2, pp. 277–290, 2007.

[82] J. Yuan, K. Luo, T. Liu, and Z. Lou, "Regulation of SIRT1 activity by genotoxic stress," *Genes & Development*, vol. 26, no. 8, pp. 791–796, 2012.

[83] C. Escande, C. C. S. Chini, V. Nin et al., "Deleted in breast cancer-1 regulates SIRT1 activity and contributes to high-fat diet-induced liver steatosis in mice," *The Journal of Clinical Investigation*, vol. 120, no. 2, pp. 545–558, 2010.

[84] C. Escande, V. Nin, T. Pirtskhalava et al., "Deleted in breast cancer 1 limits adipose tissue fat accumulation and plays a key role in the development of metabolic syndrome phenotype," *Diabetes*, vol. 64, no. 1, pp. 12–22, 2015.

[85] D. Volonte, H. Zou, J. N. Bartholomew, Z. Liu, P. A. Morel, and F. Galbiati, "Oxidative stress-induced inhibition of Sirt1 by caveolin-1 promotes p53-dependent premature senescence and stimulates the secretion of interleukin 6 (IL-6)," *The Journal of Biological Chemistry*, vol. 290, no. 7, pp. 4202–4214, 2015.

[86] E. N. Chini, "CD38 as a regulator of cellular NAD: a novel potential pharmacological target for metabolic conditions," *Current Pharmaceutical Design*, vol. 15, no. 1, pp. 57–63, 2009.

[87] J. Yoshino, K. F. Mills, M. J. Yoon, and S.-I. Imai, "Nicotinamide mononucleotide, a key NAD^+ intermediate, treats the pathophysiology of diet- and age-induced diabetes in mice," *Cell Metabolism*, vol. 14, no. 4, pp. 528–536, 2011.

[88] C. Cantó, R. H. Houtkooper, E. Pirinen et al., "The NAD^+ precursor nicotinamide riboside enhances oxidative metabolism and protects against high-fat diet-induced obesity," *Cell Metabolism*, vol. 15, no. 6, pp. 838–847, 2012.

[89] C. Escande, V. Nin, N. L. Price et al., "Flavonoid apigenin is an inhibitor of the NAD^+ase CD38: implications for cellular NAD^+ metabolism, protein acetylation, and treatment of metabolic syndrome," *Diabetes*, vol. 62, no. 4, pp. 1084–1093, 2013.

[90] M. T. P. Barbosa, S. M. Soares, C. M. Novak et al., "The enzyme CD38 (a NAD glycohydrolase, EC 3.2.2.5) is necessary for the development of diet-induced obesity," *The FASEB Journal*, vol. 21, no. 13, pp. 3629–3639, 2007.

[91] P. Bai, C. Cantó, H. Oudart et al., "PARP-1 inhibition increases mitochondrial metabolism through SIRT1 activation," *Cell Metabolism*, vol. 13, no. 4, pp. 461–468, 2011.

[92] P. Aksoy, T. A. White, M. Thompson, and E. N. Chini, "Regulation of intracellular levels of NAD: a novel role for CD38," *Biochemical and Biophysical Research Communications*, vol. 345, no. 4, pp. 1386–1392, 2006.

[93] P. Aksoy, C. Escande, T. A. White et al., "Regulation of SIRT 1 mediated NAD dependent deacetylation: a novel role for the multifunctional enzyme CD38," *Biochemical and Biophysical Research Communications*, vol. 349, no. 1, pp. 353–359, 2006.

[94] S. B. Rajamohan, V. B. Pillai, M. Gupta et al., "SIRT1 promotes cell survival under stress by deacetylation-dependent deactivation of poly(ADP-ribose) polymerase 1," *Molecular and Cellular Biology*, vol. 29, no. 15, pp. 4116–4129, 2009.

[95] N. Braidy, G. J. Guillemin, H. Mansour, T. Chan-Ling, A. Poljak, and R. Grant, "Age related changes in NAD+ metabolism oxidative stress and Sirt1 activity in wistar rats," *PLoS ONE*, vol. 6, no. 4, Article ID e19194, 2011.

[96] L. Du, X. Zhang, Y. Y. Han et al., "Intra-mitochondrial poly(ADP-ribosylation) contributes to NAD^+ depletion and cell death induced by oxidative stress," *The Journal of Biological Chemistry*, vol. 278, no. 20, pp. 18426–18433, 2003.

[97] K. T. Howitz, K. J. Bitterman, H. Y. Cohen et al., "Small molecule activators of sirtuins extend Saccharomyces cerevisiae lifespan," *Nature*, vol. 425, no. 6954, pp. 191–196, 2003.

[98] M. Kaeberlein, T. McDonagh, B. Heltweg et al., "Substrate-specific activation of sirtuins by resveratrol," *Journal of Biological Chemistry*, vol. 280, no. 17, pp. 17038–17045, 2005.

[99] J. C. Milne, P. D. Lambert, S. Schenk et al., "Small molecule activators of SIRT1 as therapeutics for the treatment of type 2 diabetes," *Nature*, vol. 450, no. 7170, pp. 712–716, 2007.

[100] C. Cantó, Z. Gerhart-Hines, J. N. Feige et al., "AMPK regulates energy expenditure by modulating NAD^+ metabolism and SIRT1 activity," *Nature*, vol. 458, no. 7241, pp. 1056–1060, 2009.

[101] S.-J. Park, F. Ahmad, A. Philp et al., "Resveratrol ameliorates aging-related metabolic phenotypes by inhibiting cAMP phosphodiesterases," *Cell*, vol. 148, no. 3, pp. 421–433, 2012.

[102] S. J. Mitchell, A. Martin-Montalvo, E. M. Mercken et al., "The SIRT1 activator SRT1720 extends lifespan and improves health of mice fed a standard diet," *Cell Reports*, vol. 6, no. 5, pp. 836–843, 2014.

[103] R. K. Minor, J. A. Baur, A. P. Gomes et al., "SRT1720 improves survival and healthspan of obese mice," *Scientific Reports*, vol. 1, article 70, 2011.

[104] M. Pacholec, J. E. Bleasdale, B. Chrunyk et al., "SRT1720, SRT2183, SRT1460, and resveratrol are not direct activators of SIRT1," *The Journal of Biological Chemistry*, vol. 285, no. 11, pp. 8340–8351, 2010.

[105] B. P. Hubbard, A. P. Gomes, H. Dai et al., "Evidence for a common mechanism of SIRT1 regulation by allosteric activators," *Science*, vol. 339, no. 6124, pp. 1216–1219, 2013.

[106] H. Dai, L. Kustigian, D. Carney et al., "SIRT1 activation by small molecules: kinetic and biophysical evidence for direct interaction of enzyme and activator," *The Journal of Biological Chemistry*, vol. 285, no. 43, pp. 32695–32703, 2010.

[107] J. J. Smith, R. D. Kenney, D. J. Gagne et al., "Small molecule activators of SIRT1 replicate signaling pathways triggered by calorie restriction in vivo," *BMC Systems Biology*, vol. 3, no. 1, article 31, 2009.

[108] G. Boily, X. H. He, B. Pearce, K. Jardine, and M. W. McBurney, "SirT1-null mice develop tumors at normal rates but are poorly protected by resveratrol," *Oncogene*, vol. 28, no. 32, pp. 2882–2893, 2009.

[109] K. J. Pearson, J. A. Baur, K. N. Lewis et al., "Resveratrol delays age-related deterioration and mimics transcriptional aspects of dietary restriction without extending life span," *Cell Metabolism*, vol. 8, no. 2, pp. 157–168, 2008.

[110] J. M. Ajmo, X. Liang, C. Q. Rogers, B. Pennock, and M. You, "Resveratrol alleviates alcoholic fatty liver in mice," *The American Journal of Physiology—Gastrointestinal and Liver Physiology*, vol. 295, no. 4, pp. G833–G842, 2008.

[111] J.-T. Hwang, D. W. Kwak, S. K. Lin, H. M. Kim, Y. M. Kim, and O. J. Park, "Resveratrol induces apoptosis in chemoresistant cancer cells via modulation of AMPK signaling pathway," *Annals of the New York Academy of Sciences*, vol. 1095, pp. 441–448, 2007.

[112] M. Lagouge, C. Argmann, Z. Gerhart-Hines et al., "Resveratrol improves mitochondrial function and protects against metabolic disease by activating SIRT1 and PGC-1α," *Cell*, vol. 127, no. 6, pp. 1109–1122, 2006.

[113] J. A. Baur, K. J. Pearson, N. L. Price et al., "Resveratrol improves health and survival of mice on a high-calorie diet," *Nature*, vol. 444, no. 7117, pp. 337–342, 2006.

[114] J. G. Wood, B. Rogina, S. Lavu et al., "Sirtuin activators mimic caloric restriction and delay ageing in metazoans," *Nature*, vol. 430, no. 7000, pp. 686–689, 2004.

[115] Y. Yamazaki, I. Usui, Y. Kanatani et al., "Treatment with SRT1720, a SIRT1 activator, ameliorates fatty liver with reduced expression of lipogenic enzymes in MSG mice," *American Journal of Physiology—Endocrinology and Metabolism*, vol. 297, no. 5, pp. E1179–E1186, 2009.

[116] J. M. Feige, M. Lagouge, C. Canto et al., "Specific SIRT1 activation mimics low energy levels and protects against diet-induced metabolic disorders by enhancing fat oxidation," *Cell Metabolism*, vol. 8, no. 5, pp. 347–358, 2008.

[117] M. Tanno, A. Kuno, T. Yano et al., "Induction of manganese superoxide dismutase by nuclear translocation and activation of SIRT1 promotes cell survival in chronic heart failure," *Journal of Biological Chemistry*, vol. 285, no. 11, pp. 8375–8382, 2010.

[118] S. M. Shin, I. J. Cho, and S. G. Kim, "Resveratrol protects mitochondria against oxidative stress through AMP-activated protein kinase-mediated glycogen synthase kinase-3β inhibition downstream of poly(ADP-ribose)polymerase-LKB1 pathway," *Molecular Pharmacology*, vol. 76, no. 4, pp. 884–895, 2009.

[119] E. D. Brookins Danz, J. Skramsted, N. Henry, J. A. Bennett, and R. S. Keller, "Resveratrol prevents doxorubicin cardiotoxicity through mitochondrial stabilization and the Sirt1 pathway," *Free Radical Biology and Medicine*, vol. 46, no. 12, pp. 1589–1597, 2009.

[120] J.-T. Hwang, D. Y. Kwon, O. J. Park, and M. S. Kim, "Resveratrol protects ROS-induced cell death by activating AMPK in H9c2 cardiac muscle cells," *Genes & Nutrition*, vol. 2, no. 4, pp. 323–326, 2008.

[121] A. Csiszar, N. Labinskyy, A. Podlutsky et al., "Vasoprotective effects of resveratrol and SIRT1: attenuation of cigarette smoke-induced oxidative stress and proinflammatory phenotypic alterations," *American Journal of Physiology—Heart and Circulatory Physiology*, vol. 294, no. 6, pp. H2721–H2735, 2008.

[122] H. Yao, I. K. Sundar, T. Ahmad et al., "SIRT1 protects against cigarette smoke-induced lung oxidative stress via a FOXO3-dependent mechanism," *American Journal of Physiology—Lung Cellular and Molecular Physiology*, vol. 306, no. 9, pp. L816–L828, 2014.

[123] A. Vaquero, M. Scher, D. Lee, H. Erdjument-Bromage, P. Tempst, and D. Reinberg, "Human SirT1 interacts with histone H1 and promotes formation of facultative heterochromatin," *Molecular Cell*, vol. 16, no. 1, pp. 93–105, 2004.

[124] S. Kong, S.-J. Kim, B. Sandal et al., "The type III histone deacetylase Sirt1 protein suppresses p300-mediated histone H3 lysine 56 acetylation at Bclaf1 promoter to inhibit T cell activation," *The Journal of Biological Chemistry*, vol. 286, no. 19, pp. 16967–16975, 2011.

[125] B. Ponugoti, D.-H. Kim, Z. Xiao et al., "SIRT1 deacetylates and inhibits SREBP-1C activity in regulation of hepatic lipid metabolism," *The Journal of Biological Chemistry*, vol. 285, no. 44, pp. 33959–33970, 2010.

[126] F. Picard, M. Kurtev, N. Chung et al., "Sirt1 promotes fat mobilization in white adipocytes by repressing PPAR-γ," *Nature*, vol. 429, no. 6993, pp. 771–776, 2004.

[127] F. Yeung, J. E. Hoberg, C. S. Ramsey et al., "Modulation of NF-κB-dependent transcription and cell survival by the SIRT1 deacetylase," *The EMBO Journal*, vol. 23, no. 12, pp. 2369–2380, 2004.

[128] I. Mattagajasingh, C.-S. Kim, A. Naqvi et al., "SIRT1 promotes endothelium-dependent vascular relaxation by activating endothelial nitric oxide synthase," *Proceedings of the National Academy of Sciences of the United States of America*, vol. 104, no. 37, pp. 14855–14860, 2007.

[129] J. Nakae, Y. Cao, H. Daitoku et al., "The LXXLL motif of murine forkhead transcription factor FoxO1 mediates Sirt1-dependent transcriptional activity," *The Journal of Clinical Investigation*, vol. 116, no. 9, pp. 2473–2483, 2006.

[130] J.-H. Lim, Y.-M. Lee, Y.-S. Chun, J. Chen, J.-E. Kim, and J.-W. Park, "Sirtuin 1 modulates cellular responses to hypoxia by deacetylating hypoxia-inducible factor 1alpha," *Molecular Cell*, vol. 38, no. 6, pp. 864–878, 2010.

[131] M. Tanno, J. Sakamoto, T. Miura, K. Shimamoto, and Y. Horio, "Nucleocytoplasmic shuttling of the NAD^+-dependent histone deacetylase SIRT1," *The Journal of Biological Chemistry*, vol. 282, no. 9, pp. 6823–6832, 2007.

[132] W. C. Hallows, S. Lee, and J. M. Denu, "Sirtuins deacetylate and activate mammalian acetyl-CoA synthetases," *Proceedings of the National Academy of Sciences of the United States of America*, vol. 103, no. 27, pp. 10230–10235, 2006.

[133] N. R. Sundaresan, V. B. Pillai, D. Wolfgeher et al., "The deacetylase SIRT1 promotes membrane localization and activation of Akt and PDK1 during tumorigenesis and cardiac hypertrophy," *Science Signaling*, vol. 4, no. 182, article ra46, 2011.

[134] Y. Liu, R. Dentin, D. Chen et al., "A fasting inducible switch modulates gluconeogenesis via activator/coactivator exchange," *Nature*, vol. 456, no. 7219, pp. 269–273, 2008.

[135] T. Yamamori, J. DeRicco, A. Naqvi et al., "SIRT1 deacetylates APE1 and regulates cellular base excision repair," *Nucleic Acids Research*, vol. 38, no. 3, Article ID gkp1039, pp. 832–845, 2009.

[136] W. Jiang, S. Wang, M. Xiao et al., "Acetylation regulates gluconeogenesis by promoting PEPCK1 degradation via recruiting the UBR5 ubiquitin ligase," *Molecular Cell*, vol. 43, no. 1, pp. 33–44, 2011.

[137] Y.-B. Teng, H. Jing, P. Aramsangtienchai et al., "Efficient demyristoylase activity of SIRT2 revealed by kinetic and structural studies," *Scientific Reports*, vol. 5, article 8529, 2015.

[138] S. C. Dryden, F. A. Nahhas, J. E. Nowak, A.-S. Goustin, and M. A. Tainsky, "Role for human SIRT2 NAD-dependent deacetylase activity in control of mitotic exit in the cell cycle," *Molecular and Cellular Biology*, vol. 23, no. 9, pp. 3173–3185, 2003.

[139] A. Vaquero, M. B. Scher, H. L. Dong et al., "SirT2 is a histone deacetylase with preference for histone H4 Lys 16 during mitosis," *Genes and Development*, vol. 20, no. 10, pp. 1256–1261, 2006.

[140] T. Chen, J. Liu, N. Li et al., "Mouse SIRT3 attenuates hypertrophy-related lipid accumulation in the heart through the deacetylation of LCAD," *PLoS ONE*, vol. 10, no. 3, Article ID e0118909, 2015.

[141] M. D. Hirschey, T. Shimazu, J. A. Capra, K. S. Pollard, and E. Verdin, "SIRT1 and SIRT3 deacetylate homologous substrates: AceCS1,2 and HMGCS1,2," *Aging*, vol. 3, no. 6, pp. 635–642, 2011.

[142] W. Yu, K. E. Dittenhafer-Reed, and J. M. Denu, "SIRT3 protein deacetylates isocitrate dehydrogenase 2 (IDH2) and regulates mitochondrial redox status," *The Journal of Biological Chemistry*, vol. 287, no. 17, pp. 14078–14086, 2012.

[143] O. Ozden, S.-H. Park, B. A. Wagner et al., "SIRT3 deacetylates and increases pyruvate dehydrogenase activity in cancer cells," *Free Radical Biology and Medicine*, vol. 76, pp. 163–172, 2014.

[144] R. A. Mathias, T. M. Greco, A. Oberstein et al., "Sirtuin 4 is a lipoamidase regulating pyruvate dehydrogenase complex activity," *Cell*, vol. 159, no. 7, pp. 1615–1625, 2014.

[145] J. Park, Y. Chen, D. X. Tishkoff et al., "SIRT5-mediated lysine desuccinylation impacts diverse metabolic pathways," *Molecular Cell*, vol. 50, no. 6, pp. 919–930, 2013.

[146] M. Tan, C. Peng, K. A. Anderson et al., "Lysine glutarylation is a protein posttranslational modification regulated by SIRT5," *Cell Metabolism*, vol. 19, no. 4, pp. 605–617, 2014.

[147] N. R. Sundaresan, P. Vasudevan, L. Zhong et al., "The sirtuin SIRT6 blocks IGF-Akt signaling and development of cardiac hypertrophy by targeting c-Jun," *Nature Medicine*, vol. 18, no. 11, pp. 1643–1650, 2012.

[148] E. Michishita, R. A. McCord, E. Berber et al., "SIRT6 is a histone H3 lysine 9 deacetylase that modulates telomeric chromatin," *Nature*, vol. 452, no. 7186, pp. 492–496, 2008.

[149] E. Michishita, R. A. McCord, L. D. Boxer et al., "Cell cycle-dependent deacetylation of telomeric histone H3 lysine K56 by human SIRT6," *Cell Cycle*, vol. 8, no. 16, pp. 2664–2666, 2009.

[150] Z. Mao, C. Hine, X. Tian et al., "SIRT6 promotes DNA repair under stress by activating PARP1," *Science*, vol. 332, no. 6036, pp. 1443–1446, 2011.

[151] S. Chen, J. Seiler, M. Santiago-Reichelt, K. Felbel, I. Grummt, and R. Voit, "Repression of RNA polymerase I upon stress is caused by inhibition of RNA-dependent deacetylation of PAF53 by SIRT7," *Molecular Cell*, vol. 52, no. 3, pp. 303–313, 2013.

[152] M. F. Barber, E. Michishita-Kioi, Y. Xi et al., "SIRT7 links H3K18 deacetylation to maintenance of oncogenic transformation," *Nature*, vol. 486, no. 7405, pp. 114–118, 2012.

[153] J. Tomé-Carneiro, M. Larrosa, A. González-Sarrías, F. A. Tomás-Barberán, M. T. García-Conesa, and J. C. Espín, "Resveratrol and clinical trials: the crossroad from in vitro studies to human evidence," *Current Pharmaceutical Design*, vol. 19, no. 34, pp. 6064–6093, 2013.

[154] A. Baksi, O. Kraydashenko, A. Zalevkaya et al., "A phase II, randomized, placebo-controlled, double-blind, multi-dose study of SRT2104, a SIRT1 activator, in subjects with type 2 diabetes," *British Journal of Clinical Pharmacology*, vol. 78, no. 1, pp. 69–77, 2014.

[155] V. Libri, A. P. Brown, G. Gambarota et al., "A pilot randomized, placebo controlled, double blind phase I trial of the novel SIRT1 activator SRT2104 in elderly volunteers," *PLoS ONE*, vol. 7, no. 12, Article ID e51395, 2012.

[156] H. Lee, K. R. Kim, S. J. Noh et al., "Expression of DBC1 and SIRT1 is associated with poor prognosis for breast carcinoma," *Human Pathology*, vol. 42, no. 2, pp. 204–213, 2011.

[157] X.-M. Yu, Y. Liu, T. Jin et al., "The expression of SIRT1 and DBC1 in laryngeal and hypopharyngeal carcinomas," *PLoS ONE*, vol. 8, no. 6, Article ID e66975, 2013.

Hindawi Publishing Corporation
Oxidative Medicine and Cellular Longevity
Volume 2016, Article ID 3480637, 12 pages
http://dx.doi.org/10.1155/2016/3480637

Research Article

Maladaptive Modulations of NLRP3 Inflammasome and Cardioprotective Pathways Are Involved in Diet-Induced Exacerbation of Myocardial Ischemia/Reperfusion Injury in Mice

Raffaella Mastrocola,[1] Massimo Collino,[2] Claudia Penna,[1] Debora Nigro,[1] Fausto Chiazza,[2] Veronica Fracasso,[1] Francesca Tullio,[1] Giuseppe Alloatti,[3,4] Pasquale Pagliaro,[1] and Manuela Aragno[1]

[1] *Department of Clinical and Biological Sciences, University of Turin, Regione Gonzole 10, Orbassano, 10043 Torino, Italy*
[2] *Department of Drug Science and Technology, University of Turin, Corso Raffaello 33, 10125 Torino, Italy*
[3] *Department of Life Sciences and Systems Biology, University of Torino, via Accademia Albertina 13, 10123 Torino, Italy*
[4] *National Institute for Cardiovascular Research, via Irnerio 48, 40126 Bologna, Italy*

Correspondence should be addressed to Massimo Collino; massimo.collino@unito.it

Received 23 July 2015; Accepted 9 September 2015

Academic Editor: Andrés Trostchansky

Excessive fatty acids and sugars intake is known to affect the development of cardiovascular diseases, including myocardial infarction. However, the underlying mechanisms are ill defined. Here we investigated the balance between prosurvival and detrimental pathways within the heart of C57Bl/6 male mice fed a standard diet (SD) or a high-fat high-fructose diet (HFHF) for 12 weeks and exposed to cardiac *ex vivo* ischemia/reperfusion (IR) injury. Dietary manipulation evokes a maladaptive response in heart mice, as demonstrated by the shift of myosin heavy chain isoform content from α to β, the increased expression of the Nlrp3 inflammasome and markers of oxidative metabolism, and the downregulation of the hypoxia inducible factor- (HIF-)2α and members of the Reperfusion Injury Salvage Kinases (RISK) pathway. When exposed to IR, HFHF mice hearts showed greater infarct size and lactic dehydrogenase release in comparison with SD mice. These effects were associated with an exacerbated overexpression of Nlrp3 inflammasome, resulting in marked caspase-1 activation and a compromised activation of the cardioprotective RISK/HIF-2α pathways. The common mechanisms of damage here reported lead to a better understanding of the cross-talk among prosurvival and detrimental pathways leading to the development of cardiovascular disorders associated with metabolic diseases.

1. Introduction

Cardiovascular disorders associated with metabolic diseases are referred to as cardiometabolic diseases (CMDs). Despite the recent publication of several documents and papers suggesting clinical and social interventions to prevent CMDs and benefit subjects afflicted with these comorbidities, the identification of common mechanisms of disease is far from clear. A growing body of evidences indicates that excessive fatty acids and sugars intake affects the development and progression of cardiovascular diseases, including myocardial infarction, by increasing the local inflammatory response and, at the same time, by reducing the efficiency of protective responses that are usually activated by transient oxygen deprivation [1–3]. However, the underlying mechanisms leading to these impairments are complex, and a more thorough understanding is needed.

When exposed to an ischemic insult the cardiomyocytes easily switch from fatty acid (FA) oxidation towards glycolytic metabolism and increase glucose uptake to sustain ATP generation and support cardiac function. The loss of this metabolic flexibility is the main feature of a maladapted heart.

For instance, mice with diet-induced obesity and exposed to daily repetitive brief-duration cardiac ischemia exhibited an early and profound downregulation of myocardial genes involved in FA oxidation, such as muscle-type carnitine palmitoyltransferase 1 (CPT-1m) and medium-chain acyl-coenzyme A dehydrogenase with respect to lean mice [2]. Besides, an excessive FA oxidation has been demonstrated to contribute to cardiac dysfunction in obesity and diabetes [4].

One of the most recently identified proinflammatory signaling pathways involved in CMDs is the NOD-like receptor pyrin domain containing 3 (Nlrp3) inflammasome, a large multimeric protein complex mediating the cleavage of inactive prointerleukin- (IL-) 1β and IL-18 into their active form [5]. We and others have recently demonstrated that activation of Nlrp3 inflammasome contributes to the development of heart failure and diet-induced renal dysfunction [6, 7], mainly by inducing IL-1β and IL-18 overproduction. These cytokines of the IL-1 family modulate the insulin-producing pancreatic β-cell function and act as inflammatory mediators in myocardial ischemia/reperfusion (IR) injury [8, 9]. Reactive oxygen species (ROS), which are produced during IR, may activate Nlrp3 inflammasome and all known Nlrp3 inflammasome activators generate ROS whereas ROS inhibitors block Nlrp3 inflammasome activation [10–12]. The ischemic injury may also evoke the transient activation of prosurvival signaling pathways and several studies demonstrate that the adaptations to hypoxic conditions are regulated by the relative activities of molecules such as Akt, extracellular-signal-regulated kinases (ERK), and glycogen synthase kinase- (GSK-) 3β that taken together constitute the so-called Reperfusion Injury Salvage Kinases (RISK) pathway [13, 14]. The activation of the RISK pathway confers cardioprotection against IR injury by avoiding the opening of the mitochondrial permeability transition pore at the onset of reperfusion [15]. Interestingly, this prosurvival RISK pathway signaling is less effective in animal models of obesity and insulin resistance [16]. For instance, hearts from mice fed a high-fat diet for 32 weeks showed compromised basal expression and activation of the prosurvival RISK pathway signaling compared to mice under normal diet [3].

Other protective pathways include the family of proteins that coordinates at the transcriptional level the cellular response to oxygen availability, mainly the hypoxia inducible factor- (HIF-) α [17]. HIF-1 and HIF-2 proteins are both increased in the peri-infarct area after myocardial infarction in rats and humans, and their powerful protection seems to implicate mechanisms modulating glucose uptake and utilization and preserving mitochondrial function [18–21]. HIF-2α expression occurs in remote areas from the infarct [18] and it is necessary to maintain normal lipid homeostasis, as constitutive HIF-2 activation in hepatocytes results in impaired fatty acid beta-oxidation, decreased lipogenic gene expression, and increased lipid storage capacity [22]. These data suggest a broader role for HIF-2α in the pathophysiology of several CMDs, including ischemic heart diseases.

Nevertheless, none of the above mentioned studies investigated the direct impact of dysmetabolic conditions (i.e., diet-induced insulin resistance) on the potential cross-talk among these different prosurvival and detrimental signaling pathways involved in ischemic myocardial dysfunction. Thus, we investigated the effects of an obesogenic/diabetogenic high-fat high-fructose (HFHF) diet on cardiac tolerance to IR challenging in mice and we validated the relevance of impaired pivotal intracellular mechanisms, in the heart, a key target organ of CMDs.

2. Materials and Methods

2.1. Animals and Dietary Manipulation. Male C57Bl/6j mice (Charles River Laboratories, Calco, LC, Italy) aged 4 weeks were randomly allocated into the following dietary regimens: a standard low-sugars low-fat diet (Control, $n = 12$) and a high-fat high-fructose diet (HFHF, $n = 12$), for twelve weeks. Standard diet (D12450K, Research Diet Inc., New Brunswick, NJ, USA) composition was as follows: 70% of calories in carbohydrates (55% from corn starch and 15% from maltodextrin), 10% of calories in fat (5% from soybean, 5% from butter). High-fat high-fructose diet (D03012907, Research Diet Inc.) composition was as follows: 35% of calories in carbohydrates (10% from maltodextrin and 25% from fructose), 45% of calories in fat (5% from soybean, 40% from lard). All groups received drink and food *ad libitum*.

The animal protocols followed in this study were approved by the local "animal use and care committee" and were in accordance with the European Directive 2010/63/EU on the protection of animals used for scientific purposes. All groups received drink and food *ad libitum*.

2.2. General Parameters. Body weight and food intake were recorded weekly. Fasting glycemia was measured at the start of the protocol and every 4 weeks by saphenous vein puncture using a glucometer (GlucoGmeter, Menarini Diagnostics, Firenze, Italy).

Systolic blood pressure and pulse rate were assessed at 11 weeks of dietary manipulation as the mean value of 10 consecutive measurements obtained in the morning using a tail-cuff sphygmomanometer (IITC; Life Sciences, Woodland Hills, CA).

2.3. Ex Vivo Ischemia/Reperfusion (IR) Injury. After 12 weeks of dietary manipulation, Control and HFHF mice were pretreated with 500 U heparin and anesthetized with sodium pentothal (50 mg/kg) by intraperitoneal injections before being culled by cervical dislocation. Hearts were rapidly excised, blood was rapidly collected from the thorax cavity, and plasma was isolated. The excised heart was rapidly perfused at 80 mmHg by the Langendorff technique with Krebs-Henseleit bicarbonate buffer containing (mM) NaCl 118, $NaHCO_3$ 25, KCl 4.7, KH_2PO_4 1.2, $MgSO_4$ 1.2, $CaCl_2$ 1.25, and glucose 11. The buffer was gassed with 95% O_2 : 5% CO_2. The temperature of the perfusion system was maintained at 37°C.

After a 30 min stabilization period, hearts were subjected to a protocol of IR, which consisted in 30 min of global no-flow, normothermic ischemia followed by a period of 60 min of reperfusion for hearts of both groups (IR Control and IR HFHF). Hearts of Control and HFHF mice, after stabilization, underwent 90 min perfusion only (Sham Control and Sham

HFHF) and served as reference groups in western blot analysis (see the following).

The perfusate flowing out of the heart was collected and measured. Collected coronary effluent was used for measurement of lactate dehydrogenase (LDH) release. To assess the conditions of experimental preparation the coronary flow rate was determined by the amount of perfusate measured in a specific time period.

At the end of perfusion period, the heart was rapidly removed from the perfusion apparatus and divided into two parts by a coronal section (perpendicular to the long axis); while the apical part (less than 1/3 of ventricular mass) was frozen rapidly in liquid nitrogen and stored at −80°C and subsequently used for western blot and histological analysis, the basal part of ventricle was used for infarct size assessment.

2.4. Infarct Size Assessment. Infarct areas were assessed at the end of the experiments with the nitroblue tetrazolium (NBT) technique [23]. The basal part of the ventricles was dissected by transverse sections into two-three slices. Following 20 min of incubation at 37°C in 0.1% solution NBT (Sigma-Aldrich, St. Louis, MO, USA) in phosphate buffer, unstained necrotic tissue was carefully separated from stained viable tissue by an independent observer, who was unaware of the protocols. Since the ischemia was global and since we analyzed only the basal part of the ventricles, the necrotic mass was expressed as a percentage of the analyzed ischemic tissue (% of infarct size on ischemic tissue, %IS/IT).

2.5. Detection of Lactate Dehydrogenase (LDH) Release. The perfusion effluent was collected for 5 min immediately before ischemia and for the entire reperfusion period. LDH released from the heart was determined by spectrophotometric analysis at 340 nm [23].

2.6. Biochemical Parameters. Plasma lipid profile was determined by standard enzymatic procedures using reagent kits (triglycerides (TG), cholesterol, and high-density lipoproteins (HDL); Hospitex Diagnostics, Florence, Italy). Low-density lipoproteins (LDL) were calculated by the formula: total cholesterol − [HDL + (TG/5)]. Plasma insulin level was measured using an enzyme-linked immunosorbent assay (ELISA) kit (Mercodia AB, Uppsala, Sweden).

2.7. Oil Red Staining. Cardiac intramyocellular lipid accumulation was evaluated by Oil Red staining on 10 μm apex cryostatic sections. Stained tissues were viewed under an Olympus Bx4I microscope (40x magnification) with an AxioCamMR5 photographic attachment (Zeiss, Gottingen, Germany).

2.8. Immunohistochemistry. GLUT-4 expression was assessed on 10 μm apex cryostatic sections by immunohistochemistry. Endogenous peroxidases were inactivated by incubating sections for 5 min with 0.3% H_2O_2. Sections were then blocked for 1 h with 3% BSA in PBS. Thus, sections were incubated overnight with rabbit anti-GLUT-4 primary antibody (Abcam, Cambridge, UK) followed by HRP-conjugated secondary antibodies. Sections were digitised with a high resolution camera (Zeiss) at 20x magnification.

2.9. Western Blot Analysis. Total proteins extracts were obtained from 10% (w/v) apex homogenates in RIPA buffer (0.5% Nonidet P-40, 0.5% sodium deoxycholate, 0.1% SDS, 10 mmol/L EDTA, and protease inhibitors). Protein content was determined using the Bradford assay. Protein extracts were stored at −80°C until use. Equal amounts of proteins were separated by SDS-PAGE and electrotransferred to nitrocellulose membrane. Membranes were probed with goat anti-α-myosin heavy chain (α-MHC), goat anti-β-MHC, rabbit anti-carnitine palmitoyltransferase (CPT) 1m, mouse anti-succinate dehydrogenase (SDH), anti-glucose transport- (GLUT-) 4 primary antibody (Abcam, Cambridge, UK), rabbit anti-phospho-insulin receptor 2 ($IRS2^{Ser270}$), and mouse anti-IRS-2 (Cell Signaling, Danvers, MA, USA), rabbit anti-Nlrp3 (Epitomics, Burlingame, CA, USA), rabbit anti-caspase-1, rabbit anti-pERK1/2, rabbit anti-ERK, rabbit anti-$pAkt^{Ser473}$, rabbit anti-Akt, rabbit anti-pGSK-3β^{Ser9}, rabbit anti-GSK-3β, mouse anti-hypoxia inducible factor- (HIF-) 2α, and goat anti-hydroxynonenal (HNE) (Novus Biologicals, Abingdon, UK) primary antibodies, followed by incubation with appropriated HRP-conjugated secondary antibodies (Bio-Rad Laboratories, Hercules, CA, USA). Proteins were detected with ECL detection system (ECL Clarity, Bio-Rad Laboratories, Hercules, CA, USA) and quantified by densitometry using analytic software (Quantity-One, Bio-Rad Laboratories, Hercules, CA, USA). Results were normalized with respect to α-tubulin densitometric value.

2.10. Materials. Unless otherwise stated, all compounds were purchased from the Sigma-Aldrich Company Ltd. (St. Louis, Missouri, USA). Antibodies were from Santa Cruz Biotechnology (Santa Cruz, CA, USA).

2.11. Statistical Analysis. All values are expressed as means ± SD. The Shapiro-Wilk test was used to assess the normality of the variable distributions. One-way ANOVA followed by Bonferroni's post hoc test was adopted for comparisons among selected pairs of groups: Control Sham versus Control IR; Control Sham versus HFHF Sham; Control IR versus HFHF IR; HFHF Sham versus HFHF IR. A P value < 0.05 was considered statistically significant. Statistical tests were performed with GraphPad Prism 6.0 software package (GraphPad Software, San Diego, CA, USA).

3. Results

3.1. General Parameters. After 12 weeks of HFHF diet, mice showed a marked increase in total body weight, accompanied by reduced heart-to-body weight ratio and a significant increase in plasma fasting levels of glucose, insulin, triglycerides, and cholesterol, when compared to Control mice (Table 1). In contrast, HFHF diet did not affect systolic blood pressure or pulse rate (data not shown).

Table 1: General parameters of mice after 12 weeks of Control or high-fat high-fructose (HFHF) diets.

	Control ($n = 10$)	HFHF ($n = 12$)
Body weight increase (g)	8.5 ± 1.6	14.7 ± 3.2***
Heart weight (% of body w.)	0.45 ± 0.02	0.35 ± 0.06**
Plasma glucose (mg/dL)	73 ± 19	139 ± 13***
Plasma insulin (mg/mL)	85.8 ± 5.3	106.8 ± 6.8***
Plasma TG (mg/dL)	32.8 ± 7.8	66.5 ± 25.5***
Plasma Chol. (mg/dL)	77.2 ± 5.7	97.2 ± 8.2**

Data are means ± SD. ** $P < 0.01$, *** $P < 0.005$ versus Control.

3.2. Diet-Induced Cardiac Adaptation. As a shift in myosin heavy chain (MHC) isoform content from α to β is known to contribute to the development of heart failure, we measured the cardiac expression of the two functionally distinct cardiac MHC isoforms by western blotting analysis. As shown in Figure 1(a), a marked increase in β-MHC expression paralleled by a slight reduction in expression of α-MHC was recorded in the hearts of mice chronically exposed to the HFHF diet in comparison to hearts from Control mice, thus confirming a significant MHC isoform shift. This effect was associated with dramatic increase of CPT-1m and SDH, two markers of oxidative metabolism, following HFHF diet exposure (Figure 1(b)).

In addition, Oil Red O staining on heart sections revealed an intramyocellular lipid accumulation in HFHF mice that was not detected in Control mice (Figure 1(c)).

3.3. Infarct Area and LDH Release Increased in HFHF Hearts. When mice underwent myocardial IR, the IR infarct size recorded in the HFHF group was doubled with respect to that recorded in the Control IR (Figure 2(a)). Total LDH release during the 60 min of reperfusion corroborated this observation as it reached a 2.5-fold increase in HFHF IR group when compared to the Control IR value (Figure 2(b)).

3.4. Effects of HFHF and IR Injury on Cardiac GLUT-4 Translocation and Expression and IRS-2 Activation. Immunohistochemistry and western blotting analysis showed that translocation from cytosol to membranes (Figure 3(a)) and expression (Figure 3(b)) of GLUT-4 were both reduced by HFHF diet, thus indicating a diet-induced insulin resistance of the cardiomyocytes. This was confirmed by the markedly increased phosphorylation rate of IRS-2 that inactivates insulin signaling in HFHF hearts assessed by western blotting (Figure 3(c)). The IR challenge induced the increase in GLUT-4 translocation and IRS-2 activation in Control mice, while in HFHF-fed mice IR did not significantly modify GLUT-4 expression and translocation or IRS-2 phosphorylation rate, with respect to HFHF Sham (Figures 3(a), 3(b), and 3(c)).

3.5. Effects of HFHF and IR Injury on Cardiac Lipid Peroxidation and Mitochondrial Oxidative Stress. As shown by western blotting analysis, HFHF diet induced a significant increase in HNE-protein adducts in both Sham and IR experimental conditions in comparison to Control mice, thus demonstrating a robust diet-induced production of lipid peroxidation products (Figure 4(a)). Interestingly, hearts exposure to the IR challenge evoked a further increase in the levels of lipid peroxidation products in both Control and HFHF groups (Figure 4(a)). When the expression of the antioxidant MnSOD enzyme was measured, a significant upregulation was recorded following chronic treatment with HFHF diet. In contrast, IR injury induced MnSOD expression in the heart of Control mice but not in the heart of HFHF mice, thus suggesting that the antioxidant defense in HFHF hearts could not be further increased by IR (Figure 4(b)).

3.6. NLRP3 Inflammasome Complex Activation. As assessed by western blot analysis, IR induced a strong upregulation of both Nlrp3 inflammasome and activated caspase-1 in the heart samples from Control and HFHF mouse, although basal expression levels of Nlrp3 inflammasome and activated caspase-1 in Sham HFHF mouse hearts were already drastically higher than those recorded in Sham Control hearts (Figure 5).

3.7. RISK Pathway Activation. In Control diet hearts, IR challenging did not induce significant variations of phospho-ERK1/2 (Figure 6(a)), while a marked increase in both phospho-Akt/Akt (Figure 6(b)) and phospho-GSK-3β/GSK-3β ratios (Figure 6(c)) was observed. The basal levels of ERK1/2, Akt, and GSK-3β phosphorylation in the hearts of the HFHF group were significantly lower than those reported in the Control diet hearts. The IR-induced upregulation of enzyme phosphorylation following dietary manipulation still remained lower than those evoked by the same insult in Control mice and no effects were recorded on ERK1/2 expression and phosphorylation.

3.8. HIF-2α Activation. Twelve weeks of HFHF diet led to a slight but not significant reduction in HIF-2α expression in heart extracts. Hearts from Control mice exposed to IR underwent a robust induction of HIF-2α expression. In contrast, in the hearts of HFHF mice, the expression level of HIF-2α was reduced by HFHF exposure and reported to Control Sham value by IR, remaining significantly lower than in IR Control hearts (Figure 7).

4. Discussion

In this study, we demonstrated that chronic feeding with an HFHF diet induces a maladaptive response in cardiac tissue, as shown by the α- to β-MHC isoform shift, the increased expression of markers of mitochondrial oxidative metabolism, such as CPT-1m and SDH, and the reduced

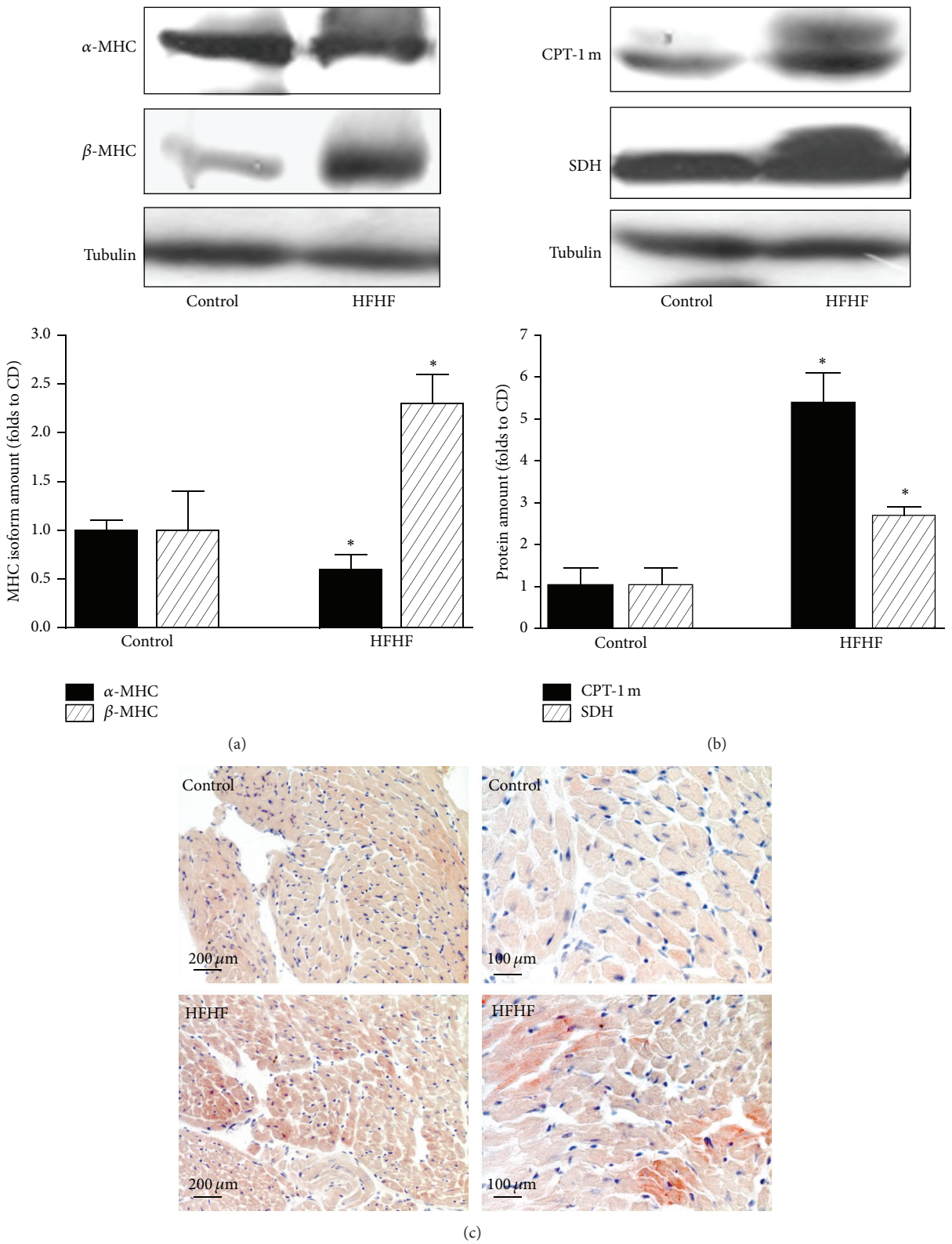

Figure 1: Cardiac metabolic adaptations to diet. Representative western blotting showing cardiac levels of α-MHC and β-MHC isoforms (a) and of markers of oxidative metabolism CPT-1 and SDH (b) assessed after 12 weeks of Control or HFHF diet in heart apex extracts. Histograms report densitometric analysis of 10–12 mice per group normalized for the corresponding tubulin content. $^{*}P < 0.05$ versus Control. (c) Representative 20x/40x magnification photomicrographs of heart apex sections from Control or HFHF diet mice showing cardiac intramyocellular lipid accumulation by Oil Red O staining.

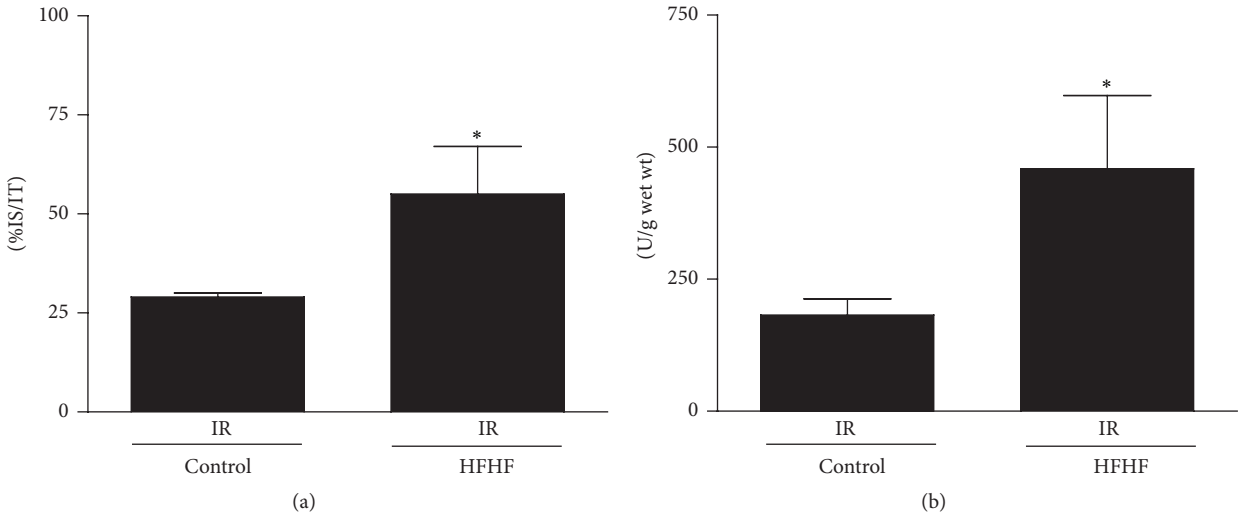

Figure 2: Infarct area and LDH release. Hearts from mice fed for 12 weeks with Control or HFHF diet, exposed to 30-minute ischemia plus 60-minute reperfusion. (a) Infarct size in the basal part of the ventricle after IR exposition is expressed as a percentage of ischemic tissue (%IS/IT). (b) LDH release in the perfusion effluent during the IR was expressed as units per mg of wet tissue weight. $^{*}P < 0.05$ versus Control.

cardiac glucose uptake. Interestingly, despite increased markers of oxidative metabolism, HFHF diet was associated with intramyocytes triglyceride accumulation, suggesting that the tightly regulated process of FA uptake and utilization was perturbed. These effects were paralleled by a robust increase in markers of mitochondrial oxidative stress and lipid peroxidation in the hearts of HFHF mice. Similar results have been previously documented in different experimental models of diabetic cardiomyopathy [24, 25] and the effect of myocardial lipid accumulation on the impairment of systolic cardiac performance is well known [26]. Although there are contrasting data on cardiac postischemic outcomes in models of diet-induced dysmetabolism [27], we here documented worsening of cardiac IR effects in animals exposed to the obesogenic/diabetogenic diet. To better elucidate the impact of dietary manipulation on myocardial IR injury, we assessed the expression and activation of IR-related signaling pathways. One of the most widely studied protective cascades which is involved in mediating the protective effects of many cardioprotective interventions is the RISK pathway [16, 28, 29]. Interestingly, the activities of members of the RISK pathway, including Akt, ERK1/2, and GSK-3β, are often impaired in conditions of diabetes, obesity, insulin resistance, and hypercholesterolemia [3, 16, 29, 30]. In this context, we previously reported that high-fat high sugar diets lead to reduced Akt-mediated insulin signaling [21, 31]. Here we show that the protective myocardial RISK pathway is upregulated by cardiac IR challenging and, most notably, this upregulation is lost in HFHF mice. These results suggest that the reduced RISK activation contributes to the exacerbated myocardial injury in HFHF mice. This is consistent with findings of other authors showing that the presence of metabolic derangements abrogates the protective preconditioning-induced activation of RISK pathway [16, 30, 32]. A consequence of the RISK pathway activation in the early response to cardiac oxygen deprivation is the increased expression of HIF-2α in remote areas from the infarct [18]. HIF-2α regulates key processes of long-term adaptation and maintains mitochondrial homeostasis by regulating production of antioxidant enzymes [33]. A recent research study reported the association between reduced Akt signaling and impaired HIF proteins activity [34]. Moreover, recent studies indicate that HIF-2α directly regulates IRS-2 transcription in diabetic mice both *in vivo* and in primary hepatocytes, thus improving insulin sensitivity and increasing Akt activation [35, 36]. Our results further extend this observation, demonstrating for the first time that an HFHF diet negatively impacts cardiac HIF-2α expression during IR, thus compromising the heart response to IR and the related activation of the insulin signalling.

Intriguingly, the diet-induced inhibition of protective signaling pathways was associated with a robust increase in myocardial protein levels of Nlrp3 inflammasome. The key role of the Nlrp3 inflammasome as central mediator in the inflammatory response to tissue injury during either myocardial infarction or insulin resistance is already known [7, 37, 38]. Strong correlations between the expression of Nlrp3 inflammasome-related genes and insulin resistance have been recently reported in obese male subjects with impaired glucose tolerance and in type 2 diabetic patients [39, 40]. Besides, genetic or pharmacological inhibition of Nlrp3 inflammasome reduces infarct size and limits the development of diet-induced obesity [41, 42]. However, the present study is, to the best of our knowledge, the first one demonstrating that the upregulation of Nlrp3 protein evoked by IR injury is drastically higher in the presence of a diet-induced metabolic derangement. These findings suggest a potential association between increased activity of Nlrp3 inflammasome following metabolic derangements and enhanced susceptibility to a myocardial ischemic insult. Overall, the diet- and IR-induced redox imbalance may

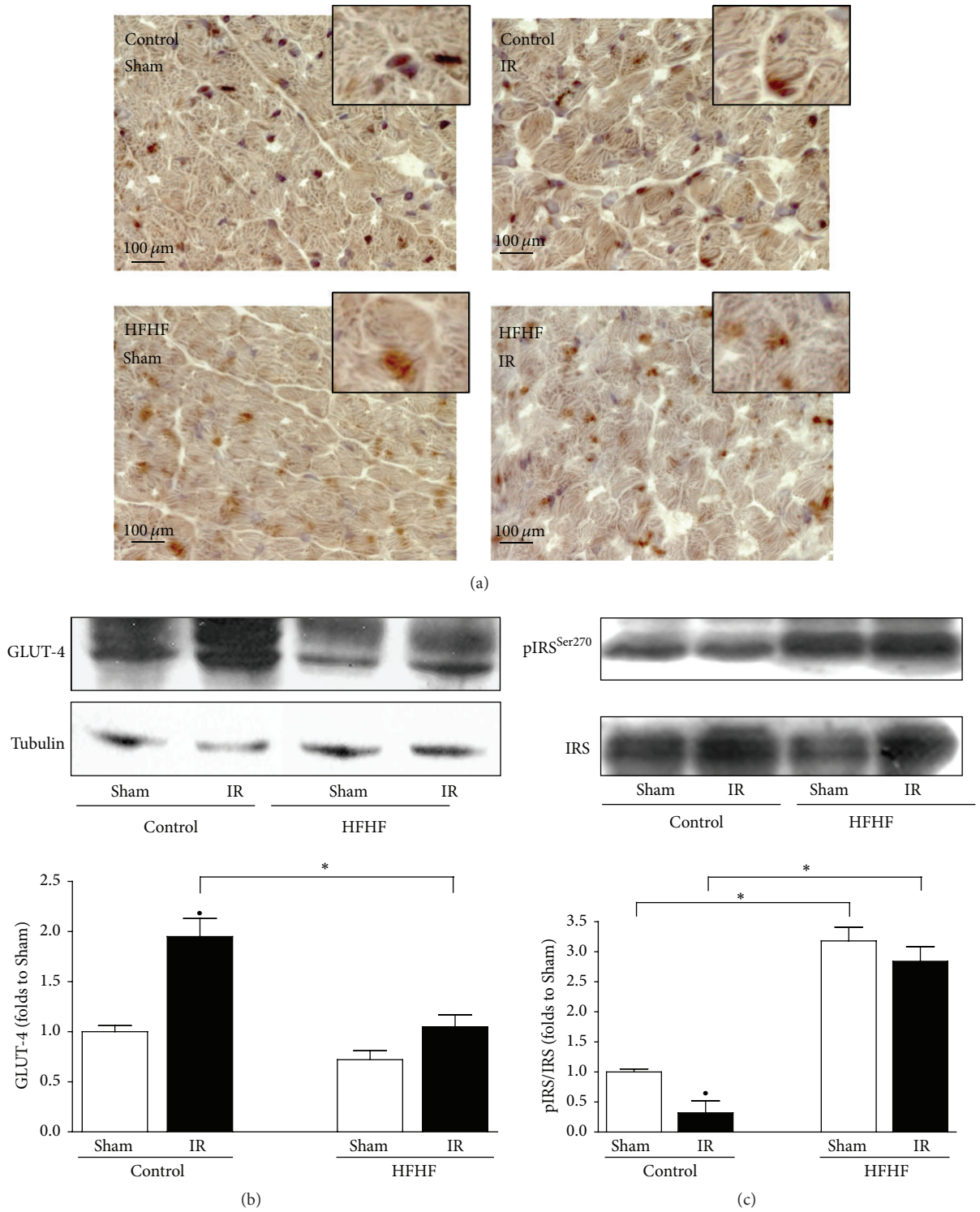

Figure 3: Localization and expression of GLUT-4 and IRS-2 activation in the mouse heart. Representative 40x magnification photomicrographs of heart apex sections and western blotting analysis on heart apex extracts from Control or HFHF diet mice, exposed or not to IR, showing GLUT-4 localization (a) and expression (b). Representative western blotting for cardiac levels of total IRS-2 and Ser270 phosphorylation performed on heart apex extracts from Control or HFHF diet mice, exposed or not to IR (c). Histogram reports densitometric analysis of the phosphorylated-to-total form ratio of 5-6 mice per group. $^{*}P < 0.05$ versus Control; $^{\bullet}P < 0.05$ versus Sham.

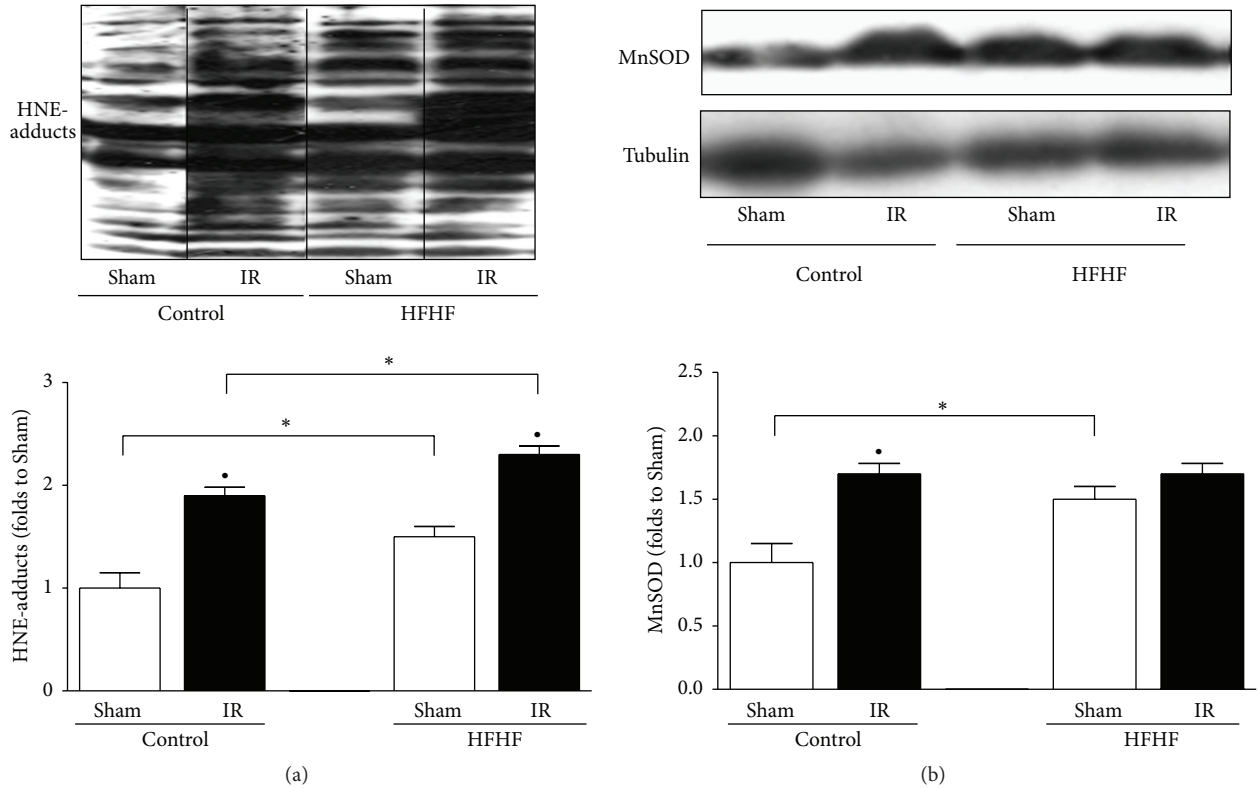

Figure 4: Oxidative stress parameters. Representative western blotting showing cardiac levels of HNE-protein adducts (a) and MnSOD (b) assessed on heart apex extracts from Control or HFHF diet mice, with or without IR. Histograms report densitometric analysis of 5-6 mice per group normalized, respectively, for the corresponding tubulin content. $^{*}P < 0.05$ versus Control; $^{\bullet}P < 0.05$ versus Sham.

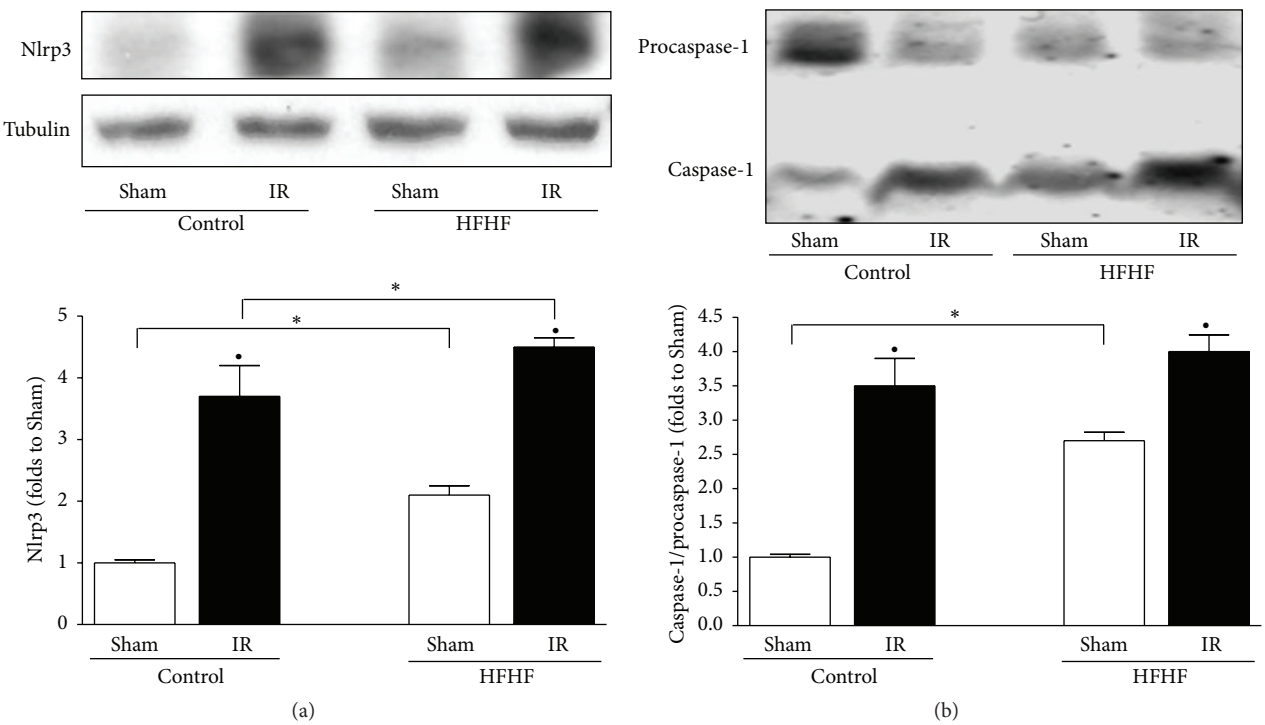

Figure 5: Inflammasome expression and activation in the mouse heart. Representative western blotting showing cardiac levels of Nlrp3 (a), the best characterized element of inflammasome complex, and of downstream activation of caspase-1 (b) assessed on heart apex extracts from Control or HFHF diet mice, with or without IR. Histograms report densitometric analysis of 5-6 mice per group normalized, respectively, for the corresponding tubulin content or the procaspase-1 content. $^{*}P < 0.05$ versus Control; $^{\bullet}P < 0.05$ versus Sham.

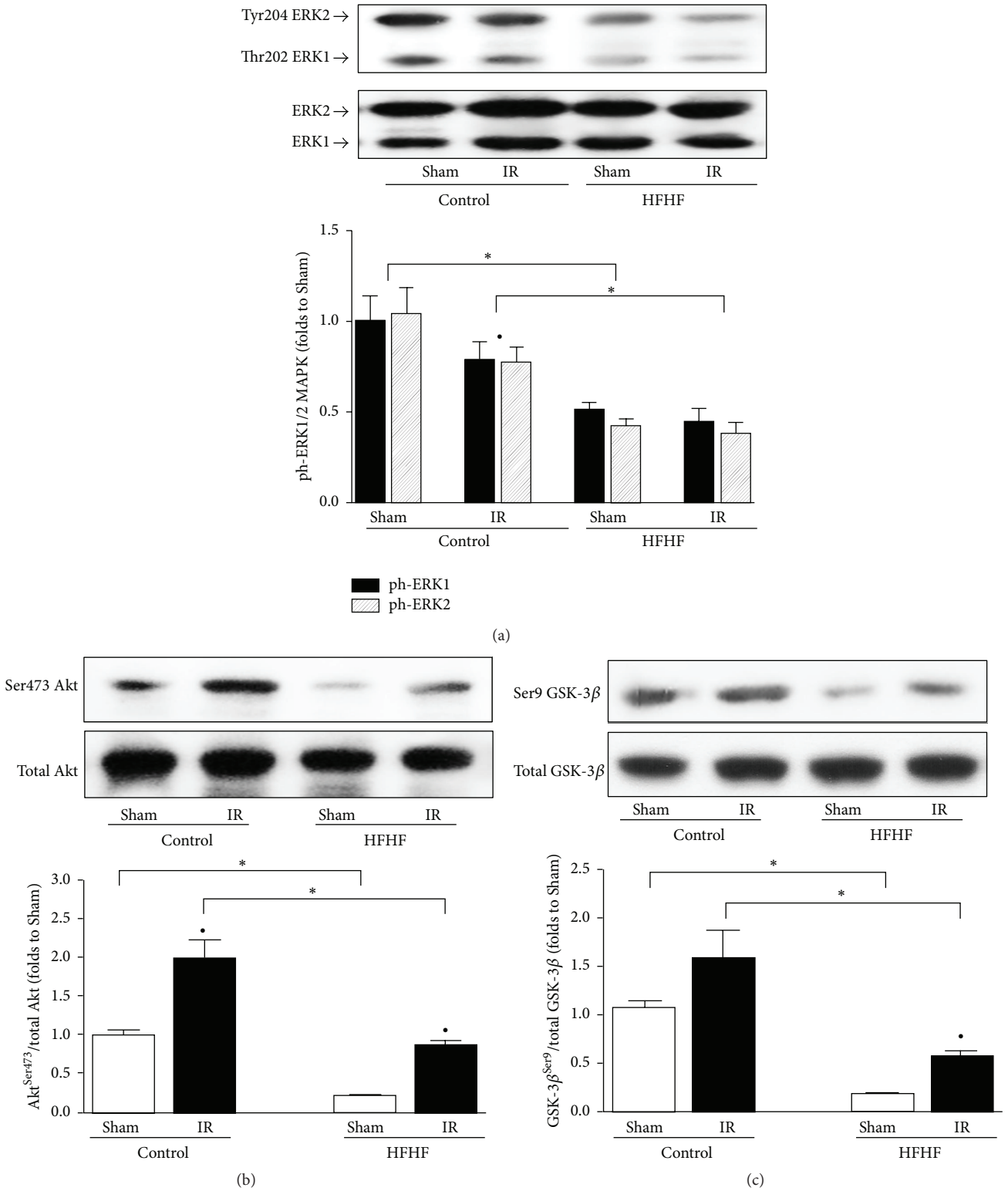

Figure 6: Prosurvival RISK pathway activation in the mouse heart. Representative western blotting for cardiac levels of total ERK1/2 expression and Thr202/Tyr204 phosphorylation, respectively, (a), total Akt protein expression and Ser473 phosphorylation (b), and total GSK-3 protein expression and Ser9 phosphorylation (c) performed on heart apex extracts from Control or HFHF diet mice, exposed or not to IR. Histograms report densitometric analysis of the phosphorylated-to-total form ratio of 5-6 mice per group. $^{*}P < 0.05$ versus Control; $^{\bullet}P < 0.05$ versus Sham.

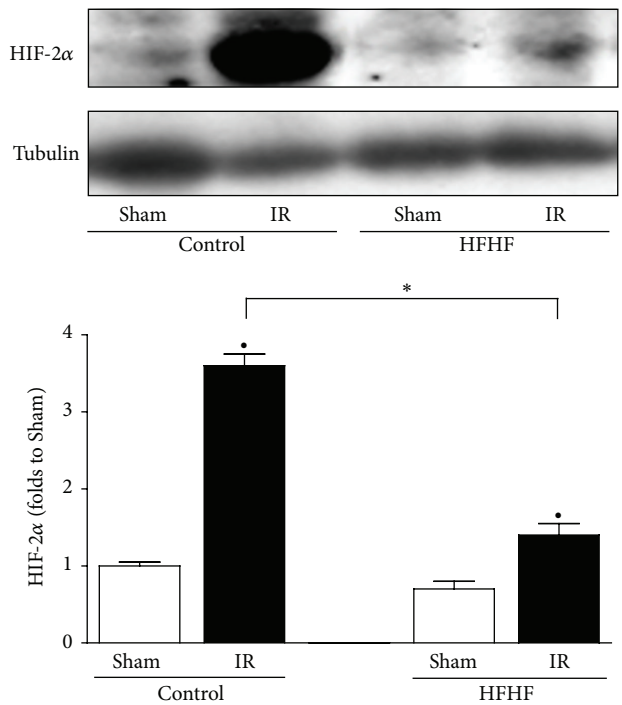

Figure 7: HIF-2α expression in the mouse heart. Representative western blotting for cardiac levels of HIF-2α performed on heart apex extracts from Control or HFHF diet mice, exposed or not to IR. Histograms report densitometric analysis of 5-6 mice per group normalized for the corresponding tubulin content. $^{*}P < 0.05$ versus Control; $^{\bullet}P < 0.05$ versus Sham.

represent the key event leading to the signaling pathways modifications. Indeed, a previous study showed that HIF-2α knockout mice show multiorgan damage due to ROS overproduction [43], and genetic deletion of HIF-2α resulted in increased levels of oxidative stress markers [33]. In keeping with these findings, we observed a reduced expression of HIF-2α and MnSOD in HFHF mice exposed to IR, which could account for the dramatic increase in HNE-adducts. Similarly, mitochondrial oxidative stress is one of the main stimuli triggering Nlrp3 activation [44–46]. For instance, HNE treatment of retinal pigment epithelial cells strongly induces Nlrp3 expression, leading to IL-1β and IL-18 production [47]. We may, thus, speculate that the oxidative unbalance due to impairments in RISK/HIF-2α pathways can worsen the proinflammatory response triggered by Nlrp3 activation. However, further investigations are required to better elucidate the intricate mechanisms of cross-talk among signaling pathways operational in the pathogenesis and potentially also the resolution of CMDs.

The experimental model here proposed allows us to study the intrinsic capacity of the myocardium to afford the IR challenge in a strictly controlled environment, avoiding extracardiac influences and the possible effect of temperature and collateral flow variations. However, we are aware of some limitations of the present study, including the lack of hemodynamic and functional data of postischemic myocardium and the impossibility to dissect between the redox effects on postischemic necrosis and stunning. Future *ad hoc* studies, with implemented technologies, are required to clarify these aspects.

In conclusion, our results clearly demonstrate that a high-fat high-fructose diet alters different signaling pathways involved in cardiac IR injury. While elements of cardioprotective pathways are downregulated, those of inflammatory processes are upregulated by HFHF diet and IR injury is exacerbated by these maladaptive pathway modulations. These results offer further improvements of our understanding of the link between cardiovascular and metabolic injuries. However, further studies are needed to better clarify the reciprocal interaction of these pathways within CMDs pathogenesis, thus allowing the identification of new therapeutic targets for improving postischemic recovery in obese/diabetic patients.

Conflict of Interests

The authors have no conflict of interests to declare.

Acknowledgment

This study was supported by a grant from the University of Turin (Ricerca Locale ex-60% 2013-2014).

References

[1] L. Pulakat, V. G. DeMarco, S. Ardhanari et al., "Adaptive mechanisms to compensate for overnutrition-induced cardiovascular abnormalities," *American Journal of Physiology—Regulatory Integrative and Comparative Physiology*, vol. 301, no. 4, pp. R885–R895, 2011.

[2] G. D. Thakker, N. G. Frangogiannis, P. T. Zymek et al., "Increased myocardial susceptibility to repetitive ischemia with high-fat diet-induced obesity," *Obesity*, vol. 16, no. 12, pp. 2593–2600, 2008.

[3] I. Wensley, K. Salaveria, A. C. Bulmer, D. G. Donner, and E. F. Du Toit, "Myocardial structure, function and ischaemic tolerance in a rodent model of obesity with insulin resistance," *Experimental Physiology*, vol. 98, no. 11, pp. 1552–1564, 2013.

[4] G. D. Lopaschuk, J. R. Ussher, C. D. L. Folmes, J. S. Jaswal, and W. C. Stanley, "Myocardial fatty acid metabolism in health and disease," *Physiological Reviews*, vol. 90, no. 1, pp. 207–258, 2010.

[5] B. Vandanmagsar, Y.-H. Youm, A. Ravussin et al., "The NLRP3 inflammasome instigates obesity-induced inflammation and insulin resistance," *Nature Medicine*, vol. 17, no. 2, pp. 179–189, 2011.

[6] M. Collino, E. Benetti, M. Rogazzo et al., "Reversal of the deleterious effects of chronic dietary HFCS-55 intake by PPAR-δ agonism correlates with impaired NLRP3 inflammasome activation," *Biochemical Pharmacology*, vol. 85, no. 2, pp. 257–264, 2013.

[7] E. Mezzaroma, S. Toldo, D. Farkas et al., "The inflammasome promotes adverse cardiac remodeling following acute myocardial infarction in the mouse," *Proceedings of the National Academy of Sciences of the United States of America*, vol. 108, no. 49, pp. 19725–19730, 2011.

[8] A. A. Wanderer, "Ischemic-reperfusion syndromes: biochemical and immunologic rationale for IL-1 targeted therapy," *Clinical Immunology*, vol. 128, no. 2, pp. 127–132, 2008.

[9] C. J. Tack, R. Stienstra, L. A. B. Joosten, and M. G. Netea, "Inflammation links excess fat to insulin resistance: the role of the interleukin-1 family," *Immunological Reviews*, vol. 249, no. 1, pp. 239–252, 2012.

[10] M. Kawaguchi, M. Takahashi, T. Hata et al., "Inflammasome activation of cardiac fibroblasts is essential for myocardial ischemia/reperfusion injury," *Circulation*, vol. 123, no. 6, pp. 594–604, 2011.

[11] J. Fuentes-Antrás, A. M. Ioan, J. Tuñón, J. Egido, and Ó. Lorenzo, "Activation of toll-like receptors and inflammasome complexes in the diabetic cardiomyopathy-associated inflammation," *International Journal of Endocrinology*, vol. 2014, Article ID 847827, 10 pages, 2014.

[12] R. Zhou, A. Tardivel, B. Thorens, I. Choi, and J. Tschopp, "Thioredoxin-interacting protein links oxidative stress to inflammasome activation," *Nature Immunology*, vol. 11, no. 2, pp. 136–140, 2010.

[13] M. Aragno, R. Mastrocola, C. Ghé et al., "Obestatin induced recovery of myocardial dysfunction in type 1 diabetic rats: underlying mechanisms," *Cardiovascular Diabetology*, vol. 11, article 129, 2012.

[14] P. Pagliaro, F. Moro, F. Tullio, M.-G. Perrelli, and C. Penna, "Cardioprotective pathways during reperfusion: focus on redox signaling and other modalities of cell signaling," *Antioxidants and Redox Signaling*, vol. 14, no. 5, pp. 833–850, 2011.

[15] D. J. Hausenloy and D. M. Yellon, "New directions for protecting the heart against ischaemia-reperfusion injury: targeting the Reperfusion Injury Salvage Kinase (RISK)-pathway," *Cardiovascular Research*, vol. 61, no. 3, pp. 448–460, 2004.

[16] P. Ferdinandy, D. J. Hausenloy, G. Heusch, G. F. Baxter, and R. Schulz, "Interaction of risk factors, comorbidities, and comedications with ischemia/reperfusion injury and cardioprotection by preconditioning, postconditioning, and remote conditioning," *Pharmacological Reviews*, vol. 66, no. 4, pp. 1142–1174, 2014.

[17] J. Hyvärinen, I. E. Hassinen, R. Sormunen et al., "Hearts of hypoxia-inducible factor prolyl 4-hydroxylase-2 hypomorphic mice show protection against acute ischemia-reperfusion injury," *The Journal of Biological Chemistry*, vol. 285, no. 18, pp. 13646–13657, 2010.

[18] J. S. Jürgensen, C. Rosenberger, M. S. Wiesener et al., "Persistent induction of HIF-1α and -2α in cardiomyocytes and stromal cells of ischemic myocardium," *The FASEB Journal*, vol. 18, no. 12, pp. 1415–1417, 2004.

[19] J. B. Pampín, S. A. García Rivero, X. L. Otero Cepeda, A. V. Boquete, J. F. Vila, and R. H. Fonseca, "Immunohistochemical expression of HIF-1α in response to early myocardial ischemia," *Journal of Forensic Sciences*, vol. 51, no. 1, pp. 120–124, 2006.

[20] S. H. Lee, P. L. Wolf, R. Escudero, R. Deutsch, S. W. Jamieson, and P. A. Thistlethwaite, "Early expression of angiogenesis factors in acute myocardial ischemia and infarction," *The New England Journal of Medicine*, vol. 342, no. 9, pp. 626–633, 2000.

[21] J. Wu, P. Chen, Y. Li et al., "HIF-1α in heart: protective mechanisms," *The American Journal of Physiology—Heart and Circulatory Physiology*, vol. 305, no. 6, pp. H821–H828, 2013.

[22] E. B. Rankin, J. Rha, M. A. Selak et al., "Hypoxia-inducible factor 2 regulates hepatic lipid metabolism," *Molecular and Cellular Biology*, vol. 29, no. 16, pp. 4527–4538, 2009.

[23] C. Penna, M. Brancaccio, F. Tullio et al., "Overexpression of the muscle-specific protein, melusin, protects from cardiac ischemia/reperfusion injury," *Basic Research in Cardiology*, vol. 109, article 418, 2014.

[24] M. Aragno, R. Mastrocola, C. Medana et al., "Oxidative stress-dependent impairment of cardiac-specific transcription factors in experimental diabetes," *Endocrinology*, vol. 147, no. 12, pp. 5967–5974, 2006.

[25] M. Rajesh, S. Bátkai, M. Kechrid et al., "Cannabinoid 1 receptor promotes cardiac dysfunction, oxidative stress, inflammation, and fibrosis in diabetic cardiomyopathy," *Diabetes*, vol. 61, no. 3, pp. 716–727, 2012.

[26] J. E. Schaffer, "Lipotoxicity: when tissues overeat," *Current Opinion in Lipidology*, vol. 14, no. 3, pp. 281–287, 2003.

[27] R. Salie, B. Huisamen, and A. Lochner, "High carbohydrate and high fat diets protect the heart against ischaemia/reperfusion injury," *Cardiovascular Diabetology*, vol. 13, article 109, 2014.

[28] Y. Xu, L.-L. Ma, C. Zhou et al., "Hypercholesterolemic myocardium is vulnerable to ischemia-reperfusion injury and refractory to sevoflurane-induced protection," *PLoS ONE*, vol. 8, no. 10, Article ID e76652, 2013.

[29] D. J. Hausenloy and D. M. Yellon, "Reperfusion injury salvage kinase signalling: taking a RISK for cardioprotection," *Heart Failure Reviews*, vol. 12, no. 3-4, pp. 217–234, 2007.

[30] N. Ghaboura, S. Tamareille, P.-H. Ducluzeau et al., "Diabetes mellitus abrogates erythropoietin-induced cardioprotection against ischemic-reperfusion injury by alteration of the RISK/GSK-3β signaling," *Basic Research in Cardiology*, vol. 106, no. 1, pp. 147–162, 2011.

[31] M. Collino, E. Benetti, M. Rogazzo et al., "A non-erythropoietic peptide derivative of erythropoietin decreases susceptibility

to diet-induced insulin resistance in mice," *British Journal of Pharmacology*, vol. 171, no. 24, pp. 5802–5815, 2014.

[32] L.-L. Ma, F.-J. Zhang, L.-B. Qian et al., "Hypercholesterolemia blocked sevoflurane-induced cardioprotection against ischemia-reperfusion injury by alteration of the MG53/RISK/GSK3β signaling," *International Journal of Cardiology*, vol. 168, no. 4, pp. 3671–3678, 2013.

[33] I. Kojima, T. Tanaka, R. Inagi et al., "Protective role of hypoxia-inducible factor-2α against ischemic damage and oxidative stress in the kidney," *Journal of the American Society of Nephrology*, vol. 18, no. 4, pp. 1218–1226, 2007.

[34] S.-G. Ong and D. J. Hausenloy, "Hypoxia-inducible factor as a therapeutic target for cardioprotection," *Pharmacology and Therapeutics*, vol. 136, no. 1, pp. 69–81, 2012.

[35] C. M. Taniguchi, E. C. Finger, A. J. Krieg et al., "Cross-talk between hypoxia and insulin signaling through Phd3 regulates hepatic glucose and lipid metabolism and ameliorates diabetes," *Nature Medicine*, vol. 19, no. 10, pp. 1325–1330, 2013.

[36] K. Wei, S. M. Piecewicz, L. M. McGinnis et al., "A liver Hif-2α-Irs2 pathway sensitizes hepatic insulin signaling and is modulated by Vegf inhibition," *Nature Medicine*, vol. 19, no. 10, pp. 1331–1337, 2013.

[37] E. Benetti, F. Chiazza, N. S. A. Patel, and M. Collino, "The NLRP3 inflammasome as a novel player of the intercellular crosstalk in metabolic disorders," *Mediators of Inflammation*, vol. 2013, Article ID 678627, 9 pages, 2013.

[38] S. Toldo, E. Mezzaroma, A. G. Mauro, F. Salloum, B. W. Van Tassell, and A. Abbate, "The inflammasome in myocardial injury and cardiac remodeling," *Antioxidants & Redox Signaling*, vol. 22, no. 13, pp. 1146–1161, 2015.

[39] G. H. Goossens, E. E. Blaak, R. Theunissen et al., "Expression of NLRP3 inflammasome and T cell population markers in adipose tissue are associated with insulin resistance and impaired glucose metabolism in humans," *Molecular Immunology*, vol. 50, no. 3, pp. 142–149, 2012.

[40] H.-M. Lee, J.-J. Kim, H. J. Kim, M. Shong, B. J. Ku, and E.-K. Jo, "Upregulated NLRP3 inflammasome activation in patients with type 2 diabetes," *Diabetes*, vol. 62, no. 1, pp. 194–204, 2013.

[41] Y. Liu, K. Lian, L. Zhang et al., "TXNIP mediates NLRP3 inflammasome activation in cardiac microvascular endothelial cells as a novel mechanism in myocardial ischemia/reperfusion injury," *Basic Research in Cardiology*, vol. 109, no. 5, article 415, 2014.

[42] C. Marchetti, J. Chojnacki, S. Toldo et al., "A novel pharmacologic inhibitor of the NLRP3 inflammasome limits myocardial injury after ischemia-reperfusion in the mouse," *Journal of Cardiovascular Pharmacology*, vol. 63, no. 4, pp. 316–322, 2014.

[43] M. Scortegagna, K. Ding, Y. Oktay et al., "Multiple organ pathology, metabolic abnormalities and impaired homeostasis of reactive oxygen species in Epas1$^{-/-}$ mice," *Nature Genetics*, vol. 35, no. 4, pp. 331–340, 2003.

[44] L. Chen, R. Na, E. Boldt, and Q. Ran, "NLRP3 inflammasome activation by mitochondrial reactive oxygen species plays a key role in long-term cognitive impairment induced by paraquat exposure," *Neurobiology of Aging*, vol. 36, no. 9, pp. 2533–2543, 2015.

[45] F. Usui, K. Shirasuna, H. Kimura et al., "Inflammasome activation by mitochondrial oxidative stress in macrophages leads to the development of angiotensin II-induced aortic aneurysm," *Arteriosclerosis, Thrombosis, and Vascular Biology*, vol. 35, no. 1, pp. 127–136, 2014.

[46] Y. Zhuang, M. Yasinta, C. Hu et al., "Mitochondrial dysfunction confers albumin-induced NLRP3 inflammasome activation and renal tubular injury," *The American Journal of Physiology—Renal Physiology*, vol. 308, no. 8, pp. F857–F866, 2015.

[47] A. Kauppinen, H. Niskanen, T. Suuronen, K. Kinnunen, A. Salminen, and K. Kaarniranta, "Oxidative stress activates NLRP3 inflammasomes in ARPE-19 cells-implications for age-related macular degeneration (AMD)," *Immunology Letters*, vol. 147, no. 1-2, pp. 29–33, 2012.

Hindawi Publishing Corporation
Oxidative Medicine and Cellular Longevity
Volume 2016, Article ID 4010357, 10 pages
http://dx.doi.org/10.1155/2016/4010357

Review Article

Dietary Restriction and Nutrient Balance in Aging

Júlia Santos,[1,2] Fernanda Leitão-Correia,[1,2] Maria João Sousa,[3] and Cecília Leão[1,2]

[1]*Life and Health Sciences Research Institute (ICVS), School of Health Sciences, University of Minho, 4710-057 Braga, Portugal*
[2]*ICVS/3B's-PT Government Associate Laboratory, Braga/Guimarães, Portugal*
[3]*Molecular and Environmental Biology Centre (CBMA), Department of Biology, University of Minho, 4710-057 Braga, Portugal*

Correspondence should be addressed to Maria João Sousa; mjsousa@bio.uminho.pt

Received 24 April 2015; Revised 23 July 2015; Accepted 28 July 2015

Academic Editor: Eric E. Kelley

Dietary regimens that favour reduced calorie intake delay aging and age-associated diseases. New evidences revealed that nutritional balance of dietary components without food restriction increases lifespan. Particular nutrients as several nitrogen sources, proteins, amino acid, and ammonium are implicated in life and healthspan regulation in different model organisms from yeast to mammals. Aging and dietary restriction interact through partially overlapping mechanisms in the activation of the conserved nutrient-signalling pathways, mainly the insulin/insulin-like growth factor (IIS) and the Target Of Rapamycin (TOR). The specific nutrients of dietary regimens, their balance, and how they interact with different genes and pathways are currently being uncovered. Taking into account that dietary regimes can largely influence overall human health and changes in risk factors such as cholesterol level and blood pressure, these new findings are of great importance to fully comprehend the interplay between diet and humans health.

1. Introduction

The primary molecular mechanisms underlying aging have attracted increased attention, as healthy aging becomes one of the main concerns of the modern society. Cellular activities such as the regulation of metabolism, growth, and aging are modulated by a network of nutrient and energy sensing signalling pathways that are highly conserved among organisms, from yeasts to mammals (reviewed in [1]). Three major signalling pathways involved in longevity regulation have been described: the insulin/insulin-like growth factor (IIS), the Target Of Rapamycin TOR/Sch9 (ortholog of the mammalian S6 kinase), and adenylate cyclase/protein kinase A (AC/PKA). Reducing activity of these pathways is known to promote health and lifespan extension [1]. Signalling through IIS/TOR pathways starts with the binding of ligands, such as insulin and insulin-like growth factor (IGF-1 and IGF-2) in the case of mammals, to specific receptors, which in turn activate the PI3K/Akt/mTOR intracellular signalling cascade that regulates metabolism and stress resistance and consequently aging [2]. Akt kinase directly inhibits the antiaging forkhead FoxO family transcription factor (FOXO), known to regulate autophagy, DNA repair, ubiquitin-proteasome system, and other stress resistance genes [3]. Besides being activated by insulin and IGF-1 via Akt, highly conserved TOR can also respond to dietary amino acids while signalling through other pathways such as the energy sensing pathway AMP-activated protein kinase (AMPK) and sirtuin pathway (SIRT1), downregulating rapamycin-sensitive TOR complex 1 (TORC1) activity. AMPK and SIRT1 are known to mediate longevity in several model organisms in response to dietary regimens [4]. Detailed description of these nutrient signalizing pathways in different models can be found in recently published reviews [5–9].

The study of aging regulating mechanisms can be accomplished by genetic manipulations of these well conserved nutrient-signalling pathways or by using dietary restriction (DR) protocols, in which the intake of one or more macronutrients is reduced without causing malnutrition. One of the best documented DR protocols involves reduction of caloric intake without lack of essential nutrients, termed calorie restriction (CR). The benefits of CR were first described in 1935, by showing that reduced food intake extended lifespan of rats [10]. Since then many studies have demonstrated the beneficial effects of CR on lifespan extension of multiple organisms (yeast, flies, worms, fish, rodents, and rhesus

monkeys), as well as on the improvement of overall health in rodent models. However, new evidences have recently emerged from studies in yeast [11, 12] and in higher eukaryotes [13–15] showing the importance of nutrient balance in dietary regimens and its effects on longevity regulation, challenging the notion that the indiscriminate reduction of caloric intake *per se* extends lifespan. These studies increasingly suggest that not only caloric restriction but rather a balance of different nutrients and their ratios have a pivotal role in regulating lifespan [13, 14, 16–18].

In the following sections we start with an overview of different eukaryotic model organisms that allowed establishing the role of metabolic and growth pathways in longevity. The subsequent sections highlight the impact of nutrient balance on the beneficial effects of dietary restriction regimes on longevity regulation and age-related pathologies.

2. Aging and Dietary Regimens in Different Eukaryotic Model Organisms

Studies in different eukaryotic model organisms revealed that the pathways regulating metabolism and growth, once active, are also able to modulate aging and increase mortality.

The yeast *Saccharomyces cerevisiae* has been a highly exploited eukaryotic model to study the mechanisms involved in longevity regulation through the assessment of cell survival in stationary phase cultures (known as chronological lifespan—CLS) [19–23]. These studies carried under different nutrient dietary regimens show that reducing glucose concentration in the media (usually from 2% to 0.5 or 0.05%) increase CLS [20, 23–28]. Furthermore, several other single nutrients from the culture medium were also shown to affect longevity regulation (reviewed in [29]). As in higher eukaryotes, in *S. cerevisiae* these nutrients, depending on their abundance, can activate multiple proaging signalling pathways, such as the TOR1-Sch9, primarily activated by amino acids, and the Ras/PKA which mainly responds to glucose but is also regulated by other major nutrients [30–32]. These pathways promote cell division and growth in response to nutrients while inhibiting the general stress response and autophagy [26, 33]. CR further promotes CLS extension in TOR and Sch9p deficient mutants, indicating the presence of other mechanisms in CR-mediated lifespan extension [26]. The Ras/PKA pathway is the primary mediator of the glucose transcriptional response [34] and deletion of *RAS2* causes lifespan extension and stress resistance [35], while imposing CR to long-lived *cdc25-10* mutants (deficient in guanine nucleotide exchange factor that regulates Ras2p activation) does not further extend lifespan of these mutants [36]. Both pathways converge on the stress resistance kinase Rim15p and its downstream transcription factors Msn2p/4p and Gis1p, all of which play key roles in mediating CR effects on longevity [26, 37]. Decreasing TOR-Sch9 signalling also extends CLS in Rim15p independent manner through the modulation of mitochondrial functions. Actually, it has been shown that, in active stages of growth, genetic or pharmacological TOR inhibition results in enhanced mitochondrial coupling, increasing mitochondrial membrane potential and reactive oxygen species (ROS) production that provides an adaptive mitochondrial signal to extend CLS in stationary phase [38, 39]. Others have also reported that CR extends CLS by reducing superoxide anion levels, independently of Rim15p, promoting a more frequent growth arrest in G_0/G_1 phase [40, 41]. It has also been shown that mitochondrial respiratory thresholds regulate yeast CLS and its extension by CR, a critical minimum respiratory capacity being crucial for such CLS extension [42].

The role of IIS in aging modulation was first discovered in the nematode *Caenorhabditis elegans* by demonstrating that the phosphatidylinositol 3-kinase (PI3K) signalling cascade is responsible for longevity regulation [43]. Since then, the IIS pathway has been implicated in other biological functions of *C. elegans* [44]. Inhibition of this pathway by using function mutations in *DAF-2*, the only *C. elegans* gene coding for an insulin/IGF-1 receptor ortholog, reduces the aging process [45] and leads to transcription changes of stress response and energy metabolism genes via DAF-16 (FOXO ortholog) [1, 45, 46]. As in yeast, downregulation of the TOR-S6K signalling pathway in *C. elegans* affects longevity by activating stress transcription factors, PHA-4, SKN-1, and DAF-16, which control genes involved in lipid metabolism and autophagy [47, 48]. Also in this model, the IIS and the TOR pathways act in synergy through partially overlapping mechanisms to control longevity [48, 49]. In *C. elegans* the most common dietary restriction protocol to reduce the intake of nutrients, without causing malnutrition (DR), is through the decrease of the bacterial food source, mainly *Escherichia coli*, either by using bacterial dilution, which can extend lifespan from 60% up to 150% [50], or by reducing feeding capability. Increased lifespan is observed in mutants affected in feeding capabilities such as deletion of *EAT-2* (pharyngeal pumping defect) as well as decreased activity of NAC-2 and NAC-3 (gut sodium dicarboxylate transporter) [16, 51, 52]. The study of the role of specific constituents of diet in longevity are still lacking due to the absence of purified diets in *C. elegans*. However, it is known that high glucose diets shorten lifespan in this model by downregulating proteins such as AMPK, FOXO, and glyoxalase [53, 54]. Recently, a glucose transporter that links nutrient restriction and signalling to aging, in this simple organism, has also been discovered. The FGT-1 glucose transporter, a mammalian GLUT-like protein paralog, seems to be responsible not only for transport activity but also for glucose signalling metabolism as reducing its activity increases lifespan to the same level obtained by decreasing DAF-2 signalling [53, 55].

In the fruit fly *Drosophila melanogaster*, reducing IIS signalling by mutations in the insulin-like peptides (DILPS) or insulin-like receptor (INR) shows increased lifespan extension, establishing the role of this pathway as being evolutionary conserved [56]. Direct inhibition of TOR pathway in flies presents a 30% increase in lifespan [57, 58]. However, mutants in the insulin receptor substrate CHICO still respond to DR as do null dFOXO mutants, suggesting only partially overlapping mechanisms for IIS and DR mediated lifespan extension, indicating the existence of other nutrient responding pathways [59, 60]. The usual DR protocol in flies is an *ad libitum* diluted diet, in which the sugar and yeast content

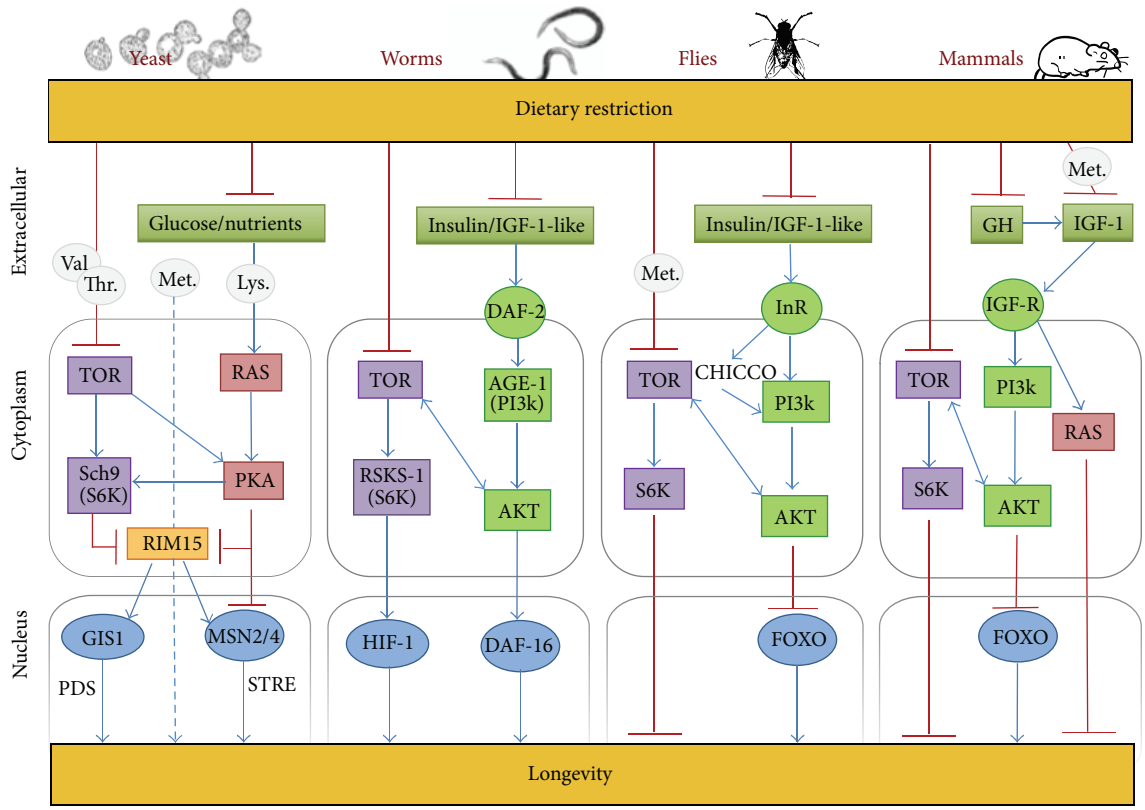

Figure 1: Scheme of longevity regulatory pathways in various model organisms (yeast, worms, flies, and mammals). Identical symbols are used for the orthologous genes in each model organism. In worms, flies, and mammals, dietary restriction reduces signalling through IIS/TOR pathways, deactivating the PI3K/Akt/TOR intracellular signalling cascade and consequently activating the antiaging FOXO family transcription factor(s), known to regulate stress resistance and aging. In yeast, dietary restriction reduces the activity of the TOR/Sch9 and RAS/PKA nutrient-signalling pathways, both converging on the protein kinase Rim15 that in consequence activates its downstream transcription factors Gis1 and Msn2/4, involved in the postdiauxic shift (PDS) element-driven gene expression and stress-responsive elements (STRE) gene expression, respectively. The involvement of RAS signalling in longevity regulation is indicated in the two models where it has been described. lysine (Lys.), methionine (Met.), threonine (Thr.), and valine (Val.). The detailed description and other abbreviations are given in the text.

can be changed to achieve maximal longevity. In fact, using fixed concentrations of sugar but reducing calories from yeast (protein source) can significantly extend longevity while restriction of dietary sugar yields only modest extension, indicating that protein restriction is more important in lifespan extension in fruit flies [60–62].

As for the other models described above, in mammals, the modulation of the conserved nutrient activated pathways IIS and mTOR, genetically, pharmacologically, or nutritionally, impacts aging and delays age-related diseases. Genetic interventions that limit signalling through IIS pathway in rodents, such as Ames and Snell dwarfs and growth hormone (GH) receptor knockout, are capable of extending lifespan in 50% by diminishing IGF-1 and insulin levels and simultaneously enhance healthspan (reviewed in [5]). Recently, the beneficial effects of CR and IGF-1 levels in longevity are proposed to act through PI3K/Akt/mTOR signalling to reduce mTOR activity, significantly increasing lifespan [2]. The most common DR protocol in mammals is the decrease of calorie intake (CR) which is the most robust dietary intervention to extend lifespan and healthspan in mammals to date. Other DR protocols include protein restriction and intermittent fasting, which do not require a reduction in calorie intake. CR animals have their caloric diet reduced normally 20 to 40% from the *ad libitum* diet given to the control animal and present extended lifespan up to 40% partially by reducing the occurrence of chronic diseases such as cancer, diabetes, and cardiovascular diseases. GH stimulates IGF-1 production, which can be arrested by CR, suggesting that CR uses longevity pathways to limit cancer probably due to energy restriction that alters cell cycle regulation and consequently inhibits cell proliferation and increases apoptosis [63]. CR has also been reported to reduce oxidative damage to DNA, by enhancing the efficiency of DNA repair mechanisms [16, 63]. A schematic illustration of the nutrient-signalling pathways involved in longevity regulation in the different model organisms is provided in Figure 1.

3. Nitrogen Sources as Key Effectors on Dietary Regimens

The results in yeast [11, 64] and in higher eukaryotes, described above, clearly favour an emerging perspective

where nutrient balance plays a predominant role in the beneficial effects of dietary restriction regimens impacting longevity regulation. Therefore recently several studies tried to clarify which nutrients are affecting longevity regulation and whether they interact. Protein and amino acids have been studied as activators of specific nutrient signalling pathways involved in longevity regulation in multiple model organisms. In the yeast *S. cerevisiae,* dietary amino acid composition has been implicated in CLS regulation. Several studies in the literature report different effects of amino acids on lifespan regulation, dependent on the TOR pathway [19, 21–23, 65]. In this context, it is known that starvation for nonessential amino acids used as preferred nitrogen sources can extend CLS [24, 36, 66], while starvation for essential amino acids reduces CLS [21, 65]. Single amino acids are known to affect longevity and, recently, it has been shown that leucine influences autophagy and extension of CLS during CR [67]. On the other hand, methionine restriction has been described to extend CLS in an autophagy-dependent manner [68] and to confer resistance to multiple cellular stresses through stress-responsive retrograde signalling [69]. Isoleucine, threonine, and valine extend CLS via the general amino acid control (GAAC) pathway [19]. The sensing of certain amino acids, such as leucine, occurs via TOR kinase while the absence of individual amino acids is recognized via GCN2 (general amino acid control nonderepressible 2) [70, 71]. Regulation of these two kinases has been highly implicated in longevity modulation by dietary restriction [72]. Besides amino acids, another nitrogen source commonly used by *S. cerevisiae* such as ammonium (NH_4^+) was identified as new key player in the modulation of yeast longevity [73, 74]. These studies reported that NH_4^+ is toxic acting as an extrinsic factor affecting yeast CLS, preferentially in amino acid restriction conditions [73]. In extreme CR conditions in water, NH_4^+ effects during yeast aging depend on the specific essential amino acid deprived from the medium, with leucine or histidine deprivation being mediated by Tor1p activation and lysine deprivation by Ras2p activation. Sch9p, contrary to Tor1p and Ras2p, mediates cell survival in response to NH_4^+ associated with Sch9p-dependent Hog1p phosphorylation [74]. These results suggest that the presence of NH_4^+ in the medium (commonly present as the nitrogen source) may be at least partly responsible for the reported decrease in CLS in leucine-starved cells [19, 67]. This work provided new insights into the modulation of CLS by several nutrients, linking NH_4^+ toxicity to amino acid limitation [74].

In *C. elegans*, amino acids and proteins are influencing its lifespan through DR. In this scope, it has been shown in a recent study that GCN2, the evolutionarily conserved kinase that directly responds to amino acid deficiency, plays a central role in mediating lifespan extension under DR conditions by converging with TOR/S6K signalling on the PHA-4/FoxA transcription factors and its downstream target genes under stressful conditions [75, 76]. Reducing the uptake of peptides, by Pep-2 deletion, also increases lifespan by reducing insulin signalling [77] and, additionally, mutations in Metr-1/methionine synthase or the use of the common antidiabetic drug metformin, which alters methionine metabolism, is also known to extend lifespan in *C. elegans* [78]. The roles of specific components of the diet in longevity regulation *versus* reduced calorie intake in *C. elegans* are still difficult to elucidate due to the deficiency of purified diets and lack of studies connecting each nutrient contribution and the various pathways implicated in aging.

In *Drosophila melanogaster,* a recent study demonstrated that adding back essential amino acids to DR flies increased fecundity and decreased lifespan back to the full feeding level, while adding back other yeast nutrients, as fatty acids, vitamins, or carbohydrates, add no effect on lifespan nor on fecundity [13]. These results demonstrate that the amount of calories *per se* does not affect lifespan. However, supplementing with methionine by itself increased fecundity to the fully fed level, without reducing lifespan, demonstrating that the assumed tight link between lifespan and fecundity could be uncoupled. Other studies support that methionine and casein supplementation led to extended longevity. On the contrary, a recent study reported positive effects of methionine restriction on longevity in a defined diet, only in the presence of relatively low total amino acids, by downregulating TOR signalling [79]. In order to clarify these different responses to amino acids and in particular to methionine which suggests a possible cross talk between the response pathways of the various amino acids, the use of a fully defined diet such as the complete chemically defined (holidic) diet available for *D. melanogaster* developed by Piper and coworkers [80] has been recommended. The use of this diet has confirmed the positive effects of amino acid dietary restriction on lifespan regulation as well as the negative effect of complete lack of methionine on lifespan extension [61, 80]. This holidic diet is now a promising tool to study the role of individual nutrients in longevity regulation in flies.

As referred above, besides CR, other DR protocols are used successfully in mammal studies on longevity. Recent reports demonstrate that rodents on low protein regimens with 5–15% protein live longer than the ones on high-protein diets with 50% protein intake [14]. This extended longevity due to the fact that protein restriction is associated with reduced mTOR activation, reduced DNA and protein oxidative damage, and reduced spontaneous tumor formation and has been demonstrated to improve renal function [81]. Restriction of single amino acids like methionine and tryptophan has also been described to have a role in longevity regulation in mammals. Studies show that rodents given 80% reduced methionine diet displayed an increase in median and maximum lifespan of 40% in comparison to the controlled fed animals. Methionine restricted rodents exhibit reduced levels of insulin, IGF-1, serum glucose, and mitochondrial ROS, similar to CR restricted animals, although by partially independent pathways [82, 83]. Also, tryptophan restriction has been described to extend mice lifespan by 23% [16] accompanied with delayed sexual maturation and tumor onset and improved hair growth and coat condition. Leucine restriction also appears to be implicated in longevity extension probably by increasing insulin sensitivity via GCN2/mTOR and AMPK pathways [81]. Accordingly, the amino acid sensing pathways GCN2 and mTOR and their cross talk can most probably be implicated in longevity regulation in protein restriction regimens [84].

4. Dietary Restriction versus Dietary Balance

As described above, traditional DR differs even within experiments using the same model organism. DR can be implemented by using a diet of constant composition or diets in which the composition varies, either by providing limited food intake or by using a diluted diet. Due to these major discrepancies in DR protocols amongst the major aging models, recent studies have been using the Geometric Framework (GF) approach, consisting of a multidimensional representation of nutrition, in order to better understand the effects of dietary nutrients on feeding behaviour, metabolic health, reproduction, and longevity, among other traits [85]. From these studies emerged the concept that macronutrient ratios between protein and carbohydrates (P : C ratio), but not fat, have key roles in longevity regulation in these models [13, 14, 18, 62]. In fruit flies increased longevity was achieved by reducing the caloric input from the protein source yeast extract. This DR-regimen ameliorated lifespan extension in comparison to isocaloric reduction of sucrose [62]. Similarly, addition of essential amino acids to dietary restriction in sucrose plus yeast-based diet diminishes longevity extension [13]. Another study demonstrated that 1P : 16C diet ratio maximized *D. melanogaster* lifespan, while reduced caloric intake did not extend lifespan [18]. In rodents, increasing the P : C ratio affects longevity without being influenced by total calorie intake, ultimately leading to an increased mTOR activation. The longest lifespan extension was achieved by a low protein high carbohydrate diet, which the authors believe to result from low mTOR activation and low insulin levels. Inhibition of mTOR, a proaging pathway, by manipulating the ratio of macronutrients is believed to extend longevity in rodents [14]. As described above, mTOR and IGF-1 signalling by amino acids and the effect of low protein diets on longevity regulation suggest further investigation into how dietary balance affects aging.

Also in primates, DR composition has a major impact in results regarding lifespan extension, supporting the notion that balance of nutrients in the diet might be more important in healthy lifespan extension than dietary restriction. Two studies, one from the Wisconsin National Primate Research Centre (WNPRC) and another from the National Institute on Aging (NIA) presented different results when subjecting rhesus monkeys to 30% CR regimen. The WNPRC study reported a decreased mortality in the CR group in comparison to the control group with a 50% lower incidence of diabetes, cancer, and cardiovascular diseases [17, 86]. On the other hand, the NIA study did not find significant differences between CR and control groups, although supporting the beneficial impact of CR on healthspan [87]. The major differences between these two studies were the dietary regimens and the protein and carbohydrate sources used in each study. In the WNPRC study, the protein source used was lactalbumin and the carbohydrate source derived from corn, starch, and 28.5% sucrose, whereas, in the NIA study, the protein source used derived from wheat, corn, soybean, fish, and alfalfa meal, and the carbohydrate source derived from ground wheat and corn with 3.9% sucrose [81]. The differences in results from the two studies could be attributed to the variations in food ingredients and possibly to the protein source; one derived from animal and the other derived from plant sources that have been previously described to affect aging [81, 88].

In humans, very recent cohort studies suggest a correlation between age-related diseases and high protein diets from animal sources. Based on the US national survey of health and nutrition, NHANES III database, a recent article reports that the 50-to-65 age group with high protein intake had a 75% increase in overall mortality and a fourfold increased risk of cancer mortality in comparison to individuals with low protein intake, which was attenuated or abolished when protein intake was derived from plants. Interestingly, in individuals over 65 years, the high protein intake was reported to reduce cancer and overall mortality. These results were confirmed in mice, proving that protein absorption is affected by aging. The study also confirms the correlation between higher IGF-1 levels with more dietary protein and the incidence and progression of both melanoma and breast cancer [15]. Likewise, a Swedish cohort reported that low carbohydrate high protein diets are associated with increased risk of cardiovascular diseases [89].

Although the yeast aging model has been pioneer in uncovering many age-related processes, only recently studies addressing dietary balance started to emerge. A recent study shows a nutritional balance occurring between glucose, amino acids, and yeast nitrogen base (YNB) as having a major role in yeast CLS through Sch9p [11]. The same authors have also shown that the ratio between essential and nonessential amino acids greatly affects CLS regulation, in a glucose dependent manner, as a significantly shorter CLS was observed under CR conditions. Methionine restriction and glutamic acid addition were also reported to maximize CLS, and a positive correlation between the additive effects of methionine restriction and glutamic acid addition with CR in CLS was also reported [90]. These reports suggest that also in yeast the well-known CR effect in longevity is strongly dependent on other nutrients in the medium compared to glucose alone. Also, a recent study uncovered how glucose and amino acids (threonine, valine, and serine) modulate stress and aging in yeast [64]. In this study it was reported that, in the presence of glucose, threonine and valine activated TORC1 pathway and serine activated the sphingolipid dependent Pkh1/2 pathway. Both activated pathways converged to active Sch9p which plays a critical role in this nutrient response mechanism. Sch9p seems to be directly involved in nutritional balance in yeast as a new study reports antagonistic effects of *SCH9* deletion on yeast cells grown in synthetic complete medium and natural grape juice, where the nitrogen : carbon ratio significantly differs [91]. In line with these latest results, the CLS shortening under amino acid restriction can be completely reverted by removing nonlimiting good nitrogen sources (NH_4^+ or glutamine) from the medium and furthermore NH_4^+ is a necessary nutrient for the beneficial effects of CR on longevity to occur [12]. The presence of ammonium is responsible for inducing replicative stress and blocking the consumption of essential amino acids. Furthermore, the negative effects of NH_4^+ are mediated by Tor1p, Ras2p, and Sch9p. These

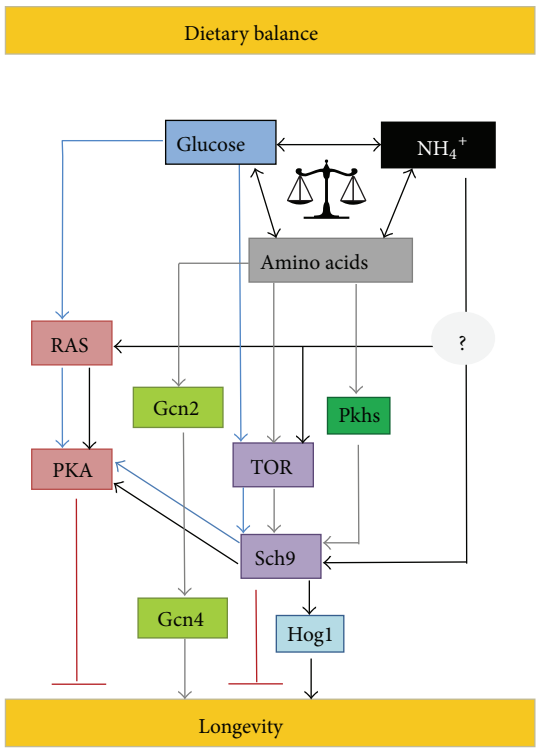

Figure 2: Schematic of nutrients (glucose, amino acids, and ammonium) that accelerate aging through different signalling pathways. A dietary balance between these nutrients is necessary for achieving maximum longevity in yeast. The detailed description and abbreviations are given in the text.

results further establish NH_4^+ as a key factor involved in the nutritional balance required between nitrogen sources and glucose, to achieve longevity promotion in yeast [12]. A schematic illustration of dietary balance in yeast is provided in Figure 2. These new reports demonstrating that extended lifespan as well as healthspan does not depend only on calorie or dietary restriction but rather on an optimal nutritional equilibrium may have significant acceptance from the general population and a broader application than dietary restriction in worldwide diet regimens [13, 14, 16–18].

5. The Interplay between Diet and Age-Related Pathologies

Dietary restriction, as mentioned above, is a potent intervention that increases lifespan and contributes to a lower incidence of chronic diseases, namely, cancer [17, 63]. However, although DR presents high advantages to the aging process and associated diseases, long-term food restriction is unfeasible for most people, therefore presenting low clinical value [92]. Also, inadequate nutrition is known to reduce reproductive function and increase the risk of osteoporotic bone fractures and cardiac arrhythmias [3]. To overcome this low compliance to food DR, a promising strategy is to use DR mimetics, by the development of pharmaceutical compounds that lead to the same physiological effects as DR without significantly reducing food intake. The best studied DR mimetics are rapamycin, metformin, and resveratrol, which have shown anticancer properties and consequently are being tested in clinical trials [63]. Several studies report the effects of metformin, a well-known antidiabetic drug, on reducing spontaneous tumor growth and also increasing the efficacy of radiation in cancer treatment [93, 94]. These beneficial effects of metformin are primarily mediated by the activation of AMPK pathway, known to regulate cellular energy homeostasis, but also by signaling suppression of mTORC1 [63, 93]. The TORC1 inhibitor rapamycin or its analogs induces cell death in breast and colorectal cancer subjected to therapeutic drugs, leading to tumor regression [63]. Resveratrol has been used as CR mimetic known to activate SIRT1 and AMPK with beneficial effects on longevity, cancer, and obesity [95]. The new field of DR mimetics brings to light the vast applications in cancer metabolism and these novel results associating DR mimetics to chemotherapy agents can help reduce the side effects of treated cells by protecting normal cells from stress induced death [63].

Fasting is a dietary regimen that has proven to trigger similar biological pathways as caloric restriction and has gained popularity over the years with people finding it easier to follow than traditional DR. Intermittent fasting (IF) involves restriction of energy intake for periods of 1-2 days a week with no restriction during feeding periods whereas periodic fasting (PF) involves fasting for 3 or more days every 2 or more weeks, also with no restriction during feeding periods. Fasting for a period of 2 or 5 days is known to promote a 50% reduction in glucose and IGF-1 levels in both mice and humans, respectively, and to promote depletion of hepatic glycogen, leading to the generation of ketone bodies [96]. In cancer treatment, fasting has shown to have more consistent positive effects than DR. Fasting generates an extreme environment that induces protective changes in normal cells, but not in cancer cells, that fail to respond to the protective signals of fasting due to the role of oncogenes as negative regulators of stress resistance. This effect is called differential stress resistance (DRS) [97]. On the contrary, long-term DR requires a period of weeks or even months to have some effect and is not capable of achieving high decreases in glucose and IGF-1 levels, besides promoting chronic weight loss, considered detrimental to patients undergoing chemotherapy [63, 96, 97]. Studies in mice have reported that combining fasting cycles and chemotherapy increased cancer-free survival in 20–60% [98, 99] and is effective in improving chemotherapeutic index [100]. Although there are no human data so far, the effect of fasting on enhancing cancer treatment is being tested in clinical trials in both Europe and the USA [96]. IF has also shown major health benefits in both rodents and humans, being able to lower the risk factors associated with metabolic syndrome (MS), such as abdominal fat, blood pressure, inflammation, and insulin resistance, and consequently diminish the risk factor for diabetes and cardiovascular diseases [101–104]. IF can reduce inflammation in rheumatoid arthritis patients and asthma-related symptoms in overweight subjects, inducing significant decreased levels in oxidative stress and inflammation markers [105, 106]. Studies linking IF and cognitive brain function in humans

are still scarce; however, recently, dietary patterns have been linked to brain biomarkers of Alzheimer's disease [107]. In fact, in rodent models of Alzheimer's, Parkinson's, and Huntington's disease, IF reduced clinical symptoms, protecting neurons against dysfunction and degeneration by inducing the expression of brain-derived neurotrophic factor (BDNF) [108–110], which suggest that IF interventions could also present benefits in the prevention of brain dysfunction in humans.

Summing up, evidence reported herewith shows that multiple dietary regimens can largely influence overall health and longevity. Nutrient modulating mechanisms are presently being uncovered in different organisms from yeast to mammals, exposing the balance between several nutrients as primordial to aging. These new findings are of great importance to fully comprehend the interplay between diet and humans health.

Conflict of Interests

The authors declare that there is no conflict of interests regarding the publication of this paper.

References

[1] L. Fontana, L. Partridge, and V. D. Longo, "Extending healthy life span-from yeast to humans," *Science*, vol. 328, no. 5976, pp. 321–326, 2010.

[2] D. W. Lamming, "Diminished mTOR signaling: a common mode of action for endocrine longevity factors," *SpringerPlus*, vol. 3, article 735, 2014.

[3] L. Fontana and L. Partridge, "Promoting health and longevity through diet: from model organisms to humans," *Cell*, vol. 161, no. 1, pp. 106–118, 2015.

[4] S. M. Solon-Biet, S. J. Mitchell, R. de Cabo, D. Raubenheimer, D. G. Le Couteur, and S. J. Simpson, "Macronutrients and caloric intake in health and longevity," *The Journal of Endocrinology*, vol. 226, no. 1, pp. R17–R28, 2015.

[5] H. M. Brown-Borg, "Hormonal regulation of longevity in mammals," *Ageing Research Reviews*, vol. 6, no. 1, pp. 28–45, 2007.

[6] M. M. Mihaylova and R. J. Shaw, "The AMPK signalling pathway coordinates cell growth, autophagy and metabolism," *Nature Cell Biology*, vol. 13, no. 9, pp. 1016–1023, 2011.

[7] M. N. Stanfel, L. S. Shamieh, M. Kaeberlein, and B. K. Kennedy, "The TOR pathway comes of age," *Biochimica et Biophysica Acta (BBA)—General Subjects*, vol. 1790, no. 10, pp. 1067–1074, 2009.

[8] J. R. Broach, "Nutritional control of growth and development in yeast," *Genetics*, vol. 192, no. 1, pp. 73–105, 2012.

[9] N. Alic and L. Partridge, "Death and dessert: nutrient signalling pathways and ageing," *Current Opinion in Cell Biology*, vol. 23, no. 6, pp. 738–743, 2011.

[10] C. M. McCay, M. F. Crowell, and L. A. Maynard, "The effect of retarded growth upon the length of life span and upon the ultimate body size: one figure," *The Journal of Nutrition*, vol. 10, no. 1, pp. 63–79, 1935.

[11] Z. Wu, S. Q. Liu, and D. Huang, "Dietary restriction depends on nutrient composition to extend chronological lifespan in budding yeast *Saccharomyces cerevisiae*," *PLoS ONE*, vol. 8, no. 5, Article ID e64448, 2013.

[12] J. Santos, F. Leitao-Correia, M. J. Sousa, and C. Leao, "Ammonium is a key determinant on the dietary restriction of yeast chronological aging in culture medium," *Oncotarget*, vol. 6, no. 9, pp. 6511–6523, 2015.

[13] R. C. Grandison, M. D. W. Piper, and L. Partridge, "Amino-acid imbalance explains extension of lifespan by dietary restriction in *Drosophila*," *Nature*, vol. 462, no. 7276, pp. 1061–1064, 2009.

[14] S. M. Solon-Biet, A. C. McMahon, J. W. O. Ballard et al., "The ratio of macronutrients, not caloric intake, dictates cardiometabolic health, aging, and longevity in ad libitum-fed mice," *Cell Metabolism*, vol. 19, no. 3, pp. 418–430, 2014.

[15] M. E. Levine, J. A. Suarez, S. Brandhorst et al., "Low protein intake is associated with a major reduction in IGF-1, cancer, and overall mortality in the 65 and younger but not older population," *Cell Metabolism*, vol. 19, no. 3, pp. 407–417, 2014.

[16] G. Taormina and M. G. Mirisola, "Calorie restriction in mammals and simple model organisms," *BioMed Research International*, vol. 2014, Article ID 308690, 10 pages, 2014.

[17] R. J. Colman, T. M. Beasley, J. W. Kemnitz, S. C. Johnson, R. Weindruch, and R. M. Anderson, "Caloric restriction reduces age-related and all-cause mortality in rhesus monkeys," *Nature Communications*, vol. 5, article 3557, 2014.

[18] K. P. Lee, S. J. Simpson, F. J. Clissold et al., "Lifespan and reproduction in *Drosophila*: new insights from nutritional geometry," *Proceedings of the National Academy of Sciences of the United States of America*, vol. 105, no. 7, pp. 2498–2503, 2008.

[19] A. L. Alvers, L. K. Fishwick, M. S. Wood et al., "Autophagy and amino acid homeostasis are required for chronological longevity in *Saccharomyces cerevisiae*," *Aging Cell*, vol. 8, no. 4, pp. 353–369, 2009.

[20] P. Fabrizio and V. D. Longo, "The chronological life span of *Saccharomyces cerevisiae*," *Aging Cell*, vol. 2, no. 2, pp. 73–81, 2003.

[21] P. Gomes, B. Sampaio-Marques, P. Ludovico, F. Rodrigues, and C. Leão, "Low auxotrophy-complementing amino acid concentrations reduce yeast chronological life span," *Mechanisms of Ageing and Development*, vol. 128, no. 5-6, pp. 383–391, 2007.

[22] C. J. Murakami, C. R. Burtner, B. K. Kennedy, and M. Kaeberlein, "A method for high-throughput quantitative analysis of yeast chronological life span," *The Journals of Gerontology Series A: Biological Sciences and Medical Sciences*, vol. 63, no. 2, pp. 113–121, 2008.

[23] D. L. Smith Jr., J. M. McClure, M. Matecic, and J. S. Smith, "Calorie restriction extends the chronological lifespan of Saccharomyces cerevisiae independently of the Sirtuins," *Aging Cell*, vol. 6, no. 5, pp. 649–662, 2007.

[24] J. C. Jiang, E. Jaruga, M. V. Repnevskaya, and S. M. Jazwinski, "An intervention resembling caloric restriction prolongs life span and retards aging in yeast," *The FASEB Journal*, vol. 14, no. 14, pp. 2135–2137, 2000.

[25] M. Kaeberlein, C. R. Burtner, and B. K. Kennedy, "Recent developments in yeast aging," *PLoS Genetics*, vol. 3, no. 5, article e84, 2007.

[26] M. Wei, P. Fabrizio, J. Hu et al., "Life span extension by calorie restriction depends on Rim15 and transcription factors downstream of Ras/PKA, Tor, and Sch9," *PLOS Genetics*, vol. 4, no. 1, article e13, 2008.

[27] M. Kaeberlein, K. T. Kirkland, S. Fields, and B. K. Kennedy, "Sir2-independent life span extension by calorie restriction in yeast," *PLoS Biology*, vol. 2, no. 9, Article ID E296, 2004.

[28] S.-J. Lin, M. Kaeberlein, A. A. Andalis et al., "Calorie restriction extends *Saccharomyces cerevisiae* lifespan by increasing respiration," *Nature*, vol. 418, no. 6895, pp. 344–348, 2002.

[29] J. Santos, C. Leão, and M. J. Sousa, "Growth culture conditions and nutrient signaling modulating yeast chronological longevity," *Oxidative Medicine and Cellular Longevity*, vol. 2012, Article ID 680304, 10 pages, 2012.

[30] C. De Virgilio and R. Loewith, "The TOR signalling network from yeast to man," *The International Journal of Biochemistry & Cell Biology*, vol. 38, no. 9, pp. 1476–1481, 2006.

[31] R. Dechant and M. Peter, "Nutrient signals driving cell growth," *Current Opinion in Cell Biology*, vol. 20, no. 6, pp. 678–687, 2008.

[32] B. Smets, R. Ghillebert, P. De Snijder et al., "Life in the midst of scarcity: adaptations to nutrient availability in *Saccharomyces cerevisiae*," *Current Genetics*, vol. 56, no. 1, pp. 1–32, 2010.

[33] V. D. Longo, "The Ras and Sch9 pathways regulate stress resistance and longevity," *Experimental Gerontology*, vol. 38, no. 7, pp. 807–811, 2003.

[34] S. Zaman, S. I. Lippman, L. Schneper, N. Slonim, and J. R. Broach, "Glucose regulates transcription in yeast through a network of signaling pathways," *Molecular Systems Biology*, vol. 5, article 245, 2009.

[35] P. Fabrizio, L.-L. Liou, V. N. Moy et al., "SOD2 functions downstream of Sch9 to extend longevity in yeast," *Genetics*, vol. 163, no. 1, pp. 35–46, 2003.

[36] S.-J. Lin, P.-A. Defossez, and L. Guarente, "Requirement of NAD and SIR2 for life-span extension by calorie restriction in saccharomyces cerevisiae," *Science*, vol. 289, no. 5487, pp. 2126–2128, 2000.

[37] P. Fabrizio, F. Pozza, S. D. Pletcher, C. M. Gendron, and V. D. Longo, "Regulation of longevity and stress resistance by Sch9 in yeast," *Science*, vol. 292, no. 5515, pp. 288–290, 2001.

[38] J. Hu, M. Wei, H. Mirzaei et al., "Tor-Sch9 deficiency activates catabolism of the ketone body-like acetic acid to promote trehalose accumulation and longevity," *Aging Cell*, vol. 13, no. 3, pp. 457–467, 2014.

[39] Y. Pan, E. A. Schroeder, A. Ocampo, A. Barrientos, and G. S. Shadel, "Regulation of yeast chronological life span by TORC1 via adaptive mitochondrial ROS signaling," *Cell Metabolism*, vol. 13, no. 6, pp. 668–678, 2011.

[40] A. Mesquita, M. Weinberger, A. Silva et al., "Caloric restriction or catalase inactivation extends yeast chronological lifespan by inducing H_2O_2 and superoxide dismutase activity," *Proceedings of the National Academy of Sciences of the United States of America*, vol. 107, no. 34, pp. 15123–15128, 2010.

[41] M. Weinberger, A. Mesquita, T. Carroll et al., "Growth signaling promotes chronological aging in budding yeast by inducing superoxide anions that inhibit quiescence," *Aging*, vol. 2, no. 10, pp. 709–726, 2010.

[42] A. Ocampo, J. Liu, E. A. Schroeder, G. S. Shadel, and A. Barrientos, "Mitochondrial respiratory thresholds regulate yeast chronological life span and its extension by caloric restriction," *Cell Metabolism*, vol. 16, no. 1, pp. 55–67, 2012.

[43] D. B. Friedman and T. E. Johnson, "A mutation in the age-1 gene in *Caenorhabditis elegans* lengthens life and reduces hermaphrodite fertility," *Genetics*, vol. 118, no. 1, pp. 75–86, 1988.

[44] C. Kenyon, "A pathway that links reproductive status to lifespan in *Caenorhabditis elegans*," *Annals of the New York Academy of Sciences*, vol. 1204, pp. 156–162, 2010.

[45] C. Kenyon, J. Chang, E. Gensch, A. Rudner, and R. Tabtiang, "A *C. elegans* mutant that lives twice as long as wild type," *Nature*, vol. 366, no. 6454, pp. 461–464, 1993.

[46] C. Kenyon, "The plasticity of aging: insights from long-lived mutants," *Cell*, vol. 120, no. 4, pp. 449–460, 2005.

[47] C. J. Kenyon, "The genetics of ageing," *Nature*, vol. 464, no. 7288, pp. 504–512, 2010.

[48] L. R. Lapierre and M. Hansen, "Lessons from *C. elegans*: signaling pathways for longevity," *Trends in Endocrinology and Metabolism*, vol. 23, no. 12, pp. 637–644, 2012.

[49] K. Seo, E. Choi, D. Lee, D.-E. Jeong, S. K. Jang, and S.-J. Lee, "Heat shock factor 1 mediates the longevity conferred by inhibition of TOR and insulin/IGF-1 signaling pathways in *C. elegans*," *Aging Cell*, vol. 12, no. 6, pp. 1073–1081, 2013.

[50] K. Houthoofd, B. P. Braeckman, I. Lenaerts et al., "Axenic growth up-regulates mass-specific metabolic rate, stress resistance, and extends life span in *Caenorhabditis elegans*," *Experimental Gerontology*, vol. 37, no. 12, pp. 1371–1378, 2002.

[51] Y.-J. Fei, K. Inoue, and V. Ganapathy, "Structural and functional characteristics of two sodium-coupled dicarboxylate transporters (ceNaDC1 and ceNaDC2) from *Caenorhabditis elegans* and their relevance to life span," *The Journal of Biological Chemistry*, vol. 278, no. 8, pp. 6136–6144, 2003.

[52] B. Lakowski and S. Hekimi, "The genetics of caloric restriction in *Caenorhabditis elegans*," *Proceedings of the National Academy of Sciences of the United States of America*, vol. 95, no. 22, pp. 13091–13096, 1998.

[53] D. Lee, W. Hwang, M. Artan, D.-E. Jeong, and S.-J. Lee, "Effects of nutritional components on aging," *Aging Cell*, vol. 14, no. 1, pp. 8–16, 2015.

[54] S.-J. Lee, C. T. Murphy, and C. Kenyon, "Glucose shortens the life span of *C. elegans* by downregulating DAF-16/FOXO activity and aquaporin gene expression," *Cell Metabolism*, vol. 10, no. 5, pp. 379–391, 2009.

[55] Y. Feng, B. G. Williams, F. Koumanov, A. J. Wolstenholme, and G. D. Holman, "FGT-1 is the major glucose transporter in *C. elegans* and is central to aging pathways," *The Biochemical Journal*, vol. 456, no. 2, pp. 219–229, 2013.

[56] M. Tatar, A. Kopelman, D. Epstein, M.-P. Tu, C.-M. Yin, and R. S. Garofalo, "A mutant *Drosophila* insulin receptor homolog that extends life-span and impairs neuroendocrine function," *Science*, vol. 292, no. 5514, pp. 107–110, 2001.

[57] I. Bjedov, J. M. Toivonen, F. Kerr et al., "Mechanisms of life span extension by rapamycin in the fruit fly *Drosophila melanogaster*," *Cell Metabolism*, vol. 11, no. 1, pp. 35–46, 2010.

[58] L. Partridge, N. Alic, I. Bjedov, and M. D. W. Piper, "Ageing in *Drosophila*: the role of the insulin/Igf and TOR signalling network," *Experimental Gerontology*, vol. 46, no. 5, pp. 376–381, 2011.

[59] M. E. Giannakou, M. Goss, and L. Partridge, "Role of dFOXO in lifespan extension by dietary restriction in *Drosophila melanogaster*: not required, but its activity modulates the response," *Aging Cell*, vol. 7, no. 2, pp. 187–198, 2008.

[60] K.-J. Min, R. Yamamoto, S. Buch, M. Pankratz, and M. Tatar, "*Drosophila* lifespan control by dietary restriction independent of insulin-like signaling," *Aging Cell*, vol. 7, no. 2, pp. 199–206, 2008.

[61] M. Tatar, S. Post, and K. Yu, "Nutrient control of *Drosophila longevity*," *Trends in Endocrinology and Metabolism*, vol. 25, no. 10, pp. 509–517, 2014.

[62] W. Mair, M. D. W. Piper, and L. Partridge, "Calories do not explain extension of life span by dietary restriction in *Drosophila*," *PLoS Biology*, vol. 3, no. 7, article e223, 2005.

[63] O. Meynet and J.-E. Ricci, "Caloric restriction and cancer: molecular mechanisms and clinical implications," *Trends in Molecular Medicine*, vol. 20, no. 8, pp. 419–427, 2014.

[64] M. G. Mirisola, G. Taormina, P. Fabrizio, M. Wei, J. Hu, and V. D. Longo, "Serine- and threonine/valine-dependent activation of PDK and Tor orthologs converge on Sch9 to promote aging," *PLoS Genetics*, vol. 10, no. 2, Article ID e1004113, 2014.

[65] V. M. Boer, S. Amini, and D. Botstein, "Influence of genotype and nutrition on survival and metabolism of starving yeast," *Proceedings of the National Academy of Sciences of the United States of America*, vol. 105, no. 19, pp. 6930–6935, 2008.

[66] R. W. Powers III, M. Kaeberlein, S. D. Caldwell, B. K. Kennedy, and S. Fields, "Extension of chronological life span in yeast by decreased TOR pathway signaling," *Genes and Development*, vol. 20, no. 2, pp. 174–184, 2006.

[67] J. P. Aris, A. L. Alvers, R. A. Ferraiuolo et al., "Autophagy and leucine promote chronological longevity and respiration proficiency during calorie restriction in yeast," *Experimental Gerontology*, vol. 48, no. 10, pp. 1107–1119, 2013.

[68] C. Ruckenstuhl, C. Netzberger, I. Entfellner et al., "Lifespan extension by methionine restriction requires autophagy-dependent vacuolar acidification," *PLoS Genetics*, vol. 10, no. 5, Article ID e1004347, 2014.

[69] J. E. Johnson and F. B. Johnson, "Methionine restriction activates the retrograde response and confers both stress tolerance and lifespan extension to yeast, mouse and human cells," *PLoS ONE*, vol. 9, no. 5, Article ID e97729, 2014.

[70] M. Binda, M.-P. Péli-Gulli, G. Bonfils et al., "The Vam6 GEF controls TORC1 by activating the EGO complex," *Molecular Cell*, vol. 35, no. 5, pp. 563–573, 2009.

[71] G. Bonfils, M. Jaquenoud, S. Bontron, C. Ostrowicz, C. Ungermann, and C. De Virgilio, "Leucyl-tRNA synthetase controls TORC1 via the EGO complex," *Molecular Cell*, vol. 46, no. 1, pp. 105–110, 2012.

[72] J. Gallinetti, E. Harputlugil, and J. R. Mitchell, "Amino acid sensing in dietary-restriction-mediated longevity: roles of signal-transducing kinases GCN2 and TOR," *Biochemical Journal*, vol. 449, no. 1, pp. 1–10, 2013.

[73] J. Santos, M. J. Sousa, and C. Leão, "Ammonium is toxic for aging yeast cells, inducing death and shortening of the chronological lifespan," *PLoS ONE*, vol. 7, no. 5, Article ID e37090, 2012.

[74] J. Santos, C. Leão, and M. J. Sousa, "Ammonium-dependent shortening of CLS in yeast cells starved for essential amino acids is determined by the specific amino acid deprived, through different signaling pathways," *Oxidative Medicine and Cellular Longevity*, vol. 2013, Article ID 161986, 10 pages, 2013.

[75] A. Rousakis, A. Vlassis, A. Vlanti, S. Patera, G. Thireos, and P. Syntichaki, "The general control nonderepressible-2 kinase mediates stress response and longevity induced by target of rapamycin inactivation in *Caenorhabditis elegans*," *Aging Cell*, vol. 12, no. 5, pp. 742–751, 2013.

[76] A. Vlanti, A. Rousakis, and P. Syntichaki, "Gcn2 and TOR converge on aging," *Aging*, vol. 5, no. 8, pp. 584–585, 2013.

[77] B. Meissner, M. Boll, H. Daniel, and R. Baumeister, "Deletion of the intestinal peptide transporter affects insulin and TOR signaling in *Caenorhabditis elegans*," *Journal of Biological Chemistry*, vol. 279, no. 35, pp. 36739–36745, 2004.

[78] F. Cabreiro, C. Au, K.-Y. Leung et al., "Metformin retards aging in *C. elegans* by altering microbial folate and methionine metabolism," *Cell*, vol. 153, no. 1, pp. 228–239, 2013.

[79] B. C. Lee, A. Kaya, S. Ma et al., "Methionine restriction extends lifespan of *Drosophila melanogaster* under conditions of low amino-acid status," *Nature Communications*, vol. 5, article 3592, 2014.

[80] M. D. W. Piper, E. Blanc, R. Leitão-Gonçalves et al., "A holidic medium for *Drosophila melanogaster*," *Nature Methods*, vol. 11, no. 1, pp. 100–105, 2014.

[81] H. Mirzaei, J. A. Suarez, and V. D. Longo, "Protein and amino acid restriction, aging and disease: from yeast to humans," *Trends in Endocrinology and Metabolism*, vol. 25, no. 11, pp. 558–566, 2014.

[82] I. Sanchez-Roman, A. Gómez, I. Pérez et al., "Effects of aging and methionine restriction applied at old age on ROS generation and oxidative damage in rat liver mitochondria," *Biogerontology*, vol. 13, no. 4, pp. 399–411, 2012.

[83] A. Sanz, P. Caro, V. Ayala, M. Portero-Otin, R. Pamplona, and G. Barja, "Methionine restriction decreases mitochondrial oxygen radical generation and leak as well as oxidative damage to mitochondrial DNA and proteins," *The FASEB Journal*, vol. 20, no. 8, pp. 1064–1073, 2006.

[84] R. Chen, Y. Zou, D. Mao et al., "The general amino acid control pathway regulates mTOR and autophagy during serum/glutamine starvation," *The Journal of Cell Biology*, vol. 206, no. 2, pp. 173–182, 2014.

[85] M. D. W. Piper, L. Partridge, D. Raubenheimer, and S. J. Simpson, "Dietary restriction and aging: a unifying perspective," *Cell Metabolism*, vol. 14, no. 2, pp. 154–160, 2011.

[86] R. J. Colman, R. M. Anderson, S. C. Johnson et al., "Caloric restriction delays disease onset and mortality in rhesus monkeys," *Science*, vol. 325, no. 5937, pp. 201–204, 2009.

[87] J. A. Mattison, G. S. Roth, T. M. Beasley et al., "Impact of caloric restriction on health and survival in rhesus monkeys from the NIA study," *Nature*, vol. 489, no. 7415, pp. 318–321, 2012.

[88] T. T. Fung, R. M. van Dam, S. E. Hankinson, M. Stampfer, W. C. Willett, and F. B. Hu, "Low-carbohydrate diets and all-cause and cause-specific mortality: two cohort studies," *Annals of Internal Medicine*, vol. 153, no. 5, pp. 289–298, 2010.

[89] P. Lagiou, S. Sandin, M. Lof, D. Trichopoulos, H.-O. Adami, and E. Weiderpass, "Low carbohydrate-high protein diet and incidence of cardiovascular diseases in Swedish women: prospective cohort study," *British Medical Journal*, vol. 344, Article ID e4026, 2012.

[90] Z. Wu, L. Song, S. Q. Liu, and D. Huang, "Independent and additive effects of glutamic acid and methionine on yeast longevity," *PLoS ONE*, vol. 8, no. 11, Article ID e79319, 2013.

[91] C. Picazo, H. Orozco, E. Matallana, and A. Aranda, "Interplay among Gcn5, Sch9 and mitochondria during chronological aging of wine yeast is dependent on growth conditions," *PLoS ONE*, vol. 10, no. 2, Article ID e0117267, 2015.

[92] L. T. Robertson and J. R. Mitchell, "Benefits of short-term dietary restriction in mammals," *Experimental Gerontology*, vol. 48, no. 10, pp. 1043–1048, 2013.

[93] R. J. O. Dowling, S. Niraula, V. Stambolic, and P. J. Goodwin, "Metformin in cancer: translational challenges," *Journal of Molecular Endocrinology*, vol. 48, no. 3, pp. R31–E43, 2012.

[94] Y. Storozhuk, S. N. Hopmans, T. Sanli et al., "Metformin inhibits growth and enhances radiation response of non-small cell lung cancer (NSCLC) through ATM and AMPK," *British Journal of Cancer*, vol. 108, no. 10, pp. 2021–2032, 2013.

[95] A. P. Sharples, D. C. Hughes, C. S. Deane, A. Saini, C. Selman, and C. E. Stewart, "Longevity and skeletal muscle mass: the role

of IGF signalling, the sirtuins, dietary restriction and protein intake," *Aging Cell*, vol. 14, no. 4, pp. 511–523, 2015.

[96] V. D. Longo and M. P. Mattson, "Fasting: molecular mechanisms and clinical applications," *Cell Metabolism*, vol. 19, no. 2, pp. 181–192, 2014.

[97] C. Lee and V. D. Longo, "Fasting vs dietary restriction in cellular protection and cancer treatment: from model organisms to patients," *Oncogene*, vol. 30, no. 30, pp. 3305–3316, 2011.

[98] C. Lee, L. Raffaghello, S. Brandhorst et al., "Fasting cycles retard growth of tumors and sensitize a range of cancer cell types to chemotherapy," *Science Translational Medicine*, vol. 4, no. 124, p. 124ra27, 2012.

[99] Y. Shi, E. Felley-Bosco, T. M. Marti, K. Orlowski, M. Pruschy, and R. A. Stahel, "Starvation-induced activation of ATM/Chk2/p53 signaling sensitizes cancer cells to cisplatin," *BMC Cancer*, vol. 12, article 571, 2012.

[100] C. Lee, F. M. Safdie, L. Raffaghello et al., "Reduced levels of IGF-I mediate differential protection of normal and cancer cells in response to fasting and improve chemotherapeutic index," *Cancer Research*, vol. 70, no. 4, pp. 1564–1572, 2010.

[101] M. N. Harvie, M. Pegington, M. P. Mattson et al., "The effects of intermittent or continuous energy restriction on weight loss and metabolic disease risk markers: a randomized trial in young overweight women," *International Journal of Obesity*, vol. 35, no. 5, pp. 714–727, 2011.

[102] M. C. Klempel, C. M. Kroeger, and K. A. Varady, "Alternate day fasting (ADF) with a high-fat diet produces similar weight loss and cardio-protection as ADF with a low-fat diet," *Metabolism: Clinical and Experimental*, vol. 62, no. 1, pp. 137–143, 2013.

[103] R. Wan, I. Ahmet, M. Brown et al., "Cardioprotective effect of intermittent fasting is associated with an elevation of adiponectin levels in rats," *The Journal of Nutritional Biochemistry*, vol. 21, no. 5, pp. 413–417, 2010.

[104] R. Wan, S. Camandola, and M. P. Mattson, "Intermittent food deprivation improves cardiovascular and neuroendocrine responses to stress in rats," *Journal of Nutrition*, vol. 133, no. 6, pp. 1921–1929, 2003.

[105] J. B. Johnson, W. Summer, R. G. Cutler et al., "Alternate day calorie restriction improves clinical findings and reduces markers of oxidative stress and inflammation in overweight adults with moderate asthma," *Free Radical Biology & Medicine*, vol. 42, no. 5, pp. 665–674, 2007.

[106] G. Smedslund, M. G. Byfuglien, S. U. Olsen, and K. B. Hagen, "Effectiveness and safety of dietary interventions for rheumatoid arthritis: a systematic review of randomized controlled trials," *Journal of the American Dietetic Association*, vol. 110, no. 5, pp. 727–735, 2010.

[107] V. Berti, J. Murray, M. Davies et al., "Nutrient patterns and brain biomarkers of Alzheimer's disease in cognitively normal individuals," *Journal of Nutrition, Health & Aging*, vol. 19, no. 4, pp. 413–423, 2015.

[108] T. V. Arumugam, T. M. Phillips, A. Cheng, C. H. Morrell, M. P. Mattson, and R. Wan, "Age and energy intake interact to modify cell stress pathways and stroke outcome," *Annals of Neurology*, vol. 67, no. 1, pp. 41–52, 2010.

[109] V. K. M. Halagappa, Z. Guo, M. Pearson et al., "Intermittent fasting and caloric restriction ameliorate age-related behavioral deficits in the triple-transgenic mouse model of Alzheimer's disease," *Neurobiology of Disease*, vol. 26, no. 1, pp. 212–220, 2007.

[110] N. Maswood, J. Young, E. Tilmont et al., "Caloric restriction increases neurotrophic factor levels and attenuates neurochemical and behavioral deficits in a primate model of Parkinson's disease," *Proceedings of the National Academy of Sciences of the United States of America*, vol. 101, no. 52, pp. 18171–18176, 2004.

Hindawi Publishing Corporation
Oxidative Medicine and Cellular Longevity
Volume 2016, Article ID 9151290, 9 pages
http://dx.doi.org/10.1155/2016/9151290

Research Article

Toll-Like Receptor 4 Reduces Oxidative Injury via Glutathione Activity in Sheep

Shoulong Deng,[1] Kun Yu,[2,3] Qian Wu,[4] Yan Li,[3] Xiaosheng Zhang,[5] Baolu Zhang,[6] Guoshi Liu,[2] Yixun Liu,[1] and Zhengxing Lian[2,3]

[1]*State Key Laboratory of Reproductive Biology, Institute of Zoology, Chinese Academy of Sciences, Beijing 100101, China*
[2]*Laboratory of Animal Genetics and Breeding, College of Animal Science and Technology, China Agricultural University, Beijing 100193, China*
[3]*State Key Laboratory of Agrobiotechnology, College of Biological Sciences, China Agricultural University, Beijing 100193, China*
[4]*School of Biological Science and Medical Engineering, Beijing University of Aeronautics and Astronautics, Beijing 100191, China*
[5]*Tianjin Institute of Animal Sciences, Tianjin 300112, China*
[6]*State Oceanic Administration, Beijing 100860, China*

Correspondence should be addressed to Yixun Liu; liuyx@ioz.ac.cn and Zhengxing Lian; lianzhx@cau.edu.cn

Received 11 March 2015; Accepted 28 June 2015

Academic Editor: Hariom Yadav

Toll-like receptor 4 (TLR4) is an important sensor of Gram-negative bacteria and can trigger activation of the innate immune system. Increased activation of TLR4 can lead to the induction of oxidative stress. Herein, the pathway whereby TLR4 affects antioxidant activity was studied. In TLR4-overexpressing sheep, TLR4 expression was found to be related to the integration copy number when monocytes were challenged with lipopolysaccharide (LPS). Consequently, production of malondialdehyde (MDA) was increased, which could increase the activation of prooxidative stress enzymes. Meanwhile, activation of an antioxidative enzyme, glutathione peroxidase (GSH-Px), was increased. Real-time PCR showed that expression of activating protein-1 (AP-1) and the antioxidative-related genes was increased. By contrast, the expression levels of superoxide dismutase 1 (SOD1) and catalase (CAT) were reduced. In transgenic sheep, glutathione (GSH) levels were dramatically reduced. Furthermore, transgenic sheep were intradermally injected with LPS in each ear. The amounts of inflammatory infiltrates were correlated with the number of TLR4 copies that were integrated in the genome. Additionally, the translation of γ-glutamylcysteine synthetase (γ-GCS) was increased. Our findings indicated that overexpression of TLR4 in sheep could ameliorate oxidative injury through GSH secretion that was induced by LPS stimulation. Furthermore, TLR4 promoted γ-GCS translation through the AP-1 pathway, which was essential for GSH synthesis.

1. Introduction

Toll-like receptor 4 (TLR4) is a pattern-recognition receptor (PRR) that plays a key role in innate immunity and host defense. TLR4 is a critical signal transducer of lipopolysaccharide (LPS), the major exocellular component of Gram-negative bacteria. The activation of TLR4 can promote cell proliferation and apoptosis [1]. TLR4 can initiate immune responses through both myeloid differentiation primary response gene 88- (MyD88-) dependent and independent pathways. In the MyD88-dependent pathway, TLR4 activates nuclear factor-κB (NF-κB) and activating protein-1 (AP-1), which leads to oxidative stress and inflammation [2, 3].

Oxidative stress was frequently observed after pathogenic microbial infections. In this condition oxidative stress is supposed to ward off pathogenic microbes. When excessive, tissue can be damaged by the overproduction of reactive oxygen species (ROS) and reactive nitrogen species (RNS). To protect organs, ROS/RNS are scavenged via antioxidant mechanisms. There are two major physiological antioxidant defense systems, endogenous antioxidants (glutathione) and membrane-protecting enzymes (superoxide dismutase

Table 1: The primer sequences.

Primer	Forward (5′-3′)	Reverse (5′-3′)
cTLR4	TACGGTAAACTGCCCACTTG	ACCTGGAGAAGTTATGGCTG
TLR4	CTGAATCTCTACAAAATCCC	CTTAATTTCGCATCTGGATA
AP-1	TGAAGGAAGAGCCGCAGAC	CCACCTGTTCCCTGAGCATA
SOD1	CGAGGCAAAGGGAGATAAA	CTCCAGCGTTTCCAGTCTT
CAT	GAAACGCCTGTGTGAGAAC	ACATAGGTGTGAACTGCGT
GSTα1	GTTCCAGCAAGTGCCAATG	GGGAGATAACGGTTTGTCG
γ-GCS	ATGGCTCAAGCGTTCGTCA	CAGTTCCCCTCTCTCGTGC
HO1	GGCGGAGAATGCCGAGTT	CCTCCTGGAGTCGCTGAACAT
β-actin	AGATGTGGATCAGCAAGCAG	CCAATCTCATCTCGTTTTCTG

(SOD), catalase (CAT), and glutathione peroxidase (GSH-Px)) [4]. Genes, such as CAT, SOD, glutathione S transferase (GST), γ-glutamylcysteine synthetase (γ-GCS), and heme oxygenase 1 (HOl), are used for monitoring antioxidant procedure, for their encode products related to antioxidative stress responses that protect cells from oxidative stress [5–7].

TLR4 pathways are crosslink to oxidative stress. After TLR4 triggers NF-κB activation, inflammatory factors, such as interleukin-6 (IL-6) and tumor necrosis factor-alpha (TNF-α), are secreted. These inflammatory factors accelerate the inflammatory response by reducing SOD activity and increasing malondialdehyde (MDA) production. As a result, the increasing of ROS/RNS production could affect the antioxidative capacity of cells [8, 9]. The AP-1 pathway is involved in regulation of GSH production [10]. As an antioxidant, GSH plays an important role in preventing oxidative damage by directly interacting with ROS/RNS or by operating as a cofactor for various enzymes [11]. Being a rate-limiting enzyme, γ-GCS has impact on GSH synthesis. The upregulation of γ-GCS can increase antioxidant capacity [12].

Many sheep diseases are closely related to increased amounts of oxidation products, because accumulation of oxidative products can reduce sheep immunity and host defense responses [13]. Studies have shown that the inflammatory response is suppressed in TLR4-mutant mice [14, 15]. Overexpression of TLR4 amplifies the host response to LPS and provides transgenic mice with a survival advantage [16]. The enhanced inflammatory response helps to remove pathogens, but excessive inflammation can result in oxidative damage. Herein, we generated lines of transgenic sheep that overexpressed TLR4 with a variety of copy numbers. LPS was administered to induce oxidative damage. The TLR4 pathway, which is involved in antioxidative damage, was studied to elucidate the antioxidative stress response in sheep.

2. Materials and Methods

2.1. Genotyping of Tg Sheep. Transgenic sheep were produced by microinjection. The transformed exogenous genes in the experimental offspring were analyzed by Southern blotting of genomic DNA from ear biopsies, and we used a PCR-based method to generate a specific Digoxigenin-labeled probe (Roche Diagnostics, Mannheim, Germany). Exogenous TLR4 was analyzed by Southern blotting with the probe cTLR4 (Table 1). Genomic DNA (20 ng/μL) was digested with *Vsp*I and *Sma*I (NEB, Beverly, MA, USA). The gene expression levels and TLR4 copy numbers were quantified by real-time PCR. Mononuclear cells were isolated from transgenic sheep peripheral blood using sheep lymphocyte separation medium (TBD, Tianjin, China). Real-time PCR was used to detect exogenous copies of TLR4. Primers were designed to target sequences located in cTLR4. *β-actin* was used as an internal standard (Table 1). Real-time PCR reactions were carried out with a Real Master Mix SYBR Green Kit (Tiangen, China) using MX300P (Stratagene) following the manufacturer's protocol.

2.2. Monocyte Cultures. Sheep with exogenous TLR4 copies ranging from 1 to 3 copies were randomly selected. Those sheep were divided into three groups based on the number of exogenous TLR4 copies. Each group included three transgenic sheep with the same number of exogenous TLR4 copies. A total of 10 mL peripheral blood from 6-month-old sheep was collected, and heparin was used for anticoagulation. Monocyte isolation and culture was carried out according to the sheep lymphocyte separation medium manufacturer's instructions. Then, 1×10^5 cells were seeded in each well of 6-well plates in triplicate wells for each group. RM1640 (Gibco, Grand Island, NY, USA) medium containing 10% FBS (Gibco) was changed every 24 h. Monocytes were stimulated using LPS (1 μg/mL; Sigma-Aldrich, St. Louis, MO, USA) after 48 h.

At 8 h after stimulation, culture medium was collected and frozen. RNA from adherent cells was isolated using TRIzol (Invitrogen, Carlsbad, CA, USA). Then, cDNA were synthesized. The mRNA transcript abundance of TLR4 was measured using real-time PCR. Gene expression levels of AP-1, SOD1, CAT, GSTα1, γ-GCS, and HO1 were quantified by RT-PCR. Primers sequences are shown in Table 1.

2.3. Measurements of Oxidative Stress-Related Enzymes. Cell suspensions were dropped in liquid nitrogen and samples were thawed on ice; this freeze/thaw cycle was repeated two more times. The activities of iNOS, T-SOD, CAT, COX-2, NADPH oxidase, MDA, GSH, and GSSH were examined by spectrophotometry using respective detection kits (Jiancheng, Nanjing, China). GSH-Px was detected

using an enzyme-linked immunosorbent assay (ELISA) kit (CUSABIO, Hubei, China) following previously published methods. The OD ratio was obtained using a microplate spectrophotometer.

2.4. In Vivo Injection of LPS. Local inflammatory responses were observed in three 3-month-old transgene-positive individuals after intradermal injection of LPS (3 mg/mL in 100 μL) in each ear. At 8 h after challenge, tissues were collected. Pathological changes were observed using hematoxylin and eosin staining. Immunohistochemically stained sections were used for observations of γ-GCS (Abcam, Cambridge, UK) protein expression.

2.5. Statistical Analyses. All the above experiments were repeated 3 times. Data were subjected to analysis of variance using the GLM procedures of Statistical Analysis System (SAS Institute, Cary, NC, USA). All data were expressed as mean ± SEM. Differences were considered to be significant when $p < 0.05$.

3. Result

3.1. Overexpression of TLR4 Increases Oxidative Damage in Sheep. Transgenic sheep that overexpressed TLR4 were produced by microinjection. Southern blot analyses were used to detect positive transgenic lambs (Figure 1(a)). By analyzing the developed blots to calculate the transgene copy number, individuals were identified that carried various copy numbers of the exogenous TLR4 gene. Real-time PCR was used to study exogenous TLR4 expression. The mRNA transcript levels of monocytes from selected lambs were observed (Figure 1(b)), and the numbers of exogenous TLR4 copies were calculated, which were 1.24, 1.30, 1.38, 1.67, 1.89, 2.46, 2.84, 3.00, and 3.23, respectively. Based on the number of exogenous TLR4 copies, nine lambs were selected and divided into three groups (Figure 1(c)).

At 8 h after LPS stimulation, TLR4 transcript levels in monocytes from nine lambs were measured. We found that the TLR4 mRNA transcript levels and MDA contents were correlated with the number of exogenous TLR4 copies (Figures 1(d) and 1(e)). Transcript levels in transgenic sheep were all significantly higher than those in wild-type (Wt) sheep ($p < 0.05$). Compared with Wt sheep, more oxygen free radicals were generated, resulting in enhanced oxidative damage in transgenic animals.

Ear tissue inflammatory reactions induced by LPS stimulation were next assessed in Wt and transgenic sheep (Figure 2). Inflammatory cell infiltrates were observed in the dermis. Inflammatory cells were found to increase in Tg-1 group animals. Many inflammatory cells were also observed in Tg-2 animals. In Tg-3 animals, the horny layer (of the epidermis) cuticle off and many inflammatory cells, including segmented cells, could be observed. Oxidative stress induced tissue disequilibrium. Subsequently, inflammatory cell infiltration and inflammatory mediator release were detected in inflammatory tissues. *In vivo* observations of tissue sections showed that the degree of inflammation was associated with the transgene copy number.

3.2. TLR4 Promotes Oxidative Stress-Related Enzyme Activation following LPS Stimulation in Sheep. Oxidation intermediate products are major drivers of oxidative stress and are mostly either NO or O_2^-. Catalysis by COX-2 can promote NO synthesis and secretion. In this present study, monocytes with various exogenous TLR4 copy numbers were challenged with 1 μg/mL LPS for 8 h. Compared with Wt sheep, activation of cellular COX-2 and iNOS was significantly higher in Tg animals (Figures 3(a) and 3(b)). Meanwhile, COX-2 and iNOS activation were well correlated with TLR4 copy number.

Enzyme activities between the transgenic groups were significantly different ($p < 0.05$). For NADPH oxidase activation, there was no significant difference between the Tg-1 and Wt groups; however, there was a significant difference between the Tg-2 and Tg-3 groups ($p < 0.05$). Levels of NADPH oxidase activation in the Tg-2 group were much higher than those in the Tg-1 and Wt groups (Figure 3(c)). These findings indicated that overexpressed TLR4 could trigger ROS/RNS release and could consequently induce oxidative stress. More copies of TLR4 enhanced free radical release and increased cellular oxidative stress.

3.3. In Response to LPS Stimulation, Overexpressed TLR4 Reduced T-SOD and Increased GSH-Px Activities. In this present study, monocytes that expressed various copy numbers of TLR4 showed similar patterns of T-SOD and CAT activation after 8 h exposure to LPS (Figures 3(d) and 3(e)). Expression levels in cells from Tg-1 sheep were higher than those from Wt sheep, but the differences were not significant ($p > 0.05$). Both of these enzymes exhibited lower expression levels in the Tg-3 group compared with the Tg-2 group ($p < 0.05$). GSH-Px activation tended to be positively correlated with TLR4 copy number (Figure 3(f)). We found that TLR4 promoted the activation of GSH-Px, T-SOD, and CAT at relatively low copy numbers to maintain the level of oxidative stress. Increased TLR4 copy numbers could reduce T-SOD and CAT activation, whereas GSH-Px activation was increased.

3.4. Reduced GSH Content in TLR4 Overexpressing Sheep. Monocytes with various TLR4 copy numbers were collected and challenged with LPS for 8 h. GSH and GSSG contents were measured (Figures 4(a) and 4(b)), and they were higher in the Tg-1 group, although there was no significant difference between the Tg-1 and Wt groups ($p > 0.05$). The GSSG contents tended to increase in correlation with the TLR4 copy number, which was in contrast to those of GSH. Overexpressed TLR4 caused more oxidative damage. During this process, oxidation intermediate products were scavenged. GSH was maintained at a higher level in transgene-positive monocytes, and this difference was significant when compared with the Wt group ($p < 0.05$). GSSG contents were negatively correlated with TLR4 copy number, indicating that the free radicals had been scavenged.

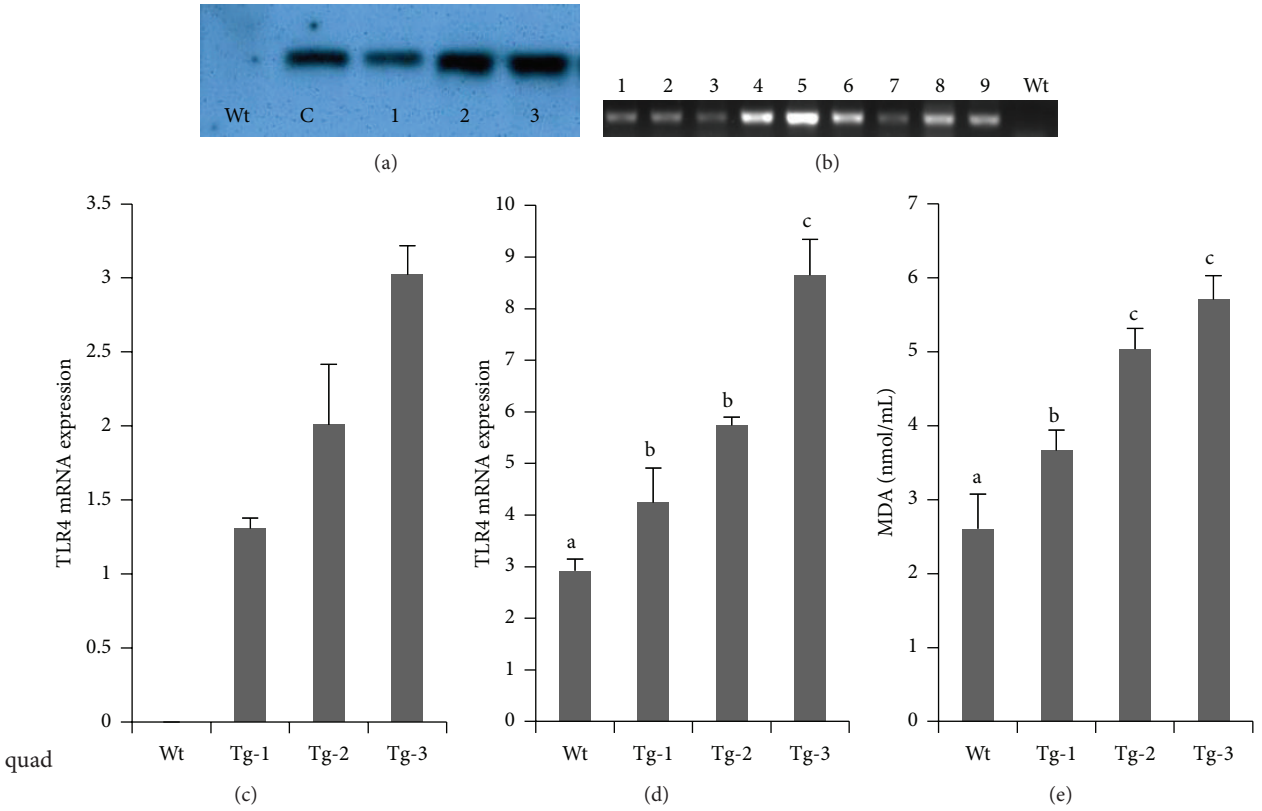

Figure 1: Oxidative damage in sheep with transgenic TLR4 overexpression. (a) Southern blot analysis; Wt, wild type; 1–3 were transgenic sheep (Tg); (c) TLR4 plasmid. (b) Real-time PCR product analysis by agarose gel electrophoresis. TLR4 expression levels were different in transgenic animals; 1–9, transgenic sheep (Tg). (c) Exogenous TLR4 copies were measured by real-time PCR. (d) Relative quantitative analysis of TLR4 expression in cells from transgenic sheep after LPS stimulation. (e) MDA constant measurements. Data represent mean ± SE. ^{a,b,c}Different superscript letters indicate significantly different values between groups ($p < 0.05$). Wt, wild type; Tg-1, Tg-2, and Tg-3 were transgenic sheep that had 1, 2, or 3 copies of TLR4.

The ratio of GSH/GSSG indirectly reflects the levels of oxidative stress, so ratios were calculated for each group at both 8 and 48 h. We found that the ratio of GSH/GSSG was negatively correlated with TLR4 copy number and was lower in the Tg-2 and Tg-3 groups compared with the Tg-1 and Wt groups at 8 h ($p < 0.05$; Figure 4(c)). At 48 h after stimulation, the ratio of GSH/GSSG had returned to the average level. These findings indicated that, in response to LPS stimulation, extra copies of TLR4 could lead to lower amounts of GSH. However, over time, the ratio could quickly increase to an average level. The period of time over which oxidative damage occurred was reduced in transgenic animals.

3.5. Overexpression of TLR4 Promoted AP-1 Expression and the Regulation of Antioxidative Stress Genes. Real-time PCR was used to study TLR4 downstream genes expressed, including AP-1, CAT, SOD1, GSTα1, γ-GCS, and HOl (Figure 4(d)). Levels of AP-1 expression increased in correlation with exogenous TLR4 copy numbers. The expression levels of GSTα1, γ-GCS, and HOl showed similar patterns. By contrast, CAT and SOD1 expression levels showed a decreasing pattern. γ-GCS could also be observed by immunohistochemistry. More γ-GCS was observed in the high TLR4 copy number group (Figure 5). Levels of CAT and SOD1 expression were suppressed in the high TLR4 copy number groups. AP-1 expression levels were higher in the high TLR4 copy number groups. In support of a feedback regulation mechanism, HO1 expression was enhanced, which could potentially neutralize any oxidative effects. The increased amounts of GSTα1 and γ-GCS expression indicated that GSH synthesis was promoted to scavenge free radicals.

4. Discussion

Both oxidative stress and LPS-induced immunity response can share TLR4 pathways. Binding with myeloid differentiation factor 2 (MD2) LPS induces TLR4 signal transduction, enhancing both phagocytosis and cytokine production in response to Gram-negative bacteria [17]. There are two major pathways for TLR4 transduction, MyD88-dependent and independent pathways. In the MyD88-dependent pathway, MyD88 triggers interleukin-1 receptor-associated kinase (IRAK) binding to TNF receptor-associated factor-6 (TRAF6), resulting in the nuclear translocation of NF-κB, and initiates the AP-1 pathway [18, 19]. Meanwhile, TLR4 pathways play important roles in oxidative stress by

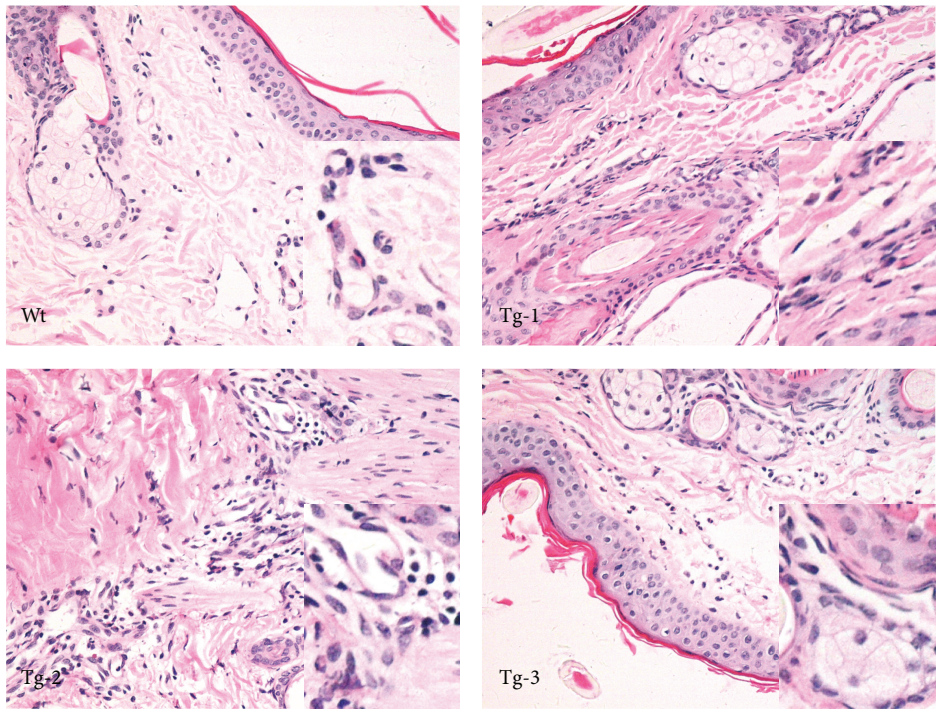

Figure 2: Inflammatory reactions in TLR4 transgenic sheep. Pathological changes were observed after the administration of LPS (hematoxylin and eosin staining; 400x magnification). Wt, wild type; Tg-1, Tg-2, and Tg-3 were transgenic sheep that had 1, 2, or 3 copies of TLR4.

promoting oxidative stress-related enzyme activation [20]. Products of oxidative stress act as second messengers to promote cytokine synthesis by activating NF-κB and AP-1 [21]. Since the iNOS is one of the downstream genes of TLR4, the TLR4 pathways contributed to upregulation of iNOS in transgenic sheep. Consequently, neutrophils were triggered to produce superoxide, which can increase macrophage activation [22]. COX-2 is the rate-limiting enzyme of prostaglandin synthesis, and COX-2 is involved in both acute and chronic inflammation under pathological conditions. Both NF-κB and AP-1 can regulate COX-2 transcription [23]. In this study, COX-2 expression tended to increase according to TLR4 copies, which indicated that COX-2 transcription was regulated by TLR4 pathway. NAPDH oxidase production is administrated by TLR4 through the IRAK4 pathway [24]. We found that LPS activated AP-1 in transgenic animals, especially in sheep with high TLR4 copy numbers. This could be a result of AP-1 interacting with NF-κB [25]. Meanwhile, expression of HO1, another important anti-inflammatory enzyme, was detected. Results showed HO1 expressions were found increasing in transgenic sheep. Previous studies showed that HO1 directly regulates AP-1 expression, independently of its catalytic activity [26, 27]. Increased HO1 activity can suppress TLR4-induced signal transduction [28]. Our results suggest the negative feedback loop was initiated to reduce the inflammatory response in TLR4-overexpressed sheep.

Oxidative stress represents disequilibrium of the oxidative system. When an organ is infected, many types of inflammatory cells are activated. NO production is promoted and a large amount of oxygen free radicals is generated to remove pathogens. Large amounts of oxidation intermediates and their derivatives can not only destroy bacteria membranes, but also cause tissue damage [29]. A key feature of oxidative damage is the breakdown of the enzymatic defense system. SOD is a crucial enzyme for scavenging oxygen free radicals. In this present study, the SOD activation was found upregulated in Tg-1 animals. This suggests that the tissue was under mild oxidative stress conditions [30]. While SOD expression was suppressed in Tg-2 and Tg-3 groups, this indicated that tissues were under acute stress conditions. SOD is consumed in the process of scavenging oxygen free radicals. Subsequently, tissues are damaged by reactive oxygen accumulation [31]. All these findings indicated that excess SOD was consumed in TLR4 transgenic sheep and that overexpressed TLR4 caused serious damage to the antioxidative stress enzyme system in transgenic sheep.

Glutathione is a nonenzymatic antioxidant component that is important for organs to guard against free radicals. In the presence of GSH, GSH-Px can catalyze almost all ROOH into ROH. In certain tissues, GSH-Px acts in place of CAT to eliminate H_2O_2 [32]. In this present study, CAT activity was reduced and GSH-Px expression was increased following LPS stimulation. GST might regulate antioxidative enzyme expression [33] and AP-1 can upregulate GST transcription, whereas GSH can downregulate GST transcription [34]. We obtained similar results, as AP-1 expression was observed to increase, and levels of GSTα1 transcription were also found to be elevated. In inflammatory conditions, ROS can be produced by macrophages and neutrophils. The inflammation caused by ROS could be reversed by the addition of exogenous GSH [35]. In this present study,

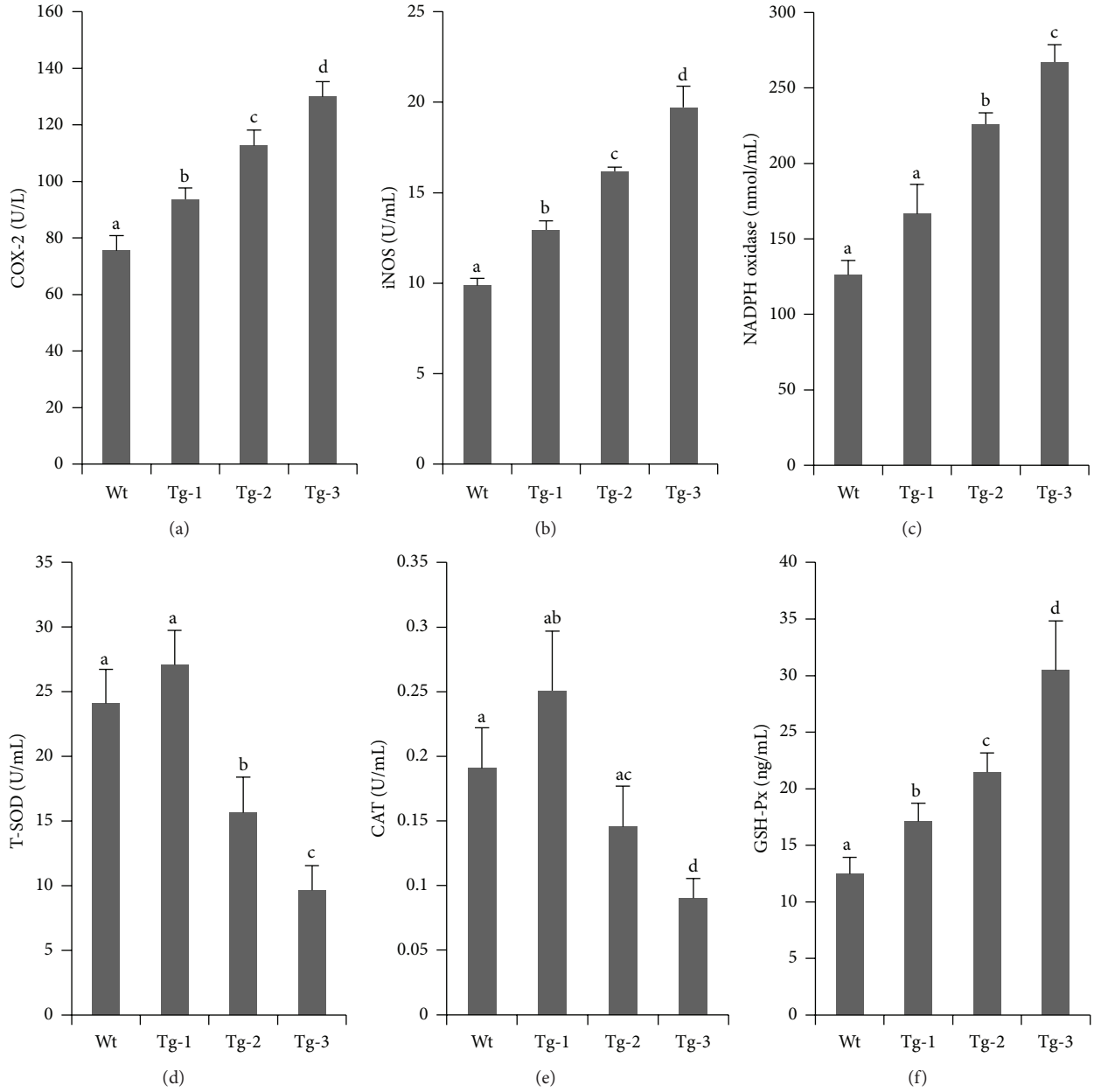

Figure 3: Expression of oxidative stress-related kinases in monocytes from transgenic sheep. Detection of the expression levels of oxidative stress kinases: (a) COX-2, (b) iNOS, and (c) NADPH oxidase. Detection of the activation of antioxidative damage-related kinases: (d) T-SOD, (e) CAT, and (f) Gsh-Px. Data represent mean ± SE. ^{a,b,c,d}Different superscripts indicate significantly different values between groups ($p < 0.05$). Wt, wild type; Tg-1, Tg-2, and Tg-3 were transgenic sheep that had 1, 2, or 3 copies of TLR4.

expressions of γ-GCS, rate-limiting enzyme for GSH synthesis, were observed to be increasing correlated with TLR4 copy numbers. Under oxidative stress conditions, γ-GCS is compensatory upregulated to increase GSH synthesis. GSH can be transferred to GSSG to eliminate free radicals avoiding tissue's oxidative damage [36, 37]. But the extra copies of the TLR4 gene led to more rapid GSH consumption and dramatically increased GSSG. This finding suggests that more severe oxidative damage occurred in TLR4 overexpressing sheep. Over time, GSH was maintained at a relatively high level and returned to an average level more quickly in transgenic animals. Accordingly, the time period of oxidative damage was shortened.

5. Conclusions

It has been established that TLR4 is related to the oxidative stress response [38]. This present study found that overexpressed TLR4 inhibited SOD activity and triggered AP-1 to

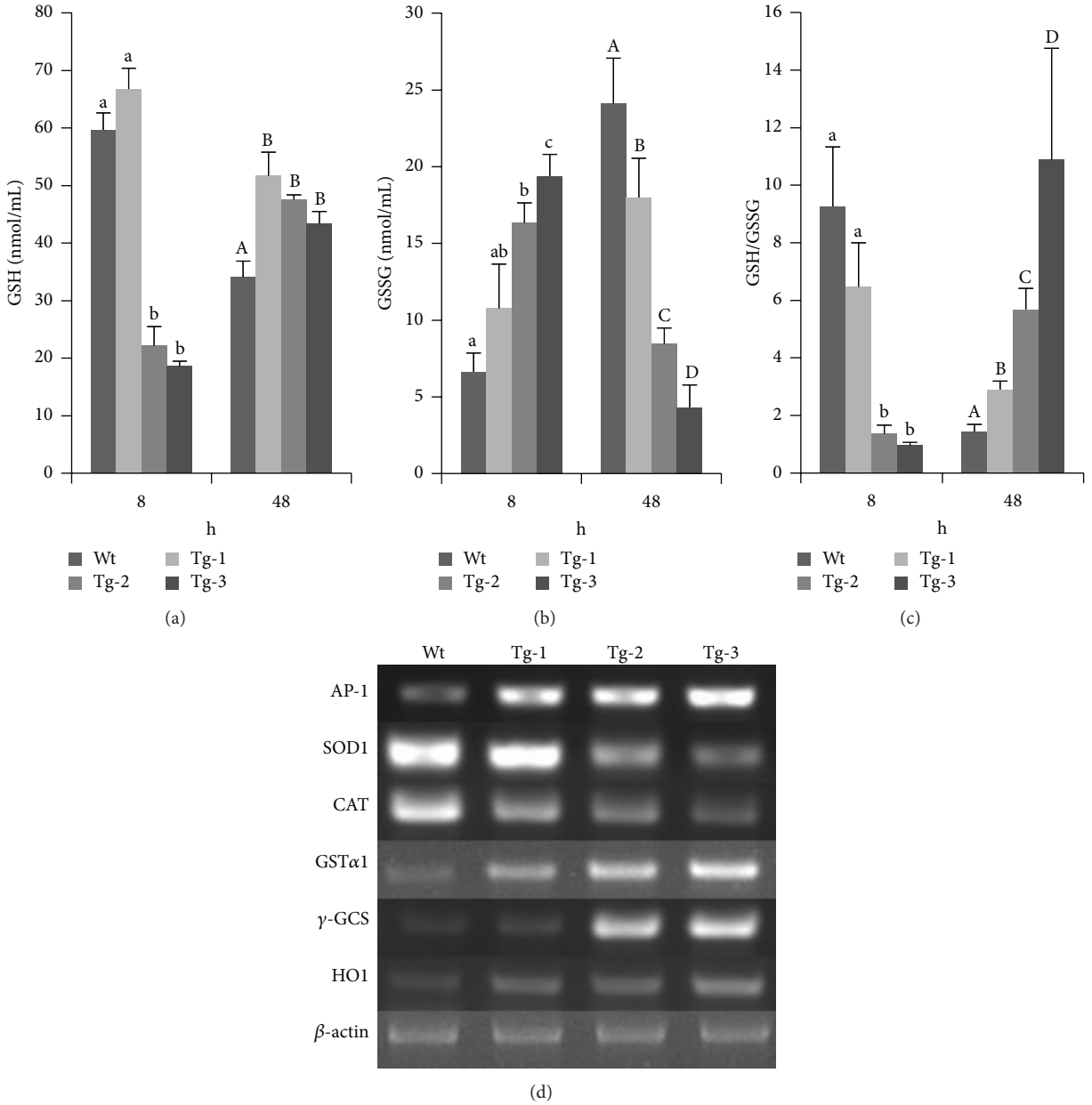

Figure 4: Contents of GSH and oxidative stress-related genes in TLR4 transgenic sheep monocytes/macrophages. (a) GSH content measurements, (b) GSSG content measurements, (c) GSH/GSSG ratio calculations, (d) RT-PCR detection of AP-1 and antioxidative-related gene expression. Data represent mean ± SE. $^{a,b,c,d;A,B,C,D}$Different superscripts indicate significantly different values between groups ($p < 0.05$). Wt, wild type; Tg-1, Tg-2, and Tg-3 were transgenic sheep that had 1, 2, or 3 copies of TLR4.

initiate downstream antioxidative genes that protect against oxidative stress. We found that overexpressed TLR4 increased antioxidative stress capacity. TLR4 promoted AP-1 expression, and subsequently γ-GCS expression was upregulated to maintain tissue homeostasis.

Ethical Approval

Artificial insemination, intradermic injection, surgical biopsy, and blood collection were performed at the experimental station of the China Agricultural University, and the whole procedure was carried out in strict accordance with the protocol approved by the Animal Welfare Committee of China Agricultural University (Permit number XK662).

Conflict of Interests

The authors declare that they have no competing interests.

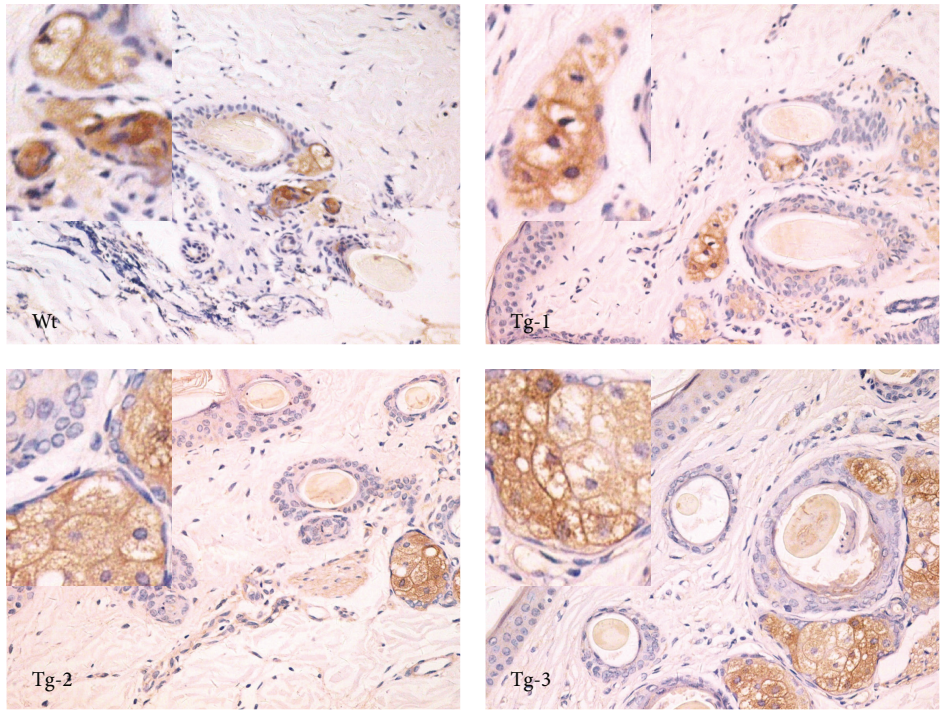

Figure 5: γ-GCS expression in TLR4 overexpressing sheep ear tissues. γ-GCS expression was detected by immunohistochemical staining (400x magnification is shown). Data represent mean ± SE. Wt, wild type; Tg-1, Tg-2, and Tg-3 were transgenic sheep that had 1, 2, or 3 copies of TLR4.

Authors' Contribution

Shoulong Deng, Kun Yu, Zhengxing Lian, and Yixun Liu conceived and designed the experiments. Shoulong Deng, Guoshi Liu, and Xiaosheng Zhang performed the experiments. Shoulong Deng and Kun Yu analyzed the data. Yan Li and Qian Wu contributed reagents/materials/analysis tools. Shoulong Deng, Kun Yu, and Baolu Zhang wrote the paper. Shoulong Deng and Kun Yu contributed equally to this work.

Acknowledgments

This work was supported by grants from National Transgenic Creature Breeding Grand Project (2013ZX08008-005), Chinese Universities Scientific Fund (2014BH032), and Youth Project of CAMA (CAMAQN201411).

References

[1] R. M. Kelsh and P. J. McKeown-Longo, "Topographical changes in extracellular matrix: activation of TLR4 signaling and solid tumor progression," *Trends in Cancer Research*, vol. 9, pp. 1–13, 2013.

[2] M. Szajnik, M. J. Szczepanski, M. Czystowska et al., "TLR4 signaling induced by lipopolysaccharide or paclitaxel regulates tumor survival and chemoresistance in ovarian cancer," *Oncogene*, vol. 28, no. 49, pp. 4353–4363, 2009.

[3] Y. Gao, X. Fang, Y. Tong, Y. Liu, and B. Zhang, "TLR4-mediated MyD88-dependent signaling pathway is activated by cerebral ischemia-reperfusion in cortex in mice," *Biomedicine and Pharmacotherapy*, vol. 63, no. 6, pp. 442–450, 2009.

[4] M. Muller, "Pyocyanin induces oxidative stress in human endothelial cells and modulates the glutathione redox cycle," *Free Radical Biology and Medicine*, vol. 33, no. 11, pp. 1527–1533, 2002.

[5] J.-W. Yao, J. Liu, X.-Z. Kong et al., "Induction of activation of the antioxidant response element and stabilization of Nrf2 by 3-(3-pyridylmethylidene)-2-indolinone (PMID) confers protection against oxidative stress-induced cell death," *Toxicology and Applied Pharmacology*, vol. 259, no. 2, pp. 227–235, 2012.

[6] K. Kato, H. Tokuda, J. Mizutani et al., "Role of HSP27 in tumor necrosis factor-α-stimulated interleukin-6 synthesis in osteoblasts," *International Journal of Molecular Medicine*, vol. 28, no. 5, pp. 887–893, 2011.

[7] K.-J. Min, J.-H. Kim, I. Jou, and E.-H. Joe, "Adenosine induces hemeoxygenase-1 expression in microglia through the activation of phosphatidylinositol 3-kinase and nuclear factor E2-related factor 2," *Glia*, vol. 56, no. 9, pp. 1028–1037, 2008.

[8] D. Altavilla, H. Marini, P. Seminara et al., "Protective effects of antioxidant raxofelast in alcohol-induced liver disease in mice," *Pharmacology*, vol. 74, no. 1, pp. 6–14, 2005.

[9] X.-M. Yao, H. Chen, and Y. Li, "Protective effect of bicyclol on liver injury induced by hepatic warm ischemia/reperfusion in rats," *Hepatology Research*, vol. 39, no. 8, pp. 833–842, 2009.

[10] G. M. Habib, "Arsenite causes down-regulation of Akt and c-Fos, cell cycle dysfunction and apoptosis in glutathione-deficient cells," *Journal of Cellular Biochemistry*, vol. 110, no. 2, pp. 363–371, 2010.

[11] V. R. Pannala, J. N. Bazil, A. K. S. Camara, and R. K. Dash, "A biophysically based mathematical model for the catalytic

mechanism of glutathione reductase," *Free Radical Biology and Medicine*, vol. 65, pp. 1385–1397, 2013.

[12] A. Kode, S. Rajendrasozhan, S. Caito, S.-R. Yang, I. L. Megson, and I. Rahman, "Resveratrol induces glutathione synthesis by activation of Nrf2 and protects against cigarette smoke-mediated oxidative stress in human lung epithelial cells," *The American Journal of Physiology—Lung Cellular and Molecular Physiology*, vol. 294, no. 3, pp. L478–L488, 2008.

[13] B. Dimitrijević, S. Borozan, S. Katić-Radivojević, and S. Stojanović, "Effects of infection intensity with Strongyloides papillosus and albendazole treatment on development of oxidative/nitrosative stress in sheep," *Veterinary Parasitology*, vol. 186, no. 3-4, pp. 364–375, 2012.

[14] H. Shi, M. V. Kokoeva, K. Inouye, I. Tzameli, H. Yin, and J. S. Flier, "TLR4 links innate immunity and fatty acid-induced insulin resistance," *The Journal of Clinical Investigation*, vol. 116, no. 11, pp. 3015–3025, 2006.

[15] T. Suganami, K. Tanimoto-Koyama, J. Nishida et al., "Role of the Toll-like receptor 4/NF-κB pathway in saturated fatty acid-induced inflammatory changes in the interaction between adipocytes and macrophages," *Arteriosclerosis, Thrombosis, and Vascular Biology*, vol. 27, no. 1, pp. 84–91, 2007.

[16] F. Bihl, L. Salez, M. Beaubier et al., "Overexpression of toll-like receptor 4 amplifies the host response to lipopolysaccharide and provides a survival advantage in transgenic mice," *Journal of Immunology*, vol. 170, no. 12, pp. 6141–6150, 2003.

[17] V. Jain, A. Halle, K. A. Halmen et al., "Phagocytosis and intracellular killing of MD-2 opsonized gram-negative bacteria depend on TLR4 signaling," *Blood*, vol. 111, no. 9, pp. 4637–4645, 2008.

[18] J. Zhu and C. Mohan, "Toll-like receptor signaling pathways—therapeutic opportunities," *Mediators of Inflammation*, vol. 2010, Article ID 781235, 7 pages, 2010.

[19] S. Janssens and R. Beyaert, "Role of Toll-like receptors in pathogen recognition," *Clinical Microbiology Reviews*, vol. 16, no. 4, pp. 637–646, 2003.

[20] P. Ma and R. L. Danner, "The many faces of sepsis-induced vascular failure," *Critical Care Medicine*, vol. 30, no. 4, pp. 947–949, 2002.

[21] I. Sigala, P. Zacharatos, D. Toumpanakis et al., "MAPKs and NF-κB differentially regulate cytokine expression in the diaphragm in response to resistive breathing: the role of oxidative stress," *American Journal of Physiology—Regulatory Integrative and Comparative Physiology*, vol. 300, no. 5, pp. R1152–R1162, 2011.

[22] M. L. Olleros, M. L. Martin, D. Vesin et al., "Fat diet and alcohol-induced steatohepatitis after LPS challenge in mice: role of bioactive TNF and Th1 type cytokines," *Cytokine*, vol. 44, no. 1, pp. 118–125, 2008.

[23] C. Luo, L. Strauss, A. Ristimäki, T. Streng, and R. Santti, "Constant expression of cyclooxygenase-2 gene in prostate and the lower urinary tract of estrogen-treated male rats," *Zeitschrift fur Naturforschung Section C*, vol. 56, no. 5-6, pp. 455–463, 2001.

[24] S. Pacquelet, J. L. Johnson, B. A. Ellis et al., "Cross-talk between IRAK-4 and the NADPH oxidase," *Biochemical Journal*, vol. 403, no. 3, pp. 451–461, 2007.

[25] V. H. Ferreira, A. Nazli, G. Khan et al., "Endometrial epithelial cell responses to coinfecting viral and bacterial pathogens in the genital tract can activate the HIV-1 LTR in an NFκB-and AP-1-dependent manner," *Journal of Infectious Diseases*, vol. 204, no. 2, pp. 299–308, 2011.

[26] L. E. Otterbein, M. P. Soares, K. Yamashita, and F. H. Bach, "Heme oxygenase-1: unleashing the protective properties of heme," *Trends in Immunology*, vol. 24, no. 8, pp. 449–455, 2003.

[27] Q. Lin, S. Weis, G. Yang et al., "Heme oxygenase-1 protein localizes to the nucleus and activates transcription factors important in oxidative stress," *The Journal of Biological Chemistry*, vol. 282, no. 28, pp. 20621–20633, 2007.

[28] X. M. Wang, H. P. Kim, K. Nakahira, S. W. Ryter, and A. M. K. Choi, "The heme oxygenase-1/carbon monoxide pathway suppresses TLR4 signaling by regulating the interaction of TLR4 with caveolin-1," *Journal of Immunology*, vol. 182, no. 6, pp. 3809–3818, 2009.

[29] A. M. Pisoschi and A. Pop, "The role of antioxidants in the chemistry of oxidative stress: a review," *European Journal of Medicinal Chemistry*, vol. 97, pp. 55–74, 2015.

[30] B. M. Rovenko, O. I. Kubrak, D. V. Gospodaryov et al., "Restriction of glucose and fructose causes mild oxidative stress independently of mitochondrial activity and reactive oxygen species in *Drosophila melanogaster*," *Comparative Biochemistry and Physiology Part A: Molecular & Integrative Physiology*, vol. 187, pp. 27–39, 2015.

[31] Y. Ikeda, S. Sciarretta, N. Nagarajan et al., "New insights into the role of mitochondrial dynamics and autophagy during oxidative stress and aging in the heart," *Oxidative Medicine and Cellular Longevity*, vol. 2014, Article ID 210934, 13 pages, 2014.

[32] J. R. Arthur, "The glutathione peroxidases," *Cellular and Molecular Life Sciences*, vol. 57, no. 13-14, pp. 1825–1835, 2000.

[33] J. D. Hayes and R. C. Strange, "Potential contribution of the glutathione S-transferase supergene family to resistance to oxidative stress," *Free Radical Research*, vol. 22, no. 3, pp. 193–207, 1995.

[34] S. Bergelson, R. Pinkus, and V. Daniel, "Intracellular glutathione levels regulate Fos/Jun induction and activation of glutathione S-transferase gene expression," *Cancer Research*, vol. 54, no. 1, pp. 36–40, 1994.

[35] M. B. Grisham, R. P. MacDermott, and E. A. Deitch, "Oxidant defense mechanisms in the human colon," *Inflammation*, vol. 14, no. 6, pp. 669–680, 1990.

[36] S. Ray, D. N. Watkins, N. L. A. Misso, and P. J. Thompson, "Oxidant stress induces gamma-glutamylcysteine synthetase and glutathione synthesis in human bronchial epithelial NCI-H292 cells," *Clinical & Experimental Allergy*, vol. 32, no. 4, pp. 571–577, 2002.

[37] I. Rahman, A. A. M. Van Schadewuk, P. S. Hiemstra et al., "Localization of γ-glutamylcysteine synthetase messenger rna expression in lungs of smokers and patients with chronic obstructive pulmonary disease," *Free Radical Biology and Medicine*, vol. 28, no. 6, pp. 920–925, 2000.

[38] X. Zhang, P. Shan, S. Qureshi et al., "Cutting edge: TLR4 deficiency confers susceptibility to lethal oxidant lung injury," *Journal of Immunology*, vol. 175, no. 8, pp. 4834–4838, 2005.

Hindawi Publishing Corporation
Oxidative Medicine and Cellular Longevity
Volume 2016, Article ID 7843685, 10 pages
http://dx.doi.org/10.1155/2016/7843685

Research Article

Correlation between Mitochondrial Reactive Oxygen and Severity of Atherosclerosis

Gabriel G. Dorighello,[1] Bruno A. Paim,[2] Samara F. Kiihl,[3] Mônica S. Ferreira,[2] Rodrigo R. Catharino,[2] Anibal E. Vercesi,[2] and Helena C. F. Oliveira[1]

[1]*Department of Structural and Functional Biology, Biology Institute, State University of Campinas, 13083-862 Campinas, SP, Brazil*
[2]*Department of Clinical Pathology, Faculty of Medical Sciences, State University of Campinas, 13083-887 Campinas, SP, Brazil*
[3]*Department of Statistics, Institute of Mathematics, Statistic and Scientific Computation, State University of Campinas, 13083-859 Campinas, SP, Brazil*

Correspondence should be addressed to Helena C. F. Oliveira; ho98@unicamp.br

Received 24 April 2015; Revised 7 June 2015; Accepted 22 June 2015

Academic Editor: Celia Quijano

Atherosclerosis has been associated with mitochondria dysfunction and damage. Our group demonstrated previously that hypercholesterolemic mice present increased mitochondrial reactive oxygen (mtROS) generation in several tissues and low NADPH/NADP+ ratio. Here, we investigated whether spontaneous atherosclerosis in these mice could be modulated by treatments that replenish or spare mitochondrial NADPH, named citrate supplementation, cholesterol synthesis inhibition, or both treatments simultaneously. Robust statistical analyses in pooled group data were performed in order to explain the variation of atherosclerosis lesion areas as related to the classic atherosclerosis risk factors such as plasma lipids, obesity, and oxidative stress, including liver mtROS. Using three distinct statistical tools (univariate correlation, adjusted correlation, and multiple regression) with increasing levels of stringency, we identified a novel significant association and a model that reliably predicts the extent of atherosclerosis due to variations in mtROS. Thus, results show that atherosclerosis lesion area is positively and independently correlated with liver mtROS production rates. Based on these findings, we propose that modulation of mitochondrial redox state influences the atherosclerosis extent.

1. Introduction

Oxidative stress seems to be a common denominator unifying a variety of classic risk factors mode of action that leads to atherosclerosis [1]. The cellular sources of reactive oxygen species (ROS) are multiple, including NAD(P)H oxidase, xanthine oxidase, lipoxygenase, and cyclooxygenase systems, mitochondrial electron transport chain, and autoxidation of diverse substances. Previous studies found that ROS specifically derived from mitochondria (mtROS) are relevant in the context of atherosclerosis. For instance, mtROS induce endothelial dysfunction, infiltration and activation of inflammatory cells, and apoptosis of endothelial and vascular smooth muscle cells [2, 3]. In addition, a role for mitochondrial DNA damage and dysfunction in atherogenesis has been proposed in the last decade [4–9].

Our group have previously shown that mitochondria from various tissues of the hypercholesterolemic atherosclerosis-prone LDL receptor knockout mice ($LDLr^{-/-}$) release more ROS than wild type controls [10]. In addition, this model presents reduced content of mitochondrial NADPH [10], the main reducing power for the antioxidant system glutathione and thioredoxine reductase/peroxidase [11]. This $LDLr^{-/-}$ mitochondrial prooxidant state rendered the organelle more susceptible to membrane permeability transition (MPT). It has been well recognized that mitochondrial dysfunctions such as opening of the permeability transition pore directly promote inflammation and oxidative stress, phenomena involved in several cardiometabolic diseases [8, 9, 12]. The mitochondrial intrinsic pathway of cell death can be triggered by cholesterol accumulation in macrophages [13], an early event in atherogenesis. In addition, oxidative

damage of mtDNA is correlated with human and mice severity of atherosclerosis [4, 9].

In a previous study, we verified that, besides NADPH deficiency, LDLr$^{-/-}$ mitochondria contained less Krebs cycle intermediates such as isocitrate and that treating the organelle with isocitrate (*in vitro*) and the LDLr$^{-/-}$ mouse model with citrate (*in vivo*) resulted in decreased mtROS production and increased NADPH content [14]. Major processes that consume cell NADPH and Krebs cycle intermediates are lipid and cholesterol biosynthesis, which are elevated in this animal model [10]. Therefore, we hypothesized that either citrate supplementation or cholesterol synthesis inhibition could increase mitochondria NADPH availability, decrease mtROS production, and decrease atherosclerosis development in LDLr$^{-/-}$ mouse.

2. Material and Methods

2.1. Animals. Mating pairs of LDLr$^{-/-}$ (B6.129S7-Ldlr<tm1Her./J, homozygous for Ldlr<tm1Her, stock number 002207) and wild type controls (C57BL6/J, stock number 000664) were purchased from The Jackson Laboratory (Bar Harbor, ME) in 2009 and both colonies have been established and maintained in strictly SPF conditions in The Multidisciplinary Center for Biological Investigation in the Area of Laboratory Animal Science (CEMIB) of the State University of Campinas (Unicamp). The CEMIB-Unicamp is part of the International Council for Laboratory Animal Science (ICLAS). The colonies are maintained through exclusive sibling mattings in order to maintain the homogeneous genetic background. When mice reach the age of 4 weeks, they are transferred to the Conventional Animal Facility in the Department of Structural and Functional Biology at Unicamp. Mice are then maintained in a temperature-controlled room (22 ± 1°C), with 12 h light/dark cycle, with 15 cycles of air changes per hour, and with free access to food (standard laboratory rodent chow diet, Nuvital CR1, Colombo, PR, Brazil) and filtered water. Four to five mice are maintained per cage. They are then enrolled in the experimental protocol which was approved by the Ethical Committee for the Use of Animal (CEUA/Unicamp, protocol # 1101-2) and by the Internal Biosecurity Committee (CIBio-IB/Unicamp, protocol # 2008/02). One-month-old male LDLr$^{-/-}$ mice were randomly separated into four groups: control (CON), citrate (CIT), pravastatin (PRA), and citrate + pravastatin (CIT + PRA). The solutions of citrate (1.34 mM citric acid + 1.1 mM sodium citrate) and pravastatin (67 mg/L) equivalent to 10 mg/Kg of body weight were offered as the only source of drinking water. The solutions were provided in dark bottles and changed every other day during 3 months. Additional experiments were performed in untreated LDLr$^{-/-}$ and wild type controls for checking differences in oxidative susceptibility status and oxidative lipid damage in their plasma VLDL particles, as well as for determining anti-inflammatory systemic markers. Control of the colony phenotype is done by measuring fasting plasma cholesterol levels (LDLr$^{-/-}$ > 200 mg/dL and WT < 80 mg/dL) and genotype by PCR in tail tip DNA samples according to The Jackson Laboratory protocol.

2.2. Plasma Biochemical Analysis. Blood samples were collected from either the retroorbital plexus or the tail tip of anesthetized and overnight fasted mice. Total cholesterol, triglycerides, and nonesterified fatty acids were measured in fresh plasma using standard commercial kits (Roche-Hitachi, Germany, and Wako, Germany). Glucose levels were measured using a hand-held glucometer (Accu-Chek Advantage, Roche Diagnostic, Switzerland). The plasma urea, creatinine, alkaline phosphatase (ALP), alanine aminotransferase (ALT), and aspartate transaminase (AST) were determined using an automated modular analyzer PP (Hitachi) with Roche reagents (Roche Diagnostic, Germany). The plasma cytokines tumoral necrosis factor alpha (TNFα), interleukin 2 (IL-2), interleukin 4 (IL-4), and Interferon gamma (IFNγ) were measured with ELISA commercial kit (eBioscience, San Diego, CA) according to the manufacturer's instructions. Plasma oxidized LDL antibodies were measured in plasma as described by Zaratin et al. [15]. Polystyrene 96-well plates were coated with human copper-oxidized LDL and incubated overnight at 4°C. Plates were then blocked with 1% gelatin in PBS for 48 h at room temperature. After washing with PBS, plasma samples (1 : 200) were added and incubated for 2 h at room temperature. After washing with PBS containing 0.2 mL/L Tween 20, plates were incubated with 50 μL of peroxidase conjugated rabbit anti-mouse IgG antibody at room temperature for 1 h. Finally, 75 μL peroxidase substrate solution was added, incubated for 15 min, and ended by 25 μL of 2 M sulfuric acid. The optical density (OD) was then measured at 450 nm. The results are presented as the OD readings (arbitrary units). $CuSO_4$-induced plasma thiobarbituric acid reactive substances (TBARS) concentrations were determined by first exposing plasma to 0.1 mM CuSO4 at 37°C for 5 hours. Then, 100 μL of oxidized plasma was incubated with 200 μL of 0.7% thiobarbituric acid in 0.05 M NaOH and 60 μL of 50% trichloroacetic acid. Samples were incubated in boiling water for 30 minutes, followed by centrifugation at 664 g for 15 minutes. The standard curve was prepared using several dilutions of 0.05 mM 1,1,3,3-tetramethoxypropane. The optical densities of samples and standard curve were measured in a microplate reader at 532 nm.

2.3. Body Composition and Tissue Lipids Analyses. The epididymal adipose tissue and liver and spleen fresh masses were determined gravimetrically. Mice carcass composition was determined by weighing carcass before and after water drying and before and after lipid extraction of the dried carcass with petroleum ether as previously described by Salerno et al. [16]. Liver lipids were extracted using the Folch method [17]. The liver content of cholesterol and triglycerides was determined using colorimetric-enzymatic assays (Roche-Hitachi, Germany) after dissolving the lipid extracts in a triton-containing buffer (0.1 M potassium phosphate, pH 7.4, 0.05 M NaCl, 5 mM cholic acid, and 0.1% Triton X-100).

2.4. Isolation of Mouse Liver Mitochondria. Mitochondria were isolated by conventional differential centrifugation at 4°C as previously described [18]. The livers were homogenized in 250 mM sucrose, 1 mM EGTA, and 10 mM Hepes

buffer (pH 7.2). The mitochondrial suspension was washed twice in the same medium containing 0.1 mM EGTA and the final pellet was resuspended in 250 mM sucrose to a final protein concentration of 80–100 mg/mL. The protein concentration was determined by a modified Biuret assay.

2.5. Reactive Oxygen Species Production (ROS). ROS production by mitochondria was monitored using the membrane-permeable fluorescent dye 2′,7′-dichloro-dihydro-fluorescein diacetate (H_2DCF-DA) according to García-Ruiz et al. [19]. Briefly, mitochondria (0.5 mg/mL) were added to HANKS medium, pH 7.2, containing 1 μM H_2DCF-DA and a 5 mM mixture of NAD-linked substrates (malate + glutamate + α-ketoglutarate + pyruvate), in a 1 mL cuvette with constant stirring at 37°C. The fluorescence signal was recorded at the excitation/emission wavelength pair of 488/525 nm using a fluorometer (Hitachi, model F4500). Calibration was performed with known concentrations of dichlorofluorescein (DCF), which is the product of H_2-DCF oxidation.

2.6. NADPH Oxidation Rates. The redox state of pyridine nucleotides was measured as previously described [10] in the mitochondrial suspension (1 mg/mL) containing 100 μM EGTA, 5 mM succinate, and 5 μM rotenone by following the fluorescence signal in a Hitachi F-4010 spectrofluorometer using excitation and emission wavelengths of 366 and 450 nm, respectively, and a slit width of 5 nm. The extent of pyridine nucleotide oxidation was calculated as a function of the fluorescence increase induced by isocitrate addition. Internal calibration was done by the addition of known amounts of NADH.

2.7. Histological Analysis of Atherosclerosis. In situ perfused hearts were excised and embedded in Tissue-Tek OCT compound (Sakura, USA), frozen at −80°C, cut in 10 μm sections along 480 μm aorta length from the aortic valve leaflets, and stained by Oil Red O according to Paigen et al. [20]. The lipid-stained lesions were quantified as described by Rubin et al. [21] using the *ImageJ* (1.45 h) software.

2.8. VLDL Oxidation Susceptibility. Plasma VLDL fractions were obtained from 12 h fasted mice by ultracentrifugation. Five hundred μL of plasma was added to the bottom of the ultracentrifuge tube and carefully overlaid with 300 μL of saline solution (150 mM NaCl, 1 mM EDTA, and density of 1.006). The samples were centrifuged at 140,000 rpm (1×10^6 g), 16°C during 50 min in a microultracentrifuge, Hitachi (model CS150GXL). Two hundred μL from the top layer containing the VLDL fraction was collected. The amount of VLDL used in the oxidation assay was normalized by the triglyceride concentration (100 mg/mL). $CuSO_4$-induced oxidation (40 μM, 37°C) was measured by detecting the formation of conjugated dienes at 234 nm over time (Spectrophotometer Fusion Packard) according to a previous report [22].

2.9. Lipid Chemical Markers Identification. VLDL samples were submitted to a Bligh-Dyer extraction [23]. Lipid extracts were resuspended in 50 μL of methanol : H_2O milliQ (1 : 1) and 10 μL of the latter was diluted in 990 μL of methanol and 0.1% formic acid. Data acquisition was performed in an LTQ-XL Orbitrap Discovery Instrument (30,000 FWHM, Thermo Scientific, Bremen, Germany) in the positive ion mode and at the m/z range of 600–1000 for complex lipid identification. Mass and intensity values for each spectrum were included in the Principal Component Analysis (PCA), which was performed using Unscrambler v.9.7 CAMO Software (Trondheim, Norway). After the discrimination of PCA, potential chemical markers were selected for identification. For this, structural propositions were performed using high resolution as the main parameter. Mass accuracy was calculated and expressed in terms of ppm shifts, according to Machado et al. [24]. Error values were considered with the assistance of online database Lipid MAPS (University of California, San Diego, CA; http://www.lipidmaps.org/) for guiding the choice of potential lipid markers.

2.10. Statistical Data Analyses. The results are presented as the means ± SE. The comparisons between the groups were analyzed by one-way ANOVA with posttest of Tukey. For correlation analyses, we performed Spearman's univariate correlation test, partial (adjusted) correlation, and multiple linear regressions models, using, respectively, GraphPad Prism 5.0, SPSS Statistics 14.0, and R package 2.9. In the multiple linear regressions analyses, variable selection in each model was performed using the *regsubsets* tool available in the *leaps* package for R [25, 26], which identifies the exploratory variables that create the best-fitting linear regression models according to Bayesian Information Criterion (BIC). The level of significance was set at $P < 0.05$.

3. Results

In a pilot experiment, diet-induced atherosclerosis was evaluated in $LDLr^{-/-}$ treated or not with 120 mM citrate drinking solution [14] during two weeks. The high citrate concentration used in this study caused a marked increase in plasma lipid levels, without changes in mtROS production, and resulted in 80% increase in aortic atherosclerosis lesion area in the citrate treated $LDLr^{-/-}$ mice (data not shown). Therefore, for the next studies, we employed a 50-fold lower citrate dose (2.4 mM) during 12 weeks and determined the spontaneous (not diet-induced) atherosclerosis development. This protocol did not cause elevation of plasma lipid levels. For the cholesterol inhibition group (statins treatment), we chose a low dose of a hydrophilic statin (pravastatin 10 mg/Kg/day) because we had previously shown that high statin dose can directly damage mitochondria [27]. This dose is proven to be still effective to reduce atherosclerosis in $LDLr^{-/-}$ mice without important plasma lipid changes [28].

Control (CON), citrate (CIT), pravastatin (PRA), and citrate + pravastatin (CIT + PRA) mice had similar body composition and plasma lipid levels (Table 1), although PRA group of mice presented lower body weight at the end of the treatment. The liver and renal functions were similar in all groups as verified through quantification of plasma

Table 1: Body composition, plasma lipids and glucose levels, renal and hepatic function markers, systemic and mitochondrial redox parameters of LDL receptor knockout mice treated during 3 months with citrate and pravastatin.

Parameters	Control	Citrate	Pravastatin	Citrate + prava.
Body weight[1]	19.7 ± 0.2	17.7 ± 0.3	17.3 ± 0.4*	18.2 ± 0.2
Carcass fat mass[2]	14.1 ± 0.7	15.6 ± 1.6	14.2 ± 1.0	13.1 ± 1.9
Carcass lean mass[2]	65.4 ± 0.9	64.5 ± 0.5	63.8 ± 0.6	64.9 ± 0.7
Visceral fat mass[3]	0.91 ± 0.08	0.93 ± 0.11	0.74 ± 0.07	0.84 ± 0.12
Liver mass[3]	4.68 ± 0.09	4.72 ± 0.08	4.63 ± 0.11	4.78 ± 0.04
Spleen mass[3]	0.27 ± 0.01	0.27 ± 0.01	0.25 ± 0.02	0.25 ± 0.00
Liver Cholesterol[4]	4.5 ± 0.6	5.1 ± 0.6	4.4 ± 0.6	5.9 ± 0.8
Liver Triglycerides[4]	79 ± 13.7	97 ± 17.8	69.3 ± 10.8	102.3 ± 15.6
Glucose[5]	85 ± 4.1	77 ± 4.1	85 ± 3.3	79 ± 4.2
Triglycerides[5]	103 ± 6.7	104 ± 6.6	110 ± 8.3	115 ± 8.8
Cholesterol[5]	234 ± 13.3	238 ± 8.4	238 ± 12.1	252 ± 9.1
Fatty acid[6]	0.80 ± 0.09	0.83 ± 0.06	0.75 ± 0.06	0.76 ± 0.03
LDLox antibodies[7]	0.34 ± 0.07	0.54 ± 0.08	0.42 ± 0.09	0.54 ± 0.07
TBARS[6]	258.5 ± 10.3	248.6 ± 7.8	234.5 ± 6.6	245.5 ± 15.2
ALT[8]	36.0 ± 2.1	48.7 ± 4.2	44.8 ± 4.5	38.7 ± 3.1
AST[8]	117.7 ± 11.4	138.1 ± 12.4	155.0 ± 27.9	130.0 ± 14.7
ALP[8]	158.1 ± 8	145.6 ± 15.7	173.1 ± 11.2	172.4 ± 7.7
Urea[5]	77.0 ± 2.4	84.7 ± 1.5	94.3 ± 5.4*	81.8 ± 4.3
Creatinine[5]	0.12 ± 0.01	0.12 ± 0.01	0.12 ± 0.01	0.12 ± 0.01
mtROS production[9]	1.71 ± 0.19	2.02 ± 0.32	1.66 ± 0.08	1.83 ± 0.18
NADPH oxidation[10]	0.95 ± 0.13	0.80 ± 0.2	0.92 ± 0.21	0.73 ± 0.22
Atherosclerotic lesion area[11]	31.6 ± 8.8	43.8 ± 4.8	61.1 ± 12.8	116.8 ± 25.0*

Data are mean ± SE (n = 8–10/group). Citrate (1.34 mM citric acid + 1.1 mM sodium citrate in the drinking water). Pravastatin (10 mg/Kg of body weight) in the drinking water (67 mg/L). [1]g, [2]% related to the dry carcass, [3]% related to the body weight, [4]mg/g of liver, [5]mg/dL, [6]μM, [7]absorbance, [8]U/L, [9]nM DCF/mg protein min^{-1}, [10]ηM NADPH/mg protein min^{-1}, [11]$\mu m^2 \times 10^3$. *$P < 0.05$.

alkaline phosphatase (ALP), alanine aminotransferase (ALT), aspartate transaminase (AST), and creatinine plasma levels. However, plasma urea levels in PRA group were 22% higher than in the other groups (Table 1). The average values of oxidative stress markers, such as susceptibility to lipid peroxidation (copper sulfate-induced thiobarbituric acid reactive substances), titles of plasma oxidized LDL antibodies, liver mitochondrial NADPH oxidation rates, and reactive oxygen species production rates (mtROS), were not significantly modified by the three treatments (Table 1). The development of spontaneous atherosclerosis, as measured by the area of lipid stained lesions in the aortic root, did not change significantly in CON, CIT, and PRA groups of mice. Surprisingly, the group CIT + PRA presented marked enhanced atherosclerosis (Table 1 and Figure 1).

Since the treatments did not alter the average values of classic atherosclerosis risk factors such as plasma lipids, obesity, and oxidative stress, statistical correlation analyses in pooled group data were performed in an attempt to explain the differences observed in the variation of atherosclerosis lesion areas. Spearman's univariate correlation test showed that the atherosclerotic lesion areas were positively correlated with plasma cholesterol ($r = 0.39$, $P = 0.046$), triglycerides ($r = 0.43$, $P = 0.026$), ALP ($r = 0.45$, $P = 0.02$), and liver mitochondria ROS production (mtROS) ($r = 0.54$, $P = 0.031$) (Figure 2). We further tested the existence of linear multiple regression models to explain the extent of atherosclerosis. Three groups of variables were tested: (1) associations with body composition variables (carcass lean and fat mass, visceral fat mass, and body weight), (2) associations with plasma variables (glucose, triglycerides, cholesterol, free fatty acids, LDLox antibodies, and TBARS), and (3) associations with hepatic variables (liver mass, cholesterol and triglycerides content, and mtROS). For each model, variables that create the best-fitting linear regression are selected by the software [25, 26] to explain the atherosclerosis variation (Table 2). The body composition variables did not have any relevance in determining atherosclerosis variation (no significant associations were found). For the plasma variables, the software selected two significant models: (a) association with plasma triglyceride level and (b) association with plasma triglyceride and glucose level. For the hepatic variables, also two significant models were found: (a) association with mtROS and (b) association with mtROS and liver triglycerides content (Table 2). According to these regression models, the impact of these variables on the atherosclerosis

Table 2: Multiple linear regression models for atherosclerosis and partial correlation adjusted by plasma triglycerides.

Statistical analyses	Significant parameters	Correlation coefficients	*P* value
(1) Body composition model[1]	None	0.06	0.12
(2) Plasma model[2]	(2a) Triglycerides	0.22	0.006
	(2b) Triglycerides and glycemia	0.25	0.01
(3) Liver model[3]	(3a) mtROS	0.23	0.035
	(3b) mtROS and liver triglycerides	0.28	0.047
Partial correlation adjusted by plasma triglycerides[4]	mtROS	0.56	0.047

Parameters tested in each model: [1]carcass fat and lean mass, visceral fat mass, and body weight; [2]plasma glucose, triglycerides, cholesterol, free fatty acids, LDLox antibodies, and TBARS; [3]liver mass, hepatic cholesterol and triglyceride contents, and liver mitochondria ROS production; [4]plasma cholesterol, plasma alkaline phosphatase, and liver mitochondria ROS production were tested after adjustment by plasma triglycerides.

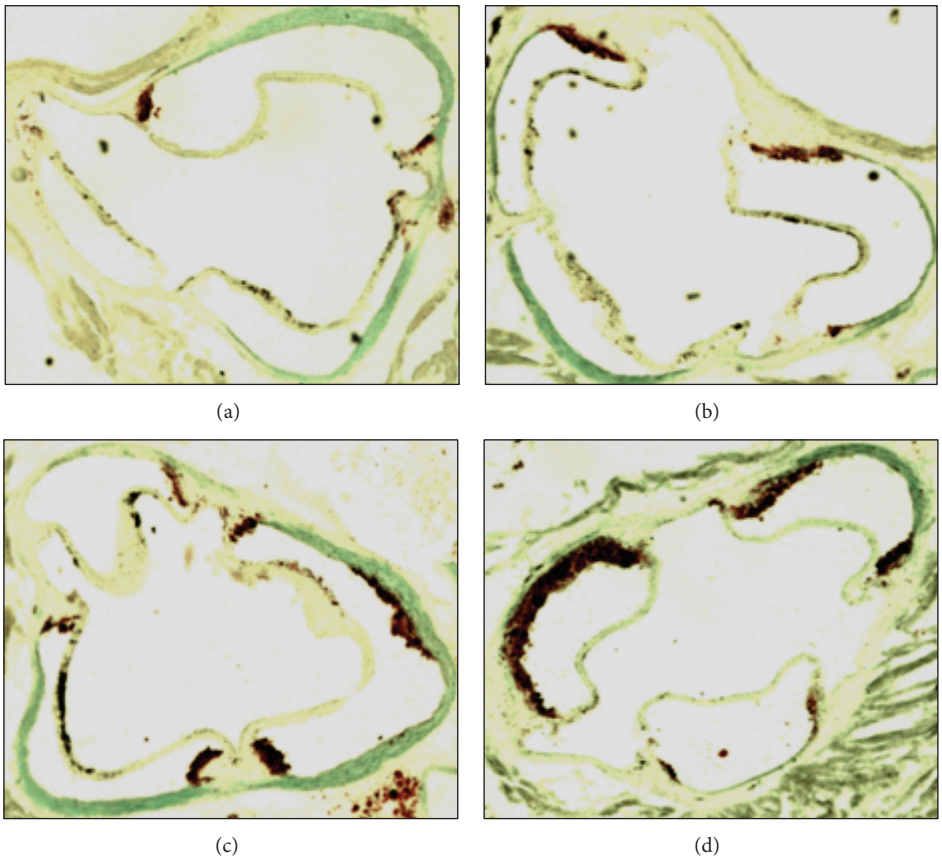

Figure 1: Representative images of aorta root with atherosclerosis lesions of LDL receptor knockout mice: control (a), treated with citrate (b), pravastatin (c), and citrate + pravastatin (d). The aortic root was cryosectioned and stained for lipids with Oil Red O and counterstained with light green.

extent can be interpreted as follows. Ten-unit increase in plasma triglycerides (10 mg/dL) is expected to increase lesion size by 17% (plasma model (2a)) and one unit increase in mtROS (nmol DCF/mg protein) is expected to increase the atherosclerotic lesion size by 370% (hepatic model (3a)).

In order to verify whether mtROS correlation with atherosclerosis was independent of the plasma triglyceride levels, we also performed the partial (adjusted) correlation test. This adjusted analysis included all variables that were significantly correlated with atherosclerosis by Spearman's correlation test (triglycerides, cholesterol, plasma ALP, and mtROS). After adjusting for plasma triglyceride levels, the only variable that remained significantly correlated with atherosclerosis was mtROS ($r = 0.56$, $P = 0.047$) (Table 2). Therefore, mtROS positive correlation with atherosclerosis is confirmed by three different statistical analyses and is independent of the variations of classical risk factors, the plasma lipid levels.

These statistical correlations between liver mtROS and atherosclerosis suggest a possible mechanistic link between liver and artery disease. The most likely connections are metabolic (for instance, secretion of oxidized VLDL) and/or

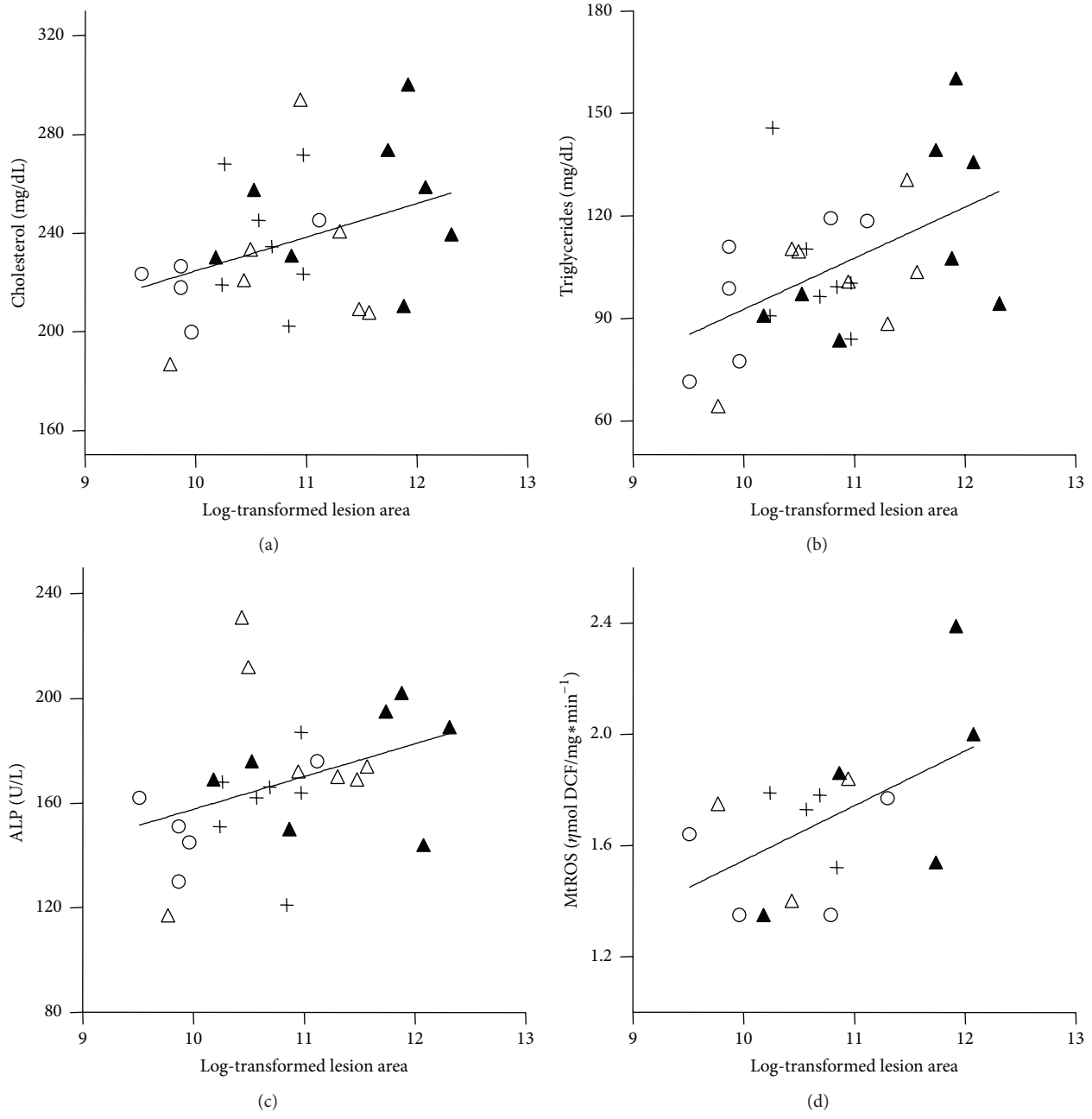

FIGURE 2: Spearman's correlations between log-transformed atherosclerosis lesion area (μm^2) and plasma cholesterol, $n = 27$ (a), plasma triglycerides, $n = 28$ (b), plasma alkaline phosphatase, $n = 26$ (ALP) (c), and liver mitochondria ROS production, $n = 16$ (d). ○ = control; + = citrate; △ = pravastatin; ▲ = citrate + pravastatin.

an oxidative induction of proinflammatory cytokines. Therefore, we compared $LDLr^{-/-}$ and wild type mice regarding VLDL susceptibility to oxidation (Figure 3) and lipid markers (Table 3) as well as the levels of plasma cytokines (Table 4). Figure 3 shows that VLDL secreted by $LDLr^{-/-}$ livers is markedly more susceptible to an oxidative insult ($CuSO_4$) than the wild type VLDL compared at the same TG content basis. Wild type VLDL shows a 5-fold greater lag time for oxidation initiation and a 50% lower rate of oxidation than VLDL from $LDLr^{-/-}$ mice. In addition, mass spectrometry analyses of VLDL lipid extracts identified oxidized lipid markers, mainly phospholipids, in VLDL from $LDLr^{-/-}$ compared with wild type mice (Table 3). Both groups were clearly separated with an accuracy of 95% and mass errors of less than 2 ppm. Regarding systemic inflammatory markers, Table 4 shows that three proinflammatory cytokines (TNFα, IL-2, and IFNγ) were augmented in the plasma of $LDLr^{-/-}$ mice.

4. Discussion

Several studies have evidenced the relevance of mitochondria functionality to the development of atherosclerosis in

Table 3: Lipid chemical markers identified by high resolution electrospray ionization mass spectrometry (ESI-MS) analysis of plasma VLDL from LDL receptor knockout and wild type mice.

	Molecule	Theoretical mass	Experimental mass	Error (ppm)	LM ID*
Wild type	$[PE(15:1/22:4)+K]^+$	790,4784	790,4769	−1,8976	LMGP02010503
	$[TG(14:0/16:1/20:1)+K]^+$	869,6995	869,7010	1,7247	LMGL03014259
	$[PG(18:0/13:0)+Na]^+$	715,4884	715,4889	0,6988	LMGP04030029
	$[PC(13:0/18:2)+H]^+$	716,5225	716,5238	1,8143	LMGP01011348
	$[PC(13:0/18:4)+Na]^+ + OH$	751,4764	751,4763	−0,1331	LMGP01011351
	$[PI(12:0/20:5)+Na]^+$	823,4368	823,4379	1,3359	LMGP06010031
	$[PE\text{-}Cer(15:2/20:0)+Na]^+ + OH$	711,5048	711,5059	1,5460	LMSP03020077
	$[PE\text{-}Cer(14:1/22:1)+K]^+$	725,4994	725,5002	1,1027	LMSP03020009
	$[PE\text{-}Cer(15:1/20:0)+K]^+ + 2OH$	729,4943	729,4934	−1,2337	LMSP03020074
	$[PA(20:4/20:0)+K]^+$	791,4988	791,4975	−1,6425	LMGP10010636
$LDLr^{-/-}$	$[PC(16:1/18:1)+H]^+ + OH$	759,5778	759,5791	1,7115	LMGP01090011
	$[PC(19:0/15:1)+H]^+$	760,5851	760,5839	−1,5777	LMGP01011732
	$[PG(19:1/18:2)+H]^+$	787,5484	787,5472	−1,5237	LMGP04010493
	$[PS(18:0/16:0)+H]^+ + OH$	781,5469	781,5477	1,0236	LMGP03010888
	$[PC(18:3/18:1)+H]^+ + OH$	783,5778	783,5765	−1,6591	LMGP01090030
	$[PC(20:5/18:1)+H]^+ + OH$	807,5778	807,5766	−1,4859	LMGP01090051
	$[PA(22:2/16:0)+K]^+ + OH$	785,5093	785,5103	1,2731	LMGP10010761
	$[PS(16:0/17:2)+H]^+ + 2OH$	762,4916	762,4901	−1,9672	LMGP03030011
	$[PS(16:0/20:5)+H]^+ + OH$	782,4967	782,4976	1,1502	LMGP03030022
	$[PI(14:0/22:6)+Na]^+$	877,4838	877,4845	0,7977	LMGP06010892

PE: phosphatidylethanolamine; TG: triacylglycerols; PG, phosphoglycerol; PC: phosphatidylcholine; PI: phosphatidylinositol; PS: phosphatidylserine; Cer: ceramide; PA: phosphatic acid. *LM ID: Lipid MAPS identity. Identification is based on exact mass of each compound and Lipid MAPS database. The assigned IDs are for general structures and can be any of the positional isomers.

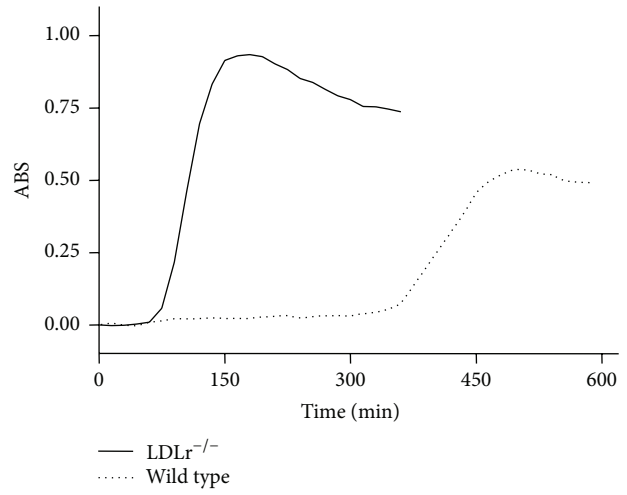

Figure 3: Representative curve of oxidation susceptibility of plasma VLDL obtained from LDL receptor knockout ($LDLr^{-/-}$) and wild type mice. The VLDL oxidation was induced by incubation with $CuSO_4$ (40 μM). Formation of conjugated dienes was followed by absorbance changes at 234 nm along time. The VLDL lag-time to start oxidation was 73 ± 4.8 and 382 ± 79.9 minutes for $LDLr^{-/-}$ and wild type mice, respectively ($P = 0.0007$). The VLDL oxidation rate, determined by the curve slopes, was about 2-fold greater ($P < 0.0001$) in the $LDLr^{-/-}$ than wild type VLDL. The n used in this experiment was of 6–8 mice.

Table 4: Plasma cytokines of LDL receptor knockout and control wild type mice.

Cytokines (pg/mL)	$LDLr^{-/-}$	Wild type	P value	N
TNFα	1364 ± 255	467 ± 53	0.007	8–10
IL-2	58.8 ± 10.7	28.1 ± 2.7	0.02	7-8
IFNγ	1553 ± 238	819 ± 124	ns	8–10

Data are mean ± SE. P value from Student's t-test. ns: nonsignificant.

humans and animals [2, 3, 7, 8]. Most studies agree that mitochondria ROS overproduction is likely implicated in atherogenesis and disease progression, although better mechanistic understanding is still needed [29].

Because we had previously found that mitochondria from atherosclerosis-prone mouse model ($LDLr^{-/-}$) had decreased content of Krebs cycle intermediates, reducing equivalent power, and increased ROS release, we hypothesized that at least part of these mitochondrial features could be attributed to an elevated cholesterol synthesis, which consume both Krebs cycle intermediates and cell reducing equivalents. Therefore, in the present work, we tested whether citrate supplementation combined or not with inhibition of cholesterol synthesis could decrease mitochondrial ROS release and atherosclerosis development. In contrast to our hypothesis, any of the treatments affected significantly the average values

of mtROS, and the combined citrate supplementation with pravastatin treatment actually increased atherogenesis.

Pravastatin alone increased plasma urea levels, and uremia *per se* appears to be proatherogenic [30]. Increased urea concentrations may increase the rate of isocyanate synthesis and increase carbamylation of lipids and proteins, including LDL [31]. Previous studies showed that carbamylated LDL dose dependently promotes proliferation of human coronary artery smooth muscle cells, endothelial cell death, and expression of adhesion molecules [32, 33]. On the other hand, in the group CIT + PRA, urea plasma levels were normal. It is possible that citrate treatment may have counteracted the effect of pravastatin on uremia, since it was previously shown that citrate reduced uremia induced by high fat diet [34]. Concerning atherosclerosis extent, it is difficult to explain why citrate + pravastatin would increase the progression of spontaneous atherosclerosis. We postulate that an interaction between these factors may have a local vascular wall harmful action, which we have not addressed in this study, but possibly related to mtROS production.

A limitation of this study is the low number (n) of mice and high variability of the responses. Therefore, we applied statistical methods to infer possible links between atherosclerosis and all measured parameters in pooled data. Correlation and regression analyses in pooled data help to identify which parameters related to risk factors (plasma lipids, obesity, and oxidative stress) have significant impact on the variation of atherosclerosis. As expected, plasma cholesterol and triglycerides were positively correlated to aortic lesion size, even within a very narrow range. Furthermore, new positive correlations were identified, named liver derived ALP and mtROS. Increasing levels of ALP suggest a correlation between liver damage and cardiovascular disease, which has already been shown by others regarding liver enzymes [35] and C-reactive protein levels [36]. However, after adjusting the analysis by plasma triglycerides, only mtROS remained positively and independently correlated with atherosclerosis. Multiple linear regression analysis also indicated that liver mtROS production could explain the extent of aortic atherosclerosis, either alone (Table 2, model (3a)) or in combination with liver triglycerides content (Table 2, model (3b)). Therefore, by using three distinct statistical tools (univariate correlation, adjusted correlation, and multiple regression) with increasing levels of stringency, we confirm a significant association between variables and further quantify the amount of variation in the dependent variable (atherosclerosis) that can be explained by the independent variable (mtROS). Although these statistical analyses do not imply causation, these results together with the whole body of evidences in the current literature lead us to propose that mechanistic links are conceivable. Liver mtROS could be linked to the arterial disease by different ways. The first one is through a metabolic connection, that is, by secreting altered amounts and/or quality of VLDL, the precursors of LDL. Secondly, liver mitochondrial oxidative stress results in activation of inflammatory pathways that may contribute to a systemic inflammation, which in turn is strongly correlated with atherosclerosis [36]. Finally, liver could be a surrogate marker of the main events occurring in the arterial wall, particularly lipid accumulation and mitochondrial oxidative stress. In support for the metabolic connection, we found that VLDL secreted by $LDLr^{-/-}$ livers is markedly more susceptible to an oxidative insult ($CuSO_4$) than the wild type VLDL, compared at the same TG content basis. In addition, these $LDLr^{-/-}$ VLDL are already secreted with several oxidized lipids compared to the wild type VLDL. At this point, it is relevant to recall and quote Davis and Hui in their George Lyman Duff Memorial Lecture "Atherosclerosis is a liver disease of the heart" [37]. In that occasion, the authors referred specifically to the complex processes involved in the liver assembly and secretion of apoB-containing lipoproteins, the precursors of the atherosclerosis culprit, the LDL.

In conclusion, our results revealed that mitochondrial reactive oxygen is a novel positive and independent risk factor for atherosclerosis. We propose that modulation of mitochondrial redox state results in significant variation of atherosclerosis extent. These findings provide support for proposed strategies of using mitochondria-targeted antioxidants as potential therapy for treatment of cardiovascular diseases.

Disclosure

The authors alone are responsible for the content and writing of the paper.

Conflict of Interests

The authors report no conflict of interests.

Acknowledgments

This study was supported by grants obtained by Helena C. F. Oliveira and Anibal E. Vercesi from the Brazilian agencies: Fundação de Amparo a Pesquisa do Estado de São Paulo (FAPESP # 2011/50400-0 and 2011/51349-8) and Conselho Nacional de Desenvolvimento Científico e Tecnológico (CNPq). Gabriel G. Dorighello and Bruno A. Paim were supported by CNPq and FAPESP fellowships, respectively. The authors thank Ms. Natalia Mayumi Inada, Edilene de Souza Siqueira Santos, and Gabriela C. Tonini for the technical assistance.

References

[1] N. R. Madamanchi, A. Vendrov, and M. S. Runge, "Oxidative stress and vascular disease," *Arteriosclerosis, Thrombosis, and Vascular Biology*, vol. 25, no. 1, pp. 29–38, 2005.

[2] M. Hulsmans, E. van Dooren, and P. Holvoet, "Mitochondrial reactive oxygen species and risk of atherosclerosis," *Current Atherosclerosis Reports*, vol. 14, no. 3, pp. 264–276, 2012.

[3] V. M. Victor, N. Apostolova, R. Herance, A. Hernandez-Mijares, and M. Rocha, "Oxidative stress and mitochondrial dysfunction in atherosclerosis: mitochondria-targeted antioxidants as

potential therapy," *Current Medicinal Chemistry*, vol. 16, no. 35, pp. 4654–4667, 2009.

[4] S. W. Ballinger, C. Patterson, C. A. Knight-Lozano et al., "Mitochondrial integrity and function in atherogenesis," *Circulation*, vol. 106, no. 5, pp. 544–549, 2002.

[5] S. W. Ballinger, "Mitochondrial dysfunction in cardiovascular disease," *Free Radical Biology and Medicine*, vol. 38, no. 10, pp. 1278–1295, 2005.

[6] C. M. Harrison, M. Pompilius, K. E. Pinkerton, and S. W. Ballinger, "Mitochondrial oxidative stress significantly influences atherogenic risk and cytokine induced oxidant production," *Environmental Health Perspectives*, vol. 119, no. 5, pp. 676–681, 2011.

[7] N. R. Madamanchi and M. S. Runge, "Mitochondrial dysfunction in atherosclerosis," *Circulation Research*, vol. 100, no. 4, pp. 460–473, 2007.

[8] E. P. K. Yu and M. R. Bennett, "Mitochondrial DNA damage and atherosclerosis," *Trends in Endocrinology and Metabolism*, vol. 25, no. 9, pp. 481–487, 2014.

[9] Y. Wang, G. Z. Wang, P. S. Rabinovitch, and I. Tabas, "Macrophage mitochondrial oxidative stress promotes atherosclerosis and nuclear factor-κB-mediated inflammation in macrophages," *Circulation Research*, vol. 114, no. 3, pp. 421–433, 2014.

[10] H. C. F. Oliveira, R. G. Cosso, L. C. Alberici et al., "Oxidative stress in atherosclerosis-prone mouse is due to low antioxidant capacity of mitochondria," *The FASEB Journal*, vol. 19, no. 2, pp. 278–280, 2005.

[11] A. J. Kowaltowski, R. F. Castilho, and A. E. Vercesi, "Mitochondrial permeability transition and oxidative stress," *FEBS Letters*, vol. 495, no. 1-2, pp. 12–15, 2001.

[12] T. R. Figueira, M. H. Barros, A. A. Camargo et al., "Mitochondria as a source of reactive oxygen and nitrogen species: from molecular mechanisms to human health," *Antioxidants and Redox Signaling*, vol. 18, no. 16, pp. 2029–2074, 2013.

[13] P. M. Yao and I. Tabas, "Free cholesterol loading of macrophages is associated with widespread mitochondrial dysfunction and activation of the mitochondrial apoptosis pathway," *The Journal of Biological Chemistry*, vol. 276, no. 45, pp. 42468–42476, 2001.

[14] B. A. Paim, J. A. Velho, R. F. Castilho, H. C. F. Oliveira, and A. E. Vercesi, "Oxidative stress in hypercholesterolemic LDL (low-density lipoprotein) receptor knockout mice is associated with low content of mitochondrial NADP-linked substrates and is partially reversed by citrate replacement," *Free Radical Biology & Medicine*, vol. 44, no. 3, pp. 444–451, 2008.

[15] Á. Zaratin, M. Gidlund, P. Boschcov, L. Castilho, and E. Cotta De Faria, "Antibodies against oxidized low-density lipoprotein in normolipidemic smokers," *The American Journal of Cardiology*, vol. 90, no. 6, pp. 651–653, 2002.

[16] A. G. Salerno, T. R. Silva, M. E. C. Amaral et al., "Overexpression of apolipoprotein CIII increases and CETP reverses diet-induced obesity in transgenic mice," *International Journal of Obesity*, vol. 31, no. 10, pp. 1586–1595, 2007.

[17] J. Folch, M. Lees, and G. H. S. Stanley, "A simple method for the isolation and purification of total lipides from animal tissues," *The Journal of Biological Chemistry*, vol. 226, no. 1, pp. 497–509, 1957.

[18] R. S. Kaplan and P. L. Pedersen, "Characterization of phosphate efflux pathways in rat liver mitochondria," *The Biochemical Journal*, vol. 212, no. 2, pp. 279–288, 1983.

[19] C. García-Ruiz, A. Colell, M. Marí, A. Morales, and J. C. Fernández-Checa, "Direct effect of ceramide on the mitochondrial electron transport chain leads to generation of reactive oxygen species: role of mitochondrial glutathione," *The Journal of Biological Chemistry*, vol. 272, no. 17, pp. 11369–11377, 1997.

[20] B. Paigen, A. Morrow, P. A. Holmes, D. Mitchell, and R. A. Williams, "Quantitative assessment of atherosclerotic lesions in mice," *Atherosclerosis*, vol. 68, no. 3, pp. 231–240, 1987.

[21] E. M. Rubin, R. M. Krauss, E. A. Spangler, J. G. Verstuyft, and S. M. Clift, "Inhibition of early atherogenesis in transgenic mice by human apolipoprotein AI," *Nature*, vol. 353, pp. 265–267, 1991.

[22] M.-F. Hau, A. H. M. Smelt, A. J. G. H. Bindels et al., "Effects of fish oil on oxidation resistance of VLDL in hypertriglyceridemic patients," *Arteriosclerosis, Thrombosis, and Vascular Biology*, vol. 16, no. 9, pp. 1197–1202, 1996.

[23] E. G. Bligh and W. J. Dyer, "A rapid method of total lipid extraction and purification," *Canadian Journal of Biochemistry and Physiology*, vol. 37, no. 8, pp. 911–917, 1959.

[24] D. Machado, S. M. Shishido, K. C. S. Queiroz et al., "Irradiated riboflavin diminishes the aggressiveness of melanoma in vitro and in vivo," *PLoS ONE*, vol. 8, no. 1, Article ID e54269, 2013.

[25] T. Lumley, *Leaps: Regression Subset Selection. R Package Version 2.9*, CRAN, 2009.

[26] R-Core-Team, *R: A Language and Environment for Statistical Computing*, R Foundation for Statistical Computing, Vienna, Austria, 2013.

[27] J. A. Velho, H. Okanobo, G. R. Degasperi et al., "Statins induce calcium-dependent mitochondrial permeability transition," *Toxicology*, vol. 219, no. 1–3, pp. 124–132, 2006.

[28] B. R. Kwak, N. Veillard, G. Pelli et al., "Reduced connexin43 expression inhibits atherosclerotic lesion formation in low-density lipoprotein receptor-deficient mice," *Circulation*, vol. 107, no. 7, pp. 1033–1039, 2003.

[29] Y. Wang and I. Tabas, "Emerging roles of mitochondria ROS in atherosclerotic lesions: causation or association?" *Journal of Atherosclerosis and Thrombosis*, vol. 21, no. 5, pp. 381–390, 2014.

[30] C. Albert, P. R. Mertens, and P. Bartsch, "Urea and atherosclerosis-evidence for a direct link involving apolipoprotein B protein modifications," *International Urology and Nephrology*, vol. 43, no. 3, pp. 933–936, 2011.

[31] A. G. Basnakian, S. V. Shah, E. Ok, E. Altunel, and E. O. Apostolov, "Carbamylated LDL," *Advances in Clinical Chemistry*, vol. 51, pp. 25–52, 2010.

[32] E. Ok, A. G. Basnakian, E. O. Apostolov, Y. M. Barri, and S. V. Shah, "Carbamylated low-density lipoprotein induces death of endothelial cells: a link to atherosclerosis in patients with kidney disease," *Kidney International*, vol. 68, no. 1, pp. 173–178, 2005.

[33] E. O. Apostolov, D. Ray, A. V. Savenka, S. V. Shah, and A. G. Basnakian, "Chronic uremia stimulates LDL carbamylation and atherosclerosis," *Journal of the American Society of Nephrology*, vol. 21, no. 11, pp. 1852–1857, 2010.

[34] K. M. Surapaneni and M. Jainu, "Pioglitazone, quercetin and hydroxy citric acid effect on hepatic biomarkers in Non Alcoholic Steatohepatitis," *Pharmacognosy Research*, vol. 6, no. 2, pp. 153–162, 2014.

[35] A. Kerner, O. Avizohar, R. Sella et al., "Association between elevated liver enzymes and C-reactive protein—possible hepatic contribution to systemic inflammation in the metabolic syndrome," *Arteriosclerosis, Thrombosis, and Vascular Biology*, vol. 25, no. 1, pp. 193–197, 2005.

[36] P. Libby, "Inflammation in atherosclerosis," *Arteriosclerosis, Thrombosis, and Vascular Biology*, vol. 32, pp. 2045–2051, 2012.

[37] R. A. Davis and T. Y. Hui, "2000 George Lyman Duff memorial lecture: atherosclerosis is a liver disease of the heart," *Arteriosclerosis, Thrombosis, and Vascular Biology*, vol. 21, no. 6, pp. 887–898, 2001.

Hindawi Publishing Corporation
Oxidative Medicine and Cellular Longevity
Volume 2015, Article ID 940627, 10 pages
http://dx.doi.org/10.1155/2015/940627

Research Article

Increased Susceptibility of *Gracilinanus microtarsus* Liver Mitochondria to Ca^{2+}-Induced Permeability Transition Is Associated with a More Oxidized State of NAD(P)

Juliana A. Ronchi,[1] Barbara Henning,[2] Felipe G. Ravagnani,[1] Tiago R. Figueira,[1] Roger F. Castilho,[1] Sergio F. dos Reis,[3] and Anibal E. Vercesi[1]

[1]*Department of Clinical Pathology, Faculty of Medical Sciences, State University of Campinas (UNICAMP), 13087-877 Campinas, SP, Brazil*
[2]*Graduate Program in Ecology, Biology Institute, State University of Campinas, 13087-877 Campinas, SP, Brazil*
[3]*Department of Animal Biology, Biology Institute, State University of Campinas, 13087-877 Campinas, SP, Brazil*

Correspondence should be addressed to Anibal E. Vercesi; anibal@unicamp.br

Received 7 April 2015; Revised 22 May 2015; Accepted 27 May 2015

Academic Editor: Andrés Trostchansky

In addition to be the cell's powerhouse, mitochondria also contain a cell death machinery that includes highly regulated processes such as the membrane permeability transition pore (PTP) and reactive oxygen species (ROS) production. In this context, the results presented here provide evidence that liver mitochondria isolated from *Gracilinanus microtarsus*, a small and short life span (one year) marsupial, when compared to mice, are much more susceptible to PTP opening in association with a poor NADPH dependent antioxidant capacity. Liver mitochondria isolated from the marsupial are well coupled and take up Ca^{2+} but exhibited a much lower Ca^{2+} retention capacity than mouse mitochondria. Although the known PTP inhibitors cyclosporin A, ADP, and ATP significantly increased the marsupial mitochondria capacity to retain Ca^{2+}, their effects were much larger in mice than in marsupial mitochondria. Both fluorescence and HPLC analysis of mitochondrial nicotinamide nucleotides showed that both content and state of reduction (mainly of NADPH) were lower in the marsupial mitochondria than in mice mitochondria despite the similarity in the activity of the glutathione peroxidase/reductase system. Overall, these data suggest that PTP opening is an important event in processes of Ca^{2+} signalling to cell death mediated by mitochondrial redox imbalance in *G. microtarsus*.

1. Introduction

It is well established that Ca^{2+} modulates many vital processes through transient increases in its free concentrations in different cell compartments [1]. This includes several pathways of energy metabolism, synaptic transmission, gene expression, and cell survival or death [2–5].

In order to fulfill these physiological roles Ca^{2+} movements across plasma cell membrane are driven directly or indirectly by ATP hydrolysis; therefore, defects in processes of cellular ATP supply may lead to dysregulation in Ca^{2+} signaling that may compromise cell functioning [1, 4]. In regard to mechanisms of survival or death, evidence has been provided that intramitochondrial Ca^{2+} signals for both (i) the control of oxidative phosphorylation, required for cell function [3, 5, 6], and (ii) reactive oxygen generation, required for both survival and death [4, 7]. Indeed, it is now generally accepted that superoxide as well as other reactive oxygen species (ROS) can function both beneficially or adversely [4, 8]. At progressively increasing physiological levels they may successively regulate cellular processes such as proliferation and differentiation, activate adaptive programs such as transcriptional upregulation of antioxidant genes and, at higher levels, they may signal to senescence and regulated cell death [8]. Direct damaging effects of free radicals may only occur under extreme conditions [9, 10]. In addition to the physiological processes, it seems that mitochondrial oxidative stress is responsible for the development and

progression of a series of pathologies such as cancer, diabetes, inflammatory diseases, hypertension, neurodegenerative, and ischemia-related diseases and aging [4, 11]. In this context, one event that may participate in all of these processes via the mitochondrial pathway of cell death, either by apoptosis or necrosis, is the so-called mitochondrial membrane permeability transition (MPT) [12, 13].

The state of MPT is characterized by the opening of a nonspecific inner membrane pore induced by the combination of high matrix [Ca^{2+}] and oxidative stress [9, 13]. Considering the understanding of how Ca^{2+} and reactive oxygen act synergistically in the process of permeability transition pore (PTP) opening, evidence has been provided that mitochondria are more susceptible to MPT when their antioxidant systems, represented mainly by NADPH, are exhausted [9, 14, 15]. In fact, MPT can be induced by prooxidants and prevented or even reversed by antioxidants [13].

Altogether the above considerations indicate that mitochondria are multifunctional organelles that control the production of ATP, participate in intracellular Ca^{2+} homeostasis, and function as a main source of reactive oxygen. Therefore, it might be reasonable to consider that genetic variations or dysfunctions in any of these vital mitochondrial properties may intrinsically modify the susceptibility to many diseases and aging [16]. In this regard, the Brazilian gracile opossum (*Gracilinanus microtarsus*) is a short lifespan marsupial with high mortality associated with heightened levels of stress due to aggressive behavior during the mating period [17–22]. *G. microtarsus* has a most unusual and remarkable reproductive pattern in that the majority of males die after the first mating period, a condition known as partial semelparity in evolutionary ecology [18, 23]. Available evidence suggests that the cost of reproduction is detrimental to the survival of *G. microtarsus* and is conceivably related to the short lifespan of this species in nature.

The aims of the present work were, firstly, the analysis of mitochondrial bioenergetics in isolated liver mitochondria from *G. microtarsus*, taking into consideration the possible role of these organelles as key players in lifespan regulation of this marsupial and, secondly, to verify whether MPT plays any role in the process.

2. Material and Methods

2.1. Chemicals. Most of the reagents used were obtained from Sigma-Aldrich. Calcium Green-5N hexapotassium salt was purchased from Invitrogen (Invitrogen, Carlsbad, CA, USA).

2.2. Animals. C57BL/6/JUnib mice were provided by the Campinas University Multidisciplinary Center for Biological Research in Laboratory Animals (CEMIB/UNICAMP, Campinas, Brazil). The C57BL/6/JUnib mice substrain does not carry the mutation in the nicotinamide nucleotide transhydrogenase (*Nnt*) gene [15] that affects the mitochondrial function of some other C57BL/6 mice substrains [24]. *Nnt* is a well conserved gene and is present in marsupials (*Monodelphis domestica*, gene ID: 100012732). Mice were kept under standard laboratory conditions (20–22°C and 12 h/12 h light/dark cycle) with free access to a standard diet (Labina/Purina, Campinas, SP, Brazil) and tap water. Although mice are phylogenetically distant from marsupials, mouse features a similar body size to *G. microtarsus* and is one of the most well-characterized species in terms of mitochondrial bioenergetics.

Marsupials (*G. microtarsus*) were captured in the municipality of Américo Brasiliense, *ca* 300 km northwest of São Paulo in southeastern Brazil (collection permit number from the Brazilian Institute of Environment (IBAMA): SISBIO #36133). Vegetation at the location consists of forested remnants of Cerrado characterized by dense semideciduous forest with canopy cover varying from 50 to 90 percent, trees 8–15 m tall, and little herbaceous vegetation. The climate of the region has two well-defined seasons: a warm-wet season from October to March and a cool-dry season from April to September. Traps were set for four consecutive nights every month from February to November 2012. Animals were captured using a 11×8 trapping grid with 88 trapping stations located 10 m apart. A single Sherman live trap (7.5 × 9.0 × 23.5 cm) was set on trees at each trapping station *ca* 1.75 m aboveground and baited with banana, peanut butter, and cod-liver oil.

The marsupials (*G. microtarsus*) were returned to the Universidade Estadual de Campinas (UNICAMP) and housed in individual cages in an animal room maintained at approximately 23°C with a 12 h/12 h light/dark cycle. Marsupials were provided with *ad libitum* water and the appropriated amount of food (dry cat and dog food and mango) to maintain their weight gain similar to that expected under natural conditions. The individuals were kept in this animal room for approximately 3 months before the beginning of the experiments.

Experimental protocols used were approved by the local Committee for Ethics in Animal Research (CEUA-UNICAMP). Animal experiments followed the Guide for the care and use of laboratory animals published by the U.S. National Institutes of Health (NIH publication 85-23, revised 1996).

2.3. Isolation of Liver Mitochondria. Liver mitochondria were isolated concomitantly from mice and marsupials by differential centrifugation [25] and partially purified by a discontinuous Percoll gradient. Male animals were used for all experiments except that for quantification of mitochondrial NAD(P) contents. The animals were decapitated and the livers were rapidly removed, finely minced, and homogenized in an ice-cold isolation medium containing 250 mM sucrose, 1 mM EGTA, and 10 mM HEPES buffer (pH 7.2). The homogenates were centrifuged for 10 min at 800 *g*. The supernatants were centrifuged at 7750 *g* for 10 min. The mitochondrial pellet was purified using a discontinuous Percoll gradient according to Lopez-Mediavilla et al. [26]. After centrifugation for 10 min at 7750 *g*, the mitochondrial fraction obtained from the interface between 19 and 52% Percoll layers was resuspended in buffer containing 250 mM sucrose, 0.3 mM EGTA, and 10 mM HEPES buffer (pH 7.2) and recentrifuged at 7750 *g* for 10 min. The final pellet containing liver mitochondria was resuspended in an EGTA-free buffer at approximate protein concentrations of 50 mg/mL.

The entire procedure was carried out at 4°C. The protein content of the mitochondrial suspensions was determined by Biuret assay in the presence of 0.2% deoxycholate [27] with bovine serum albumin as the standard.

2.4. Standard Incubation Procedure. Measurements of mitochondrial oxygen consumption, membrane potential, Ca^{2+} uptake, redox state of endogenous nicotinamide nucleotides, and activity of glutathione peroxidase/redutase system were carried out at 28°C with continuous magnetic stirring in a standard reaction medium containing 125 mM sucrose, 65 mM KCl, 2 mM KH_2PO_4, 1 mM $MgCl_2$, 10 mM HEPES buffer (pH 7.2), and ~15 μM contaminant Ca^{2+}. Other additions are indicated in the figure legends. Except for the O_2 consumption measurements, which were performed in a 1.4 mL chamber, a 2 mL final volume was used in the experiments that were performed in cuvettes.

2.5. Oxygen Consumption Measurements. Oxygen consumption by the mitochondria (0.5 mg/mL) was measured in a temperature controlled chamber equipped with a magnetic stirrer, using a Clark-type electrode (Yellow Spring Instruments Company, Yellow Spring, OH, USA) in standard reaction medium containing 0.3 mM EGTA and a NADH-linked substrate mixture (2 mM malate, 1 mM pyruvate, 1 mM α-ketoglutarate, and 1 mM glutamate).

2.6. Measurement of Transmembrane Electrical Potential. Mitochondrial membrane potential was monitored by following the changes in 5 μM safranine fluorescence [28], which were recorded on a Hitachi F-4500 spectrofluorometer operating at excitation and emission wavelengths of 495 and 586 nm, respectively, with slit widths of 5 nm.

2.7. Measurements of Mitochondrial Ca^{2+} Retention Capacity. The Ca^{2+} retention capacity was determined in liver mitochondria (0.5 mg/mL) incubated in standard reaction medium containing 0.2 μM Calcium Green-5N as a probe. Levels of external free Ca^{2+} were measured by recording the fluorescence of Calcium Green-5N on a spectrofluorometer (Hitachi F-4500) operating at excitation and emission wavelengths of 506 and 532 nm, respectively, with slit widths of 5 nm and continuous magnetic stirring. Five minutes after the addition of mitochondria (0.5 mg/mL) to the cuvette, boluses of 5 μM (control conditions) or 30 μM (when cyclosporin A, ADP, or ATP plus Mg^{2+} was present) of $CaCl_2$ were sequentially added every 2.5 min until the mitochondria began to release Ca^{2+} into the medium. The amount of $CaCl_2$ added prior to mitochondrial Ca^{2+} release was taken as the mitochondrial Ca^{2+} retention capacity, a quantitative approach to compare MPT between groups.

2.8. Determination of NAD(P) Redox State in Intact Mitochondria. Changes in the redox state of nicotinamide nucleotides (NAD(P)) in the mitochondrial suspensions (0.5 mg/mL) in standard reaction medium supplemented with 300 μM EGTA, 1 μM rotenone, and 5 mM succinate were monitored in a spectrofluorometer (Hitachi F-4500) using excitation and emission wavelengths of 366 and 450 nm, respectively, and slit widths of 5 nm [15]. Of note, only the reduced forms of NAD(P) exhibit a strong endogenous fluorescence signal. As a reference, known amounts of NADPH were added to the reaction medium in the absence of mitochondria. Succinate was chosen as an energizing substrate to allow the endogenous content of substrates, which was apparently different between species, to play a role in the metabolism of tert-butyl hydroperoxide (*t*-BOOH), an exogenous peroxide that was used to challenge the mitochondrial antioxidant system.

2.9. Mitochondrial Activity of Glutathione Peroxidase/Reductase System. Liver mitochondria (1 mg/mL) were lysed by the presence of 0.1% Triton X-100 in standard medium reaction containing 500 μM GSH and 100 μM NADPH. The activity of the mitochondrial glutathione peroxidase/reductase system was estimated by the rate of NADPH oxidation after the addition of 0.5 mM tert-butyl hydroperoxide (*t*-BOOH; an oxidant agent) [29]. NADPH oxidation was followed by monitoring the fluorescence at excitation and emission wavelengths of 366 and 450 nm, respectively, and slit widths of 5 nm. In this assay, added glutathione is recycled thought the action of both redox enzymes consuming the NADPH, thus revealing the maximal flux through this enzymatic system.

2.10. Nicotinamide Nucleotide Transhydrogenase (NNT) Assay. NNT was assayed as conducted before in our laboratory [15]. Briefly, the changes in differential absorbance (375–425 nm) due to the reduction of APAD, which is a NAD^+ analogue, were monitored for 5 min at 37°C (Shimadzu UV-1800 Spectrophotometer, Kyoto, Japan). The assay medium contained 100 mM sodium phosphate (pH 6.5), 1 mg/mL lysolecithin, 0.5% Brij-35, 1 μM rotenone, 300 μM APAD, and 400 μg/mL liver mitochondrial protein; the reaction was initiated with 300 μM NADPH after 5 min preincubation. The slopes of absorbance over time were converted to nmol APAD reduced/min using the molar extinction coefficient of 5.1 $mM^{-1} \times cm^{-1}$ for reduced APAD.

2.11. Quantification of Mitochondrial NAD(P) Contents. Oxidized and reduced forms of NAD and NADP were determined by fluorometric detection using high-performance liquid chromatography (HPLC) as described by Klaidman et al. [30] with minor modifications [15]. Calibration curves were built with known amounts of standards. All samples concomitantly isolated from marsupials and mice were immediately frozen and maintained at −80°C until analysis a week later.

2.12. Statistics. Results are presented as representatives or averages ± standard errors (SEM) of at least three experiments with different preparations. Mann-Whitney (nonparametric) test or Student's *t*-test was used for statistical analyses. A P value less than 0.05 was considered significant.

3. Results

3.1. Respiratory Coupling. In order to assess the functional integrity of isolated mitochondrial preparations, respiration

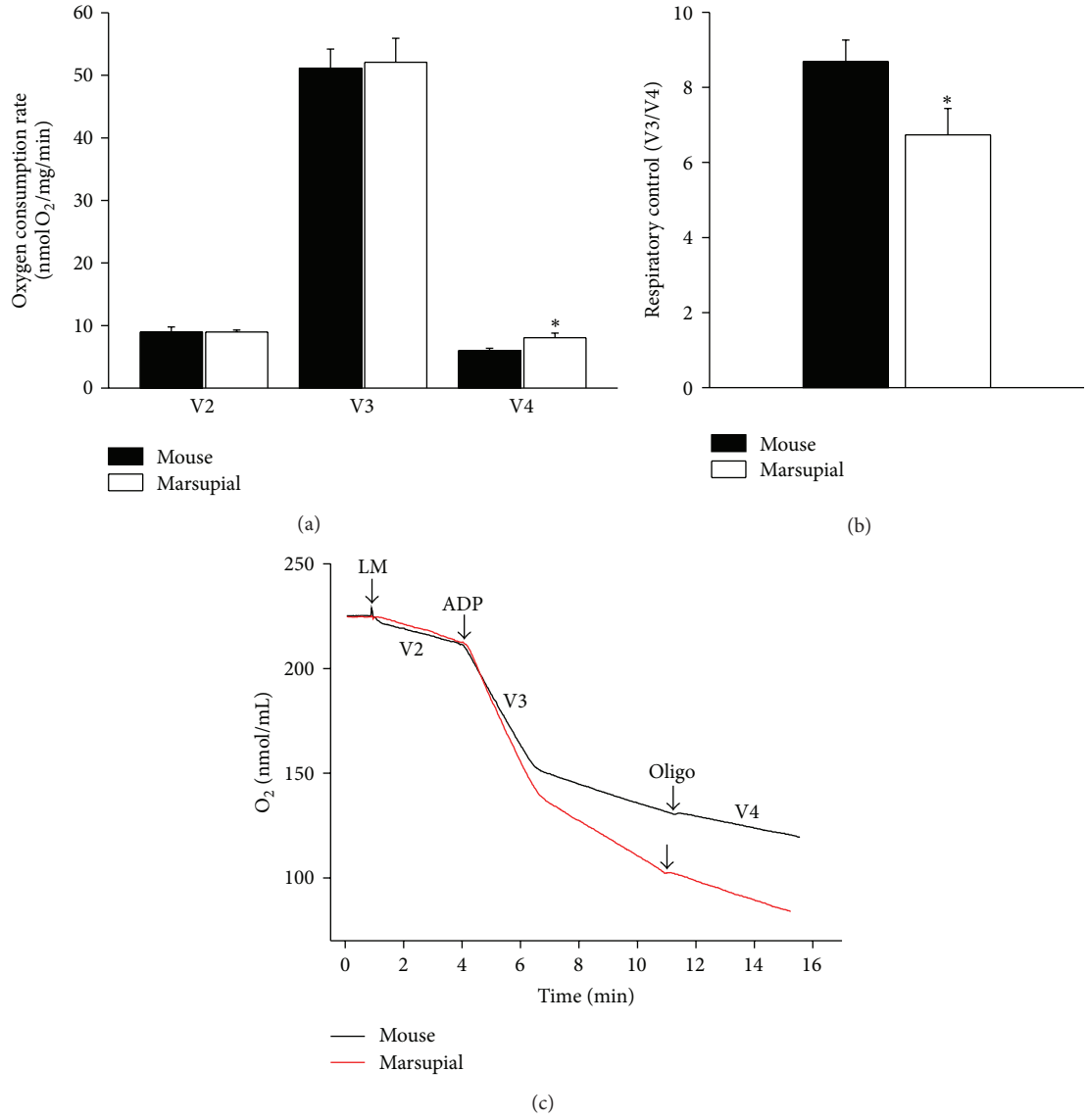

Figure 1: Oxidative phosphorylation parameters in mouse and marsupial liver mitochondria. (a) *Mus musculus* (mouse) and *Gracilinanus microtarsus* (marsupial) isolated liver mitochondria (0.5 mg/mL) were incubated in standard reaction medium containing NADH-linked respiratory substrates (2 mM malate, 1 mM pyruvate, 1 mM α-ketoglutarate, and 1 mM glutamate) and 200 μM EGTA. Respiratory states were determined under basal conditions (V2) and after sequential additions of ADP (300 μM) and 1 μg/mL oligomycin (Oligo) to achieve respiratory states 3 (V3) and 4 (V4), respectively. The results are expressed as means ± SEM ($n = 8$). $^*P < 0.05$ versus mouse mitochondria. (b) Respiratory control ratios (V3/V4). (c) Representative traces of oxygen consumption by mouse and marsupial liver mitochondria (LM).

experiments were performed (Figures 1(a)–1(c)). Both marsupial and mouse liver mitochondria demonstrated well-coupled respiration although the respiration in the presence of oligomycin (state 4 respiration; V4) was significantly higher in the marsupial liver mitochondria. The mean respiratory control ratio (RCR) was slightly higher in mice than in marsupial.

3.2. Electrical Membrane Potential ($\Delta\Psi$): Effect of Ca^{2+}. The experiment depicted in Figure 2 demonstrated that energization of both types of mitochondria was followed by safranine uptake and adsorption to the polarized inner membrane, processes associated with safranine fluorescence decrease [28]. It can be observed that the initial decreases in fluorescence were quantitatively similar in both mitochondria and stabilized at membrane potentials close to −180 mV (Figure 2(a)). ADP addition to mouse liver mitochondria induced the expected transient decrease in $\Delta\Psi$, returning to the previous value after a short period of ADP phosphorylation. ADP addition to the marsupial mitochondria also caused the expected $\Delta\Psi$ decrease with a slow return to initial values. $\Delta\Psi$ was estimated by calibration through potassium titration after the ionophore valinomycin was included in the medium [28].

Interestingly, Figure 2(b) shows that the marsupial mitochondria quickly released the $\Delta\Psi$ after the addition of a small pulse of Ca^{2+} (30 μM) via a mechanism sensitive

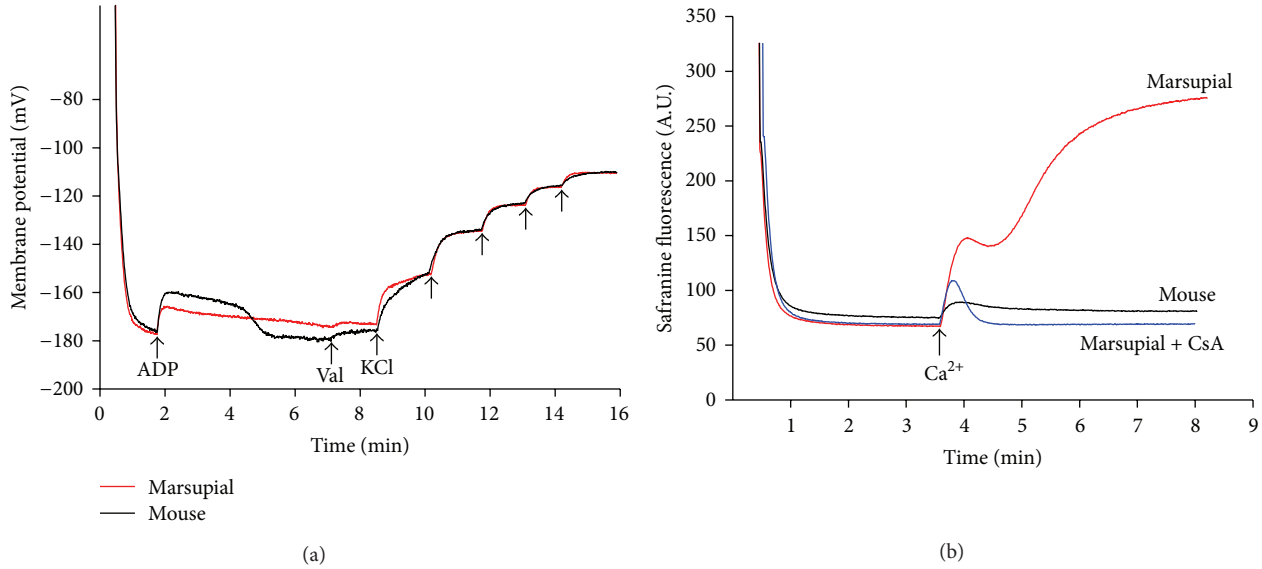

FIGURE 2: Effect of micromolar Ca^{2+} concentration on membrane potential of mouse and marsupial liver mitochondria. (a) Determination of membrane potential in isolated mouse and marsupial liver mitochondria. Liver mitochondria (0.5 mg/mL) were added to the incubation medium containing 200 μM EGTA, NADH-linked respiratory substrates (2 mM malate, 1 mM pyruvate, 1 mM α-ketoglutarate and 1 mM glutamate), and 5 μM safranine. The arrows indicate where 150 μM ADP, 40 ng/mL valinomycin (Val), and KCl (each addition: 350 μM) were added to the experiments. (b) Effect of Ca^{2+} on mitochondrial membrane potential. Ca^{2+} (40 μM) was added to the experiments which was indicated by the arrow. Cyclosporin A (CsA; 1 μM), a mitochondrial permeability transition inhibitor, was present in the incubation medium where indicated. Traces are representative of 3 independent experiments.

to cyclosporin A. In contrast, mouse liver mitochondria sustained a very stable membrane potential after the transient decrease in $\Delta\Psi$ induced by the same pulse of Ca^{2+}.

3.3. Ca^{2+} Retention Capacity. Considering that Ca^{2+}-induced MPT is an event that is redox sensitive and may promote cell death [4, 13], we determined the mitochondrial Ca^{2+} retention capacity of both types of mitochondria as an assessment of their susceptibility to MPT. Figure 3(a) depicts representative experiments of mitochondria oxidizing NAD-linked substrates, in the presence of ADP, and subjected to successive additions of Ca^{2+} pulses, to the point of MPT-mediated Ca^{2+} release. It can be seen that the marsupial liver mitochondria exhibited a significantly lower Ca^{2+} retention capacity than mouse mitochondria. Although the known MPT inhibitors cyclosporin A, ADP, and ATP plus Mg^{2+} [12, 13, 31, 32] significantly increased the capacity of the marsupial mitochondria to retain the cation, their effects were much larger in mice mitochondria (Figure 3(b)). For example, in the presence of ADP the capacity of Ca^{2+} retention by the marsupial liver mitochondria was almost ten times lower than that of the mice liver mitochondria.

3.4. Mitochondrial Nicotinamide Nucleotide Content and Redox State. It has long been known [33] that the reduced state of mitochondrial nicotinamide nucleotides, mainly NADPH [14], favors Ca^{2+} retention by mitochondria. To assess the participation of these nucleotides in these mechanisms, we monitored fluorimetrically the changes in redox state of mitochondrial NAD(P)H during the detoxification of exogenously added tert-butyl hydroperoxide (*t*-BOOH) in both types of mitochondria. Firstly we analyzed the activity of the glutathione peroxidase/reductase system that catalyzes this reaction using reducing equivalents from NADPH [29]. Figure 4(a) provided evidence that the activities of these enzymes are quite similar in both marsupial and mice mitochondria but the results presented in Figure 4(b) indicated that (i) upon the addition of mitochondria to the reaction medium, the mice nicotinamide nucleotides fluorescence was at the maximum value and maintained a plateau while the marsupial nicotinamide nucleotides were not at the maximal value but steadily increased their fluorescence toward a lower plateau value than that of the mice nicotinamide nucleotides fluorescence, (ii) the extent of the redox changes induced by *t*-BOOH was much smaller in marsupial mitochondria, and (iii) the time to restore the *t*-BOOH induced NAD(P)H oxidation was much longer in marsupial mitochondria. Taken together these results indicate that both content and state of reduction were lower in the marsupial mitochondria than in mice mitochondria. Under the conditions with succinate as an energy substrate that was used to obtain data shown in Figure 4(b), the function of NNT is required (as demonstrated in [15]) to support $NADP^+$ reduction. For this reason and because the rereduction of NAD(P) was much slower in marsupial than in mouse mitochondria following *t*-BOOH addition, we assayed NNT activity in isolated liver mitochondria from both species. The measured activity of NNT was not different between marsupial (28.0 ± 1.12 mU/mg; $n = 3$) and mouse (30.9 ± 5.02 mU/mg; $n = 3$), thus ruling out the involvement of NNT activity in the slower

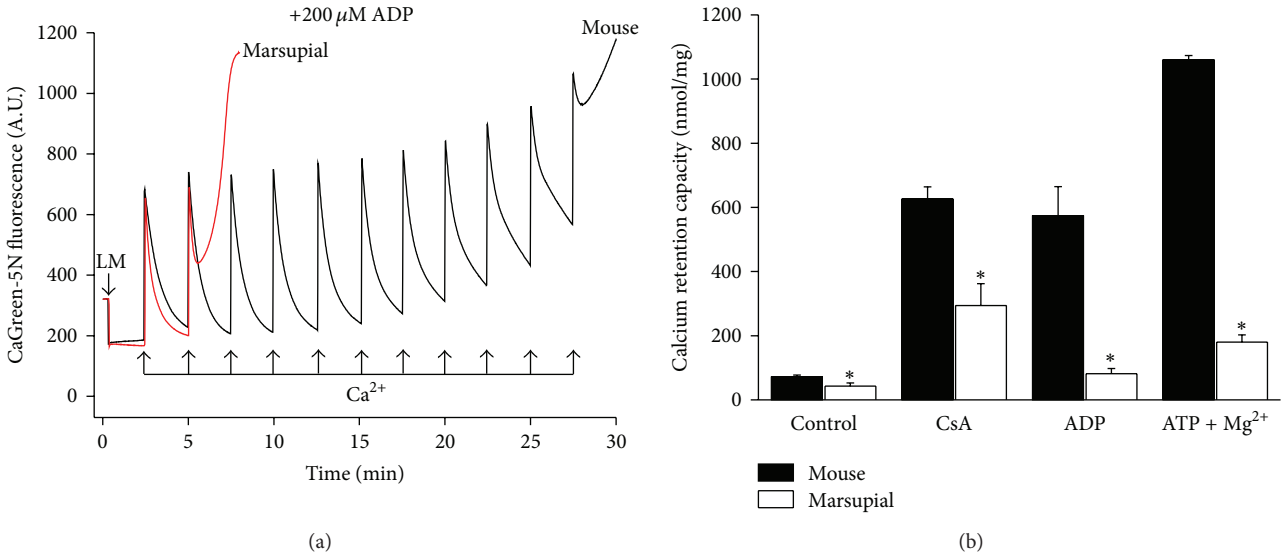

FIGURE 3: Effect of mitochondrial permeability transition (MPT) inhibitors on the Ca^{2+} retention capacity of mouse and marsupial liver mitochondria. Isolated mouse and marsupial liver mitochondria (LM; 0.5 mg/mL) were incubated in standard reaction medium supplemented with NADH-linked (2 mM malate, 1 mM pyruvate, 1 mM α-ketoglutarate, and 1 mM glutamate) respiratory substrates and 0.2 μM Calcium Green-5N. Some experiments were conducted in the presence of the MPT inhibitors: 1 μM cyclosporin A (CsA), 200 μM ADP, or 200 μM ATP plus 3 mM $MgCl_2$, as indicated in the figure. (a) Representative experiments for estimation of calcium retention capacity of mouse and marsupial liver mitochondria in the presence of ADP. (b) To assess the mitochondrial Ca^{2+} retention capacity, pulses of Ca^{2+} (5 μM for control conditions or 30 μM for the conditions in the presence of MPT inhibitors CsA, ADP, or ATP plus Mg^{2+}) were added until mitochondrial Ca^{2+} release occurred. The sum of Ca^{2+} pulses prior to MPT pore opening was taken as the mitochondrial Ca^{2+} retention capacity ($n = 7$ for all conditions except for "ATP+Mg^{2+}," where $n = 3$). $^*P < 0.05$ versus respective condition in mouse mitochondria.

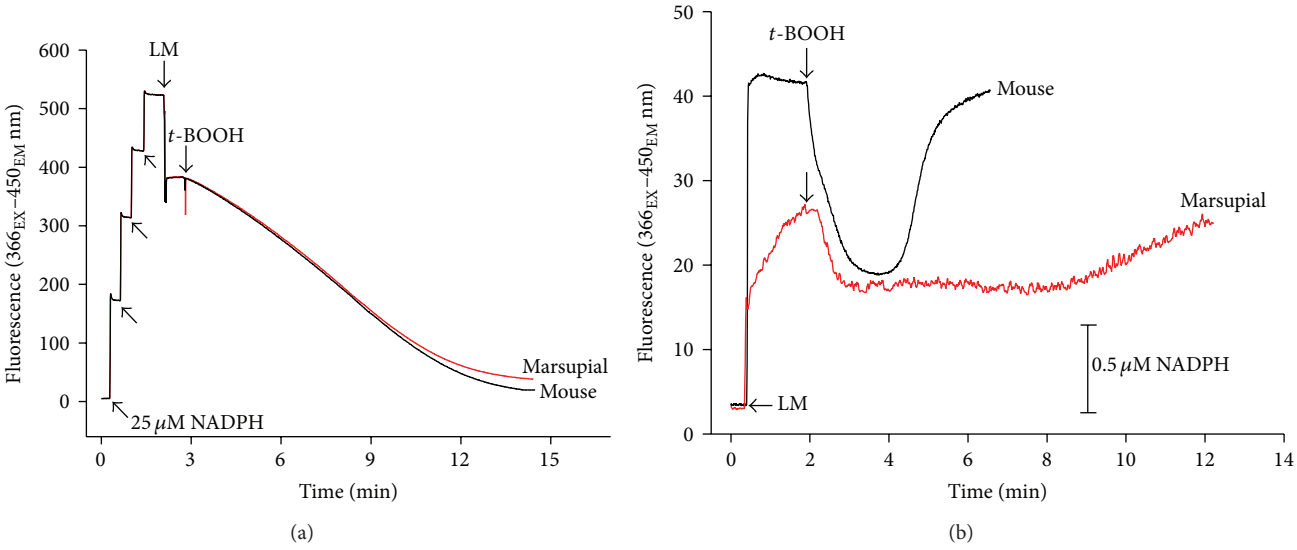

FIGURE 4: Determination of the mitochondrial activity of glutathione peroxidase/reductase system and ability to metabolize organic peroxide. (a) Isolated mouse and marsupial liver mitochondria (LM; 1 mg/mL) were added to standard reaction medium containing 500 μM GSH and 100 μM NADPH. Triton X-100 (0.1%) was also presented to lyse the mitochondria. The reaction started after the addition of 0.5 mM tert-butyl hydroperoxide (t-BOOH). Lines are representative of three independent experiments. (b) LM (0.5 mg/mL) were incubated in standard medium containing 5 mM succinate, 1 μM rotenone, and 300 μM EGTA. Where indicated by the arrow, 15 μM t-BOOH was added. Traces are representative of 4 independent experiments.

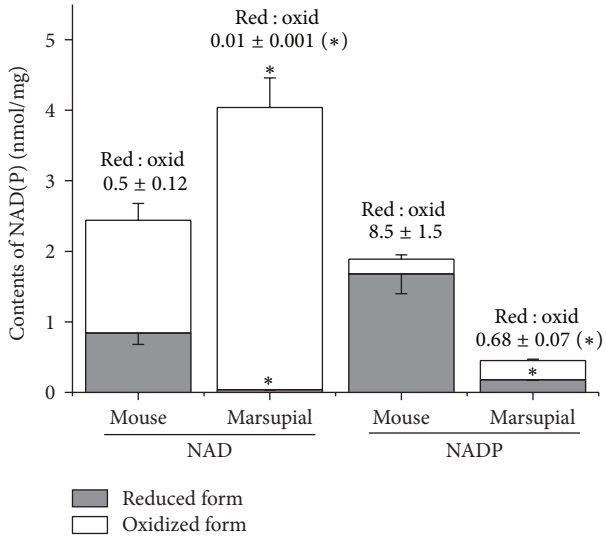

Figure 5: Determination of nicotinamide nucleotide content in isolated mitochondria. HPLC analysis of NAD and NADP contents in mouse and marsupial mitochondria ($n = 3$ for mouse and 5 for marsupial). The ratio of reduced to oxidized NAD(P) (Red : Oxid) is shown above the bars. $^{*}P < 0.05$ versus respective parameter in mouse mitochondria.

peroxide metabolism by marsupial mitochondria compared to that of mouse.

In order to further investigate the redox state and the content of nicotinamide nucleotides in mitochondria, we performed HPLC analysis of these nucleotides. The bars presented in Figure 5 show that the content of total NAD is higher in the marsupial than in mice mitochondria (4.02 ± 0.42 versus 2.44 ± 0.62 nmol/mg) and that, in contrast, the content of total NADP is much lower in the marsupial mitochondria (0.44 ± 0.03 versus 1.89 ± 0.32 nmol/mg). Most interesting, and in agreement with the data presented in Figure 4(b), both nicotinamide nucleotides were much more oxidized in the marsupial mitochondria. Overall, data in Figures 4(b) and 5 seem to indicate that marsupial liver mitochondria possess a lower content of endogenous substrates linked to $NAD(P)^+$ reduction than that of mice.

4. Discussion

Mitochondrial dysfunction and opening of the PTP are thoroughly implicated in the development of several diseases and aging, in various animal models [4, 11–13]. In this regard, the present work demonstrates that isolated liver mitochondria from the short life span marsupial *G. microtarsus* presented three main functional differences when compared to mice mitochondria, which were used here as an established mammalian model, for comparative purposes. First, the marsupial mitochondria showed a significant higher rate of resting (state-4) respiration; second, they are much more susceptible to PTP opening; and third, they have a much lower constitutive antioxidant capacity represented by the $NADPH/NADP^+$ content and redox potential.

The higher state-4 respiration was present in all marsupial liver mitochondrial preparations as compared to mouse. From the stand point of redox regulation of MPT that will be approached below, it might be worth mentioning that higher mitochondrial respiration rates are associated with lower rates of superoxide radical production by mitochondria [4]. Since the most frequently used technique to assess ROS production from mitochondria (Amplex Red/horseradish peroxidase assay) may not be suitable to compare isolated liver mitochondria from different species [34], we performed analyses of the mitochondrial antioxidant system. These evaluations indeed revealed main mitochondrial redox differences between these two species with regard to the regulation of MPT. It might be speculated that the higher state-4 respiration in marsupial could be linked to an impaired clearance process of old or damaged mitochondria that may contribute to a fast process of senescence related to the short life span of this marsupial [35, 36]. Except for this presumed subpopulation of uncoupled mitochondria and the higher susceptibility to Ca^{2+}-induced MPT the marsupial and mice liver mitochondria exhibited similar bioenergetics properties when evaluated under the same experimental conditions. As shown in the results section, liver mitochondria from both species were well coupled and presented comparable values of electrical membrane potential and maximal rates of ADP-stimulated respiration. Therefore, the difference in susceptibilities to MPT cannot be attributed to differences in quality between the two mitochondrial preparations. Indeed, research in progress in this laboratory provides evidence that fish liver mitochondria present lower respiratory control ratio and higher state-4 respiration than rat liver mitochondria; but in contrast to these marsupial mitochondria, fish liver mitochondria have a much higher capacity to retain Ca^{2+} than rat (G. A. Dal'Bó, F. G. Sampaio, A. E. Vercesi, unpublished results). In fact, the present experiments demonstrate that marsupial and mice mitochondria share some MPT properties and differ in some other properties. The results depicted in Figure 3 indicate that the marsupial mitochondria present a lower threshold for Ca^{2+} induced PTP opening. However, it should be emphasized that even when PTP is inhibited by CsA the ability of the marsupial mitochondria to accumulate and retain Ca^{2+} is significantly lower than that of the mice mitochondria. In addition, MPT in the marsupial mitochondria is less sensitive to the inhibition by adenine nucleotides ATP or ADP, especially to the latter. For example, while the mice mitochondria accumulated and retained ten pulses of 60 nmol Ca^{2+}/mg before opening the PTP in the presence of ADP, marsupial mitochondria were able to accumulate and retain only one pulse (Figure 3(a)).

Despite the large number of studies approaching the PTP structure, its composition remains unresolved and controversial. Several studies suggest that it is minimally composed of or modulated by matrix, inner and outer membrane proteins such as the CsA-binding protein cyclophilin D (CypD), the adenine nucleotide transporter (ANT), the ATP synthase, hexokinase, phosphate carrier, and the voltage dependent anion channel (VDAC) (for recent reviewers see [37, 38]). Other studies using submitochondrial particles, mitoplasts,

or mitochondria naturally or genetically modified provided evidence that PTP opening may take place although with different characteristics even in the absence of some of these proteins [39–43]. Therefore, the present results showing different properties between marsupial and mice PTP can be interpreted taking into consideration the different plasticity and protein composition of the putative PTP pore. In addition, oxidative stress may also contribute to the lower inhibitory effect of adenine nucleotides on Ca^{2+} induced MPT [31] in marsupial mitochondria.

Perhaps the most intriguing characteristic of the marsupial liver mitochondria is their low capacity for Ca^{2+} retention. This recall pioneering data from Lehninger laboratory demonstrating that Ca^{2+} release from liver mitochondria was favored by the oxidized state of endogenous nicotinamide nucleotides [33]. The progress in the understanding of these data provided evidence that PTP opening is associated with membrane protein thiol crosslinking via thiol oxidation linked to the redox state of mitochondrial NADP [39]. In fact, MPT can be stimulated in Ca^{2+} loaded mitochondria by prooxidants such as *t*-BOOH, diamide, suramin, and/or by various experimental conditions that lead to oxidative stress either in isolated mitochondria, intact cells, or isolated organs [13, 14, 44, 45].

In the present work, a more oxidized state of the mitochondrial NADP was demonstrated by HPLC analysis which strongly supports the idea that the mitochondrial NADPH-dependent antioxidant systems glutathione and thioredoxin peroxidases/reductases are less effective in the marsupial due to a lower reducing power provided by NADPH (Figure 4(a)). This hypothesis was further corroborated by the experiment depicted in Figure 4(b) showing a much slower rate of *t*-BOOH metabolization by the marsupial than by the mouse liver mitochondria. This is also in agreement with the recent studies from this laboratory showing that liver mitochondria isolated from the expontaneously mutated C57BL/6J mice lacking functional mitochondrial nicotinamide nucleotide transhydrogenase (NNT), an enzyme that reduces $NADP^+$ using reducing equivalents from NADH, are more susceptible to MPT [15]. Although the marsupial and the NNT-mutated mice exhibit a compromised NADPH reducing power via different mechanisms, they share common mitochondrial characteristics namely low antioxidant mitochondrial capacity and high susceptibility to MPT.

A complex phenotype, as the short life span of this marsupial, may be determined by the interaction of many variables, among which the observed mitochondrial characteristics may comprise an intrinsic biochemical factor reducing survival upon environmental challenges.

Abbreviations

ADP: Adenosine diphosphate
ATP: Adenosine triphosphate
CsA: Cyclosporin A
KCl: Potassium chloride
LM: Liver mitochondria
MPT: Mitochondrial permeability transition
NAD: β-Nicotinamide adenine dinucleotide
NADH: Reduced form of NAD
NAD^+: Oxidized form of NAD
NADP: β-Nicotinamide adenine dinucleotide phosphate
NADPH: Reduced form of NADP
$NADP^+$: Oxidized form of NADP
NNT: Nicotinamide nucleotide transhydrogenase
Oligo: Oligomycin
PTP: Permeability transition pore
ROS: Reactive oxygen species
t-BOOH: tert-Butyl hydroperoxide
Val: Valinomycin.

Conflict of Interests

The authors declare that there is no conflict of interests regarding the publication of this paper.

Acknowledgments

The authors thank Dr. Prianda R. Laborda for discussions about marsupial genetics. Research funding was provided by FAPESP (2011/50400-0) and CNPq. B. Henning has been supported by CAPES and CNPq fellowships.

References

[1] M. J. Berridge, M. D. Bootman, and H. L. Roderick, "Calcium signalling: dynamics, homeostasis and remodelling," *Nature Reviews Molecular Cell Biology*, vol. 4, no. 7, pp. 517–529, 2003.

[2] C. Hidalgo and P. Donoso, "Crosstalk between calcium and redox signaling: from molecular mechanisms to health implications," *Antioxidants and Redox Signaling*, vol. 10, no. 7, pp. 1275–1312, 2008.

[3] B. Glancy and R. S. Balaban, "Role of mitochondrial Ca^{2+} in the regulation of cellular energetics," *Biochemistry*, vol. 51, no. 14, pp. 2959–2973, 2012.

[4] T. R. Figueira, M. H. Barros, A. A. Camargo et al., "Mitochondria as a source of reactive oxygen and nitrogen species: from molecular mechanisms to human health," *Antioxidants & Redox Signaling*, vol. 18, no. 16, pp. 2029–2074, 2013.

[5] G. Huang, A. E. Vercesi, and R. Docampo, "Essential regulation of cell bioenergetics in *Trypanosoma brucei* by the mitochondrial calcium uniporter," *Nature Communications*, vol. 4, article 2865, 2013.

[6] R. M. Denton and J. G. McCormack, "Ca^{2+} as a second messenger within mitochondria of the heart and other tissues," *Annual Review of Physiology*, vol. 52, no. 1, pp. 451–466, 1990.

[7] R. F. Feissner, J. Skalska, W. E. Gaum, and S.-S. Sheu, "Crosstalk signaling between mitochondrial Ca^{2+} and ROS," *Frontiers in Bioscience*, vol. 14, no. 4, pp. 1197–1218, 2009.

[8] R. B. Hamanaka and N. S. Chandel, "Mitochondrial reactive oxygen species regulate cellular signaling and dictate biological outcomes," *Trends in Biochemical Sciences*, vol. 35, no. 9, pp. 505–513, 2010.

[9] A. J. Kowaltowski, N. C. de Souza-Pinto, R. F. Castilho, and A. E. Vercesi, "Mitochondria and reactive oxygen species," *Free Radical Biology and Medicine*, vol. 47, no. 4, pp. 333–343, 2009.

[10] S. Dikalov, "Cross talk between mitochondria and NADPH oxidases," *Free Radical Biology and Medicine*, vol. 51, no. 7, pp. 1289–1301, 2011.

[11] A. K. S. Camara, E. J. Lesnefsky, and D. F. Stowe, "Potential therapeutic benefits of strategies directed to mitochondria," *Antioxidants & Redox Signaling*, vol. 13, no. 3, pp. 279–347, 2010.

[12] M. Crompton, "The mitochondrial permeability transition pore and its role in cell death," *The Biochemical Journal*, vol. 341, pp. 233–249, 1999.

[13] A. J. Kowaltowski, R. F. Castilho, and A. E. Vercesi, "Mitochondrial permeability transition and oxidative stress," *FEBS Letters*, vol. 495, no. 1-2, pp. 12–15, 2001.

[14] A. E. Vercesi, "The participation of NADP, the transmembrane potential and the energy-linked NAD(P) transhydrogenase in the process of Ca^{2+} efflux from rat liver mitochondria," *Archives of Biochemistry and Biophysics*, vol. 252, no. 1, pp. 171–178, 1987.

[15] J. A. Ronchi, T. R. Figueira, F. G. Ravagnani, H. C. F. Oliveira, A. E. Vercesi, and R. F. Castilho, "A spontaneous mutation in the nicotinamide nucleotide transhydrogenase gene of C57BL/6J mice results in mitochondrial redox abnormalities," *Free Radical Biology and Medicine*, vol. 63, pp. 446–456, 2013.

[16] D. C. Wallace, "A mitochondrial paradigm of metabolic and degenerative diseases, aging, and cancer: a dawn for evolutionary medicine," *Annual Review of Genetics*, vol. 39, pp. 359–407, 2005.

[17] E. G. Martins, V. Bonato, C. Q. Silva, and S. F. Reis, "Seasonality in reproduction, age structure and density of the gracile mouse opossum *Gracilinanus microtarsus* (Marsupialia: Didelphidae) in a Brazilian cerrado," *Journal of Tropical Ecology*, vol. 22, no. 4, pp. 461–468, 2006.

[18] E. G. Martins, V. Bonato, C. Q. Da-Silva, and S. F. Dos Reis, "Partial semelparity in the neotropical didelphid marsupial *Gracilinanus microtarsus*," *Journal of Mammalogy*, vol. 87, no. 5, pp. 915–920, 2006.

[19] E. G. Martins, V. Bonato, H. P. Pinheiro, and S. F. Dos Reis, "Diet of the gracile mouse opossum (*Gracilinanus microtarsus*) (Didelphimorphia: Didelphidae) in a Brazilian cerrado: patterns of food consumption and intrapopulation variation," *Journal of Zoology*, vol. 269, no. 1, pp. 21–28, 2006.

[20] E. G. Martins, M. S. Araújo, V. Bonato, and S. F. D. Reis, "Sex and season affect individual-level diet variation in the neotropical marsupial *Gracilinanus microtarsus* (Didelphidae)," *Biotropica*, vol. 40, no. 1, pp. 132–135, 2008.

[21] C. Q. da-Silva, E. G. Martins, V. Bonato, and S. F. dos Reis, "Bayesian capture-recapture analysis: an application in modeling semelparity of a neotropical didelphid marsupial," *Communications in Statistics. Simulation and Computation*, vol. 37, no. 3–5, pp. 816–828, 2008.

[22] C. Q. Silva, A. E. Gomes, E. G. Martins, V. Bonato, and S. F. Reis, "A Bayesian change-point model for describing partial semelparity of a Neotropical didelphid marsupial," *Revista Brasileira de Biometria*, vol. 26, pp. 31–44, 2008.

[23] R. Boonstra, "Equipped for life: the adaptive role of the stress axis in male mammals," *Journal of Mammalogy*, vol. 86, no. 2, pp. 236–247, 2005.

[24] T. R. Figueira, "A word of caution concerning the use of Nnt-mutated C57BL/6 mice substrains as experimental models to study metabolism and mitochondrial pathophysiology," *Experimental Physiology*, vol. 98, no. 11, pp. 1643–1643, 2013.

[25] R. S. Kaplan and P. L. Pedersen, "Characterization of phosphate efflux pathways in rat liver mitochondria," *Biochemical Journal*, vol. 212, no. 2, pp. 279–288, 1983.

[26] C. Lopez-Mediavilla, A. Orfao, M. Gonzalez, and J. M. Medina, "Identification by flow cytometry of two distinct rhodamine-123-stained mitochondrial populations in rat liver," *FEBS Letters*, vol. 254, no. 1-2, pp. 115–120, 1989.

[27] A. G. Gornall, C. J. Bardawill, and M. M. David, "Determination of serum proteins by means of the biuret reaction," *The Journal of Biological Chemistry*, vol. 177, no. 2, pp. 751–766, 1949.

[28] T. R. Figueira, D. R. Melo, A. E. Vercesi, and R. F. Castilho, "Safranine as a fluorescent probe for the evaluation of mitochondrial membrane potential in isolated organelles and permeabilized cells," *Methods in Molecular Biology*, vol. 810, pp. 103–117, 2012.

[29] B. A. Paim, J. A. Velho, R. F. Castilho, H. C. F. Oliveira, and A. E. Vercesi, "Oxidative stress in hypercholesterolemic LDL (low-density lipoprotein) receptor knockout mice is associated with low content of mitochondrial NADP-linked substrates and is partially reversed by citrate replacement," *Free Radical Biology and Medicine*, vol. 44, no. 3, pp. 444–451, 2008.

[30] L. K. Klaidman, A. C. Leung, and J. D. Adams Jr., "High-performance liquid chromatography analysis of oxidized and reduced pyridine dinucleotides in specific brain regions," *Analytical Biochemistry*, vol. 228, no. 2, pp. 312–317, 1995.

[31] A. P. Halestrap, K.-Y. Woodfield, and C. P. Connern, "Oxidative stress, thiol reagents, and membrane potential modulate the mitochondrial permeability transition by affecting nucleotide binding to the adenine nucleotide translocase," *The Journal of Biological Chemistry*, vol. 272, no. 6, pp. 3346–3354, 1997.

[32] Â. Saito and R. F. Castilho, "Inhibitory effects of adenine nucleotides on brain mitochondrial permeability transition," *Neurochemical Research*, vol. 35, no. 11, pp. 1667–1674, 2010.

[33] A. L. Lehninger, A. Vercesi, and E. A. Bababunmi, "Regulation of Ca^{2+} release from mitochondria by the oxidation-reduction state of pyridine nucleotides," *Proceedings of the National Academy of Sciences of the United States of America*, vol. 75, no. 4, pp. 1690–1694, 1978.

[34] S. Miwa and T. von Zglinicki, "Measuring hydrogen peroxide release from isolated liver mitochondria using Amplex Red: a critical evaluation," *Biochimica et Biophysica Acta: Bioenergetics*, vol. 1837, supplement, p. e62, 2014.

[35] J. Viña, C. Borras, K. M. Abdelaziz, R. Garcia-Valles, and M. C. Gomez-Cabrera, "The free radical theory of aging revisited: the cell signaling disruption theory of aging," *Antioxidants and Redox Signaling*, vol. 19, no. 8, pp. 779–787, 2013.

[36] H.-M. Ni, J. A. Williams, and W.-X. Ding, "Mitochondrial dynamics and mitochondrial quality control," *Redox Biology*, vol. 20, pp. 6–13, 2014.

[37] P. Bernardi and F. Di Lisa, "The mitochondrial permeability transition pore: molecular nature and role as a target in cardioprotection," *Journal of Molecular and Cellular Cardiology*, vol. 78, pp. 100–106, 2015.

[38] A. P. Halestrap and A. P. Richardson, "The mitochondrial permeability transition: a current perspective on its identity and role in ischaemia/reperfusion injury," *Journal of Molecular and Cellular Cardiology*, vol. 78, pp. 129–141, 2015.

[39] M. M. Fagian, L. Pereira-da-Silva, I. S. Martins, and A. E. Vercesi, "Membrane protein thiol cross-linking associated with the permeabilization of the inner mitochondrial membrane by Ca^{2+} plus prooxidants," *Journal of Biological Chemistry*, vol. 265, no. 32, pp. 19955–19960, 1990.

[40] J. E. Kokoszka, K. G. Waymire, S. E. Levy et al., "The ADP/ATP translocator is not essential for the mitochondrial permeability transition pore," *Nature*, vol. 427, no. 6973, pp. 461–465, 2004.

[41] C. P. Baines, R. A. Kaiser, N. H. Purcell et al., "Loss of cyclophilin D reveals a critical role for mitochondrial permeability transition in cell death," *Nature*, vol. 434, no. 7033, pp. 658–662, 2005.

[42] J. A. Ronchi, A. E. Vercesi, and R. F. Castilho, "Reactive oxygen species and permeability transition pore in rat liver and kidney mitoplasts," *Journal of Bioenergetics and Biomembranes*, vol. 43, no. 6, pp. 709–715, 2011.

[43] J. Šileikyte, V. Petronilli, A. Zulian et al., "Regulation of the inner membrane mitochondrial permeability transition by the outer membrane translocator protein (peripheral benzodiazepine receptor)," *The Journal of Biological Chemistry*, vol. 286, no. 2, pp. 1046–1053, 2011.

[44] A. E. Vercesi, "Possible participation of membrane thiol groups on the mechanism of $NAD(P)^+$-stimulated Ca^{2+} efflux from mitochondria," *Biochemical and Biophysical Research Communications*, vol. 119, no. 1, pp. 305–310, 1984.

[45] R. F. Castilho, A. J. Kowaltowski, A. R. Meinicke, E. J. H. Bechara, and A. E. Vercesi, "Permeabilization of the inner mitochondrial membrane by Ca^{2+} ions is stimulated by t-butyl hydroperoxide and mediated by reactive oxygen species generated by mitochondria," *Free Radical Biology and Medicine*, vol. 18, no. 3, pp. 479–486, 1995.

Hindawi Publishing Corporation
Oxidative Medicine and Cellular Longevity
Volume 2015, Article ID 482582, 10 pages
http://dx.doi.org/10.1155/2015/482582

Review Article

Mitochondrial Retrograde Signaling: Triggers, Pathways, and Outcomes

Fernanda Marques da Cunha,[1] Nicole Quesada Torelli,[2] and Alicia J. Kowaltowski[2]

[1]*Departamento de Bioquímica, Escola Paulista de Medicina, Universidade Federal de São Paulo, 04044-020 São Paulo, SP, Brazil*
[2]*Departamento de Bioquímica, Instituto de Química, Universidade de São Paulo, 05508-000 São Paulo, SP, Brazil*

Correspondence should be addressed to Alicia J. Kowaltowski; alicia@iq.usp.br

Received 2 April 2015; Revised 8 May 2015; Accepted 13 May 2015

Academic Editor: Adriana Maria Cassina

Mitochondria are essential organelles for eukaryotic homeostasis. Although these organelles possess their own DNA, the vast majority (>99%) of mitochondrial proteins are encoded in the nucleus. This situation makes systems that allow the communication between mitochondria and the nucleus a requirement not only to coordinate mitochondrial protein synthesis during biogenesis but also to communicate eventual mitochondrial malfunctions, triggering compensatory responses in the nucleus. Mitochondria-to-nucleus retrograde signaling has been described in various organisms, albeit with differences in effector pathways, molecules, and outcomes, as discussed in this review.

1. Introduction

Mitochondria are believed to be former free-living bacteria that established a successful symbiosis with preeukaryotic cells billions of years ago [1]. Today, while being unquestionably essential for eukaryotic aerobic metabolism, they also exhibit multiple alternative functions, including the biosynthesis of intermediary metabolites, regulation of cytosolic Ca^{2+} homeostasis [2–6], and coordination of cell death [7–9], among others. Many age-induced processes (for review see [10]) and degenerative diseases (for review see [11]) are related to mitochondrial dysfunction, further highlighting the critical importance of this organelle.

The evolution of this endosymbiotic relationship between mitochondria and the host cell resulted in transfer of genetic material so that, currently, most mitochondrial proteins (but not all of them) are coded in the nucleus. In this scenario, the need for a communication system between mitochondria and the nucleus becomes evident, necessary not only to coordinate mitochondrial protein synthesis during biogenesis of the organelle, but also to communicate eventual mitochondrial malfunctions, triggering compensatory responses in the nucleus. This communication system was described to operate in various organisms and involves antegrade (nucleus to mitochondria), retrograde (mitochondria-to-nucleus) as well as intermitochondrial pathways [12]. Mitochondrial signaling continues to be studied and is uncovering a central role of mitochondria in an increasing number of homeostatic systems. This review focuses on retrograde signaling, discussing triggers, molecular pathways, and outcomes known so far. Special attention is devoted to mitochondrial-derived peptides as signaling molecules.

2. Mitochondrial Retrograde Signaling Pathways

Saccharomyces cerevisiae's RTG-dependent retrograde signaling was the first retrograde pathway to be described and is extensively characterized [13, 14]. It depends on three cytosolic proteins: Rtg1p, Rtg2p, and Rtg3p. Rtg1p and Rtg3p are basic helix-loop-helix/leucine zipper (bHLH/LeuZip) transcription factors that bind as heterodimers to the GTCAC DNA binding site. When activated, the Rtg1/3p complex translocates from the cytoplasm to the nucleus [15], where it

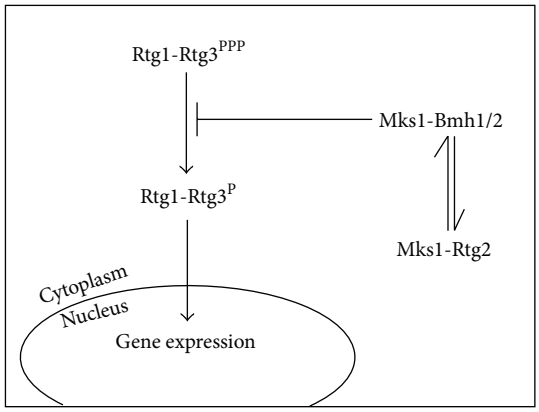

Figure 1: Simplified scheme of the RTG-dependent retrograde signaling pathway. In *Saccharomyces cerevisiae* this pathway depends on three proteins. Rtg1 and Rtg3 form a transcription factor that translocates to the nucleus when the pathway is activated. In the nucleus, Rtg1 and Rtg3 control the expression of a set of genes that code for mitochondrial proteins. Rtg2 is an activator of the pathway that allows the nuclear translocation of Rtg1 and Rtg3.

controls the expression of genes that encode mitochondrial proteins (Figures 1 and 2). Although only Rtg3p contains a transcription activation domain, Rtg1p and Rtg3p are both required for DNA binding [16].

Rtg1/3p translocation is dependent on partial dephosphorylation of Rtg3p [15]. Thus, inhibition of retrograde signaling occurs through the prevention of Rtg3p dephosphorylation mediated by Mks1p, a cytosolic phosphoprotein, when it is hyperphosphorylated and bound to Bmh1/2p (Figures 1 and 2). Rtg2p is an activator of the pathway that binds to the hypophosphorylated form of Mks1p, keeping it from binding to Bmh1/2p and allowing partial dephosphorylation of Rtg3p and Rtg1/3p translocation [17, 18]. Mks1p thus works through a dynamic switch between Rtg2p and Bmh1/2p: when bound to Rtg2p, retrograde signaling is active; when bound to Bmh1/2p, it is inactive. The Mks1p levels in the cell are controlled by SCF^{Grr1} E3 ubiquitin ligase-dependent polyubiquitination and degradation of free Msk1p, enhancing the efficiency of the Rtg2p/Bmh1/2p switch by keeping the concentration of free Mks1p low [19]. Rtg2p has an N-terminal HSP70-like ATP-binding domain that is required for the interaction with Mks1p [18]. In addition to its function as an activator of Rtg1/Rtg3p, Rtg2p is also a component of the transcriptional coactivator SAGA-like (SLIK) complex, which is required for *CIT2* expression, the prototypical reporter of RTG signaling [20].

In addition to coordinating the production of mitochondrial proteins, the retrograde signaling pathway has been found to coordinate carbon and nitrogen metabolism, since Rtg1/3p subcellular localization and activity are also regulated by the target of rapamycin (TOR) kinase pathway [21]. Inhibition of TOR function by rapamycin mimics nutrient starvation and affects genes involved in protein biosynthesis, the glycolytic pathway, the tricarboxylic acid cycle, and nitrogen metabolism, including permeases and degradation enzymes required for the use of different sources of assimilable nitrogen [22, 23]. Lst8p, a component of the target of rapamycin complex 1 (TORC1), is a negative regulator of the RTG-dependent retrograde signaling pathway [24] acting at two sites, one upstream of Rtg2p and one between Rtg2p and Rtg1/3p. Upstream regulation is believed to involve Lst8p in the activity or assembly of the SPS (Ssy1p, Ptr3p, and Ssy5p) amino acid-sensing system, affecting external glutamate sensing and consequently the retrograde response [25, 26]. The mechanism of Lst8p inhibition downstream of Rtg2p remains unknown. Treatment with rapamycin inhibits TOR function and thus activates retrograde signaling, inducing the expression of RTG-target genes [26]. It is also known that mitochondrial dysfunction leads to decreased phosphorylation and reduced activity of Sch9p [27], a target of TORC1 important for ribosome biosynthesis, cell-size control, inhibition of entry into the stationary phase, and translation initiation [28]. This is yet another possible link between retrograde signaling and the TOR kinase pathway.

Resistance to osmotic stress is also related to RTG-dependent retrograde signaling. Exposure to external hyperosmolarity activates Hog1 stress-activated protein kinase (SAPK), which controls several transcription factors such as Sko1p, Hot1p, Msn2p and Msn4p, and Smp1p. These in turn regulate the expression of stress-response genes. Expression of RTG-dependent genes is also induced under osmotic stress and is dependent on Hog1 SAPK. Hog1 SAPK binds to the Rtg1/3p transcription factor and allows its translocation to the nucleus. Although only the presence of Hog1 SAPK is required for Rtg1/3p nuclear translocation, its activity is necessary for the transcription factor to bind to the chromatin [29].

Despite the fact that it is more extensively described, RTG-dependent signaling is not the only pathway through which yeast mitochondria communicate with the nucleus. A number of genes whose transcription is altered in response to mitochondrial dysfunction are not under the control of Rtg proteins. Additionally, depending on the yeast strain or the culture condition, a different set of genes have their expression modified when compared to the genes affected by mtDNA depletion [30], the classical paradigm for RTG-dependent signaling activation. One example is the upregulation of the ATP-binding cassette protein Pdr5p, a multidrug resistance transporter, shown to be driven by the Pdr1p/Pdr3p transcription complex and not by the Rtg1p/Rtg3p complex [31].

Arnold et al. [32] reported another kind of retrograde signaling in null mutants for the i-AAA-protease coded by *YME1* when growing on respiratory substrates. Interestingly, the response was recapitulated by inhibition of the Fo-F1 ATP synthase in wild-type cells but was abrogated by respiratory chain inhibition as well as by membrane potential dissipation.

Mutant yeast strains with impaired mitochondrial proteostasis also seem to display active retrograde signaling independent of Rtg proteins. In a null mutant for a component of the large subunit of the mitochondrial ribosome (Afo1p), an alternative retrograde pathway was shown to

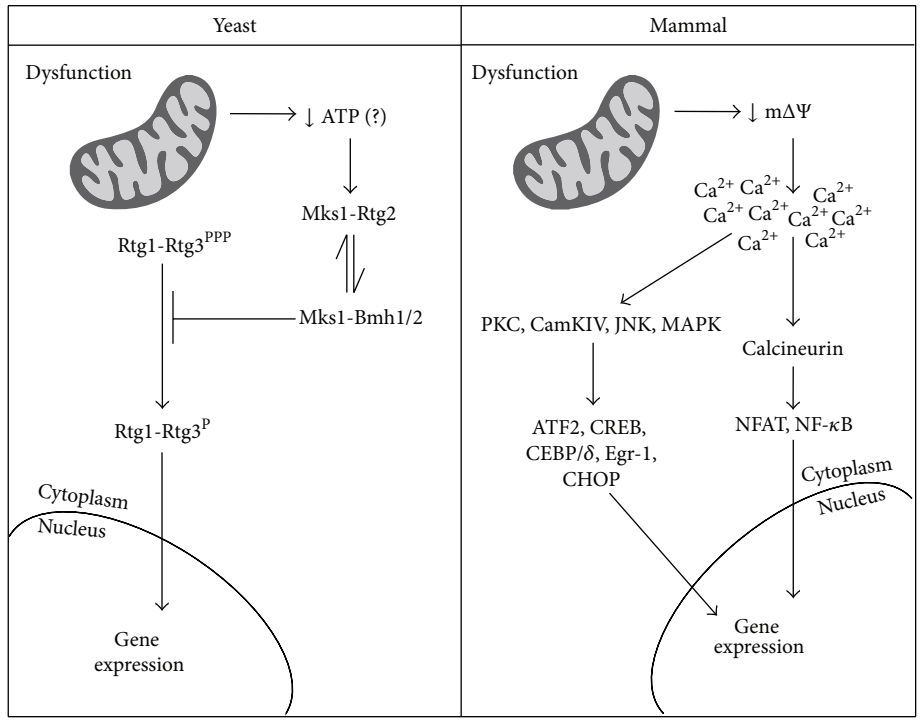

Figure 2: Scheme comparing the classical retrograde signaling pathways in yeast and mammals. In yeast, mitochondrial dysfunction leads to decreases in intracellular ATP concentration, which may favor Rtg2-Mks1 interaction [54] allowing Rtg1-Rtg3 activation. In mammals, mitochondrial dysfunction translates into drops in mitochondrial membrane potential, causing increments in intracellular calcium. Calcium-dependent kinases and phosphatases are then activated culminating with the activation of different transcription factors. Alternative retrograde signaling pathways in yeast, mammals, and other model organisms are discussed in the text.

be dependent on active TORC1 and the transcription factor Spf1p [33]. In mutants that lack Sov1p, a protein of the mitochondrial translation control module, the retrograde pathway was shown to require Sir2p and *PCN1* [34]. Mitochondrial proteostasis impairments were also shown to be central to the mitochondrial unfolded protein response (mtUPR), another kind of mitochondrial retrograde signaling pathway described in *Caenorhabditis elegans*, *Drosophila melanogaster*, and mammalian cells [35–37]. In *C. elegans*, perturbation of mitochondrial protein handling by either genetic or pharmacological means induced mitochondrial retrograde signaling culminating with the selective expression of mitochondrial matrix chaperones encoded in the nucleus [36]. Additional data indicate that mtUPR in *C. elegans* may also be activated by RNAi-mediated knockdown of factors required for mtDNA expression [37] as well as knockdown of some respiratory chain components [38–40]. The same is also true for *D. melanogaster*, for which experimental evidences are less numerous but nonetheless indicate the activation of mtUPR when different respiratory chain components are knocked out or down [41–43].

In mammalian cells, altered nuclear expression in response to mitochondrial dysfunction has long been reported [44, 45], with a number of signaling pathways implicated in this retrograde communication [46]. Indeed calcineurin, PKC, CamKIV, JNK, and MAPK (kinases) as well as the transcription factors ATF2, CEBP/δ, NFAT, CREB, Egr-1, CHOP, and NFκB participate in mammalian mitochondrial retrograde signaling [46–49] (Figure 2). Interestingly, evidence of retrograde signaling was also reported at the level of whole mammalian organisms. Despite their dysfunctional mitochondria and increased reactive oxygen species (ROS) production, knockout mutants with reduced *MCLK1* activity (involved in coenzyme Q synthesis) or *SURF1* (COX assembly factor) have increased life span [50, 51] as well as significant resistance to brain damage following global cerebral ischemia-reperfusion injury [52] or excitotoxic insults [51]. Interestingly, *MCKL1* heterozygous mice also have enhanced immune function [53], suggesting a new outcome of mitochondrial retrograde signaling activation, further discussed below.

3. Triggers and Relay Molecules of Retrograde Signaling Pathways

Retrograde signaling must be triggered by a mitochondrial signal that in turn is relayed to one or more molecules that finally reach the nucleus. While the yeast RTG-dependent retrograde signaling is molecularly well characterized, the same is not true for other retrograde pathways. In this section,

events that may function as triggers and relaying molecules will be discussed.

ATP is one of the main mitochondrial products and would be an obvious trigger molecule. Some evidences suggest that this may be the case, at least in specific situations. In yeast, Mks1p release from Rtg2p is dependent on ATP hydrolysis and is ATP-specific, suggesting that loss of mitochondrial DNA activates the pathway possibly through a decrease in ATP concentration, allowing Mks1p-Rtg2p association and Rtg1/3p nuclear translocation (Figure 2) [54]. While decreases in ATP concentrations may occur in drastic situations, retrograde signaling was shown to be active during normal replicative [55] or chronological [56] aging, situations in which decreases in ATP are less likely. Drops in mitochondrial membrane potential were shown to trigger the retrograde response during replicative aging [55], although the mechanism through which this decrease in potential is relayed to Rtg2p is not defined [57]. In mammalian cells, disruption of the mitochondrial membrane potential is also the main trigger of retrograde signaling, impairing mitochondrial Ca^{2+} uptake and causing an elevation in free Ca^{2+} in the cytoplasm [58–61]. This, in turn, activates Ca^{2+}-dependent protein kinase C (PKC), CamKIV, JNK, and MAPK, which then activate the transcription factors ATF2, CEBP/δ, CREB, Egr-1, and CHOP [46]. Elevated Ca^{2+} levels also activate calcineurin, a calcium-dependent serine-threonine phosphatase that induces NFAT and NF-κB, which is considered to have evolved from RTG-dependent retrograde signaling (Figure 2) [47, 48]. Importantly, the causal relationship between mitochondrial dysfunction and calcium signaling was established by studies in which the chelation of free calcium was sufficient to abolish downstream signaling [58, 61]. Although determinant for retrograde signaling activation in different organisms, overt alterations in mitochondrial membrane potential do not seem to be the trigger of RTG-dependent signaling in yeast grown in raffinose, since RTG signaling was shown to be active and confer acetic acid resistance with no detected changes in membrane potentials [62].

An interesting possibility raised by Arnold et al. [32] is that mitochondria-derived peptides are involved in the activation of retrograde signaling in yeast, under certain circumstances. They showed that deletion of *YME1*, coding for i-AAA-protease in the inner membrane, abolished peptide generation in the intermembrane space and led to biogenesis of the respiratory chain and the induction of nuclear genes with functions in mitochondrial gene expression. The mitochondrial membrane potential was shown to be essential for the response, since the induction of nuclear genes was abolished by antimycin (an inhibitor of electron transport chain) or CCCP (a mitochondrial uncoupler), suggesting that mitochondrial transport of a yet uncharacterized relay molecule is part of the process.

In *C. elegans* with reduced expression of *SPG7* (a mitochondrial protease), the mitochondrial unfolded protein response (mtUPR) was shown to be activated in a manner dependent on *HAF1*, a gene encoding a mitochondria-localized ATP-binding cassette transporter [63]. The mechanism involves the transport and degradation of the transcription factor Atfs1p, which is normally imported into mitochondria and degraded. During mitochondrial stress, the import efficiency is reduced, allowing the traffic of Atfs1p to the nucleus and the consequent alteration of transcription of components of mtUPR [64]. It would be interesting to check whether, in this case, alterations in mitochondrial membrane potential are the primary cause of transport impairment. It would also be interesting to know if the reported alterations in mitochondrial membrane potential in mammalian or yeast cells affect the import/export of proteins and peptides and if this would in turn affect downstream signaling pathways as described for *C. elegans* [63, 64].

In *D. melanogaster*, a mutant defective in coenzyme Q synthesis (*SBO* gene mutant) presents activation of mtUPR together with attenuation of the insulin/insulin-like growth factor signaling (IIS) pathway [42]. In a more recent study with mutants for muscle *NDUFS1*/*ND75*, a component of complex I, nonautonomous attenuation of insulin/insulin-like growth factor signaling was shown to be responsible for life span extension [43]. Interestingly, the increase in life span was suppressed by forced expression of catalase or glutathione peroxidase I, uncovering a pivotal role for H_2O_2 in the signaling pathway. ROS (the specific chemical species is not characterized) were also shown to be part of the mtUPR induced by knockdown of *CCO1* (a subunit of mitochondrial cytochrome oxidase) in *C. elegans*. Indeed, the lifespan extension of this mutant partially depends on mild increases in mitochondrial ROS, a production that in turn activated the hypoxia-inducible transcription factor Hif1p [65]. Neuronal-limited knockdown of *cco-1* activates the mtUPR in the intestine in a cell nonautonomous manner, influencing the whole organism [66]. Whether the relaying factor (coined mitokine) is some oxygen-derived species was not investigated, but, as shown for *D. melanogaster*, this may be a possibility. Indeed, mitochondrial ROS have been implicated in mitochondria-to-nucleus signaling in different organisms, regulating the expression of enzymes involved in oxidative detoxification ([67], for review see [56, 68–73]). Even though the pathway by which mitochondria-derived ROS induces a protective response was dubbed mitohormesis [74], it is nonetheless a form of mitochondrial retrograde signaling that involves a mitochondrially derived signal inducing alterations in nuclear gene expression.

Increasing evidence indicates that a number of short open reading frames (sORFs) in the mtDNA can give rise to biologically active peptides that differ from those mentioned above in that they are not the product of degradation of existent mitochondrial proteins. The most prominent example is humanin, a 21- or 24-amino-acid peptide (depending on whether the translation occurs in the mitochondrion or the cytoplasm, resp.), discovered in 2001 during a search for protective molecules against Alzheimer's disease [75]. It is interesting to note that expressed sequence tags related to humanin were also found in rat [76] and *C. elegans* [77], suggesting its biological relevance. Humanin and a G14S modified version (HNG) were shown to protect cells against

most Alzheimer-relevant insults [77] without changing Aβ or fibril amounts [78]. Additionally, cultured cells died less after challenges with H_2O_2, $CoCl_2$, or oxidized LDL when treated with humanin [79–81]. This peptide or its modified version (HNG) also proved to be active in murine models of cardiac isquemia/reperfusion injury and stroke, decreasing the infarcted area [82, 83].

In addition to its cytoprotective effects, humanin was also shown to affect metabolism. Indeed, Muzumdar et al. [84] demonstrated that centrally administered HNG sensitizes rats toward insulin signaling through STAT3 activation in the hypothalamus. The link is further supported by the finding that endothelial cells of ApoE-deficient mice on a hypercholesterolemic diet have increased humanin levels [85]. In the same line, Ames mice (that have decreased signaling through the GH/IGF-1 axis) have increased humanin levels while GH transgenic mice that have increased signaling through the GH/IGF-1 axis show the opposite effect [86]. Increased levels of humanin were detected in mouse myocytes after cardiac ischemia/reperfusion injury [83], the skeletal muscle of patients with MELAS (Mitochondrial Encephalomyopathy with Lactic Acidosis and Stroke-like Episodes) [87], and neurons and glia of the occipital lobe of patients with Alzheimer's disease [88]. While it is clear that stress conditions lead to increments in humanin levels, very little is known about humanin regulation.

Humanin is not the only metabolically active mitochondrial sORF-derived peptide. MOTS-c (mitochondrial open reading frame of the 12S rRNA-C), a 16-amino-acid peptide coded by sORF of the mitochondrial 12S rRNA, was recently found to regulate insulin sensitivity and metabolic homeostasis by acting primarily on skeletal muscle in mice. Importantly, treatment of mice with MOTS-c prevented not only age-dependent and high fat diet-induced insulin resistance but also diet-induced obesity. MOTS-c was detected in different mouse and rat tissues as well as in human and rodent circulation. Its levels were decreased after fasting in skeletal muscle, testes, and plasma, whereas brain and heart presented sustained levels [89].

Increasing evidences indicate that mitochondrial sORF-derived peptides are potent and evolutionarily conserved mitochondrial signals able to affect various physiological processes. Because of their relevance, further studies aiming to characterize the molecules and mechanisms involved in mitochondrial sORF-derived peptides expression and modulation are needed.

4. Outcomes of Retrograde Signaling Activation

Independently of the organism or the pathway activated, the hallmark of mitochondrial retrograde signaling is the modification of the expression of nuclear genes induced by a signal from mitochondria. In *S. cerevisiae* treated with oligomycin or in a null strain for the *YME1* gene, the activation of a retrograde pathway leads to the expression of a number of genes involved in mitochondrial biogenesis [32]. Similarly, RTG-dependent signaling was shown to alter the expression of several genes [30, 90], including *CIT1* (encoding mitochondrial citrate synthase), *CIT2* (peroxisomal citrate synthase), *PYC1* (pyruvate carboxylase), *ACS1* (acetyl-coenzyme A synthetase), *ACO1* (aconitase), *IDH1/2* (NAD^+-dependent isocitrate dehydrogenase), and *DLD3* (D-lactate dehydrogenase) [91–95], ensuring that there is sufficient glutamate for biosynthetic pathways in cells with reduced respiratory capacity. Indeed, cells with mutant alleles of *RTG1* or *RTG2* are unable to grow in acetate as the sole carbon source, a sign of a defective tricarboxylic acid cycle, and are auxotrophic for glutamate or aspartate. Obstructions in the tricarboxylic acid cycle alone do not lead to glutamate or aspartate auxotrophy since its precursors can be provided by intermediates of the glyoxylate cycle. However, *RTG1*, *RTG2*, or *RTG3* deletion impairs both cycles, thus making cells unable to grow without glutamate or aspartate [92, 96]. Retrograde signaling was also shown to affect amino acid metabolism, since *RTG1* or *RTG3* deletion results in increased levels of polyamine biosynthetic intermediates (putrescine, ornithine, and spermidine). Polyamines are known to have cytoprotective effects against oxidative imbalance and thus may act as stress defense systems in cells lacking retrograde signaling, in which the levels of other stress-response metabolites such as glutathione and trehalose are reduced during the stationary phase [97]. Additional evidence shows that cells impaired in RTG-dependent signaling have decreased catalase and glutathione peroxidase activity in the stationary phase and are more vulnerable to oxidative insults due to decreased hormetic concentrations of H_2O_2 [56]. Thus, an optimal redox defense system seems to be an important outcome of RTG-dependent retrograde signaling activation.

Not surprisingly, activation of RTG-dependent retrograde signaling in yeast was reported to extend replicative lifespan [55, 98–100]. The mechanisms are not entirely clear but seem to involve *RAS2* [99] as well as a counteraction of negative effects that rise from the age-induced increase in the generation of extrachromosomal rDNA (ribosomal DNA) circles (ERCs) [55, 98, 100, 101].

Replicative lifespan increases are also a reported outcome of the activation of RTG-independent retrograde pathways. Indeed, the aforementioned null mutant for Afo1p showed increased replicative lifespan and resistance to oxidants, despite its inability to grow in respiratory media [33]. This is also the case for the null mutant for *SOV1*, in which the mutation impaired the growth on respiratory media but improved protein homeostasis, increased genomic silencing, and induced a Sir2p- and *PCN1*-dependent extension in replicative life span [34]. Interestingly, the life span extension of this *SOV1* mutant was demonstrated to be due to the absence of mitochondrial translation control module proteins rather than the loss of mtDNA or respiratory activity [34]. It would be interesting to check whether the response activated in *SOV1* mutants has some parallels with mtUPR described in *C. elegans* or *D. melanogaster*.

In *C. elegans*, the main reported outcome of mtUPR activation has been life span extension (for review see [102]). The causal relationship between mtUPR and longevity, however, was recently questioned [66, 103, 104], and more data are

needed to clarify this point. The data available on *C. elegans* and mtUPR suggest that, in spite of having common features like, for example, the induction of Hsp6p and Hsp60p, the effectors and signaling pathways may display some specificity related to the nature and/or the location of mitochondrial disturbance, which in turn may alter the outcome of the response (i.e., induce or not a nonautonomous response).

Similarly to *C. elegans*, the main reported outcome of mtUPR activation in *D. melanogaster* is increased life span [41]. One interesting point, however, is that some long-lived mutant flies also presented attenuation of the insulin/insulin-like growth factor signaling pathway [42]. Recently this nonautonomous attenuation was shown to be responsible for life span extension of mutants for muscle *NDUFS1*/*ND75* (a component of complex I) with an attenuation in insulin/insulin-like growth factor signaling caused by increased expression of ImpL2p (that can bind and inhibit *Drosophila* insulin-like peptides) [43]. It would be interesting to verify whether the insulin/insulin-like growth factor signaling pathway also plays a role in lifespan extension in long-lived *C. elegans* mitochondrial mutants.

As mentioned earlier, mitochondrial proteolysis perturbation by Spg7p protease inhibition in *C. elegans* led to mtUPR that required the transcription factor Atfs1p [63, 64]. One of the outcomes of this phenomenon was the production of antimicrobial molecules such as the peptide Abf2p and the lysozyme Lys2p [64]. Pellegrino et al. [105] found that worms preexposed to *SPG7* RNAi to induce mtUPR were more resistant to the pathogen *P. aeruginosa* when compared to animals exposed to control RNAi. Improved immune performance was also observed in long-lived *MCKL1* heterozygous mice [53], as previously mentioned. Indeed, these mutants had better outcomes, including less hepatic damage, after *Salmonella typhimurium* and *Salmonella enteritidis* infection [53]. Inducers of such improved immune function were not determined, but it is tempting to speculate, based on findings with *C. elegans*, that antimicrobial molecules induced by mtUPR in *MCKL1* mutants may be involved.

5. Conclusions

It has been a long time since mitochondria were believed to be organelles specifically responsible for ATP production. The vast array of data generated today indicate that mitochondria are metabolic hubs that detect and decode metabolic cues, generating signals which in turn are relayed by different molecules and pathways which finally reach the nucleus (Figure 3). Because of the diversity of mitochondria-derived signals, different retrograde communication pathways are employed to relay these signals to the nucleus.

It is interesting to note that the outcomes of mitochondrial retrograde signaling go far beyond the maintenance or biogenesis of the organelle, affecting the homeostasis of the whole organism through body weight or immunity, for example.

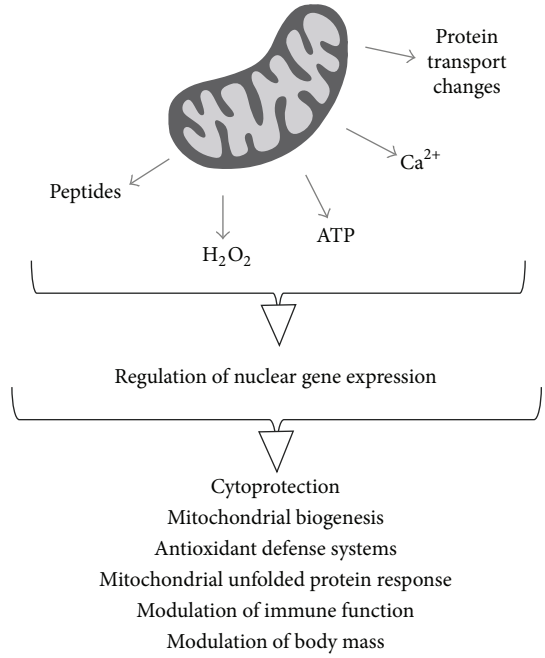

Figure 3: General view of mitochondrial signals and outcomes of retrograde communication. Diverse mitochondrial signals elicit varied responses, ranging from the increased synthesis of mitochondrial chaperones to improvement of immunity.

Conflict of Interests

The authors declare that there is no conflict of interests regarding the publication of this paper.

References

[1] L. Sagan, "On the origin of mitosing cells," *Journal of Theoretical Biology*, vol. 14, no. 3, pp. 225–274, 1967.

[2] H. F. Deluca and G. W. Engstrom, "Calcium uptake by rat kidney mitochondria," *Proceedings of the National Academy of Sciences of the United States of America*, vol. 47, no. 11, pp. 1744–1750, 1961.

[3] F. D. Vasington and J. V. Murphy, "Ca^{++} ion uptake by rat kidney mitochondria and its dependence on respiration and phosphorylation," *The Journal of Biological Chemistry*, vol. 237, no. 8, pp. 2670–2677, 1962.

[4] K. Mallilankaraman, P. Doonan, C. Cárdenas et al., "MICU1 is an essential gatekeeper for mcu-mediated mitochondrial Ca^{2+} uptake that regulates cell survival," *Cell*, vol. 151, no. 3, pp. 630–644, 2012.

[5] K. Mallilankaraman, C. Cárdenas, P. J. Doonan et al., "MCUR1 is an essential component of mitochondrial Ca^{2+} uptake that regulates cellular metabolism," *Nature Cell Biology*, vol. 14, no. 12, pp. 1336–1343, 2012.

[6] Y. Sancak, A. L. Markhard, T. Kitami et al., "EMRE is an essential component of the mitochondrial calcium uniporter complex," *Science*, vol. 342, no. 6164, pp. 1379–1382, 2013.

[7] D. Hockenbery, G. Niñez, C. Milliman, R. D. Schreiber, and S. J. Korsmeyer, "Bcl-2 is an inner mitochondrial membrane protein that blocks programmed cell death," *Nature*, vol. 348, no. 6299, pp. 334–336, 1990.

[8] J. Yang, X. Liu, K. Bhalla et al., "Prevention of apoptosis by Bcl-2: release of cytochrome c from mitochondria blocked," *Science*, vol. 275, no. 5303, pp. 1129–1132, 1997.

[9] G. Kroemer, L. Galluzzi, and C. Brenner, "Mitochondrial membrane permeabilization in cell death," *Physiological Reviews*, vol. 87, no. 1, pp. 99–163, 2007.

[10] D. F. Dai, Y. A. Chiao, D. J. Marcinek, H. H. Szeto, and P. S. Rabinovitch, "Mitochondrial oxidative stress in aging and healthspan," *Longevity & Healthspan*, vol. 3, no. 1, article 6, 2014.

[11] P. K. Kamat, A. Kalani, P. Kyles, S. C. Tyagi, and N. Tyagi, "Autophagy of mitochondria: a promising therapeutic target for neurodegenerative disease," *Cell Biochemistry and Biophysics*, vol. 70, no. 2, pp. 707–719, 2014.

[12] S. P. Whelan and B. S. Zuckerbraun, "Mitochondrial signaling: forwards, backwards, and in between," *Oxidative Medicine and Cellular Longevity*, vol. 2013, Article ID 351613, 10 pages, 2013.

[13] V. S. Parikh, M. M. Morgan, R. Scott, L. S. Clements, and R. A. Butow, "The mitochondrial genotype can influence nuclear gene expression in yeast," *Science*, vol. 235, no. 4788, pp. 576–580, 1987.

[14] Z. Liu and R. A. Butow, "Mitochondrial retrograde signaling," *Annual Review of Genetics*, vol. 40, pp. 159–185, 2006.

[15] T. Sekito, J. Thornton, and R. A. Butow, "Mitochondria-to-nuclear signaling is regulated by the subcellular localization of the transcription factors Rtg1p and Rtg3p," *Molecular Biology of the Cell*, vol. 11, no. 6, pp. 2103–2115, 2000.

[16] B. A. Rothermel, J. L. Thornton, and R. A. Butow, "Rtg3p, a basic helix-loop-helix/leucine zipper protein that functions in mitochondrial-induced changes in gene expression, contains independent activation domains," *The Journal of Biological Chemistry*, vol. 272, no. 32, pp. 19801–19807, 1997.

[17] T. Sekito, Z. Liu, J. Thornton, and R. A. Butow, "RTG-dependent mitochondria-to-nucleus signaling is regulated by *MKS1* and is linked to formation of yeast prion [URE3]," *Molecular Biology of the Cell*, vol. 13, no. 3, pp. 795–804, 2002.

[18] Z. Liu, T. Sekito, M. Špírek, J. Thornton, and R. A. Butow, "Retrograde signaling is regulated by the dynamic interaction between Rtg2p and Mks1p," *Molecular Cell*, vol. 12, no. 2, pp. 401–411, 2003.

[19] Z. Liu, M. Spírek, J. Thornton, and R. A. Butow, "A novel degron-mediated degradation of the RTG pathway regulator, Mks1p, by SCF^{Grr1}," *Molecular Biology of the Cell*, vol. 16, no. 10, pp. 4893–4904, 2005.

[20] M. G. Pray-Grant, D. Schieltz, S. J. McMahon et al., "The novel SLIK histone acetyltransferase complex functions in the yeast retrograde response pathway," *Molecular and Cellular Biology*, vol. 22, no. 24, pp. 8774–8786, 2002.

[21] A. Komeili, K. P. Wedaman, E. K. O'Shea, and T. Powers, "Mechanism of metabolic control: target of rapamycin signaling links nitrogen quality to the activity of the Rtg1 and Rtg3 transcription factors," *The Journal of Cell Biology*, vol. 151, no. 4, pp. 863–878, 2000.

[22] M. E. Cardenas, N. S. Cutler, M. C. Lorenz, C. J. Di Como, and J. Heitman, "The TOR signaling cascade regulates gene expression in response to nutrients," *Genes & Development*, vol. 13, no. 24, pp. 3271–3279, 1999.

[23] J. S. Hardwick, F. G. Kuruvilla, J. K. Tong, A. F. Shamji, and S. L. Schreiber, "Rapamycin-modulated transcription defines the subset of nutrient-sensitive signaling pathways directly controlled by the Tor proteins," *Proceedings of the National Academy of Sciences of the United States of America*, vol. 96, no. 26, pp. 14866–14870, 1999.

[24] S. Giannattasio, Z. Liu, J. Thornton, and R. A. Butow, "Retrograde response to mitochondrial dysfunction is separable from TOR1/2 regulation of retrograde gene expression," *The Journal of Biological Chemistry*, vol. 280, no. 52, pp. 42528–42535, 2005.

[25] H. Forsberg, C. F. Gilstring, A. Zargari, P. Martínez, and P. O. Ljungdahl, "The role of the yeast plasma membrane SPS nutrient sensor in the metabolic response to extracellular amino acids," *Molecular Microbiology*, vol. 42, no. 1, pp. 215–228, 2001.

[26] Z. Liu, T. Sekito, C. B. Epstein, and R. A. Butow, "RTG-dependent mitochondria to nucleus signaling is negatively regulated by the seven WD-repeat protein Lst8p," *The EMBO Journal*, vol. 20, no. 24, pp. 7209–7219, 2002.

[27] S. Kawai, J. Urban, M. Piccolis, N. Panchaud, C. de Virgilio, and R. Loewith, "Mitochondrial genomic dysfunction causes dephosphorylation of Sch9 in the yeast *Saccharomyces cerevisiae*," *Eukaryotic Cell*, vol. 10, no. 10, pp. 1367–1369, 2011.

[28] J. Urban, A. Soulard, A. Huber et al., "Sch9 is a major target of TORC1 in *Saccharomyces cerevisiae*," *Molecular Cell*, vol. 26, no. 5, pp. 663–674, 2007.

[29] C. Ruiz-Roig, N. Noriega, A. Duch, F. Posas, and E. de Nadal, "The Hog1 SAPK controls the Rtg1/Rtg3 transcriptional complex activity by multiple regulatory mechanisms," *Molecular Biology of the Cell*, vol. 23, no. 21, pp. 4286–4296, 2012.

[30] A. Traven, J. M. S. Wong, D. Xu, M. Sopta, and C. J. Ingles, "Interorganellar communication. Altered nuclear gene expression profiles in a yeast mitochondrial DNA mutant," *The Journal of Biological Chemistry*, vol. 276, no. 6, pp. 4020–4027, 2001.

[31] X. Zhang and W. S. Moye-Rowley, "*Saccharomyces cerevisiae* multidrug resistance gene expression inversely correlates with the status of the F(o) component of the mitochondrial ATPase," *The Journal of Biological Chemistry*, vol. 276, no. 51, pp. 47844–47852, 2001.

[32] I. Arnold, M. Wagner-Ecker, W. Ansorge, and T. Langer, "Evidence for a novel mitochondria-to-nucleus signalling pathway in respiring cells lacking i-AAA protease and the ABC-transporter Mdl1," *Gene*, vol. 367, no. 1-2, pp. 74–88, 2006.

[33] G. Heeren, M. Rinnerthaler, P. Laun et al., "The mitochondrial ribosomal protein of the large subunit, Afo1p, determines cellular longevity through mitochondrial back-signaling via TOR1," *Aging*, vol. 1, no. 7, pp. 622–636, 2009.

[34] A. Caballero, A. Ugidos, B. Liu et al., "Absence of mitochondrial translation control proteins extends life span by activating sirtuin dependent silencing," *Molecular Cell*, vol. 42, no. 3, pp. 390–400, 2011.

[35] Q. Zhao, J. Wang, I. V. Levichkin, S. Stasinopoulos, M. T. Ryan, and N. J. Hoogenraad, "A mitochondrial specific stress response in mammalian cells," *The EMBO Journal*, vol. 21, no. 17, pp. 4411–4419, 2002.

[36] T. Yoneda, C. Benedetti, F. Urano, S. G. Clark, H. P. Harding, and D. Ron, "Compartment-specific perturbation of protein handling activates genes encoding mitochondrial chaperones," *Journal of Cell Science*, vol. 117, no. 18, pp. 4055–4066, 2004.

[37] R. H. Houtkooper, L. Mouchiroud, D. Ryu et al., "Mitonuclear protein imbalance as a conserved longevity mechanism," *Nature*, vol. 497, no. 7450, pp. 451–457, 2013.

[38] A. Dillin, A.-L. Hsu, N. Arantes-Oliveira et al., "Rates of behavior and aging specified by mitochondrial function during development," *Science*, vol. 298, no. 5602, pp. 2398–2401, 2002.

[39] S. S. Lee, R. Y. N. Lee, A. G. Fraser, R. S. Kamath, J. Ahringer, and G. Ruvkun, "A systematic RNAi screen identifies a critical role for mitochondria in *C. elegans* longevity," *Nature Genetics*, vol. 33, no. 1, pp. 40–48, 2003.

[40] D. Cristina, M. Cary, A. Lunceford, C. Clarke, and C. Kenyon, "A regulated response to impaired respiration slows behavioral rates and increases lifespan in *Caenorhabditis elegans*," *PLoS Genetics*, vol. 5, no. 4, Article ID 1000450, 2009.

[41] J. M. Copeland, J. Cho, T. Lo Jr. et al., "Extension of *Drosophila* life span by RNAi of the mitochondrial respiratory chain," *Current Biology*, vol. 19, no. 19, pp. 1591–1598, 2009.

[42] J. Liu, Q. Wu, D. He et al., "*Drosophila* sbo regulates lifespan through its function in the synthesis of coenzyme Q *in vivo*," *Journal of Genetics and Genomics*, vol. 38, no. 6, pp. 225–234, 2011.

[43] E. Owusu-Ansah, W. Song, and N. Perrimon, "Muscle mitohormesis promotes longevity via systemic repression of insulin signaling," *Cell*, vol. 155, no. 3, pp. 699–712, 2013.

[44] M. F. Marusich, B. H. Robinson, J.-W. Taanman et al., "Expression of mtDNA and nDNA encoded respiratory chain proteins in chemically and genetically-derived Rho0 human fibroblasts: a comparison of subunit proteins in normal fibroblasts treated with ethidium bromide and fibroblasts from a patient with mtDNA depletion syndrome," *Biochimica et Biophysica Acta*, vol. 1362, no. 2-3, pp. 145–159, 1997.

[45] H. Wang and R. Morais, "Up-regulation of nuclear genes in response to ihnibition of mitochondrial DNA expression in chicken cells," *Biochimica et Biophysica Acta—Gene Structure and Expression*, vol. 1352, no. 3, pp. 325–334, 1997.

[46] R. A. Butow and N. G. Avadhani, "Mitochondrial signaling: the retrograde response," *Molecular Cell*, vol. 14, no. 1, pp. 1–15, 2004.

[47] V. Srinivasan, A. Kriete, A. Sacan, and S. M. Jazwinski, "Comparing the yeast retrograde response and NF-κB stress responses: implications for aging," *Aging Cell*, vol. 9, no. 6, pp. 933–941, 2010.

[48] S. M. Jazwinski and A. Kriete, "The yeast retrograde response as a model of intracellular signaling of mitochondrial dysfunction," *Frontiers in Physiology*, vol. 3, article 139, Article ID Article 139, 2012.

[49] U. Cagin and J. A. Enriquez, "The complex crosstalk between mitochondria and the nucleus: what goes in between?" *The International Journal of Biochemistry & Cell Biology*, vol. 63, pp. 10–15, 2015.

[50] J. Lapointe and S. Hekimi, "Early mitochondrial dysfunction in long-lived *Mclk*$^{1+/-}$ mice," *The Journal of Biological Chemistry*, vol. 283, no. 38, pp. 26217–26227, 2008.

[51] C. Dell'Agnello, S. Leo, A. Agostino et al., "Increased longevity and refractoriness to Ca^{2+}-dependent neurodegeneration in Surf1 knockout mice," *Human Molecular Genetics*, vol. 16, no. 4, pp. 431–444, 2007.

[52] H. Zheng, J. Lapointe, and S. Hekimi, "Lifelong protection from global cerebral ischemia and reperfusion in long-lived Mclk1$^{+/-}$ mutants," *Experimental Neurology*, vol. 223, no. 2, pp. 557–565, 2010.

[53] D. Wang, Y. Wang, C. Argyriou, A. Carrière, D. Malo, and S. Hekimi, "An enhanced immune response of *Mclk1*$^{+/-}$ mutant mice is associated with partial protection from fibrosis, cancer and the development of biomarkers of aging," *PLoS ONE*, vol. 7, no. 11, Article ID e49606, 2012.

[54] F. Zhang, T. Pracheil, J. Thornton, and Z. Liu, "Adenosine triphosphate (ATP) is a candidate signaling molecule in the mitochondria-to-nucleus retrograde response pathway," *Genes*, vol. 4, no. 1, pp. 86–100, 2013.

[55] C. Borghouts, A. Benguria, J. Wawryn, and S. M. Jazwinski, "Rtg2 protein links metabolism and genome stability in yeast longevity," *Genetics*, vol. 166, no. 2, pp. 765–777, 2004.

[56] N. Q. Torelli, J. R. Ferreira-Júnior, A. J. Kowaltowski, and F. M. da Cunha, "RTG1- and RTG2-dependent retrograde signaling controls mitochondrial activity and stress resistance in *Saccharomyces cerevisiae*," *Free Radical Biology and Medicine*, vol. 81, pp. 30–37, 2015.

[57] M. V. Miceli, J. C. Jiang, A. Tiwari, J. F. Rodriguez-Quiñones, and S. M. Jazwinski, "Loss of mitochondrial membrane potential triggers the retrograde response extending yeast replicative lifespan," *Frontiers in Genetics*, vol. 2, article 102, 2012.

[58] Y. Luo, J. D. Bond, and V. M. Ingram, "Compromised mitochondrial function leads to increased cytosolic calcium and to activation of MAP kinases," *Proceedings of the National Academy of Sciences of the United States of America*, vol. 94, no. 18, pp. 9705–9710, 1997.

[59] G. Biswas, O. A. Adebanjo, B. D. Freedman et al., "Retrograde Ca^{2+} signaling in C2C12 skeletal myocytes in response to mitochondrial genetic and metabolic stress: A novel mode of inter-organelle crosstalk," *The EMBO Journal*, vol. 18, no. 3, pp. 522–533, 1999.

[60] G. Amuthan, G. Biswas, H. K. Ananadatheerthavarada, C. Vijayasarathy, H. M. Shephard, and N. G. Avadhani, "Mitochondrial stress-induced calcium signaling, phenotypic changes and invasive behavior in human lung carcinoma A549 cells," *Oncogene*, vol. 21, no. 51, pp. 7839–7849, 2002.

[61] T. Arnould, S. Vankoningsloo, P. Renard et al., "Creb activation induced by mitochondrial dysfunction is a new signaling pathway that impairs cell proliferation," *The EMBO Journal*, vol. 21, no. 1-2, pp. 53–63, 2002.

[62] N. Guaragnella, M. Ždralević, P. Lattanzio et al., "Yeast growth in raffinose results in resistance to acetic-acid induced programmed cell death mostly due to the activation of the mitochondrial retrograde pathway," *Biochimica et Biophysica Acta—Molecular Cell Research*, vol. 1833, no. 12, pp. 2765–2774, 2013.

[63] C. M. Haynes, Y. Yang, S. P. Blais, T. A. Neubert, and D. Ron, "The matrix peptide exporter HAF-1 signals a mitochondrial UPR by activating the transcription factor ZC376.7 in *C. elegans*," *Molecular Cell*, vol. 37, no. 4, pp. 529–540, 2010.

[64] A. M. Nargund, M. W. Pellegrino, C. J. Fiorese, B. M. Baker, and C. M. Haynes, "Mitochondrial import efficiency of ATFS-1 regulates mitochondrial UPR activation," *Science*, vol. 337, no. 6094, pp. 587–590, 2012.

[65] S.-J. Lee, A. B. Hwang, and C. Kenyon, "Inhibition of respiration extends C. elegans life span via reactive oxygen species that increase HIF-1 activity," *Current Biology*, vol. 20, no. 23, pp. 2131–2136, 2010.

[66] J. Durieux, S. Wolff, and A. Dillin, "The cell-non-autonomous nature of electron transport chain-mediated longevity," *Cell*, vol. 144, no. 1, pp. 79–91, 2011.

[67] D. Martins and A. M. English, "Catalase activity is stimulated by H_2O_2 in rich culture medium and is required for H_2O_2 resistance and adaptation in yeast," *Redox Biology*, vol. 2, no. 1, pp. 308–313, 2014.

[68] M. Ristow and S. Schmeisser, "Extending life span by increasing oxidative stress," *Free Radical Biology and Medicine*, vol. 51, no. 2, pp. 327–336, 2011.

[69] I. Martins, L. Galluzzi, and G. Kroemer, "Hormesis, cell death and aging," *Aging*, vol. 3, no. 9, pp. 821–828, 2011.

[70] S. G. Rhee, T.-S. Chang, Y. S. Bae, S.-R. Lee, and S. W. Kang, "Cellular regulation by hydrogen peroxide," *Journal of the American Society of Nephrology*, vol. 14, no. 3, pp. S211–S215, 2003.

[71] A. J. Kowaltowski, R. G. Fenton, and G. Fiskum, "Bcl-2 family proteins regulate mitochondrial reactive oxygen production and protect against oxidative stress," *Free Radical Biology and Medicine*, vol. 37, no. 11, pp. 1845–1853, 2004.

[72] A. J. Kowaltowski and G. Fiskum, "Redox mechanisms of cytoprotection by Bcl-2," *Antioxidants & Redox Signaling*, vol. 7, no. 3-4, pp. 508–514, 2005.

[73] S. Krishna, I. C. C. Low, and S. Pervaiz, "Regulation of mitochondrial metabolism: yet another facet in the biology of the oncoprotein Bcl-2," *Biochemical Journal*, vol. 435, no. 3, pp. 545–551, 2011.

[74] M. Ristow and K. Zarse, "How increased oxidative stress promotes longevity and metabolic health: the concept of mitochondrial hormesis (mitohormesis)," *Experimental Gerontology*, vol. 45, no. 6, pp. 410–418, 2010.

[75] Y. Hashimoto, T. Niikura, H. Tajima et al., "A rescue factor abolishing neuronal cell death by a wide spectrum of familial Alzheimer's disease genes and Aβ," *Proceedings of the National Academy of Sciences of the United States of America*, vol. 98, no. 11, pp. 6336–6341, 2001.

[76] A. Caricasole, V. Bruno, I. Cappuccio, D. Melchiorri, A. Copani, and F. Nicoletti, "A novel rat gene encoding a Humanin-like peptide endowed with broad neuroprotective activity," *The FASEB Journal*, vol. 16, no. 10, pp. 1331–1333, 2002.

[77] T. Niikura, T. Chiba, S. Aiso, M. Matsuoka, and I. Nishimoto, "Humanin: after the discovery," *Molecular Neurobiology*, vol. 30, no. 3, pp. 327–340, 2004.

[78] S. S. Jung and W. E. Van Nostrand, "Humanin rescues human cerebrovascular smooth muscle cells from Aβ-induced toxicity," *Journal of Neurochemistry*, vol. 84, no. 2, pp. 266–272, 2003.

[79] Z. Yang, Q. Zhang, J. Ge, and Z. Tan, "Protective effects of tetramethyl-pyrazine on rat retinal cell cultures," *Neurochemistry International*, vol. 52, no. 6, pp. 1176–1187, 2008.

[80] J. Men, X. Zhang, Y. Yang, and D. Gao, "An AD-related neuroprotector rescues transformed rat retinal ganglion cells from $CoCl_2$-induced apoptosis," *Journal of Molecular Neuroscience*, vol. 47, no. 1, pp. 144–149, 2012.

[81] A. R. Bachar, L. Scheffer, A. S. Schroeder et al., "Humanin is expressed in human vascular walls and has a cytoprotective effect against oxidized LDL-induced oxidative stress," *Cardiovascular Research*, vol. 88, no. 2, pp. 360–366, 2010.

[82] X. Xu, C. C. Chua, J. Gao, R. C. Hamdy, and B. H. L. Chua, "Humanin is a novel neuroprotective agent against stroke," *Stroke*, vol. 37, no. 10, pp. 2613–2619, 2006.

[83] R. H. Muzumdar, D. M. Huffman, J. W. Calvert et al., "Acute humanin therapy attenuates myocardial ischemia and reperfusion injury in mice," *Arteriosclerosis, Thrombosis, and Vascular Biology*, vol. 30, no. 10, pp. 1940–1948, 2010.

[84] R. H. Muzumdar, D. M. Huffman, G. Atzmon et al., "Humanin: a novel central regulator of peripheral insulin action," *PLoS ONE*, vol. 4, no. 7, Article ID e6334, 2009.

[85] Y. K. Oh, A. R. Bachar, D. G. Zacharias et al., "Humanin preserves endothelial function and prevents atherosclerotic plaque progression in hypercholesterolemic ApoE deficient mice," *Atherosclerosis*, vol. 219, no. 1, pp. 65–73, 2011.

[86] C. Lee, J. Wan, B. Miyazaki et al., "IGF-I regulates the age-dependent signaling peptide humanin," *Aging Cell*, vol. 13, no. 5, pp. 958–961, 2014.

[87] S. Kariya, M. Hirano, Y. Furiya, K. Sugie, and S. Ueno, "Humanin detected in skeletal muscles of MELAS patients: a possible new therapeutic agent," *Acta Neuropathologica*, vol. 109, no. 4, pp. 367–372, 2005.

[88] H. Tajima, T. Niikura, Y. Hashimoto et al., "Evidence for in vivo production of Humanin peptide, a neuroprotective factor against Alzheimer's disease-related insults," *Neuroscience Letters*, vol. 324, no. 3, pp. 227–231, 2002.

[89] C. Lee, J. Zeng, B. Drew et al., "The mitochondrial-derived peptide MOTS-c promotes metabolic homeostasis and reduces obesity and insulin resistance," *Cell Metabolism*, vol. 21, no. 3, pp. 443–454, 2015.

[90] C. B. Epstein, J. A. Waddle, W. Hale IV et al., "Genome-wide responses to mitochondrial dysfunction," *Molecular Biology of the Cell*, vol. 12, no. 2, pp. 297–308, 2001.

[91] X. S. Liao, W. C. Small, P. A. Srere, and R. A. Butow, "Intramitochondrial functions regulate nonmitochondrial citrate synthase (CIT2) expression in *Saccharomyces cerevisiae*," *Molecular and Cellular Biology*, vol. 11, no. 1, pp. 38–46, 1991.

[92] X. Liao and R. A. Butow, "RTG1 and RTG2: two yeast genes required for a novel path of communication from mitochondria to the nucleus," *Cell*, vol. 72, no. 1, pp. 61–71, 1993.

[93] Z. Liu and R. A. Butow, "A transcriptional switch in the expression of yeast tricarboxylic acid cycle genes in response to a reduction or loss of respiratory function," *Molecular and Cellular Biology*, vol. 19, no. 10, pp. 6720–6728, 1999.

[94] A. Chelstowska, Z. Liu, Y. Jia, D. Amberg, and R. A. Butow, "Signalling between mitochondria and the nucleus regulates the expression of a new D-lactate dehydrogenase activity in yeast," *Yeast*, vol. 15, no. 13, pp. 1377–1391, 1999.

[95] C. Vélot, P. Haviernik, and G. J.-M. Lauquin, "The Saccharomyces cerevisiae RTG2 gene is a regulator of aconitase expression under catabolite repression conditions," *Genetics*, vol. 144, no. 3, pp. 893–903, 1996.

[96] Y. Jia, B. Rothermel, J. Thornton, and R. A. Butow, "A basic helix-loop-helix-leucine zipper transcription complex in yeast functions in a signaling pathway from mitochondria to the nucleus," *Molecular and Cellular Biology*, vol. 17, no. 3, pp. 1110–1117, 1997.

[97] Z. Hashim, Y. Mukai, T. Bamba, and E. Fukusaki, "Metabolic profiling of retrograde pathway transcription factors rtg1 and rtg3 knockout yeast," *Metabolites*, vol. 4, no. 3, pp. 580–598, 2014.

[98] P. A. Kirchman, S. Kim, C.-Y. Lai, and S. M. Jazwinski, "Interorganelle signaling is a determinant of longevity in *Saccharomyces cerevisiae*," *Genetics*, vol. 152, no. 1, pp. 179–190, 1999.

[99] J. Sun, S. P. Kale, A. M. Childress, C. Pinswasdi, and S. M. Jazwinski, "Divergent roles of RAS1 and RAS2 in yeast longevity," *Journal of Biological Chemistry*, vol. 269, no. 28, pp. 18638–18645, 1994.

[100] H. Conrad-Webb and R. A. Butow, "A polymerase switch in the synthesis of rRNA in *Saccharomyces cerevisiae*," *Molecular and Cellular Biology*, vol. 15, no. 5, pp. 2420–2428, 1995.

[101] S. M. Jazwinski, "Metabolic control and gene dysregulation in yeast aging," *Annals of the New York Academy of Sciences*, vol. 908, pp. 21–30, 2000.

[102] E. Munkácsy and S. L. Rea, "The paradox of mitochondrial dysfunction and extended longevity," *Experimental Gerontology*, vol. 56, pp. 221–233, 2014.

[103] C. F. Bennett, H. V. Wende, M. Simko et al., "Activation of the mitochondrial unfolded protein response does not predict longevity in *Caenorhabditis elegans*," *Nature Communications*, vol. 5, article 3483, 2014.

[104] S. Hill and H. van Remmen, "Mitochondrial stress signaling in longevity: a new role for mitochondrial function in aging," *Redox Biology*, vol. 2, pp. 936–944, 2014.

[105] M. W. Pellegrino, A. M. Nargund, N. V. Kirienko, R. Gillis, C. J. Fiorese, and C. M. Haynes, "Mitochondrial UPR-regulated innate immunity provides resistance to pathogen infection," *Nature*, vol. 516, no. 7531, pp. 414–417, 2014.

Hindawi Publishing Corporation
Oxidative Medicine and Cellular Longevity
Volume 2015, Article ID 359315, 11 pages
http://dx.doi.org/10.1155/2015/359315

Research Article

Toll-Like Receptor 4 Promotes NO Synthesis by Upregulating GCHI Expression under Oxidative Stress Conditions in Sheep Monocytes/Macrophages

Shoulong Deng,[1] Kun Yu,[2,3] Baolu Zhang,[3] Yuchang Yao,[4] Zhixian Wang,[2] Jinlong Zhang,[5] Xiaosheng Zhang,[5] Guoshi Liu,[2] Ning Li,[3] Yixun Liu,[1] and Zhengxing Lian[2,3]

[1]*State Key Laboratory of Reproductive Biology, Institute of Zoology, Chinese Academy of Sciences, Beijing 100101, China*
[2]*Laboratory of Animal Genetics and Breeding, College of Animal Science and Technology, China Agricultural University, Beijing 100193, China*
[3]*National Key Laboratory of Agrobiotechnology, College of Biological Sciences, China Agricultural University, Beijing 100193, China*
[4]*College of Animal Science and Technology, Northeast Agricultural University, Harbin 150030, China*
[5]*Tianjin Institute of Animal Sciences, Tianjin 300112, China*

Correspondence should be addressed to Yixun Liu; liuyx@ioz.ac.cn and Zhengxing Lian; lianzhx@cau.edu.cn

Received 15 October 2014; Accepted 26 February 2015

Academic Editor: Hariom Yadav

Many groups of Gram-negative bacteria cause diseases that are harmful to sheep. Toll-like receptor 4 (TLR4), which is critical for detecting Gram-negative bacteria by the innate immune system, is activated by lipopolysaccharide (LPS) to initiate inflammatory responses and oxidative stress. Oxidation intermediates are essential activators of oxidative stress, as low levels of free radicals form a stressful oxidative environment that can clear invading pathogens. NO is an oxidation intermediate and its generation is regulated by nitric oxide synthase (iNOS). Guanosine triphosphate cyclohydrolase (GCHI) is the rate-limiting enzyme for tetrahydrobiopterin (BH4) synthesis, which is essential for the production of inducible iNOS. Previously, we made vectors to overexpress the sheep *TLR4* gene. Herein, first generation (G1) of transgenic sheep was stimulated with LPS *in vivo* and *in vitro*, and oxidative stress and GCHI expression were investigated. Oxidative injury caused by TLR4 overexpression was tightly regulated in tissues. However, the transgenic (Tg) group still secreted nitric oxide (NO) when an iNOS inhibitor was added. Furthermore, GCHI expression remained upregulated in both serum and monocytes/macrophages. Thus, overexpression of TLR4 in transgenic sheep might accelerate the clearance of invading microbes through NO generation following LPS stimulation. Additionally, TLR4 overexpression also enhances GCHI activation.

1. Introduction

In both host defense and inflammation, monocytes/macrophages are the most prominent immune cell type activated by lipopolysaccharide (LPS) to release various pro- and anti-inflammatory mediators. Toll-like receptor 4 (TLR4) interacts with several proteins to form the myeloid differentiation factor 2 (MD2)/CD14/TLR4 complex that binds to LPS [1]. TLR4 then recruits downstream adaptors to activate both the myeloid differentiation primary response gene 88 (MyD88) and TIR-domain-containing adaptor-inducing interferon-β- (TRIF-) dependent pathways, which function through nuclear factor-κB- (NF-κB-) associated signaling events [2]. The actions of these proteins trigger the release of oxidation intermediates, including reactive oxygen species (ROS), reactive nitrogen species (RNS), and cytokines [3]. Apart from the inflammatory reaction, oxidation intermediates are also involved in many pathological processes, such as insulin resistance and type 2 diabetes [4]. They are extremely important for the intracellular environment. To maintain physiological homeostasis, ROS are maintained at a certain level to induce enough oxidative stress to eliminate pathogenic microorganisms. However, large amounts of oxidation

intermediates and derivatives can both destroy bacterial membranes and cause host tissue damage.

ROS are mainly produced by nicotinamide adenine dinucleotide phosphate (NADPH) oxidase. NADPH oxidase is a multisubunit enzyme complex. When electrons are transported across membranes, the membranes are depolarized. These changes lead to compensatory ion flux. NADPH oxidase has specialized domains for the dismutation of O_2^- and H_2O_2 production [5]. NAPDH oxidase activation is critically regulated by cytokines produced in response to activation of the TLR4 pathway. Interleukin-1 receptor-associated kinase-4 (IRAK-4), the regulatory kinase, which is downstream of TLR4 signaling, regulates NADPH oxidase through the phosphorylation of $p47^{phox}$ [6]. Tumor necrosis factor-alpha (TNF-α) enhances the activity of NADPH oxidase through the NF-κB pathway by upregulating mRNA expression levels of transcripts that encode $gp91^{phox}$ [7]. NF-κB activation is mediated by direct interactions of TLR4 with Nox4 and Nox2, two subunits of NAPDH oxidase [8, 9].

NO is the major component of RNS. In mononuclear macrophages, inducible nitric oxide synthase (iNOS) is the rate-limiting enzyme for NO synthesis. Along with NAPDH, O_2, and tetrahydrobiopterin (BH4), NO is synthesized from L-arginine by the enzyme iNOS. In the inflammatory response, transcription of iNOS is regulated by the NF-κB and MAPK pathways. Increasing levels of downstream factors, such as interleukin-1 (IL-1), TNF-α, and interferon-gamma (IFN-γ), result in increased iNOS expression [10].

Another essential enzyme for iNOS *de novo* biosynthesis is BH4. BH4 deficiency causes a reduction in iNOS uncoupling. The rate-limiting enzyme for BH4 is GTP cyclohydrolase, which is encoded by GCHI [11]. GCHI is important in iNOS activation and is closely linked to various pathological processes, such as vasofunctional disturbances and dyskinesia [12].

Innate immunity is the major type of defense against Gram-negative bacterial infection. TLR4 participates in innate immunity in various ways, not only in resistance to Gram-negative bacterial infections, but also in many autoimmune and inflammatory disease settings, including atherosclerosis, diabetes mellitus, cancer, and rheumatoid arthritis. Previous studies have shown that the susceptibility or sensitivity of TLR4-mutant cells to LPS is lower than that of wild-type cells [13, 14]. Furthermore, TLR4-deficient mice stimulated with LPS cannot secrete IL-1 or IL-12 [15] and also show reduced expression of IL-6 [16]. However, TLR4 overexpression in mice results in increased disease resistance [17]. We previously reported the generation of TLR4-transgenic sheep [18]. The effect of bacteria on the sensitivity of transgenic animals to disease resistance is dependent on transgene copy number [19]. Notably, excessive inflammation and oxidative stress can cause tissue damage [20]. To better understand the biological basis for a role of overexpressed TLR4 in the immune response and oxidative stress, we isolated monocytes/macrophages from the peripheral blood of first-generation (G1) transgenic sheep with two transgene copies and stimulated them with LPS. Immunoactivity and oxidative damage were investigated. Furthermore, we added iNOS and NADPH oxidase inhibitors to LPS-stimulated monocytes/macrophages to study the relationship between TLR4 and oxidative stress. Herein, we first demonstrate that overexpression of TLR4 promotes NO synthesis by upregulating GCHI expression under oxidative stress conditions in sheep monocytes/macrophages. Innate immune responses and oxidative stress in TLR4-transgenic sheep were tightly regulated.

2. Materials and Methods

2.1. Ethics Statement. Artificial insemination, intradermic injection, and blood collection were performed at the experimental station of the China Agricultural University, and the whole procedure was carried out in strict accordance with the protocol approved by the Animal Welfare Committee of China Agricultural University (Permit Number: XK662).

2.2. Screening of Transgenic Sheep Overexpressing TLR4. Genomic DNA from TLR4-transgenic sheep was extracted from sperm and a 623-bp fragment was amplified with the following pair of primers: Forward, TAC GGT AAA CTG CCC ACT TG; Reverse, ACC TGG AGA AGT TAT GGC TG. In mating season, ewes of natural estrus were inseminated with sperm from positive sheep. The presence of a transgene in offspring was analyzed by Southern blotting. We used polymerase chain reaction (PCR) to generate specific digoxigenin-labeled probes (Roche Diagnostics, Mannheim, Germany) using the primer sequences indicated above. Genomic DNA was isolated from ear tissue and digested with VspI and SmaI (NEB, Beverly, MA, USA).

Mononuclear cells were isolated from the peripheral blood of G1 transgenic sheep using sheep lymphocyte separation medium (TBD, Tianjin, China). Total RNA was extracted. The mRNA abundance of the *TLR4* gene was measured by real-time PCR, using a SYBR Green kit (Tiangen, China) with the following primers: TLR4-forward, CTG AAT CTCTAC AAA ATC CC; TLR4-reverse, CTT AAT TTC GCA TCT GGA TA; β-actin-forward, AGA TGT GGA TCA GCA AGC AG; β-actin-reverse, CCA ATC TCA TCT CGT TTT CTG. TLR4 protein levels were measured by enzyme-linked immunosorbent assay (ELISA; Shanghai Xin Le, Shanghai, China).

Peripheral blood was collected for routine blood and serum biochemical parameter testing at 120 days. Testing included analysis of red blood cells, white blood cells, hemoglobin, albumin, globulin, alanine aminotransferase, aspartate aminotransferase, glucose, blood urea nitrogen, and serum total protein concentrations.

2.3. Detection of Acute Inflammatory Responses in G1 Transgenic Sheep In Vivo. The ears of five 3-month-old transgene-positive sheep were injected with 100 μL 3 mg/mL LPS (Sigma-Aldrich, St. Louis, MO, USA); then tissues were collected at 1, 8, and 48 h. Samples were fixed with 4% paraformaldehyde and embedded in paraffin. Hematoxylin and eosin staining was used to investigate the inflammatory response and immunohistochemistry was used to detect

MD2 protein expression (Abcam, Cambridge, UK). Peripheral blood was also collected at 1, 4, 8, and 48 h. RNA was isolated from mononuclear cells and real-time PCR was used to detect the expression of *TLR4*, *CD14*, and *NF-κB*. Primer sequences were as follows: TLR4: as above; CD14-forward, ATA TCT AGC ACT ACG CAA CGC; CD14-reverse, CTT GGT CGG CAG TCC TTT; NF-κB-forward, TTC TCC AAA TGG CTG AAG GTA; NF-κB-reverse, TTG TTT GAG GGC CAT AAG GAT. ELISA kits were used to detect levels of TLR4, GCHI, and various cytokines, including IFN-γ, TNF-α, IL-6, IL-8, IL-12, and IL-10 in serum (Shanghai Xin Le).

2.4. Oxidative Stress in LPS-Stimulated Sheep Mononuclear Cells. Sheep peripheral blood mononuclear cells were isolated and cultured in RM1640 (Gibco, Grand Island, NY, USA) medium containing 10% fetal bovine serum (Gibco) for 48 h. After stimulation with LPS (1 μg/mL), cell suspensions were collected at 0, 1, 8, and 48 h. The activities of iNOS and NADPH oxidase, as well as the ROS, RNS, and malonaldehyde (MDA) contents of the cells, were examined by spectrophotometry (Nanjing Jiancheng Bioengineering Institute, Nanjing, China). The activity of GCHI was examined by an enzymatic method (Nanjing Jiancheng Bioengineering Institute). After 1 h stimulation with LPS, 4% paraformaldehyde was used to fix cells; then immunofluorescence was used to detect protein oxidation products. Thioredoxin- (TRX-) TRITC (Abcam) and TLR4-FITC (Abcam) were used to detect changes in protein expression, and DAPI was used to counterstain nuclei. Confocal microscopy was used to detect staining results.

NADPH oxidase and iNOS inhibitors were added to monocytes/macrophages during stimulation with 1 μg/mL LPS to study the relationship between TLR4 and oxidative damage. Apocynin (Sigma-Aldrich) is an inhibitor of NADPH oxidase and inhibits the production of O_2^-. Nitro-L-arginine (L-NNA) (Sigma-Aldrich) is an inhibitor of iNOS and inhibits the production of NO. Inhibitors were used at concentrations of 10 and 20 mmol/L. A TLR4 inhibitor, anti-TLR4 antibody, was added to the Tg group culture media at a dilution of 1 : 500. After 1 h, cell suspensions were collected. The NO, O_2^-, and MDA concentrations were determined by spectrophotometry according to the manufacturer's instructions (Nanjing Jiancheng Bioengineering Institute).

2.5. Statistical Analyses. All experiments repeated 3 times. All data were subjected to analysis of variance using the GLM procedures of Statistical Analysis System (SAS Institute, Cary, NC, USA). All data were expressed as mean ± SEM. Differences were considered to be significant when $P < 0.05$.

3. Results

3.1. Overexpression of TLR4 in G1 Transgenic Sheep. We previously generated transgenic sheep using the microinjection technique. Transgenic sheep had two TLR4 copies integrated into germ cells, as determined by PCR (Figure 1(a)). Artificial insemination was then used for the propagation of sheep. Southern blot detection showed that the G1 sheep were positive for exogenous TLR4 (Figure 1(b)). Real-time PCR and ELISA were performed to determine the expression levels of TLR4. The expression of TLR4 in Tg sheep was significantly higher than in WT sheep (Figures 1(c) and 1(d)). There were no statistically significant differences in the analysis of the routine blood counts or biochemical serum parameters between transgenic and WT sheep at 120 days (Figures 1(e) and 1(f)).

3.2. TLR4 Overexpression in G1 Tg Sheep Triggered Rapid Neutrophil Infiltration. LPS was injected into the ears of transgenic sheep and the resulting inflammatory infiltrate was observed under a light microscope after hematoxylin and eosin staining (Figure 2(a)). In the Tg group, many segmented neutrophils infiltrated the dermis at 1 h, and after 8 h more inflammatory cells, including many neutrophils, had infiltrated the dermis and many erythrocytes had infiltrated the connective tissues. Fewer inflammatory cells were observed in Tg animals at 48 h after stimulation. This finding suggested that the inflammatory reaction in Tg animals was negatively regulated by a feedback loop in order to avoid inflammatory injury. However, no significant lesions were observed after 48 h. In the WT group, dermis bleeding also occurred with inflammatory cell infiltration at 1 h. After 8 h, many erythrocytes were spread across the surface of the skin and between connective tissues, and inflammatory cells—including many neutrophils—had infiltrated around the blood vessels. Few infiltrating inflammatory cells were evident after 48 h. Immunohistochemistry was used to observe MD2 protein expression. MD2-positive tissues showed claybank, which was primarily expressed by sebaceous gland cells and infiltrating inflammatory cells (Figure 2(b)).

Real-time PCR showed that CD14 and TLR4 transcription reached a peak at 8 h. By contrast, TLR4 transcription continued to rise in the WT group (Figures 2(c) and 2(e)). These above findings showed that, at 8 h, the inflammatory response of the Tg group was stronger than that of the WT group. After 48 h, the inflammatory response of the Tg group had finished, whereas the inflammatory response of the WT group remained in progress, indicating that Tg sheep can launch a more rapid inflammatory reaction. Transcription of the TLR4 downstream factor NF-κB was also significantly higher in the Tg group than in the WT group at 1 and 8 h (Figure 2(d)). These results suggest overexpression of *TLR4* gene could trigger rapid neutrophil infiltration.

3.3. Overexpression of TLR4 Enhanced Oxidative Stress in Sheep Monocytes/Macrophages. After stimulation with LPS, ROS expression increased in the Tg group, with significant differences compared with the WT group evident at 1 and 8 h ($P < 0.05$). By contrast, the expression of ROS was maximal at 48 h in the WT group (Figure 3(a)). Compared with the WT group, the expression of RNS was also significantly higher at 1 h in the Tg group ($P < 0.05$); however, there was no significant difference between groups at 48 h (Figure 3(b)). In the Tg group, the release of ROS/RNS was increased, indicating that overexpression of TLR4 could upregulate the expression of ROS/RNS, inducing a stronger oxidative stress response

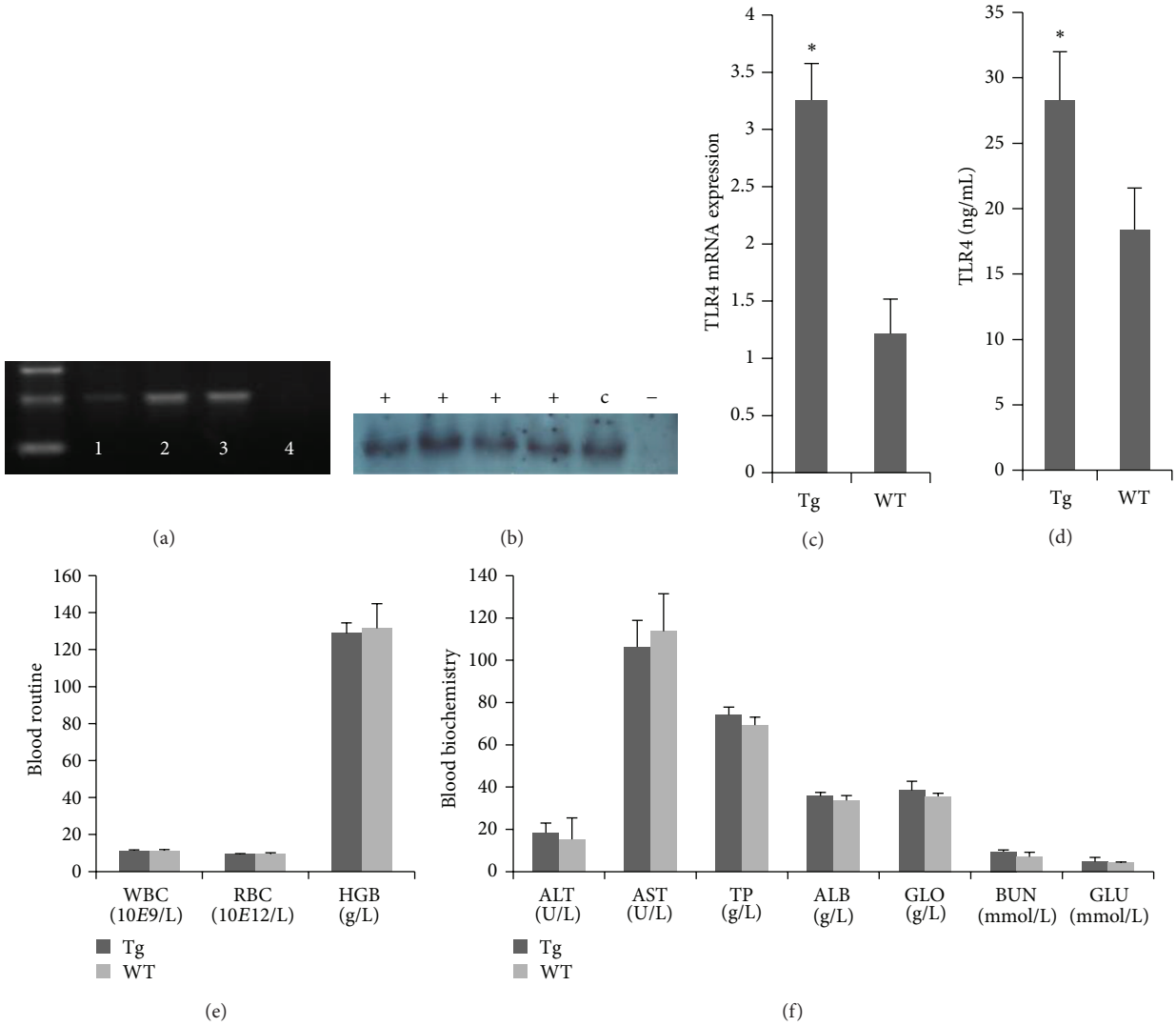

Figure 1: Overexpression of TLR4 in G1 transgenic sheep. (a) Transgene-positive sperm from transgenic sheep were detected by PCR. Lanes: (1) TLR4-positive ovine sperm genomic DNA, (2) TLR4-positive ovine ear genomic DNA, (3) expression vector (p3S-LoxP-TLR4), and (4) negative control. (b) Southern blot analysis of the TLR4 transgene insert in transgenic G1 lambs. "+": TLR4-transgenic G1 lambs, "−": negative control, and "c": TLR4-transgenic sheep. TLR4 expression and translation in mononuclear cells from G1 transgenic lambs were detected by real-time quantitative PCR and ELISA; more TLR4 was detected in transgenic lambs (c) and (d). Blood routine (e) and blood biochemistry (f) examinations were carried out on TLR4-transgenic sheep. There were no statistically significant differences between G1 and WT lambs. Tg: TLR4-transgenic G1 lambs, WT: wild-type. The results are expressed as mean ± SE; $^{*}P < 0.05$ in Tg versus WT groups.

in monocytes/macrophages. The expression of MDA also showed a significant difference at 1 and 8 h ($P < 0.05$) between the Tg and WT groups, indicating that overexpression of TLR4 in monocytes/macrophages enhanced oxidative damage. However, at 48 h, MDA expression returned to normal levels in the Tg group (Figure 3(c)). The expression of TRX protein in monocytes/macrophages 1 h after stimulation with LPS was assessed by immunofluorescence. Compared with the WT group, expression of both TLR4 and TRX protein in the Tg group was higher and the degree of oxidative damage was stronger (Figure 3(d)).

3.4. TLR4-Mediated Oxidative Stress Triggered by Monocyte/Macrophage NO Secretion. *In vivo*, NO and O_2^- are mainly released by mononuclear macrophages. TLR4 regulates the expression of NADPH oxidase, iNOS, and apocynin, which is an inhibitor of NADPH oxidase that can inhibit the release of O_2^-. Furthermore, L-NNA, which is an inhibitor of iNOS, can inhibit NO production. Monocytes/macrophages were stimulated with 1 μg/mL LPS, and 10 mmol/L of apocynin and/or L-NNA were added to inhibit the expression of NADPH oxidase and iNOS, respectively. The cellular content of O_2^-, NO, and MDA was then determined (Figures 4(a), 4(b), and 4(c)). Our results showed that the expression of NO increased in the LPS-stimulated Tg group treated with 10 mmol/L L-NNA, whereas the expression of O_2^- was reduced. Expression of NADPH oxidase was inhibited in the LPS-stimulated Tg group by 10 mmol/L apocynin,

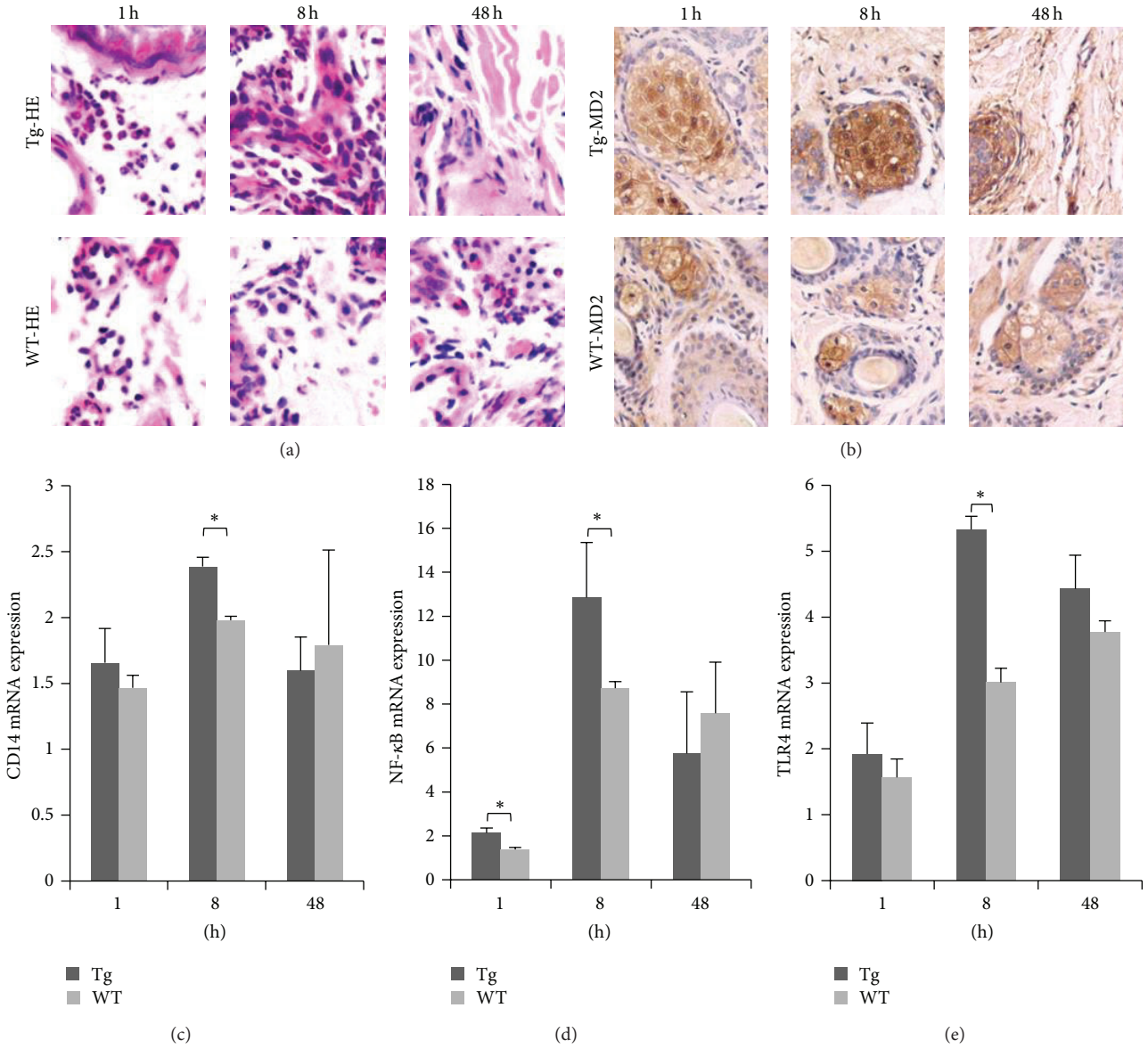

Figure 2: LPS stimulation triggered rapid infiltration of neutrophils in transgenic sheep. (a) Pathological changes were examined microscopically (hematoxylin and eosin staining, ×400). (b) MD2 expression was detected by immunohistochemistry (×200). (c) CD14, (d) NF-κB, and (e) TLR4 transcription in mononuclear cells from G1 transgenic lambs were detected by real-time quantitative PCR. Tg: transgenic sheep, WT: wild-type. The results are expressed as mean ± SE; $^{*}P < 0.05$ in Tg versus WT groups.

while O_2^- concentrations were also reduced. For expression of NO, the difference in the Tg group with inhibitor was more significant than that in the Tg group without inhibitor ($P < 0.05$). Then, 20 mmol/L L-NNA was added (Figures 4(d), 4(e), and 4(f)) and this inhibited the expression of iNOS. In the Tg group, expression of NO was also inhibited, the content of O_2^- was reduced, and there was no strong oxidative damage. Although 20 mmol/L apocynin inhibited the expression of NADPH oxidase and the content of O_2^- was reduced, NO was still secreted by the Tg group. Compared with controls, expression of MDA in the Tg group was significantly different ($P < 0.05$). These data indicated that TLR4 induced oxidative stress by promoting the release of NO by monocytes/macrophages.

3.5. TLR4 Upregulation of GCHI Activation in Sheep Monocytes/Macrophages and Serum. In macrophages of the Tg group stimulated with LPS, expression of NADPH oxidase and iNOS was significantly greater than that of the WT group at 1 and 8 h ($P < 0.05$) but returned to a normal level at 48 h (Figures 5(a) and 5(b)). This finding indicates that TLR4 could regulate the expression of NADPH oxidase and iNOS. GCHI plays an important role in the regulation of iNOS expression. The expression of GCHI in the Tg group was also

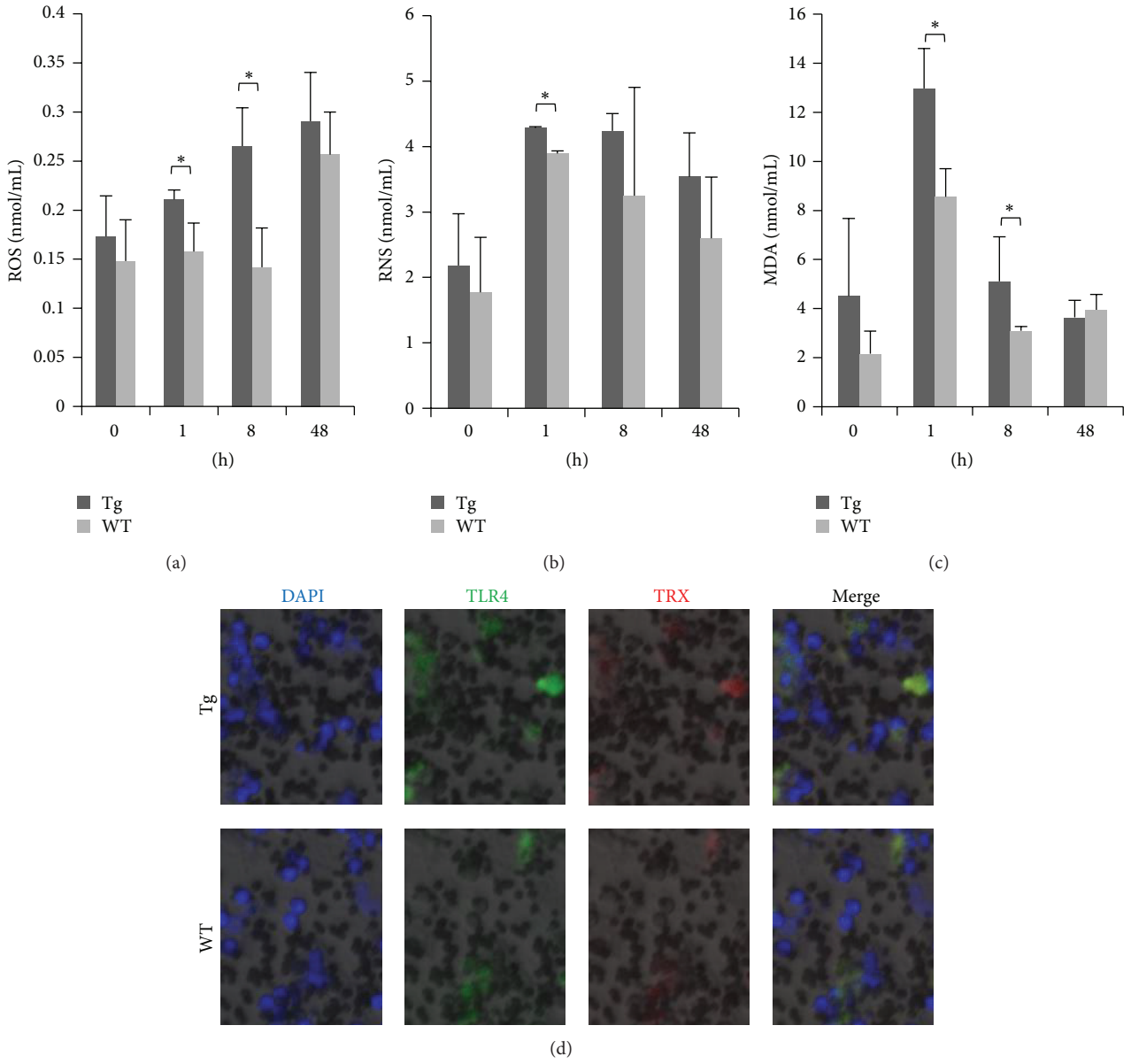

Figure 3: Overexpression of TLR4 enhances oxidative stress in monocytes/macrophages. Expression patterns of ROS, RNS, and MDA after stimulation with 1 μg/mL LPS ((a), (b), and (c), resp.). (d) TLR4 and TRX protein expression levels were detected by immunofluorescence (×200), DAPI (blue), TLR4-FITC (green), and TRX (red). Tg: transgenic sheep, WT: wild-type. Results were expressed as mean ± SE; $^*P < 0.05$ in Tg versus WT groups.

significantly higher at 1 and 8 h ($P < 0.05$) and returned to a normal level at 48 h, similar to iNOS (Figure 5(c)). These findings indicated that TLR4 enhances the activity of iNOS by upregulating GCHI to promote synthesis and secretion. In serum, during an acute inflammatory reaction, expression of TLR4 protein was significantly different between groups at 1 and 8 h ($P < 0.05$). Furthermore, the Tg group showed attenuated TLR4 expression at 48 h, while TLR4 expression in the WT group continued to increase (Figure 5(d)). We detected proinflammatory cytokines downstream of TLR4 at various time points, IFN-γ (1 h), TNF-α (1 h), IL-6 (8 h), IL-12 (8 h), and IL-8 (8 h), and anti-inflammatory cytokines IL-10 (48 h), and all showed significant differences between the Tg and WT group ($P < 0.05$; Figure 5(e)). This finding indicates that overexpression of the *TLR4* gene in sheep can promote the expression of downstream inflammatory cytokines, inducing rapid inflammatory reactions. Expression levels of GCHI protein in serum of the Tg group were significantly higher than those in the WT group at 4, 8, and 48 h ($P < 0.05$; Figure 5(f)). This finding indicates that TLR4 regulates the expression of GCHI through downstream inflammatory cytokines.

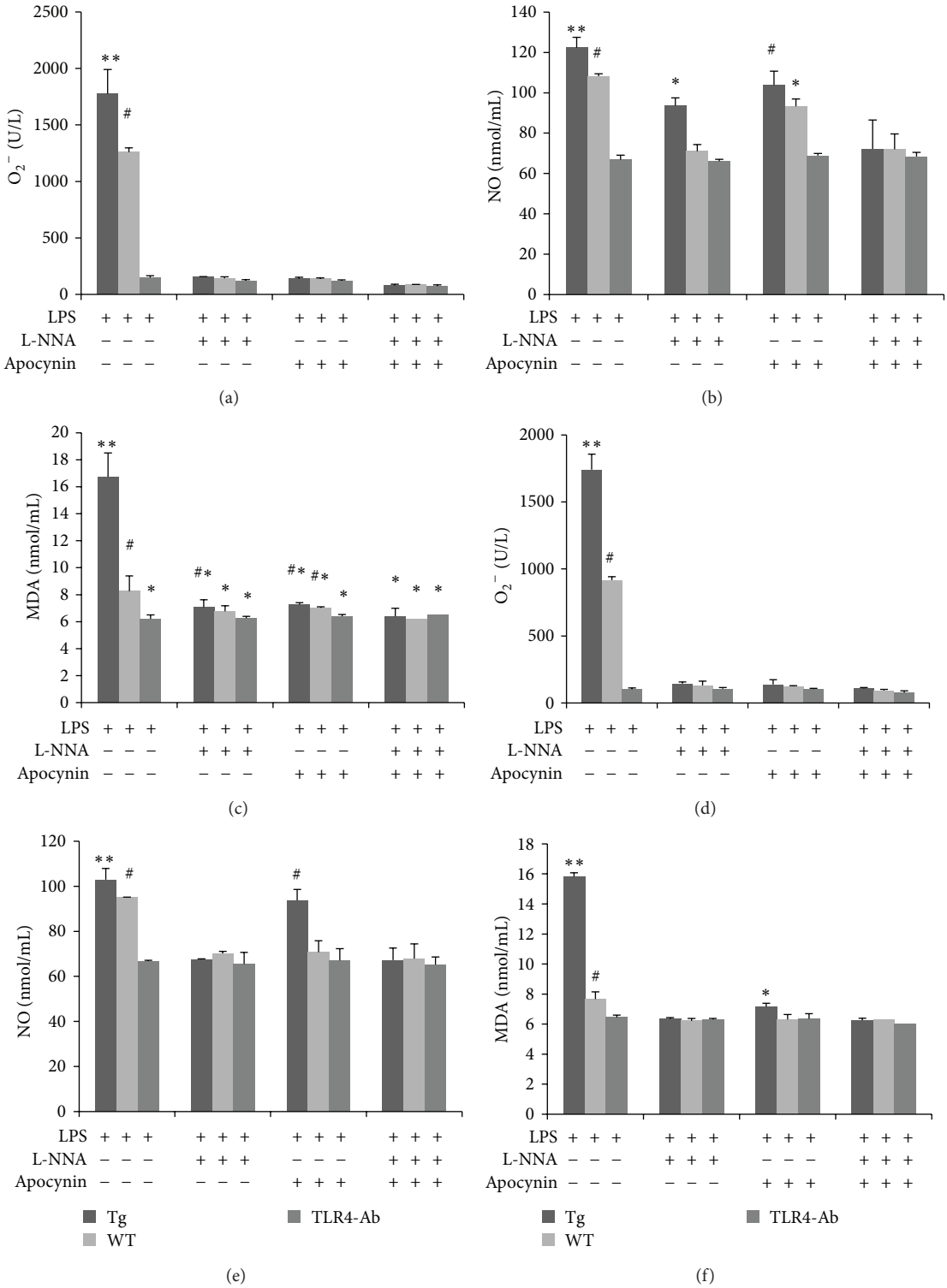

Figure 4: Overexpression of TLR4 induced oxidative stress via the secretion of NO by monocytes/macrophages. Levels of O_2^-, NO, and MDA were examined in monocytes/macrophages after LPS stimulation. Cells were treated with various combinations of the inhibitors apocynin (10 mmol/L) and L-NNA (10 mmol/L; (a), (b), and (c)). Similar patterns were observed when inhibitor concentrations were raised to 20 mmol/L ((d), (e), and (f)). Tg: transgenic sheep, WT: wild-type, and TLR4-Ab: anti-TLR4 antibody. The results are expressed as mean ± SE. $^{*,**,\#}$Values were found to be significantly different between groups ($P < 0.05$).

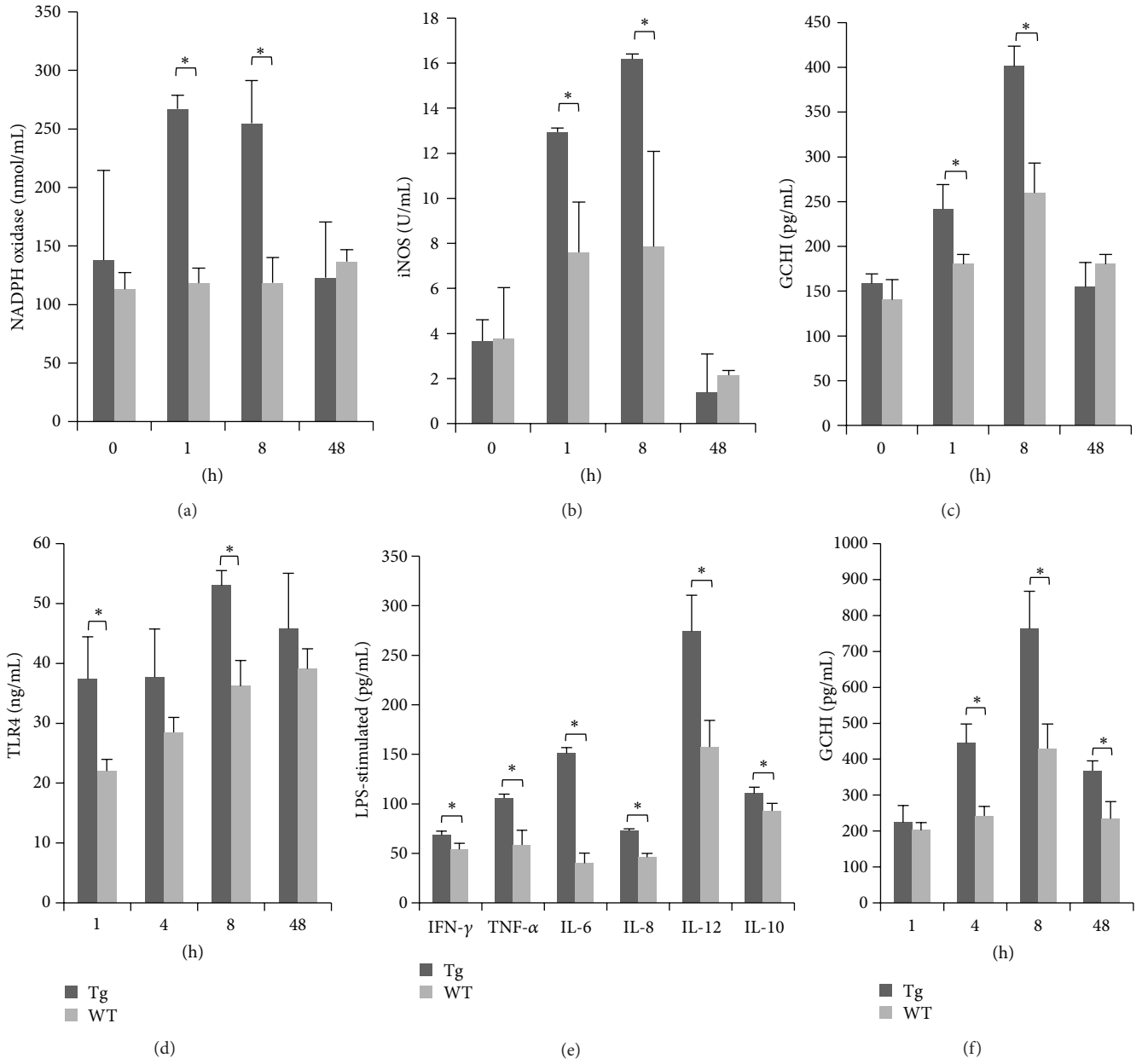

Figure 5: TLR4 enhanced GCHI activity in monocytes/macrophages and serum. The activities of NADPH oxidase, iNOS, and GCHI in monocytes/macrophages were examined after LPS stimulation ((a), (b), and (c), resp.). (d) Levels of TLR4 in the serum after LPS stimulation were measured by ELISA. (e) The effects of LPS stimulation on the expression of immune factors (TNF-α, IFN-γ, IL-6, IL-8, IL-12, and IL-10) in serum. (f) GCHI expression in serum was detected by ELISA. Tg: transgenic sheep, WT: wild-type. Data are expressed as mean ± SE; $^{*}P < 0.05$ in Tg versus WT groups.

4. Discussion

When pathogenic microorganisms invade animals, the TLR4 signaling pathway is activated and triggers a cascade of reactions to promote the production and release of inflammatory cytokines, inducing the chemotactic aggregation of granulocytes and macrophages, increased capillary permeability, and lymphocyte infiltration. The TLR4 signal transduction pathway is involved in many distinct diseases [21–23]. Current research on TLR4 signaling is concentrated in the areas of infectious disease, pulmonary infections, cancer, type 2 diabetes, and sepsis [24, 25]. Activation of TLR4 is beneficial for the elimination of exogenous pathogens. A TLR4 activator, BCG (Bacillus Calmette, Guérin), has been used in bladder cancer treatment for its ability to trigger the production of cytokines and enhance immune responses [26]. TLR4 induced large amounts of cytokine release, which is also observed in insulin resistance. Through those preinflammatory kinases and ROS, TLR4 directly represses insulin action [27]. This current study reports the generation of

TLR4-transgenic sheep with stable transgene transmission. We have shown that TLR4 was overexpressed at the RNA level and protein levels. Overexpression of TLR4 did not show any harmful effects on animal health. The result of an acute inflammatory reaction triggered by LPS indicates that overexpression of the *TLR4* gene induced the rapid infiltration of neutrophils. Thus, TLR4 can upregulate the expression of cytokines, such as TNF-α, IFN-γ, IL-6, IL-8, IL-12, and IL-10, thereby increasing resistance to pathogen invasion and infection.

As an important immune receptor, TLR4 plays a central role in oxidative stress. Research of oxidative lung injury in mice with targeted deletions of multiple inflammatory, immune, and antioxidant genes indicated that TLR4 is an important candidate gene related to oxidative-stimulated inflammation [28, 29]. TLR4 can trigger transcription of the iNOS gene and promote production of NO. The main function of NO is clearing pathogenic bacteria by producing peroxidase and superoxide radicals [30]. ROS are mainly induced by NADPH oxidase, whose activity is regulated by TLR4 through the composition of the NADPH multisubunit enzyme complex. ROS could oxidize the iNOS cofactor BH4, reduce the expression of BH4, and lead to uncoupling of iNOS to form more O_2^-. ROS are produced under conditions of the uncoupling of NADPH oxidase and mitochondria when the body is stimulated by oxidative stress. ROS can induce NF-κB activation and upregulate the cytokine-induced iNOS gene, resulting in excessive release of NO [31]. When the levels of NO are higher than those of ROS, NO can clear ROS. Currently, NOS uncoupling is thought to play a major role in the induction of oxidative stress [32, 33]. In the present study, NO was expressed in TLR4-overexpressing cells stimulated with LPS, even after NADPH oxidase was added. This finding indicates that, in sheep mononuclear macrophages, TLR4 promotes the secretion of NO by regulating iNOS expression. Similarly, when NO and O_2^- production were investigated in NOS-transfected cells, an iNOS-specific inhibitor could drastically reduce the production of O_2^- [34]. Our results are in accordance with this, as L-NNA inhibited the expression of iNOS and reduced the expression of O_2^-. TLR4 overexpression could also protect against oxidative stress [35], and NO could clear O_2^- [36]. TLR4 induces the expression of NO by upregulating iNOS, and NO induces expression of many genes that can reduce oxidative stress and help cells resist injury [37]. The present study suggests that TLR4-overexpressing sheep could reduce oxidative injury more efficiently.

GCHI is the rate-limiting enzyme in BH4 biosynthesis. BH4 is an important cofactor for NOS. When the production of BH4 is limited, coupling of O_2 and L-arginine are reduced, resulting in increased O_2^- catalyzed by NOS and no increase in NO. Recent studies showed that reductions in BH4 are linked to hypertension, arteriosclerosis, diabetes mellitus, cardiac hypertrophy, and myocardial ischemia [38, 39]. Sakai et al. found that a phosphatidylinositol 3-kinase (PI3K) inhibitor could inhibit the synthesis of NO in macrophages stimulated by LPS, while synthesis of NO and the activation of GCHI could both be inhibited in PI3K-deficient macrophages [40]. After stimulation with cytokines (IFN-γ or TNF-α) or LPS, the expression of iNOS increased significantly, resulting in increased synthesis of NO, which had a direct relationship with the increased BH4 synthesis caused by the activated GCHI gene [41]. A study of GCHI-transgenic mice stimulated with LPS showed that the expression of renal iNOS and NO content increased dramatically [42]. A GCHI inhibitor could significantly inhibit the production of NO induced by LPS [43]. LPS binds to macrophage TLR4 and activates downstream signaling pathways, including NF-κB, mitogen-activated protein kinase (MAPK), and PI3K. These signaling pathways can promote macrophages to release cytokines, including IFN-γ and TNF-α. We used LPS to stimulate transgenic sheep overexpressing TLR4 as a model of acute inflammation. TLR4 overexpression *in vivo* could enhance expression of downstream inflammatory factors and GCHI. This finding indicates that TLR4 regulates GCHI expression through downstream inflammatory factors. In endothelial cells, GCHI overexpression could enhance 10-fold the production of BH4, accompanied with significant increases in NO [44]. Overexpression of GCHI in transgenic mouse endothelial cells could reduce O_2^- significantly and decrease production of superoxide, while bioavailability of NO was well maintained in GCHI-transgenic mice [45]. Our results show that TLR4 could upregulate the expression of NADPH oxidase and iNOS in mononuclear macrophages. The Tg cells stimulated with LPS plus an iNOS inhibitor still secreted NO, and the expression of GCHI was upregulated. These findings indicate that TLR4 enhances the activity of iNOS by upregulating GCHI, which then promotes the synthesis and secretion of NO.

In summary, these experiments document that the novel overexpression of TLR4 in transgenic sheep enhanced oxidative stress and that TLR4-induced oxidative stress was caused by NO. TLR4 and its downstream signaling pathways play important roles in the activation of GCHI expression. This study provides valuable insights into oxidative disease caused by Gram-negative bacterial infection in sheep.

Conflict of Interests

The authors declare no competing financial interests.

Authors' Contribution

Shoulong Deng, Kun Yu, Zhengxing Lian, Ning Li, and Yixun Liu conceived and designed the experiments. Shoulong Deng, Guoshi Liu, Jinlong Zhang, and Xiaosheng Zhang performed the experiments. Shoulong Deng, Kun Yu, and Zhengxing Lian analyzed the data. Zhixian Wang, Yuchang Yao, and Zhengxing Lian contributed reagents/materials/analysis tools. Shoulong Deng, Kun Yu, and Baolu Zhang wrote the paper. Shoulong Deng and Kun Yu contributed equally to this work.

Acknowledgments

This work was supported by grants from National Transgenic Creature Breeding Grand Project (2013ZX08008-005) and Chinese Universities Scientific Fund (2014BH032).

References

[1] L. Hoareau, K. Bencharif, P. Rondeau et al., "Signaling pathways involved in LPS induced TNFalpha production in human adipocytes," *Journal of Inflammation*, vol. 7, article 1, 2010.

[2] K.-H. Tse, K. B. S. Chow, W. K. Leung, Y. H. Wong, and H. Wise, "Lipopolysaccharide differentially modulates expression of cytokines and cyclooxygenases in dorsal root ganglion cells via Toll-like receptor-4 dependent pathways," *Neuroscience*, vol. 267, pp. 241–251, 2014.

[3] K. A. Ryan, M. F. Smith Jr., M. K. Sanders, and P. B. Ernst, "Reactive oxygen and nitrogen species differentially regulate Toll-like receptor 4-mediated activation of NF-kappa B and interleukin-8 expression," *Infection and Immunity*, vol. 72, no. 4, pp. 2123–2130, 2004.

[4] K. Uchimura, M. Hayata, T. Mizumoto et al., "The serine protease prostasin regulates hepatic insulin sensitivity by modulating TLR4 signalling," *Nature Communications*, vol. 5, article 3428, 2014.

[5] O. O. Zaitseva, T. V. Polezhaeva, A. N. Khudyakov et al., "Influence of pectins on NADPH oxidase and phagocytic activity of neutrophils during cryopreservation," *Cryo-Letters*, vol. 34, no. 5, pp. 544–548, 2013.

[6] S. Pacquelet, J. L. Johnson, B. A. Ellis et al., "Cross-talk between IRAK-4 and the NADPH oxidase," *Biochemical Journal*, vol. 403, no. 3, pp. 451–461, 2007.

[7] K. A. Gauss, L. K. Nelson-Overton, D. W. Siemsen, Y. Gao, F. R. DeLeo, and M. T. Quinn, "Role of NF-κB in transcriptional regulation of the phagocyte NADPH oxidase by tumor necrosis factor-α," *Journal of Leukocyte Biology*, vol. 82, no. 3, pp. 729–741, 2007.

[8] Y. Suzuki, K. Hattori, J. Hamanaka et al., "Pharmacological inhibition of TLR4-NOX4 signal protects against neuronal death in transient focal ischemia," *Scientific Reports*, vol. 2, article 896, 2012.

[9] I.-T. Lee, R.-H. Shih, C.-C. Lin, J.-T. Chen, and C.-M. Yang, "Role of TLR4/NADPH oxidase/ROS-activated p38 MAPK in VCAM-1 expression induced by lipopolysaccharide in human renal mesangial cells," *Cell Communication and Signaling*, vol. 10, no. 1, article 33, 2012.

[10] Y. Y. Choi, M. H. Kim, J. M. Han et al., "The anti-inflammatory potential of Cortex Phellodendron in vivo and in vitro: down-regulation of NO and iNOS through suppression of NF-κB and MAPK activation," *International Immunopharmacology*, vol. 19, no. 2, pp. 214–220, 2014.

[11] M. Ohtsuki, T. Nomura, S.-I. Morimoto et al., "Suppressed expression of GTP cyclohydrolase I mRNA and accelerated expression of inducible nitric oxide synthase mRNA in endomyocardial biopsy specimens from patients with dilated cardiomyopathy," *Clinica Chimica Acta*, vol. 353, no. 1-2, pp. 103–107, 2005.

[12] J.-Y. Lee, H. J. Yang, J.-M. Kim, and B. S. Jeon, "Novel *GCH-1* mutations and unusual long-lasting dyskinesias in Korean families with dopa-responsive dystonia," *Parkinsonism & Related Disorders*, vol. 19, no. 12, pp. 1156–1159, 2013.

[13] T. Jilling, D. Simon, J. Lu et al., "The roles of bacteria and TLR4 in rat and murine models of necrotizing enterocolitis," *The Journal of Immunology*, vol. 177, no. 5, pp. 3273–3282, 2006.

[14] E. Faure, O. Equils, P. A. Sieling et al., "Bacterial lipopolysaccharide activates NF-κB through toll-like receptor 4 (TLR-4) in cultured human dermal endothelial cells. Differential expression of TLR-4 and TLR-2 in endothelial cells," *Journal of Biological Chemistry*, vol. 275, no. 15, pp. 11058–11063, 2000.

[15] E. Seki, H. Tsutsui, H. Nakano et al., "Lipopolysaccharide-induced IL-18 secretion from murine Kupffer cells independently of myeloid differentiation factor 88 that is critically involved in induction of production of IL-12 and IL-1β," *The Journal of Immunology*, vol. 166, no. 4, pp. 2651–2657, 2001.

[16] L. M. Haynes, D. D. Moore, E. A. Kurt-Jones, R. W. Finberg, L. J. Anderson, and R. A. Tripp, "Involvement of Toll-like receptor 4 in innate immunity to respiratory syncytial virus," *Journal of Virology*, vol. 75, no. 22, pp. 10730–10737, 2001.

[17] M.-F. Roy, L. Larivière, R. Wilkinson, M. Tam, M. M. Stevenson, and D. Malo, "Incremental expression of Tlr4 correlates with mouse resistance to *Salmonella* infection and fine regulation of relevant immune genes," *Genes and Immunity*, vol. 7, no. 5, pp. 372–383, 2006.

[18] S. Deng, Q. Wu, K. Yu et al., "Changes in the relative inflammatory responses in sheep cells overexpressing of toll-like receptor 4 when stimulated with LPS," *PLoS ONE*, vol. 7, no. 10, Article ID e47118, 2012.

[19] F. Bihl, L. Salez, M. Beaubier et al., "Overexpression of toll-like receptor 4 amplifies the host response to lipopolysaccharide and provides a survival advantage in transgenic mice," *The Journal of Immunology*, vol. 170, no. 12, pp. 6141–6150, 2003.

[20] J. H. Yu and H. Kim, "Oxidative stress and inflammatory signaling in cerulein pancreatitis," *World Journal of Gastroenterology*, vol. 20, no. 46, pp. 17324–17329, 2014.

[21] I. Gunjaca, J. Zunic, M. Gunjaca, and Z. Kovac, "Circulating cytokine levels in acute pancreatitis—model of SIRS/CARS can help in the clinical assessment of disease severity," *Inflammation*, vol. 35, no. 2, pp. 758–763, 2012.

[22] M. Szajnik, M. J. Szczepanski, M. Czystowska et al., "TLR4 signaling induced by lipopolysaccharide or paclitaxel regulates tumor survival and chemoresistance in ovarian cancer," *Oncogene*, vol. 28, no. 49, pp. 4353–4363, 2009.

[23] J. Zhao, S. Zhao, G. Zhou et al., "Altered biliary epithelial cell and monocyte responses to lipopolysaccharide as a TLR ligand in patients with primary biliary cirrhosis," *Scandinavian Journal of Gastroenterology*, vol. 46, no. 4, pp. 485–494, 2011.

[24] C. De Loera-Rodriguez, V. Delgado-Rizo, A. Alvarado-Navarro, J. Agraz-Cibrian, J. E. Segura-Ortega, and M. Fafutis-Morris, "Over-expression of TLR4-CD14, pro-inflammatory cytokines, metabolic markers and NEFAs in obese non-diabetic Mexicans," *Journal of Inflammation*, vol. 11, no. 1, p. 39, 2014.

[25] X. Wittebole, D. Castanares-Zapatero, and P. F. Laterre, "Toll-like receptor 4 modulation as a strategy to treat sepsis," *Mediators of Inflammation*, vol. 2010, Article ID 568396, 9 pages, 2010.

[26] H. LaRue, C. Ayari, A. Bergeron, and Y. Fradet, "Toll-like receptors in urothelial cells—targets for cancer immunotherapy," *Nature Reviews Urology*, vol. 10, no. 9, pp. 537–545, 2013.

[27] J. J. Kim and D. D. Sears, "TLR4 and insulin resistance," *Gastroenterology Research and Practice*, vol. 2010, Article ID 212563, 11 pages, 2010.

[28] H.-Y. Cho and S. R. Kleeberger, "Genetic mechanisms of susceptibility to oxidative lung injury in mice," *Free Radical Biology & Medicine*, vol. 42, no. 4, pp. 433–445, 2007.

[29] D. Nackiewicz, M. Dan, W. He et al., "TLR2/6 and TLR4-activated macrophages contribute to islet inflammation and impair beta cell insulin gene expression via IL-1 and IL-6," *Diabetologia*, vol. 57, no. 8, pp. 1645–1654, 2014.

[30] S.-K. Heo, H.-J. Yun, E.-K. Noh, W.-H. Park, and S.-D. Park, "LPS induces inflammatory responses in human aortic vascular smooth muscle cells via Toll-like receptor 4 expression and nitric oxide production," *Immunology Letters*, vol. 120, no. 1-2, pp. 57–64, 2008.

[31] B. S. Taylor, M. E. de Vera, R. W. Ganster et al., "Multiple NF-κB enhancer elements regulate cytokine induction of the human inducible nitric oxide synthase gene," *The Journal of Biological Chemistry*, vol. 273, no. 24, pp. 15148–15156, 1998.

[32] A. E. Dikalova, M. C. Góngora, D. G. Harrison, J. D. Lambeth, S. Dikalov, and K. K. Griendling, "Upregulation of Nox1 in vascular smooth muscle leads to impaired endothelium-dependent relaxation via eNOS uncoupling," *The American Journal of Physiology: Heart and Circulatory Physiology*, vol. 299, no. 3, pp. H673–H679, 2010.

[33] N. Xia, A. Daiber, A. Habermeier et al., "Resveratrol reverses endothelial nitric-oxide synthase uncoupling in apolipoprotein E knockout mice," *Journal of Pharmacology and Experimental Therapeutics*, vol. 335, no. 1, pp. 149–154, 2010.

[34] B. Gopalakrishnan, K. M. Nash, M. Velayutham, and F. A. Villamena, "Detection of nitric oxide and superoxide radical anion by electron paramagnetic resonance spectroscopy from cells using spin traps," *Journal of Visualized Experiments*, no. 66, Article ID e2810, 2012.

[35] X. Zhang, P. Shan, S. Qureshi et al., "Cutting edge: TLR4 deficiency confers susceptibility to lethal oxidant lung injury," *Journal of Immunology*, vol. 175, no. 8, pp. 4834–4838, 2005.

[36] A. P. Bautista and J. J. Spitzer, "Inhibition of nitric oxide formation in vivo enhances superoxide release by the perfused liver," *The American Journal of Physiology: Gastrointestinal and Liver Physiology*, vol. 266, no. 5, part 1, pp. G783–G788, 1994.

[37] W. A. Pryor and G. L. Squadrito, "The chemistry of peroxynitrite: a product from the reaction of nitric oxide with superoxide," *The American Journal of Physiology—Lung Cellular and Molecular Physiology*, vol. 268, no. 5, pp. L699–L722, 1995.

[38] A. L. Moens and D. A. Kass, "Therapeutic potential of tetrahydrobiopterin for treating vascular and cardiac disease," *Journal of Cardiovascular Pharmacology*, vol. 50, no. 3, pp. 238–246, 2007.

[39] T. S. Schmidt, E. McNeill, G. Douglas et al., "Tetrahydrobiopterin supplementation reduces atherosclerosis and vascular inflammation in apolipoprotein E-knockout mice," *Clinical Science*, vol. 119, no. 3, pp. 131–142, 2010.

[40] K. Sakai, H. Suzuki, H. Oda et al., "Phosphoinositide 3-kinase in nitric oxide synthesis in macrophage: critical dimerization of inducible nitric-oxide synthase," *The Journal of Biological Chemistry*, vol. 281, no. 26, pp. 17736–17742, 2006.

[41] S. S. Gross and R. Levi, "Tetrahydrobiopterin synthesis. An absolute requirement for cytokine-induced nitric oxide generation by vascular smooth muscle," *Journal of Biological Chemistry*, vol. 267, no. 36, pp. 25722–25729, 1992.

[42] W. Wang, E. Zolty, S. Falk et al., "Endotoxemia-related acute kidney injury in transgenic mice with endothelial overexpression of GTP cyclohydrolase-1," *The American Journal of Physiology—Renal Physiology*, vol. 294, no. 3, pp. F571–F576, 2008.

[43] D. A. Geller, M. di Silvio, T. R. Billiar, and K. Hatakeyama, "GTP cyclohydrolase I is coinduced in hepatocytes stimulated to produce nitric oxide," *Biochemical and Biophysical Research Communications*, vol. 276, no. 2, pp. 633–641, 2000.

[44] S. Cai, N. J. Alp, D. McDonald et al., "GTP cyclohydrolase I gene transfer augments intracellular tetrahydrobiopterin in human endothelial cells: effects on nitric oxide synthase activity, protein levels and dimerisation," *Cardiovascular Research*, vol. 55, no. 4, pp. 838–849, 2002.

[45] N. J. Alp, S. Mussa, J. Khoo et al., "Tetrahydrobiopterin-dependent preservation of nitric oxide-mediated endothelial function in diabetes by targeted transgenic GTP-cyclohydrolase I overexpression," *The Journal of Clinical Investigation*, vol. 112, no. 5, pp. 725–735, 2003.

Hindawi Publishing Corporation
Oxidative Medicine and Cellular Longevity
Volume 2015, Article ID 839748, 7 pages
http://dx.doi.org/10.1155/2015/839748

Research Article

Insulin Therapy of Nondiabetic Septic Patients Is Predicted by *para*-Tyrosine/Phenylalanine Ratio and by Hydroxyl Radical-Derived Products of Phenylalanine

Szilárd Kun,[1] Gergő A. Molnár,[1] Eszter Sélley,[1] Lívia Szélig,[2] Lajos Bogár,[2] Csaba Csontos,[2] Attila Miseta,[3] and István Wittmann[1]

[1] *2nd Department of Medicine and Nephrological Centre, Faculty of Medicine, University of Pécs, Pacsirta Street 1, Pécs 7624, Hungary*
[2] *Department of Anaesthesia and Intensive Care, Faculty of Medicine, University of Pécs, Rákóczi Street 2, Pécs 7623, Hungary*
[3] *Department of Laboratory Medicine, Faculty of Medicine, University of Pécs, Ifjúság Street 13, Pécs 7624, Hungary*

Correspondence should be addressed to István Wittmann; istvan.wittmann@aok.pte.hu

Received 10 January 2015; Accepted 3 March 2015

Academic Editor: Eric E. Kelley

Hydroxyl radical converts Phe to *para*-, *meta*-, and *ortho*-Tyr (*p*-Tyr, *m*-Tyr, *o*-Tyr), while Phe is converted enzymatically to *p*-Tyr in the kidney and could serve as substrate for gluconeogenesis. Pathological isoforms *m*- and *o*-Tyr are supposed to be involved in development of hormone resistances. Role of Phe and the three Tyr isoforms in influencing insulin need was examined in 25 nondiabetic septic patients. Daily insulin dose (DID) and insulin-glucose product (IGP) were calculated. Serum and urinary levels of Phe and Tyr isoforms were determined using a rpHPLC-method. Urinary *m*-Tyr/*p*-Tyr ratio was higher in patients with DID and IGP over median compared to those below median ($P = 0.005$ and $P = 0.01$, resp.). Urinary *m*-Tyr and *m*-Tyr/*p*-Tyr ratio showed positive correlation with DID ($P = 0.009$ and $P = 0.023$, resp.) and with IGP ($P = 0.004$ and $P = 0.008$, resp.). Serum Phe was a negative predictor, while serum *p*-Tyr/Phe ratio was positive predictor of both DID and IGP. Urinary *m*-Tyr and urinary *m*-Tyr/*p*-Tyr, *o*-Tyr/*p*-Tyr, and (*m*-Tyr+*o*-Tyr)/*p*-Tyr ratios were positive predictors of both DID and IGP. Phe and Tyr isoforms have a predictive role in carbohydrate metabolism of nondiabetic septic patients. Phe may serve as substrate for renal gluconeogenesis via enzymatically produced *p*-Tyr, while hydroxyl radical derived Phe products may interfere with insulin action.

1. Introduction

Kidney has an important role in carbohydrate metabolism. There are evidences that renal glucose release contributes to a significant proportion in maintaining fasting plasma glucose level (~25%) [1, 2]. As the length of fasting increases, the proportion of overall glucose release accounted for by renal gluconeogenesis increases [3]. Releasing glucose from the kidney is solely the result of gluconeogenesis [2]. In type 2 diabetic humans, the rate of renal glucose release is increased in a large extent (~300%) and it becomes comparable with hepatic glucose release [4]. Also in hyperepinephrinemia, kidney is responsible for approximately 40% of increased gluconeogenesis [5]. Renal glucose release is inhibited by insulin. This inhibitory effect involves both direct activation or deactivation of enzymes and lowered availability of gluconeogenic substrates [6, 7].

Renal gluconeogenesis is connected to Phe and Tyr metabolism, since phenylalanine hydroxylase, which converts Phe to *para*-Tyr (*p*-Tyr), is located in renal epithelial cells [8] and since Tyr can serve as a substrate for gluconeogenesis through its metabolites, as fumarate [9]. Sepsis is described as a catabolic state with overproduction of endogenous cortisol with increased gluconeogenesis [10]. Moreover, patients with septic shock are often requiring intravenous administration of hydrocortisol, which has a contrainsular effect. Glucose homeostasis in sepsis is also a complex issue, involving endogenous glucose production, endogenous insulin production, and exogenous substitution of either glucose or insulin.

A hallmark of sepsis is oxidative stress. In former studies of our workgroup, we found elevated levels of malondialdehyde (MDA) and myeloperoxidase (MPO) in the early phase of sepsis. There was an increased production of phorbol

12-myristate 13-acetate (PMA) which stimulated reactive oxygen species (ROS) in whole blood on first and second days in septic patients [11]. In the study of Ware et al. higher levels of lipid peroxidation products like plasma F2-isoprostane and isofuran were found in septic patients when organ failure developed [12].

The resulting reactive oxygen species may exert damage among others to amino acids. Overproduction of hydroxyl radical ($HO^{\bullet}$) converts Phe into *para*-, *meta*-, and *ortho*-Tyr (*p*-, *m*-, and *o*-Tyr) [13, 14]. On the other hand, export *p*-Tyr (which is used by other organs for protein synthesis) is formed enzymatically from Phe under physiological circumstances in the kidney, through Phe hydroxylase, as mentioned above [15]. Thus, *p*-Tyr may be formed physiologically and in the oxidative processes as well, while *m*- and *o*-Tyr are oxidative stress markers only. Consequently, elevated levels of *m*- and *o*-Tyr detect hydroxyl radical-induced tissue damage. Many studies have proved that *m*- and *o*-Tyr levels correlated with other oxidative stress markers [16–18].

Increasing number of studies assessed serum and urinary Tyr isoforms in different illnesses. Serum and urinary *o*- and *p*-Tyr levels were measured by our group in patients suffering from diabetes mellitus and chronic kidney disease (CKD). Significantly lower plasma *p*-Tyr levels were found in CKD group, while increased urinary excretion of *o*-Tyr was observed in diabetic/CKD patients [19]. Interestingly, total urinary albumin/creatinine and nonimmunoreactive albumin/creatinine ratios showed a good correlation with urinary *o*-Tyr/creatinine ratio in patients suffering from ischemic stroke in our other study [20]. Also, we found higher levels of *m*-Tyr and *o*-Tyr in the total homogenates of cataractous lenses [21]. These pathological Tyr isoforms may have a role in development of hormone resistances, as insulin or erythropoietin resistance. This has recently been proved by our group in both *in vitro* and human studies [22–24].

Based on the previous data we postulated that elevated levels of hydroxyl radical-derived Tyr isoforms along with enzymatically produced *p*-Tyr could contribute to altered carbohydrate metabolism in nondiabetic septic subjects and thus predict insulin therapy of these patients. Phe and *p*-Tyr contribute to renal gluconeogenesis while pathological isoforms (*m*- and *o*-Tyr) may interfere with insulin action in the kidney, thus leading to insulin resistance.

2. Methods

2.1. Subjects and Study Design. The study protocol was approved by the Ethical Committee of the Medical Faculty of the University of Pécs (4422/2012) and it was completed in accordance with the ethical guidelines of the 2003 Declaration of Helsinki. All the patients or the nearest relatives provided a written informed consent after enlightenment. The study was performed on 25 patients admitted to the Department of Anaesthesia and Intensive Care, Faculty of Medicine, University of Pécs, between September 2012 and October 2013. Those patients who presented with severe sepsis or septic shock at admission were included in the study. The diagnosis of sepsis was based on the ACCP/SCCM consensus guideline [25].

Exclusion criteria were medication (e.g., chronic steroid use and immunosuppressive medication) or treatment (e.g., radio- and chemotherapy) affecting the normal immune response and hematologic malignant disease and oliguria at admission (collection of urine samples was impossible). Patients were treated according to the recent sepsis guideline [26]. Blood samples were taken on admission (day 1) and on the four consecutive days (days 2–5). Urine has been collected every 24 hours and the daily amount has been noticed.

A five-day long study period has been chosen because we had presumed that a 5-day period would open a wide time window that could be enough for detecting early changes in *p*-, *m*-, and *o*-Tyr and Phe levels in patients suffering from sepsis. Serum and urinary creatinine, serum hsCRP, and PCT levels were measured. Daily hsCRP, PCT, and creatinine measurements were part of the routine monitoring of septic patients and they were carried out at the Institute of Laboratory Medicine, University of Pécs.

Patients received insulin intravenously using perfusor according to a sliding-scale to maintain blood glucose level in the range of 6–8 mmol/L. Glucose levels were measured using arterial blood gas analysis at minimum 5 times per day. Data of daily insulin dose (DID) and glucose profile were assessed. An insulin-glucose product (IGP) was calculated based on DID and mean daily glucose levels.

In case of septic shock, after fluid resuscitation (20 mL/kg crystalloid solution) hydrocortisone (200 mg/24 h) and norepinephrine were administered to maintain MAP > 70 mmHg. Invasive haemodynamic monitoring was started too. If central venous saturation of hemoglobin (ScVO2) remained lower than 70% and cardiac index (CI) was below 2.5 L/min/m^2 despite adequate preload (intrathoracic blood volume index (ITBVI)) dobutamine was added to the treatment. Daily doses of these agents were also noticed.

2.2. Measurement of p-, m-, and o-Tyr and Phe Levels. Blood samples of septic patients were obtained from a central venous catheter. Serum was obtained by centrifugation. Serum and urine samples were stored at −80°C until further examinations. Thereafter, 125 μL trichloroacetic acid (TCA; Reanal Private Ltd., Budapest, Hungary) was added to 500 μL serum or urine and then samples were incubated on ice for 30 min. Subsequently precipitate was separated by centrifugation. The supernatant was filtered by a syringe filter (0.2 μm) (Millipore, Billerica, MA, USA) before analysis. Finally serum and urinary *m*-, *o*-, and *p*-Tyr and Phe levels were determined using reverse phase-HPLC (Shimadzu USA Manufacturing INC, Canby, OR, USA) (C_{18} silica column, 250 × 4 mm) with fluorescence detection (λ_{EX} = 275 nm; λ_{EM} = 305 nm for the tyrosines and λ_{EX} = 258 nm; λ_{EM} = 288 nm for Phe) as described earlier [19]. Concentrations were calculated using an external standard. Representative HPLC profiles of a standard and of serum and urine samples of a septic patient are presented in Figure 1.

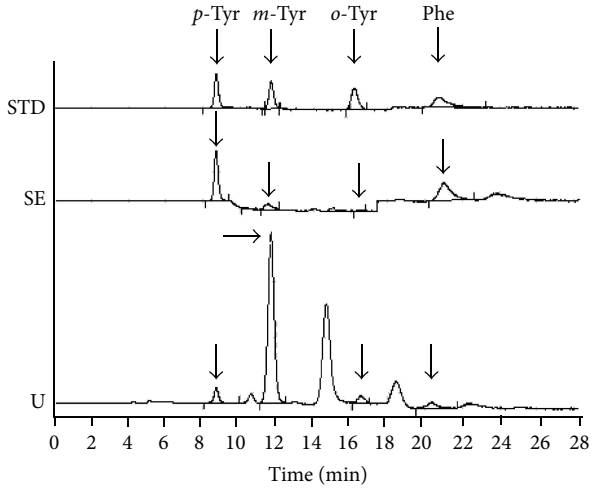

Figure 1: Chromatograms of a standard (STD), a serum (SE), and a urine sample of a septic patient (U). *p*-Tyr, *para*-tyrosine; *m*-Tyr, *meta*-tyrosine; *o*-Tyr, *ortho*-tyrosine; Phe, phenylalanine.

Fractional excretions (FE) of the three Tyr isoforms were calculated ($FE_{p\text{-Tyr}}$, $FE_{m\text{-Tyr}}$, and $FE_{o\text{-Tyr}}$) to determine tubular handling of them. FE of a certain substance can be used to examine renal handling of that particular substance. It is calculated by dividing the clearance of the measured substance by the clearance of creatinine. FE shows how much of the filtered substance is excreted with the urine. It therefore indicates whether a clearance of the particular substance is greater or smaller than or equal to the clearance of creatinine. If FE of a substance is 100%, it is freely filtered, and the net renal reabsorption and secretion are zero. If FE is smaller than 100%, it indicates an active renal reabsorption of the substance. If FE exceeds 100%, it indicates active secretion or *in loco* renal production of the substance. For calculating 24-hour clearance and FE the respective blood sample has to be obtained during the urine collection.

2.3. Statistical Analysis. Statistical Package for the Social Sciences (SPSS) Statistics software, version 20.0 (IBM Corporation, USA), was used for statistical analysis. Data were expressed as median, interquartile range (IQR (standard 25th–75th percentile)) and whiskers represent 5th and 95th percentiles since their distribution was not normal by Kolmogorov-Smirnov test. Intergroup analyses were performed using Mann-Whitney *U* test. Correlations between variables were assessed using Spearman's rho test. Multivariate linear regression models with stepwise method were used to determine predictors of insulin demand. Values of $P < 0.05$ were considered significant.

Table 1: Baseline demographics, clinical data, and amino acid parameters of patients.

n	25
Age [years]	69 ± 14
Male/female	14/11
Body weight [kg]	80 (13)
Source of sepsis	
Lung	13
Kidney	2
Burned skin	7
Wound	1
Abdomen	2
APACHE II	16 (10)
MODS	5 (5)
SAPS II	37.5 (20)
Serum creatinine [μmol/L]	118 95.5
hsCRP [mg/L]	154.2 ± 92.8
PCT [ng/mL]	7.62 19.23
Daily urine output [mL]	2055 (1775)
Mean daily glucose [mmol/L]	9.0 2.5
DID [U/day]	19 (25)
IGP [U∗mmol/L]	183.4223 261.2992
Number of patients receiving hydrocortisone	18 (72%)
Daily hydrocortisone dose [mg/day]	200 (100)
Number of patients receiving dobutamine	10 (40%)
Daily dobutamine dose [mg/day]	275.0 537.5
Serum *p*-Tyr [μmol/L]	45.177 ± 18.049
Serum *m*-Tyr [nmol/L]	14 (27)
Serum *o*-Tyr [nmol/L]	14 (15)
Serum Phe [μmol/L]	65.374 ± 27.519
Serum *p*-Tyr/Phe [μmol/μmol]	0.654 0.292
Serum *m*-Tyr/Phe [nmol/μmol]	0.2 0.4
Serum *o*-Tyr/Phe [nmol/μmol]	0.2 0.4
Serum *m*-Tyr/*p*-Tyr [nmol/μmol]	0.3 0.5
Serum *o*-Tyr/*p*-Tyr [nmol/μmol]	0.3 0.5
Serum (*m*-Tyr+*o*-Tyr)/Phe [nmol/μmol]	0.5 0.7
Serum (*m*-Tyr+*o*-Tyr)/*p*-Tyr [nmol/μmol]	0.6 1.1
Urinary *p*-Tyr [μmol/L]	25.394 44.402
Urinary *m*-Tyr [nmol/L]	123 (351)
Urinary *o*-Tyr [nmol/L]	194 (661)
Urinary *m*-Tyr/*p*-Tyr [nmol/μmol]	4 (17)
Urinary *o*-Tyr/*p*-Tyr [nmol/μmol]	9 (39)
Urinary (*m*-Tyr+*o*-Tyr)/*p*-Tyr [nmol/μmol]	21 (85)
Urinary *p*-Tyr/creatinine [μmol/mmol]	6.952 11.645
Urinary *m*-Tyr/creatinine [nmol/mmol]	29 (68)
Urinary *o*-Tyr/creatinine [nmol/mmol]	61 (220)
Daily excretion of *p*-Tyr [μmol/day]	56.268 116.710
Daily excretion of *m*-Tyr [nmol/day]	259 (607)
Daily excretion of *o*-Tyr [nmol/day]	304 (1786)
Clearance of *p*-Tyr [mL/min]	0.605 1.720
Clearance of *m*-Tyr [mL/min]	9.011 27.413*
Clearance of *o*-Tyr [mL/min]	17.198 105.512*†
$FE_{p\text{-Tyr}}$ [%]	1.783 2.160
$FE_{m\text{-Tyr}}$ [%]	25.104 54.305‡
$FE_{o\text{-Tyr}}$ [%]	85.645 639.219‡§

*$P < 0.001$ versus clearance of *p*-Tyr; †$P = 0.019$ versus clearance of *m*-Tyr; ‡$P < 0.001$ versus FE*p*-Tyr; §$P = 0.006$ vs. FE*m*-Tyr.

APACHE II, acute physiology and chronic health evaluation II; MODS, multiple organ dysfunction score; SAPS II, simplified acute physiology score II; DID, daily insulin dose; IGP, insulin-glucose product; FE, fractional excretion.

Data expressed as mean ± SD or median (interquartile range).

3. Results

3.1. Demographic Data of Patients. Twenty-five septic patients were involved in the study. Demographic data, source of infections, and amino acid parameters are summarized in Table 1. Eight patients suffered from severe sepsis and 17 from septic shock and 19 patients required mechanical ventilation during ICU stay. Out of 25 patients, 11 were discharged from the ICU, while 7 patients died during the study period and 7 patients thereafter.

Table 2: Predictors of carbohydrate metabolism parameters among septic patients, across the whole study period.

	DID		IGP*	
	β	P	β	P
Serum Phe	−0.450	0.001	−0.460	0.001
Serum *p*-Tyr/Phe	0.507	<0.001	0.554	<0.001
Serum *o*-Tyr/Phe	—	—	0.280	0.049
Urinary *m*-Tyr	0.381	0.007	0.382	0.007
Urinary *m*-Tyr/*p*-Tyr	0.359	0.011	0.351	0.013
Urinary *o*-Tyr/*p*-Tyr	0.322	0.023	0.308	0.030
Urinary (*m*-Tyr+*o*-Tyr)/*p*-Tyr	0.389	0.006	0.376	0.008

Model: body weight, hsCRP, PCT, daily hydrocortisone dose, daily dobutamine dose, and the actual amino acid parameter.
DID, daily insulin dose; IGP, insulin-glucose product.
*Calculated by average daily glucose level (mmol/L) multiplied by daily insulin dose (U).
Method: stepwise.

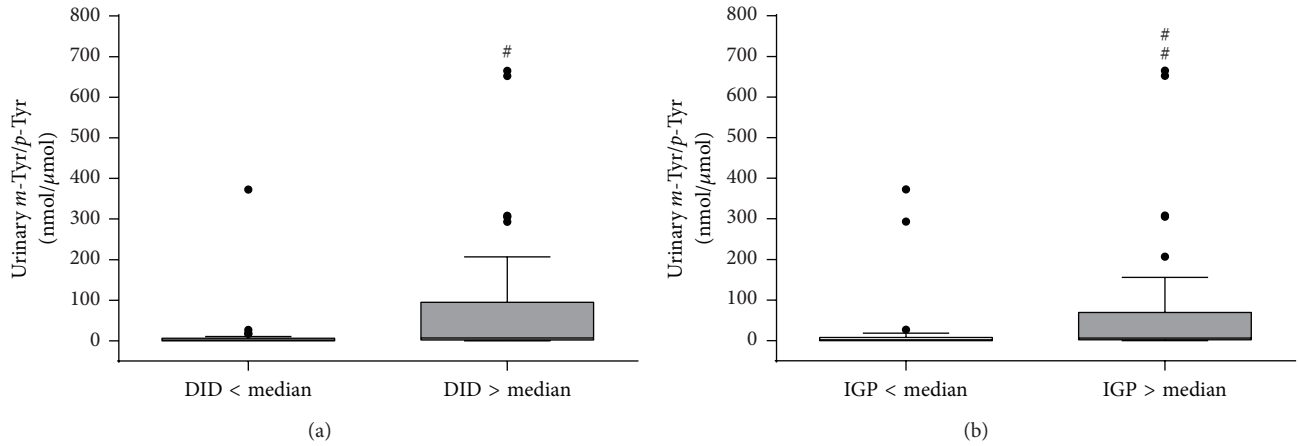

Figure 2: Urinary *m*-Tyr/*p*-Tyr ratio in septic patients requiring insulin administration, according to (a) daily insulin dose or (b) insulin-glucose product. $^{\#}P = 0.005$ versus DID < median; $^{\#\#}P = 0.01$ versus IGP < median. DID, daily insulin dose; IGP, insulin-glucose product.

We examined the association of amino acid parameters and clinical outcomes. None of these metabolites showed any difference between survivor and nonsurvivor subjects on day 1 (data not shown).

3.2. Urinary m-Tyr Levels and Insulin Demand. Urinary *m*-Tyr/*p*-Tyr ratio was significantly higher in patients with DID over median compared to those with DID below median (7.3 92.3 versus 1.7 6.3, resp.; $P = 0.005$) (Figure 2(a)). Similarly, urinary *m*-Tyr/*p*-Tyr ratio was significantly higher in patients with IGP over median compared to those with IGP below median (6.6 67.5 versus 1.7 7.5, resp.; $P = 0.010$) (Figure 2(b)).

3.3. Association of Tyr Parameters with Insulin Demand. Urinary *m*-Tyr concentration showed a positive correlation with DID ($r = 0.310$; $P = 0.009$) (Figure 3(a)) and with IGP ($r = 0.343$; $P = 0.004$) (Figure 3(c)). Similarly, urinary *m*-Tyr/*p*-Tyr ratio showed a positive correlation with DID ($r = 0.271$; $P = 0.023$) (Figure 3(b)) and with IGP ($r = 0.315$; $P = 0.008$) (Figure 3(d)).

Amino acid parameters were tested separately in multivariate linear regression models as predictors of insulin demand (DID and IGP). The components of this model were body weight, hsCRP, PCT, daily hydrocortisone dose, and daily dobutamine dose. Serum Phe was a negative predictor of both DID and IGP, while serum *p*-Tyr/Phe ratio associated positively and strongly with these carbohydrate metabolism parameters. Serum *o*-Tyr/Phe ratio was a positive predictor of IGP only, but not of DID (Table 2). Urinary level of *m*-Tyr and ratios of urinary *m*-Tyr/*p*-Tyr, *o*-Tyr/*p*-Tyr, and (*m*-Tyr+*o*-Tyr)/*p*-Tyr were positive predictors of both DID and IGP (Table 2). The abovementioned amino acid parameters were tested also in another model, in which serum creatinine level was included instead of body weight. In this model, similar results were obtained compared to the case of body weight (data not shown).

3.4. Fractional Excretion of Tyr Isoforms. Both $FE_{m\text{-Tyr}}$ and $FE_{o\text{-Tyr}}$ were significantly higher than $FE_{p\text{-Tyr}}$ ($P < 0.001$, for both). There was also a significant difference between $FE_{m\text{-Tyr}}$ and $FE_{o\text{-Tyr}}$, as $FE_{o\text{-Tyr}}$ was more than threefold higher than $FE_{m\text{-Tyr}}$ ($P = 0.006$) (Table 1). No direct connection between FE values of any of the investigated amino acid and carbohydrate parameters was found.

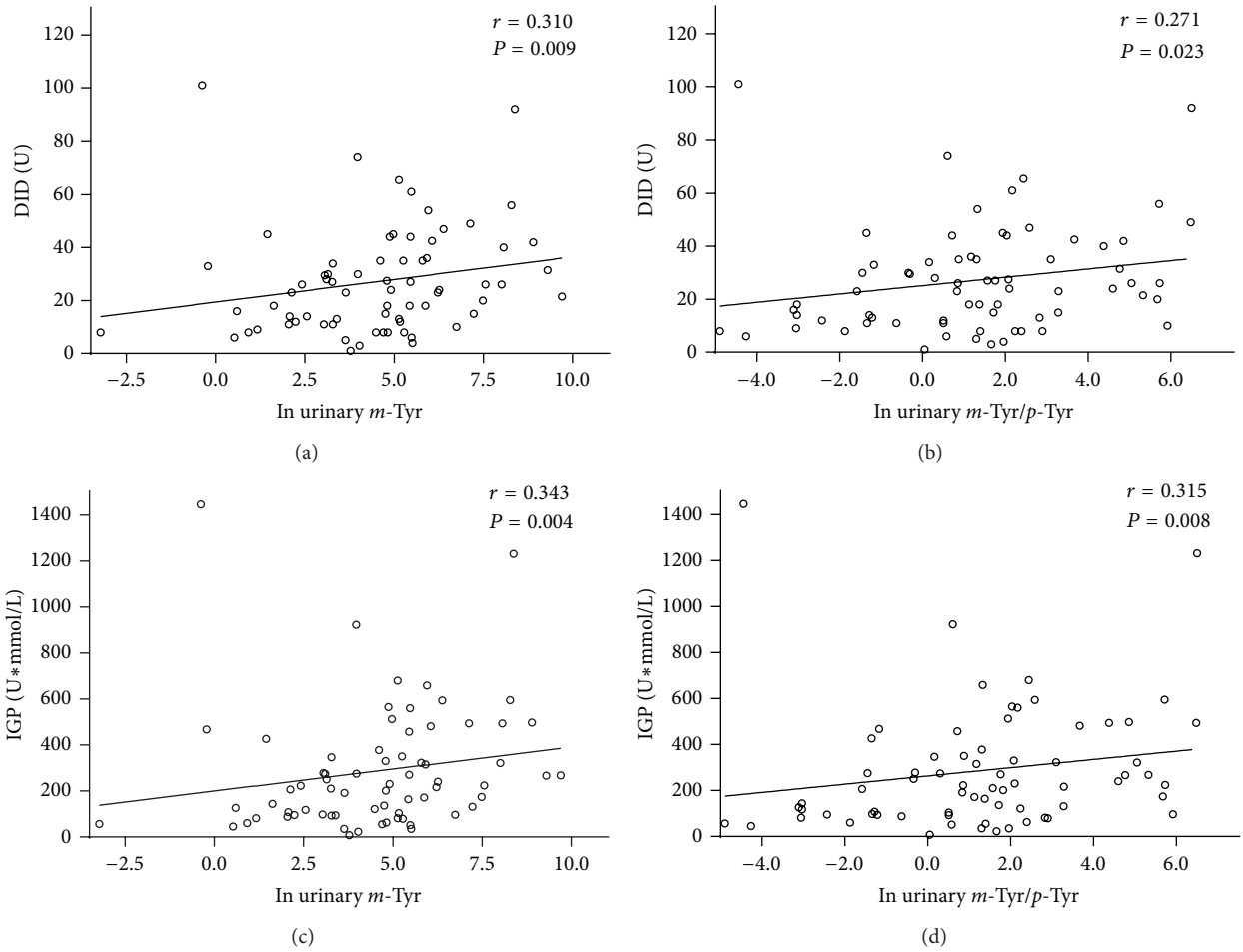

Figure 3: Correlation of urinary *m*-Tyr concentration with (a) DID and (c) IGP. Correlation of urinary *m*-Tyr/*p*-Tyr ratio with (b) DID and (d) IGP in septic patients requiring insulin administration. DID, daily insulin dose; IGP, insulin-glucose product.

4. Discussion

In our study, we provided evidence that elevated levels of hydroxyl radical-derived Tyr isoforms along with enzymatically produced *p*-Tyr could contribute to altered carbohydrate metabolism in nondiabetic septic subjects and thus predict insulin therapy of these patients.

Serum and urinary levels and ratios of the abovementioned amino acids were strong predictors of both DID and IGP in a model which was composed by the known predictors of elevated insulin demand. In another model, with serum creatinine level instead of body weight, the same results were obtained, indicating that these associations are independent of renal function.

A potential cause of the abovementioned association of serum level of Phe with DID and with IGP could be a generalized hypoaminoacidemia due to malnutrition. We tested this possibility by performing correlation tests between serum level of albumin and DID or IGP. Neither DID nor IGP showed correlation with serum albumin level ($r = 0.056$, $P = 0.646$; $r = 0.048$, $P = 0.693$, resp.) (data not shown).

The fact that (i) serum level of Phe proved to be a negative predictor of DID and IGP and (ii) serum *p*-Tyr/Phe ratio proved to be a stronger positive one, while (iii) serum *p*-Tyr alone was not a predictor and (iv) serum *p*-Tyr level was slightly but not significantly lower in septic patients compared to that of healthy subjects [19, 23] may suggest that in septic patients the conversion of Phe to *p*-Tyr—at a normal Phe level—results not only in the production of export *p*-Tyr, but the produced *p*-Tyr is also consumed for gluconeogenesis *in loco* in the kidney.

We are aware that, beyond oxidative stress, also other factors (such as metabolic status, actual level of inflammation, anthropometric parameters, and medications) may also have a strong influence on glycemic control. That is why we subsequently performed linear regression analyses, where correction to body weight, inflammatory markers, and doses of gluconeogenesis-stimulating agents did not lead to a disappearance of the association between *m*-Tyr and markers of glycemic status. Indeed, in this analysis, a statistically highly significant connection was observed. This suggests that, besides already known parameters, independently of them, the oxidative stress-derived amino acid does play a role in determining carbohydrate control.

Furthermore, our aim was mainly not to establish a new daily clinical routine marker for managing individual septic

patients, but rather to enlighten the underlying mechanisms of carbohydrate metabolism of these patients in light of Phe and Tyr metabolism. However, we also think that these metabolites could be used as clinical markers as well, if they are considered together with other current routine clinical parameters, also mentioned in our study. As in many other cases, individual consideration will be the right way also in this certain issue.

There was a significant difference between $FE_{m\text{-Tyr}}$ and $FE_{o\text{-Tyr}}$. $FE_{o\text{-Tyr}}$ was more than threefold higher than $FE_{m\text{-Tyr}}$. At the same time serum concentrations of the two Tyr isoforms were equal. This could indicate that renal retention of *m*-Tyr is much higher than that of *o*-Tyr, which results in a higher intracellular concentration of *m*-Tyr in renal cells. This could explain better predictive role of *m*-Tyr.

A septic model has been chosen because rapid changes occur in carbohydrate metabolism and also serum and urinary levels of amino acids can be well monitored in these circumstances. Also short-term associations can be observed between carbohydrate metabolism and these amino acids.

In our study, the investigated parameters did not show any difference between groups based on ICU survival (data not shown). However, in the comparison of ICU-surviving versus nonsurviving patients, the number of cases in the two groups was only $n = 18$ versus $n = 7$. The low number of cases could be in part in the background of the lack of significance; the absolute values seemed to show a tendency that corresponds to our hypothesis; that is, markers of oxidative stress-derived amino acids seemed somewhat higher in the nonsurvival than in the survival group.

IGP in describing carbohydrate metabolism was used as a parameter referring to insulin resistance. This is similar to $HOMA_{IR}$ in which plasma levels of fasting glucose and fasting endogenous insulin are included. If plasma level of glucose increases at a constant plasma level of endogenous insulin or vice versa the product rises, that refers to insulin resistance. The same conception was applied in case of IGP, in which the amount of exogenously administered insulin was multiplied with average plasma glucose level. On the other hand, according to our opinion, insulin need (thus DID and IGP) is predicted also by gluconeogenesis, as also endogenously produced glucose needs to be overcome by exogenously administered insulin. Furthermore, on the routine, no exogenous glucose infusion was applied in these patients, making the estimation of glucose metabolism somewhat easier. Thus we believe that DID and IGP mainly serve as descriptors of insulin resistance + gluconeogenesis.

A five-day long study period is appropriate for better observing the role of kidney, as in this duration renal glucose release contributes to total glucose release in an increasing proportion, as hepatic glucose output decreases, because of lowered glycogenolysis [3].

Aromatic amino acids, as Phe and Tyr, were assessed as predictors of glycemia cross-sectionally in a recent study in young adults. Serum Phe was positively associated with HOMA-IR in both males and females, while Tyr was only predictor of HOMA-IR in men [27].

Limitations of our study are the fact that (i) this is a pilot study with a relative low number of cases, (ii) correlational and linear regression analyses at each day separately were lacking, due to relatively low number of cases, and (iii) effect of hydroxyl radical-derived Phe products on insulin action in the kidney has not been proved directly.

5. Conclusions

Concluding, we provided evidence that Phe and its hydroxyl radical-derived products, along with enzymatically produced *p*-Tyr, predict insulin therapy of nondiabetic septic patients, which reflects (i) the role of kidney in gluconeogenesis, (ii) involvement of Phe and *p*-Tyr in gluconeogenesis, and (iii) the possible inhibitory effect of hydroxyl radical-derived Phe products (*m*- and *o*-Tyr) on insulin action.

Conflict of Interests

The authors declare that there is no conflict of interests regarding the publication of this paper.

References

[1] M. Stumvoll, U. Chintalapudi, G. Perriello, S. Welle, O. Gutierrez, and J. Gerich, "Uptake and release of glucose by the human kidney: postabsorptive rates and responses to epinephrine," *The Journal of Clinical Investigation*, vol. 96, no. 5, pp. 2528–2533, 1995.

[2] C. Meyer, V. Nadkarni, M. Stumvoll, and J. Gerich, "Human kidney free fatty acid and glucose uptake: evidence for a renal glucose-fatty acid cycle," *American Journal of Physiology: Endocrinology and Metabolism*, vol. 273, no. 3, pp. E650–E654, 1997.

[3] M. B. Davidson and A. L. Peters, "An overview of metformin in the treatment of type 2 diabetes mellitus," *American Journal of Medicine*, vol. 102, no. 1, pp. 99–110, 1997.

[4] C. Meyer, M. Stumvoll, V. Nadkarni, J. Dostou, A. Mitrakou, and J. Gerich, "Abnormal renal and hepatic glucose metabolism in type 2 diabetes mellitus," *The Journal of Clinical Investigation*, vol. 102, no. 3, pp. 619–624, 1998.

[5] C. Meyer, M. Stumvoll, S. Welle, H. J. Woerle, M. Haymond, and J. Gerich, "Relative importance of liver, kidney, and substrates in epinephrine-induced increased gluconeogenesis in humans," *American Journal of Physiology: Endocrinology and Metabolism*, vol. 285, no. 4, pp. E819–E826, 2003.

[6] C. Meyer, J. Dostou, V. Nadkarni, and J. Gerich, "Effects of physiological hyperinsulinemia on systemic, renal and hepatic substrate metabolism," *The American Journal of Physiology—Renal Physiology*, vol. 275, no. 6, pp. F915–F921, 1998.

[7] E. Cersosimo, P. Garlick, and J. Ferretti, "Insulin regulation of renal glucose metabolism in humans," *American Journal of Physiology—Endocrinology and Metabolism*, vol. 276, no. 1, pp. E78–E84, 1999.

[8] Y. Wang, J. L. DeMayo, T. M. Hahn et al., "Tissue- and development-specific expression of the human phenylalanine hydroxylase/chloramphenicol acetyltransferase fusion gene in transgenic mice," *The Journal of Biological Chemistry*, vol. 267, no. 21, pp. 15105–15110, 1992.

[9] D. N. Rao and S. Kaufman, "Purification and state of activation of rat kidney phenylalanine hydroxylase," *Journal of Biological Chemistry*, vol. 261, no. 19, pp. 8866–8876, 1986.

[10] E. Crimi, V. Sica, A. S. Slutsky et al., "Role of oxidative stress in experimental sepsis and multisystem organ dysfunction," *Free Radical Research*, vol. 40, no. 7, pp. 665–672, 2006.

[11] D. Mühl, G. Woth, L. Drenkovics et al., "Comparison of oxidative stress & leukocyte activation in patients with severe sepsis & burn injury," *Indian Journal of Medical Research*, vol. 134, no. 7, pp. 69–78, 2011.

[12] L. B. Ware, J. P. Fessel, A. K. May, and L. J. Roberts, "Plasma biomarkers of oxidant stress and development of organ failure in severe sepsis," *Shock*, vol. 36, no. 1, pp. 12–17, 2011.

[13] E. R. Stadtman and B. S. Berlett, "Fenton chemistry: amino acid oxidation," *The Journal of Biological Chemistry*, vol. 266, no. 26, pp. 17201–17211, 1991.

[14] A. Galano and A. Cruz-Torres, "OH radical reactions with phenylalanine in free and peptide forms," *Organic and Biomolecular Chemistry*, vol. 6, no. 4, pp. 732–738, 2008.

[15] J. E. Ayling, W. D. Pirson, J. M. Al-Janabi, and G. D. Helfand, "Kidney phenylalanine hydroxylase from man and rat. Comparison with the liver enzyme," *Biochemistry*, vol. 13, no. 1, pp. 78–85, 1974.

[16] B. Lubec, M. Hayn, W. Denk, and G. Bauer, "Brain lipid peroxidation and hydroxy radical attack following the intravenous infusion of hydrogen peroxide in an infant," *Free Radical Biology and Medicine*, vol. 21, no. 2, pp. 219–223, 1996.

[17] P. Dandona, P. Mohanty, W. Hamouda et al., "Rapid communication: inhibitory effect of a two day fast on reactive oxygen species (ROS) generation by leucocytes and plasma orthotyrosine and meta-tyrosine concentrations," *Journal of Clinical Endocrinology and Metabolism*, vol. 86, no. 6, pp. 2899–2902, 2001.

[18] R. A. Jörres, O. Holz, W. Zachgo et al., "The effect of repeated ozone exposures on inflammatory markers in bronchoalveolar lavage fluid and mucosal biopsies," *The American Journal of Respiratory and Critical Care Medicine*, vol. 161, no. 6, pp. 1855–1861, 2000.

[19] G. A. Molnár, Z. Wagner, L. Markó et al., "Urinary orthotyrosine excretion in diabetes mellitus and renal failure: evidence for hydroxyl radical production," *Kidney International*, vol. 68, no. 5, pp. 2281–2287, 2005.

[20] P. Toth, A. Koller, G. Pusch et al., "Microalbuminuria, indicated by total versus immunoreactive urinary albumins, in acute ischemic stroke patients," *Journal of Stroke and Cerebrovascular Diseases*, vol. 20, no. 6, pp. 510–516, 2011.

[21] G. A. Molnár, V. Nemes, Z. Biró, A. Ludány, Z. Wagner, and I. Wittmann, "Accumulation of the hydroxyl free radical markers meta-, ortho-tyrosine and DOPA in cataractous lenses is accompanied by a lower protein and phenylalanine content of the water-soluble phase," *Free Radical Research*, vol. 39, no. 12, pp. 1359–1366, 2005.

[22] I. A. Szijártó, G. A. Molnár, E. Mikolás et al., "Increase in insulin-induced relaxation of consecutive arterial segments toward the periphery: role of vascular oxidative state," *Free Radical Research*, vol. 48, no. 7, pp. 749–757, 2014.

[23] S. Kun, E. Mikolás, G. A. Molnár et al., "Association of plasma ortho-tyrosine/para-tyrosine ratio with responsiveness of erythropoiesis-stimulating agent in dialyzed patients," *Redox Report*, vol. 48, pp. 749–757, 2014.

[24] E. Mikolás, S. Kun, B. Laczy et al., "Incorporation of ortho- and meta-tyrosine into cellular proteins leads to erythropoietin-resistance in an erythroid cell line," *Kidney & Blood Pressure Research*, vol. 38, no. 2-3, pp. 217–225, 2014.

[25] M. M. Levy, M. P. Fink, J. C. Marshall et al., "2001 SCCM/ESICM/ACCP/ATS/SIS international sepsis definitions conference," *Critical Care Medicine*, vol. 31, no. 4, pp. 1250–1256, 2003.

[26] R. P. Dellinger, M. M. Levy, A. Rhodes et al., "Surviving sepsis campaign: international guidelines for management of severe sepsis and septic shock 2012," *Intensive Care Medicine*, vol. 39, no. 2, pp. 165–228, 2013.

[27] P. Würtz, P. Soininen, A. J. Kangas et al., "Branched-chain and aromatic amino acids are predictors of insulin resistance in young adults," *Diabetes Care*, vol. 36, no. 3, pp. 648–655, 2013.